



UNIVERSITY *of the*
WESTERN CAPE

**Geochemical evaluation of source rocks
within the upper Ecca, main Karoo**

MASTERS THESIS



BY

Zainab Mowzer

Supervisor: Prof. P. Carey
Department of Earth Sciences,
University of the Western Cape

Co-supervisors: Dr. M. Opuwari and Prof. J. van
Bever Donker
Department of Earth Sciences,
University of the Western Cape

*A thesis submitted in fulfillment of the requirements for the degree of
Magister Scientiae in the Department of Earth Sciences, University of the
Western Cape*

Geochemical evaluation of source rocks within the upper Ecca, main Karoo

Zainab Mowzer

KEYWORDS

main Karoo

Laingsburg subbasin

Source Rocks

Maturity

Mineralogy



Declaration

I declare that, *Geochemical evaluation of source rocks within the upper Ecca, main Karoo*, is my own work, that it has not been submitted before for any degree or examination in any other university, and that all the sources I have used or quoted have been indicated and acknowledged as complete references.

Zainab Mowzer

Date.....

Signed.....



Abstract

Early works completed by Bouma, Johnson, Catuneanu, Wickens and others have paved the way in gaining a better understanding of the Karoo complex, from a sedimentology perspective. Research in this area is becoming more readily available as the oil industry seeks to gain more knowledge in this area for exploration purposes. Understanding this area can help aid in offshore development that is not as readily accessible as the onshore sediments. Using new modern technologies as well as old geochemical techniques we can expand our knowledge on hydrocarbons within this onshore environment.

The Karoo in South Africa is an area in which petroleum studies are being reviewed with particular interest, especially within the Tanqua and Laingsburg subbasins of the Karoo. The particular formations of interest comprises of the Laingsburg, Fort Brown, Kookfontein and Vischkuil of the Upper Ecca group, located within the Laingsburg subbasin as well as the Kookfontein formation found within the Tanqua subbasin.

The present work dealt with interpreting and distinguishing the different types of source rock lithologies, to identify the source rock zones and organic matter within the Laingsburg, Fort Brown, Kookfontein and Vischkuil formations. This was achieved by utilising different geochemical analyses (such as rock eval pyrolysis and TOC) and organic chemistry (XRD) to assess the maturity, mineralogy and the quality of the source rocks.

Forty samples were sent for TOC analyses. Rock samples were taken at various localities in the Fort Brown, Vischkuil and Laingsburg Formations, within the Laingsburg subbasin, whereas, Kookfontein core samples were obtained from the Tanqua subbasin.

Overall, ten samples were selected from the 40 samples that had undergone TOC analysis. Using XRD, the core and rock outcrop samples showed clay minerals predominantly of illite, montmorillonite and chlorite.

The TOC and rock-eval S1 and S2 values from the formations within this study were anomalously low. The HI vs. TOC contained Type 1 and Type 2 kerogen plots, but this did not correspond with the HI vs. OI index, because the samples were heavily oxidised.



Acknowledgements

I would like to thank Inkaba ye Africa for providing the resources so that I may complete my research, Dr.Mikes at Stellenbosch for the access and availability of the core samples and reports that were used, Ithemba Laboratory, for their assistance in XRD analysis, Weatherford Labs for the Rock Eval analyses and Bemlab for the TOC analyses.

An immense thanks goes out to Dr.Carey (supervisor), Prof J.van Bever Donker (co-supervisor) and Dr.Opuwari (co-supervisor) for carefully reading, criticising and correcting all drafts, and making useful suggestions which are integrated into this study to improve its standard. They provided encouragement, enthusiasm, and were my guides when I entered uncharted territory during this study.

I am highly grateful to Dr. Remy Bucher of iThemba labs for his kind and tireless assistance with respect to X-Ray Diffraction measurements, analyses techniques and software which proved very helpful.

My deepest appreciation goes to Janine Becorny, of the University of Western Cape, Department of Geological Sciences, for her assistance during the sample preparation processes.

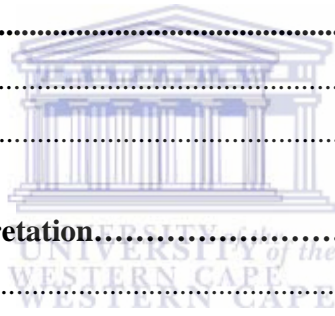
I would also like to thank my fellow graduate students who have assisted and guided me throughout this project. Special thanks go out to Janine Ferreira and Ghaarith Edries, for providing assistance when it was needed. To everyone in the Masters lab I am grateful for your friendships and continued support, you kept me sane throughout this undertaking.

Furthermore, I want to thank my friends and family who have encouraged me throughout this endeavour, I owe much of my success to you.

Table of Contents

<u>Contents</u>	<u>Page Numbers</u>
Title page.....	i
Keywords.....	ii
Declaration.....	iii
Abstract.....	iv-v
Acknowledgements.....	vi
Table of Contents.....	vii-viii
List of Figures.....	ix-xi
List of Tables.....	xii
List of Appendices.....	xiii
Thesis Outline.....	xiv
Part I.....	xiv
Part II.....	xiv
Part III.....	xiv
CHAPTER ONE: Introduction.....	1-43
1.1 Preamble.....	1-2
1.2 Research Problem.....	2
1.3 Study Area.....	3-4
-1.3.1 Sample Collection.....	5-21
1.4 Previous Work.....	21-24
Geological Framework.....	25-43
1.5 Geological Background of the main Karoo.....	25-28
1.6 Tectonic Setting.....	28-30
1.7 Lithostratigraphy.....	31-40
1.8 Chronostratigraphy.....	41
2.5 Depositional History.....	41-43

CHAPTER TWO.....	44-73
Concepts.....	44-54
2.1 Geochemical Methods.....	44-45
2.2 Time Temperature Index (TTI).....	45
2.3 Vitrinite Reflectance (R _o).....	46
2.4 Thermal Alteration Index (TAI).....	46
2.5 Elemental analyses.....	46
2.6 Extent of Kerogen Reaction.....	46-47
2.7 Gas Chromatography (GC).....	47
2.8 Rock Eval Pyrolysis.....	47-50
2.9 TOC (Total Organic Carbon).....	51-53
2.10 X-Ray Diffraction (XRD).....	53-54
Methodology and Data.....	55-73
2.11 Research Design.....	55
2.12 Analytical Techniques.....	56-73
CHAPTER THREE: Interpretation.....	74-81
Geochemistry.....	74-81
3.1. Total Organic Carbon (TOC) Interpretation.....	74
3.2 Rock eval pyrolysis Interpretation.....	75-77
3.3 X-Ray Diffraction (XRD) Interpretation.....	77
-3.3.1 Clay Interpretation.....	77-78
-3.3.2 Clay minerals and studied clay samples.....	78
-3.3.2.1 Montmorillonite.....	79
-3.3.2.2 Chlorite.....	80
-3.3.2.3 Illite.....	80-81
CHAPTER FOUR.....	82-84
4.1 Conclusion and Discussion.....	82-83
4.2 Recommendation.....	84
References.....	86-104



List of Figures

<u>Figures</u>	<u>Page Numbers</u>
Figure 1.3.1: Base map of sample points (Google Earth, AfriGIS (Pty) Ltd).....	4
Figure 1.3.2: Location map of the study area within the Bitteberg area of the Tanqua basin in which the Kookfontein samples were obtained.....	20
Figure 1.3.3: Locality map of the two subbasins in which this study is based on. (Google Earth, AfriGIS (Pty) Ltd)	20
Figure 1.3.4: Location map of the study areas within the Laingsburg basin. The Ladismith area map 3320, 1:250 000, Geological survey of South Africa.....	21
Figure 1.5.1: Location of the Tanqua and Laingsburg basin floor fan-complex in the southwestern corner of the Karoo Basin (Wickens, 1992)	26
Figure 1.5.2: Lithostratigraphic units within the main Karoo Basin (modified from Johnson et al., 1996)	28
Figure 1.6.1: The Karoo basin shown in context of the Pan Gondwanian foreland system (modified from Catuneanu & Bowker, 2001)	29
Figure 1.6.2: The three flexural provinces present within the Karoo (Catuneanu <i>et al.</i> , 2002).....	30
Figure 1.6.3: Location of the Karoo Basin and crustal terranes of South Africa, Antarctica and the Falkland Plateau prior to the breakup of Gondwana (modified by Andersson <i>et al.</i> , 2004).....	30

Figure 1.7.1: Lithostratigraphic column for the Cape Fold Belt and SW Karoo Basin (after Besaans, 1973; Dingle & Siesser, 1977; Steyn, 1983; Theron, 1986; Cole, 1992; Wickens, 1994; Thomas, 1997; De Beer, 1999; Flint et al., 2004).....	39
Figure 1.7.2: Stratigraphic chart with the major lithostratigraphic subdivisions of the Karoo Supergroup in the main Karoo Basin of South Africa (modified from Catuneanu <i>et al.</i> , 2005).....	40
Figure 1.9.1: Paleogeographic reconstruction of the environments established in relation to the Ecca seaway of the Karoo basin (modified from Catuneanu <i>et al.</i> , 2002).....	43
Figure 2.1.1: A typical geochemical analyses diagram for a possible source rock sample. (modified from Murray, 1992).....	45
Figure 2.8.1: Pyrolysis Method of source rock analysis	48
Figure 2.8.2: Time against temperature peaks (S1, S2 and S3), rock eval pyrolysis.....	49
Figure 2.8.3: The van Krevelen diagram.....	50
Figure 2.9.1: Components and classification of TOC.....	52
Figure 2.10.1: The configuration for an XRD unit.....	54
Figure 2.11.1: Flow chart of the methodology.....	55
Figure 2.12.1: HI vs. OI diagram.....	61
Figure 2.12.2: HI vs. TOC diagram.....	62
Figure 2.12.3: The Vischkuil formation minerals displayed by the XRD spikes.....	63

Figure 2.12.4: The Fort Brown formation minerals displayed by the XRD spikes.....64

Figure 2.12.5: The Kookfontein formation minerals displayed by the XRD spikes.....65

Figure 2.12.6: The Laingsburg formation minerals displayed by the XRD spikes.....66

Figure 2.12.7 Sedimentary log and of the Vischkuil Formation.....67-72

Figure 2.12.8 Legend of the Vischkuil Formation.....73



List of Tables

<u>Tables</u>	<u>Page Numbers</u>
Table 2.9.1: TOC classification with relative percentages.....	51
Table 2.12.1: TOC results.....	58
Table 2.12.2: Rock Eval results.....	60



List of Appendices

<u>Appendices</u>	<u>Page Numbers</u>
Appendix A: XRD profiles of the Kookfontein, Fort Brown, Laingsburg and Vischkuil Formations.....	106-125
- Appendix A-1 to A-10: XRD profiles of the Kookfontein Formation.....	106-110
- Appendix A-11 to A-20: XRD profiles of the Fort Brown Formation.....	111-115
- Appendix A-21 to A-30: XRD profiles of the Laingsburg Formation.....	116-120
- Appendix A-31 to A-40: XRD profiles of the Vischkuil Formation.....	121-125
Appendix B: Sedimentary log and Legend of the Laingsburg Formation.....	126-139
- Appendix B-1: Sedimentary Log of the Laingsburg Formation.....	126-139
- Appendix B-2: Legend of the Laingsburg Log.....	139
Appendix C: Sedimentary log and Legend of the Fort Brown Formation.....	140-163
- Appendix C-1: Sedimentary Log of the Fort Brown Formation.....	140-163
- Appendix C-2: Legend of the Fort Brown Log.....	163
Appendix D: Sedimentary log and Legend of the Kookfontein Formation.....	164-168
- Appendix D-1: Sedimentary Log of the Kookfontein Formation.....	164-167
- Appendix D-2: Legend of the Kookfontein Log.....	168

Thesis Outline

This thesis embodies the written report of the study work carried out to assess the source rock potential of the upper Ecca, main Karoo, South Africa. It consists of three major parts which are subdivided into five chapters. The major parts are named Part I, Part II and Part III.

Part I

Part I gives the broad overview of what this thesis is about. It starts with chapter one which presents the research framework background, aims and study area localities. Consulted publications relating to general geology, stratigraphy, geological background of the Karoo basin and petroleum studies within the study area are discussed under literature review. It concludes with chapter two which contains the basic geochemical methods and literature utilised within this study.

Part II

Part II is divided into two chapters. It is comprised of chapter three and chapter four which lays out the methodology, data analysis and interpretation of the results obtained in this study. Chapter four concludes part II. Chapter four is centered on the geochemistry; it discusses the interpreted rock eval and TOC data, as well as the mineralogical XRD interpretations.

Part III

Part III comprises of chapter five and deals with the conclusion discussion and recommendations of the study. Recommendations were made based on the observations made in the various phases of analyses.

Chapter One

Introduction

1.1 Preamble

Petroleum plays a pivotal role in society, so much so that petroleum accounts for a huge percentage of the world's energy consumption. The population boom has made the demand for this commodity increase exponentially. New ventures into the petroleum sector are increasing to keep up with the demand of hydrocarbons.

The Karoo Supergroup in Southern Africa, forms part of the main Karoo and has a number of basins that extends into Zimbabwe, Namibia, Mozambique and Botswana (Johnson et al., 1996a). The Great Karoo basin covers an area of over 700,000 km² and constitutes a retro-arc foreland basin (Raseroka & McLachlan, 2009). The Karoo is world renowned for the Tanqua basin submarine fans, which exhibits deep marine sedimentary rocks. There are three basins present within the main Karoo, which are the Laingsburg subbasin, Southern subbasin and the Tanqua subbasin. These sedimentary rocks are important for hydrocarbon exploration research due to the fact that it is found onshore and has not been altered by faulting, fracturing and metamorphism.

The search for hydrocarbons on the onshore Karoo was undertaken by Soeker in 1965 (Loon, 2007). Coal beds have been found all over the Karoo, although it has only been economically exploitable within the Vryheid Formation of the main Karoo basin (Johnson et al., 1996b). Statoil and the University of Liverpool have done research in the Tanqua basin area of the Karoo, although their research has been more focused on reservoir characterisation and modelling within this area than the source rock potential, but recent studies by Shell (and some other petroleum companies) has started delving into the source rock potential within the Karoo.

The present research work deals with identifying the mineralogy within the formations of interest, interpreting and distinguishing, the different type of source rock lithologies,

and determining the source rock zones within the Fort Brown, Kookfontein, Laingsburg and Vischkuil formations. This will be achieved by utilising different geochemical analyses to assess the maturity and the quality of the source rocks.

1.2 Research Problems

The following list was provided as problems to solve within the area of interest:

- To determine the extent of oil and gas generation in the Karoo
- To provide information on the hydrocarbon potential within the upper Ecca (Kookfontein, Vischkuil, Laingsburg and Kookfontein formations).
- If there are hydrocarbons present, then what restrictions would it have on oil/gas production?
- To determine the kerogen type and quality of the collected samples.

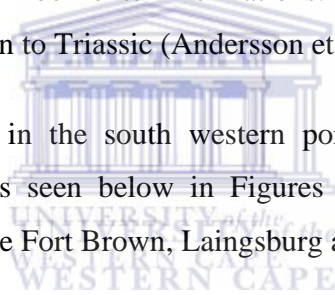
The research will be done by analysing core (Kookfontein formation) and rock outcrop samples (Laingsburg, Fort Brown and Vischkuil formations) to evaluate the geochemical characteristics of the upper Ecca, main Karoo. It will define the physical rock characteristics such as lithology and mineralogy (XRD). Geochemical analyses such as total organic carbon (TOC) and rock eval pyrolysis will be utilised to determine the thermal maturity of the identified source rocks, to quantify the nature of the organic rich rocks to determine the source rock quality, organic richness of the sediments and the kerogen type.

1.3 Study Area

The Karoo covers a vast area of 700 000km² and was formed within a retro-arc foreland basin (Raseroka & McLachlan, 2009). Sedimentary deposits of the Karoo cover two-thirds of the surface area of South Africa (Andersson et al., 2004). The Karoo ranges from the Late Carboniferous to the Middle Jurassic (Catuneanu et al., 2002) and has a maximum thickness of 6-8 km in the southern section (Rubidge, 1995).

The Dwyka is the oldest succession in the Karoo, (Herbert & Compton, 2007) that is followed by the Ecca Group, Beaufort Groups and Stormberg series. The Ecca Group consists of the Prince Albert, Whitehill, Collingham, Vischkuil, Laingsburg, Fort Brown and Waterford from the Laingsburg subbasin. The Tanqua subbasin equivalents consist of Tierberg, Skoorsteenberg and Kookfontein formations. The formations from the Ecca group vary in age from Permian to Triassic (Andersson et al., 2004).

The study areas are located in the south western portion of the Karoo within the Laingsburg subbasin which is seen below in Figures 1.3.1 to 1.3.4. Rock outcrop samples were obtained from the Fort Brown, Laingsburg and Vischkuil formations.



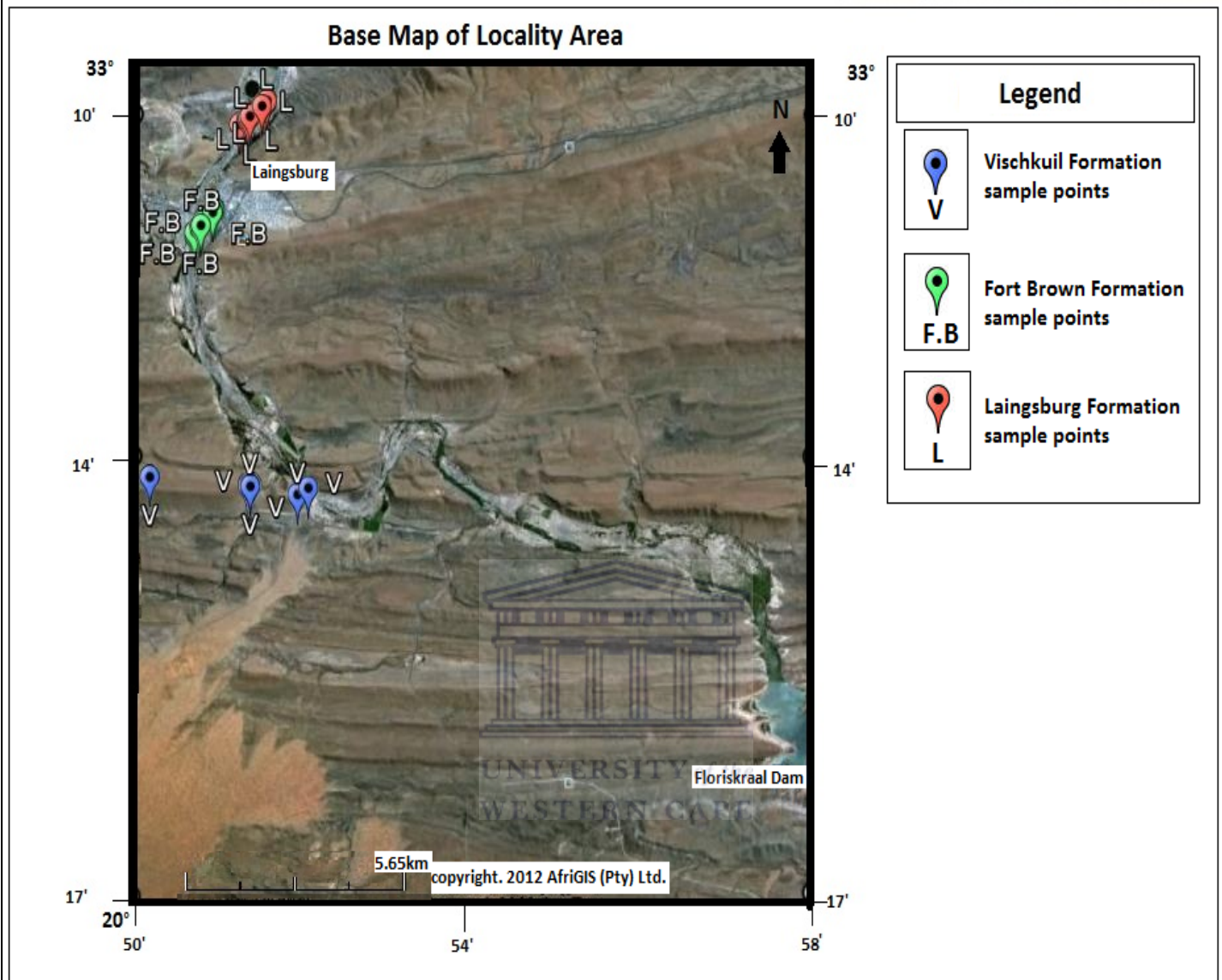


Figure 1.3.1: Sample locality points displayed on base map in the vicinity of the Laingsburg area (Google Earth, 2012).

1.3.1 Sample Collection

- ❖ Vischkuil Formation Sample 1
S 33° 14' 17.8"
E 20° 51' 57.1"
Elev: 682m



04/08/2010: Contact between the Collingham and the Vischkuil Formation. Shale is highly fractured and the outcrop is well exposed. Pencil cleavage is visible along the shale unit.

UNIVERSITY of the
WESTERN CAPE

- ❖ Vischkuil Formation Sample 2
S 33° 14' 17.9"
E 20° 51' 57.1"
Elev: 673m



04/08/2010: Shale exhibits pencil cleavage. Plant root found within the unit

❖ Vischkuil Formation Sample 3

S 33° 14' 17.5"

E 20° 51' 56.8"

Elev: 671m



04/08/2010: Shale exhibiting pencil cleavage, highly fractured and well exposed.

❖ Vischkuil Formation Sample 4

S 33° 14' 17.1"

E 20° 51' 56.8"

Elev: 679m



04/08/2010: Well exposed outcrop which displays pencil cleavage and concretions

❖ Vischkuil Formation Sample 5

S 33° 14' 17.0"

E 20° 51' 58.2"

Elev: 682m



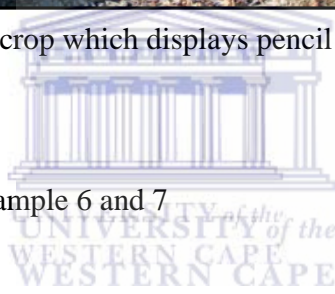
04/08/2010: Well exposed outcrop which displays pencil cleavage and parallel laminations.

❖ Vischkuil Formation Sample 6 and 7

S 33° 14' 17.2"

E 20° 51' 55.4"

Elev: 675m



04/08/2010: Well exposed outcrop of thin bedded coal and shale which is highly fractured and displays pencil cleavage.

- ❖ Vischkuil Formation Sample 8|
S 33° 14' 22.1"
E 20° 52' 30.5"
Elev: 792m



05/08/2010: Well exposed outcrop of thin bedded shale which displays pencil cleavage.

- ❖ Vischkuil Formation Sample 9
S 33° 14' 18.3"
E 20° 52' 39.7"
Elev: 665m



05/08/2010: Well exposed outcrop of thicker bedded shale which displays pencil cleavage

- ❖ Vischkuil Formation Sample 10
S 33° 14' 13.2"
E 20° 50' 47.5"
Elev: 681m



06/08/2010: Outcrop of thin bedded shale which displays pencil cleavage, wavy and parallel laminations

- ❖ Fort Brown Formation Sample 1
S 33° 12' 06.2"
E 20° 51' 21.3"
Elev: 691m



07/08/2010: Well exposed thick shale outcrop, exhibiting pencil cleavage and parallel laminations

- ❖ Fort Brown Formation Sample 2
S 33° 12' 05.5"
E 20° 51' 22.3"
Elev: 692m



07/08/2010: Well exposed thick shale outcrop, exhibiting wavy laminations and parallel laminations

- ❖ Fort Brown Formation Sample 3
S 33° 12' 02.7"
E 20° 51' 23.8"
Elev: 745m

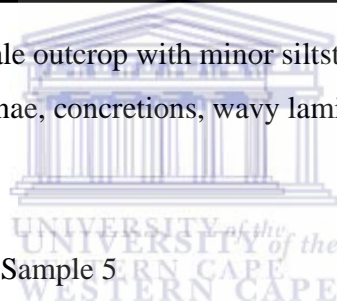


07/08/2010: Thin shale outcrop interbedded with siltstone, exhibiting calcite veins and pencil cleavage.

- ❖ Fort Brown Formation Sample 4
S 33° 12' 02.3"
E 20° 51' 25.7"
Elev: 687m



08/08/2010: Well exposed shale outcrop with minor siltstone counterpart, exhibiting pencil cleavage, slumped laminae, concretions, wavy laminations and parallel laminations



- ❖ Fort Brown Formation Sample 5
S 33° 11' 59.1"
E 20° 51' 30.1"
Elev: 719m



09/08/2010: Shale outcrop with minor siltstone counterpart, exhibiting pencil cleavage and fractures.

- ❖ Fort Brown Formation Sample 6
S 33° 11' 58.9"
E 20° 51' 30.1"
Elev: 723m



09/08/2010: Thin bedded shale outcrop interbedded with siltstone. Pencil cleavage and fractures are visible along the unit.

- ❖ Fort Brown Formation Sample 7
S 33° 11' 59.0"
E 20° 51' 30.7"
Elev: 689m



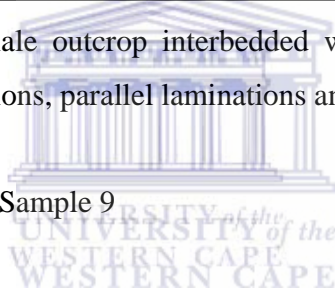
09/08/2010: Well exposed shale outcrop, exhibiting pencil cleavage and fractures.

- ❖ Fort Brown Formation Sample 8
S 33° 11' 57.6"
E 20° 51' 32.2"
Elev: 670m



09/08/2010: Well exposed shale outcrop interbedded with minor siltstone, exhibiting pencil cleavage, wavy laminations, parallel laminations and fractures.

- ❖ Fort Brown Formation Sample 9
S 33° 12' 09.0"
E 20° 51' 17.7"
Elev: 700m

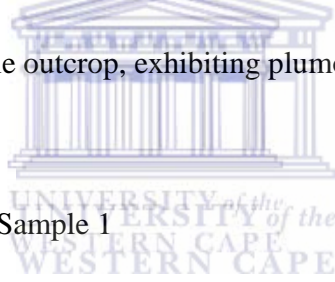


20/08/2010: Well exposed shale outcrop, exhibiting pencil cleavage, parallel laminations, concretions and fractures.

- ❖ Fort Brown Formation Sample 10
S 33° 12' 12.2"
E 20° 51' 17.8"
Elev: 688m



20/08/2010: Well exposed shale outcrop, exhibiting plumose structures, concretions, calcite veins and fractures.



- ❖ Laingsburg Formation Sample 1
S 33° 11' 10.2"
E 20° 51' 56.8"
Elev: 682m



11/08/2010: Well exposed shale outcrop, exhibiting wavy laminations, and fractures.

- ❖ Laingsburg Formation Sample 2
S 33° 11' 11.1"
E 20° 51' 55.5"
Elev: 698m



11/08/2010: Well exposed shale outcrop. Pencil cleavage and fractures are visible on the unit.

- ❖ Laingsburg Formation Sample 3
S 33° 11' 11.6"
E 20° 51' 54.5"
Elev: 701m



11/08/2010: Well exposed shale outcrop. Pencil cleavage and fractures are visible on the unit.

- ❖ Laingsburg Formation Sample 4
S 33° 11' 12.5"
E 20° 51' 52.7"
Elev: 693m



11/08/2010: Well exposed shale outcrop. Pencil cleavage, wavy laminations, parallel laminations, load casts and fractures are visible on the unit.

- ❖ Laingsburg Formation Sample 5
S 33° 11' 12.9"
E 20° 51' 52.4"
Elev: 687m



12/08/2010: Well exposed shale outcrop interbedded with siltstone. Pencil cleavage, wavy laminations, parallel laminations and fractures are visible on the unit.

- ❖ Laingsburg Formation Sample 6
S 33° 11' 13.8"
E 20° 51' 50.4"
Elev: 694m



12/08/2010: Well exposed shale outcrop interbedded with siltstone. Pencil cleavage, concretions, parallel laminations, wavy laminations and fractures are visible on the unit.

- ❖ Laingsburg Formation Sample 7
S 33° 11' 14.5"
E 20° 51' 49.2"
Elev: 688m

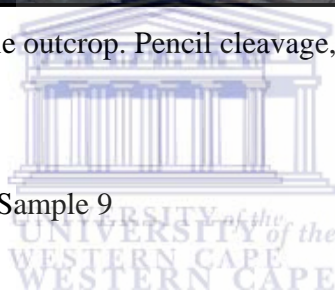


12/08/2010: Well exposed shale outcrop interbedded with sandstone. Pencil cleavage, parallel laminations, wavy laminations and slumped laminae are visible on the unit.

- ❖ Laingsburg Formation Sample 8
S 33° 11' 05.1"
E 20° 52' 05.3"
Elev: 687m



14/08/2010: Well exposed shale outcrop. Pencil cleavage, parallel lamination and fractures are visible.



- ❖ Laingsburg Formation Sample 9
S 33° 11' 02.6"
E 20° 52' 09.0"
Elev: 692m

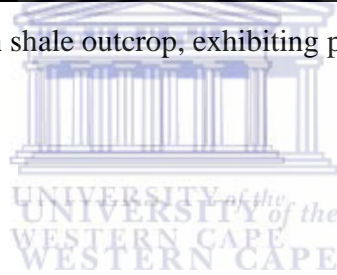


14/08/2010: Well exposed shale outcrop, exhibiting pencil cleavage and fractures.

- ❖ Laingsburg Formation Sample 10
S 33° 11' 03.3"
E 20° 52' 08.2"
Elev: 735m



14/08/2010: Well exposed thin shale outcrop, exhibiting pencil cleavage and fractures.



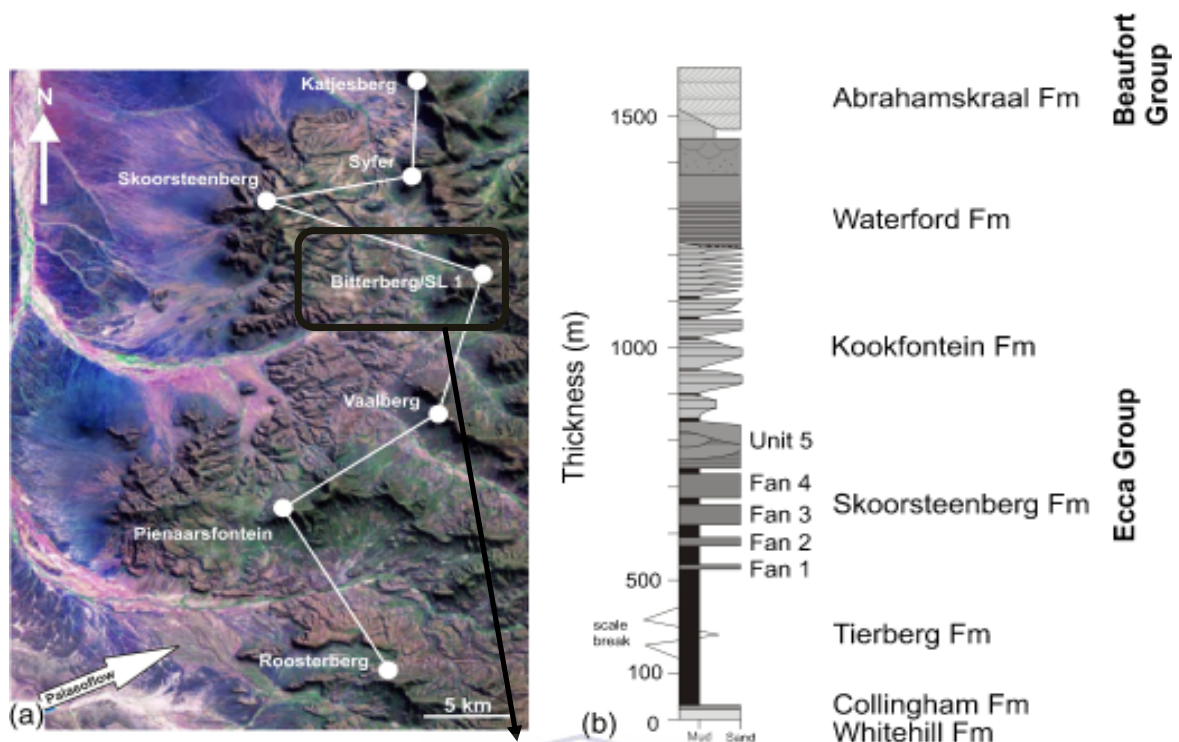


Figure 1.3.2: Location map of the study area within the Bitterberg area of the Tanqua basin in which the Kookfontein samples were obtained. (Google Earth, 2011).

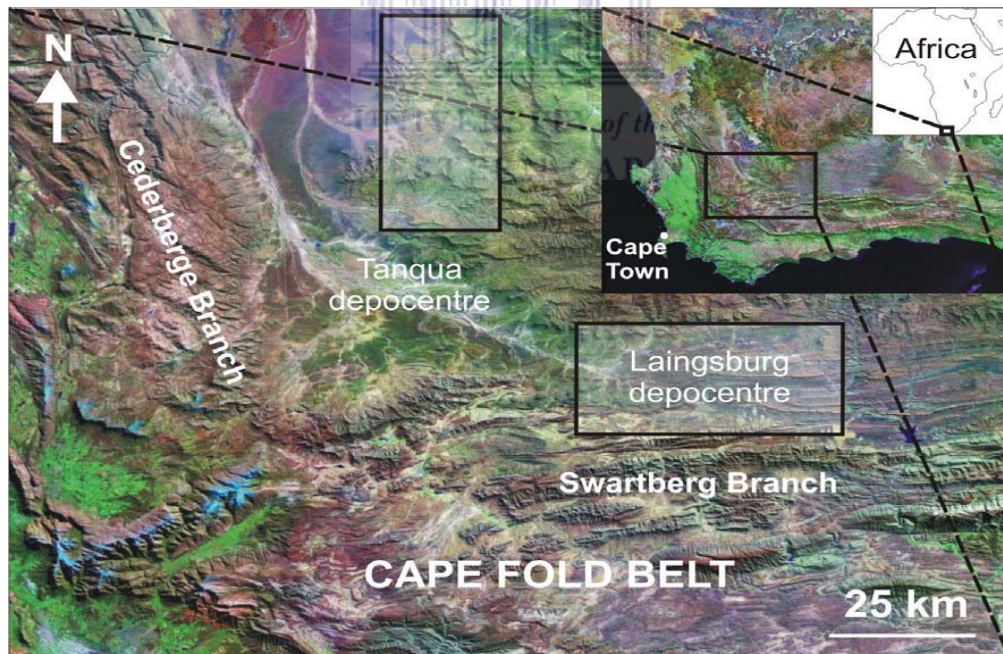


Figure 1.3.3: Locality map of the two subbasins in which this study is based on (Google Earth, 2011).

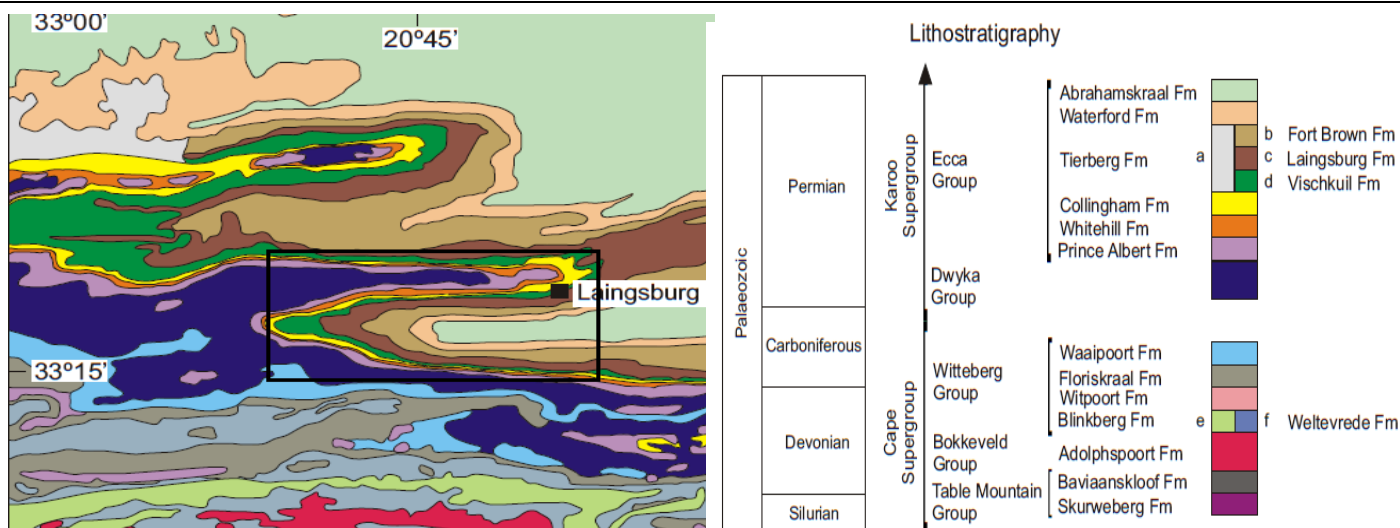


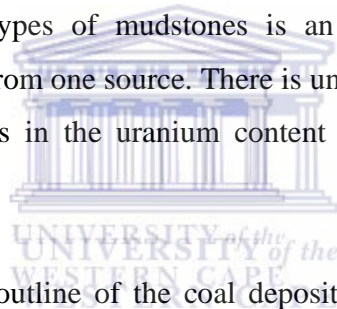
Figure 1.3.4: Location map of the study area (Vischkuil, Laingsburg and Fort Brown Formations) within the Laingsburg basin. The map originates from Besaans (1976).

1.4 Previous Work

This section looks at the different geological, structural, tectonic and stratigraphic features within the Karoo basin, based upon previous studies undertaken, to assess the hydrocarbon potential within this area of study, as well as source rock studies undertaken in other areas.

Andersson et al, (2004), geochemical analyses was undertaken on mudstones from borehole and outcrop samples in the Skoorsteenbergr formation, Karoo, to determine the provenance evolution (i.e. reconstructing the history from the sediment supply) and similarities in the sedimentary setting. The geochemical trend produced across the basin is interpreted as an unremitting evolution of the source area. The changes in chemicals such as TiO_2/Al_2O_3 , $La/(La+Lu)$ and $Th/(Th+Y)$ is an indication of a gaining mafic content that influences the depositional environment. The rise in the Zr and Hf content is suggests a more felsic content. The opposing felsic and mafic contents could be postulated as a result of the source area trending towards a more igneous suite, but for this to happen the rocks have to have been predominantly mafic in nature. The set of geochemical data obtained from the Skoorsteenbergr Formation suggests that chemostratigraphy is not the ideal manner in which to obtain a correlation, owing to the high statistical noise factor that interferes with the geochemical signal.

Andersson & Worden, (2004), used mudstones present within the Tanqua basin to determine the vertical and stratigraphic alterations within the mudstones and develop a comparison study, between and within interfan and intrafan turbidite fans. Wireline logs (used to determine the sedimentology), SGR logs (used to determine the radioactivity); XRD (used to determine the mineralogy), TOC (to determine the total carbon content) and ICP-AES (used to determine the major and minor trace elements) were some of the techniques used within the study. A statistics study was done to determine the relationship between the interfan and intrafan mudstones. Interfan mudstones are interpreted to have been formed in a period of transgression and high sea level, whereas, intrafan mudstones developed in a regressive, low sea level setting. Geochemical analyses done within this study indicates differences in the interfan and intrafan source lithologies, which might be as a result of sea level changes. The geochemical trend that develops between the two types of mudstones is an indication of denudation and weathering of the lithologies from one source. There is uniformity in the flow direction of the mudstones but differences in the uranium content which is as a result of clastic dilution.



Cairncross, (2001), gives an outline of the coal deposits in Southern Africa. The coal seams developed amid the early to late Permian period. The coals from the period are linked to non-marine terrestrial clastic sedimentary cycles. During the Artinskian-Kungurian period, coals were predominantly contained within sandstone bodies, whilst in younger coals it forms within mudstones. The tectonic setting, maturity and depositional environments of the coal within these areas are discussed. Four factors are responsible for coal formation which is: time, climate, vegetation and geology.

Catuneanu et al, (2002) looks at the foredeep submarine fans and forebulge delta that extends across the lower Ecca (Ripon formation in the south and the Vryheid formation in the north). A sequence stratigraphic correlative study was done in this area to determine the tectonic setting, accommodation, subsidence, sea level changes and forces responsible for the foredeep and forebulge.

Catuneanu et al, (2005), deals with the development of the Karoo basin in south-central Africa. It details the inception of Pangaea to the breakup of the supercontinent into the Gondwana basin. The tectonic setting, sea level changes, climatic factors, sedimentation rates are determined by using sedimentary and stratigraphic data collected from the eastern and western part of the Karoo basin and covers the entire Ecca.

Catuneanu & Bowker, (2001), dealt with the sequence stratigraphy within Koonap and Middleton formations in the Karoo. The cycles and stratigraphy were used to correlate and determine the tectonics, sea level changes, climatic controls and accommodation rates that influenced the two aforementioned formations within this study.

Herbert & Compton, (2007), looked at the Dwyka and Ecca groups in the Karoo basin. Prince Albert shale and Dwyka diamictite were used to determine the climatic and paleoenvironmental variability's that led to the last deglaciation of the Gondwana supercontinent. Different geochemical analyses were undertaken using the chert and calcite concretions gathered from the Ecca and Dwyka respectively. The concretions were used to determine the depositional environment. The overall interpreted environment was that of a fresh water environment.

Johnson et al, (2001), has compiled a comparison report based on the lithostratigraphy, biostratigraphy and chronostratigraphy of the sedimentary successions within the Karoo, defining the main basins of the Karoo, as well as its subsidiary basins, aerial extent and environments in which the strata were deposited in. From the results of this study it can be concluded that: the identical mechanisms and string of actions within the main Karoo are shown in the singular basin fills and that the main Karoo is a retro-arc foreland basin, whereas other basins are rift or intracratonic sag basins.

Werff & Johnson, (2003), used 3D modelling with isopach maps to look at the turbidite fan system within the Tanqua basin, South Africa. The data was used to determine the depositional rates, depositional setting, stratigraphy and sedimentology. There are four

basin floor fans and one slope fan complex within the Tanqua. Of the above mentioned fans, fan 3 was looked at in detail since it had the best turbidite exposure.

Van Lente, (2004), looked at the structural evolutionary and depositional relationship between the Tanqua and Laingsburg depocenters within the Karoo basin. Geochemical and chemostratigraphic analyses were done on core and outcrop data attained from the two depocenters. A stratigraphic correlation was achievable between the Skoorsteenberg, Kookfontein and Waterford formations of the Tanqua basin, so too of the Laingsburg and Fort Brown formations within the Laingsburg basin. Overall, it was found that the Tanqua and Laingsburg depocenters exhibited a uniformed provenance.

Wild et al, (2009), dealt with the Eccca group of rocks within the Tanqua depocenter. The Eccca group of rocks was used to determine the stratigraphic changes from the upper shelf to the shelf edge setting within the Karoo. The Kookfontein was one of the formations that were looked at to observe the depositional changes. The data from this study suggests that the younger slope system of the Kookfontein formation was varied from the older system that loaded the underlying sand-rich basin floor fans.

Geological Framework

1.5 Geological background of the main Karoo

Cole, 1992, describes the Karoo basin as a, Palaeozoic sedimentary basin formed above the Archaean Kaapvaal Province, Kheis Province, the Kibaran Namaqua-Natal belt and the Pan-African Saldania-Gariep Province (Andersson, et al., 2004). The Karoo basin is defined as a foreland basin, developed in front of a thrust and fold belt, known as the Cape Fold belt (CFB) (Cole, 1992). The Cape Fold belt changed in retort to continuous tectonic shortening that started in the late Palaeozoic by the subduction of the Palaeo-Pacific plate below the southern rim of Gondwana (Andersson et al., 2004).

Not much is acknowledged of the level of metamorphism within the Karoo Supergroup; nonetheless rocks of the Cape Fold Belt have been altered, for the most part, to the lower greenschist grade metamorphism (Herbert & Compton, 2007). Compression in the western and southern division of the Cape Fold belt resulted in the formation of an important anticlinorium, in which the branches unite (Andersson et al., 2004). This is displayed within Figure 1.5.1.

Herbert & Compton, (2007: 264) describe the anticlinorium as a, “basin-floor far above the ground that resulted in the formation of the Tanqua and Laingsburg subbasins in the south-west part of the Karoo Basin”. The infill of the Karoo Basin started with the Dwyka Group, in which sedimentation was dominated from the Late Carboniferous to the Early Permian (Herbert & Compton, 2007). The Dwyka Group is divided into two facies (Visser, 1986): a valley highland facies (containing a heterolithic succession of changeable thickness) and a shelf facies (containing enormous stratified diamictites and clasts with several consistent thicknesses).

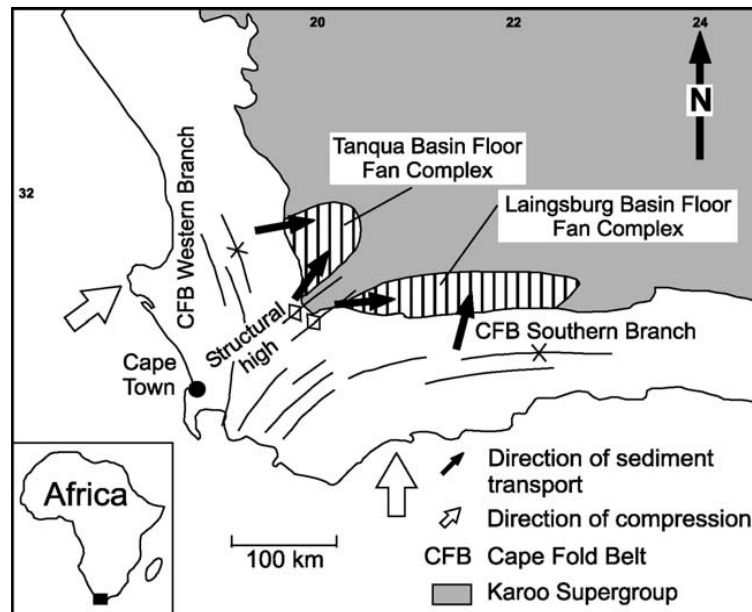


Figure 1.5.1: Locality of the Laingsburg and Tanqua basin floor fan complex, situated in the southwestern proximity of Karoo basin, relative to the Cape Fold Belt (Wickens, 1992).

After the Dwyka deglaciation event and the related marine transgression, mudstones of the Prince Albert and Whitehill formations of the Ecca Group were deposited in a huge shallow sea that was originally marine but later became brackish (Andersson et al., 2004:481). The Whitehill formation is the main contributor of organic-rich shale within the Ecca group, with total organic carbon contents in the vicinity reaching 15 wt% (Faure & Cole, 1999).

The Ecca Group comprises the Prince Albert, Whitehill and Collingham, Tierberg, Vischkuil, Laingsburg, Fort Brown, Skoorsteenberg, Kookfontein and Waterford formations, and it is early Permian in age (Smith, 1990). The Ecca units are displayed in Figure 1.5.2 modified from Johnson, 1996a. The Prince Albert, Whitehill and Collingham formations represent the post-glacial environment with thin-bedded dark mudstones and sandstones. Black clays and muds represent the Prince Albert and Whitehill formations which accumulated on the submerged glaciated platform (Smith, 1990). The Whitehill Formation also contains thin bands of yellow illite-rich claystone, which is interpreted as air-fall tuff (Martini, 1974). The Collingham Formation includes a distinctive white chert band, known as the Matijesfontein Chert, and thin white ash bands dated by Turner

(1975) as Early Permian (approximately 270 Ma). The Vischkuil, Laingsburg and Fort Brown formations represent the basin-floor to shelf-edge successions of the Laingsburg depocentre. The Vischkuil Formation is a series of mass transport complexes interpreted as the initiation of turbidite deposition of the Laingsburg Formation (Flint et al., 2004). The Laingsburg Formation is a sequence of five sand-rich turbidite deposits (Fan A and Units B-F) intercalated with dark mudstones. The turbidite deposits have been described in detail by Grecula (2000) and Sixsmith (2000). The Fort Brown Formation consists of fine grained sandstone and mudstone representative of slope deposits, the result of the overall prograding system (Smith, 1990). The Tierberg Formation is thick black shale that represents a period of regional sediment starvation.

In ascending order, the formations of the Ecca group are (Veevers et al., 1994):

- Prince Albert Formation: comprised of dark grey shale, with reddish brown weathering siltstone
- Whitehill Formation: made up of dark grey shale, light grey weathering
- Collingham Formation: comprises interlaminated tuffaceous siltstones and mudstones; chert and sandstones interbedded shale and yellow weathering tuff or mudstones
- Vischkuil Formation: comprises arenaceous shale, siltstone and thin sandstone beds
- Laingsburg Formation: consists of sandstone, greywacke and siltstone
- Fort Brown Formation: is comprised of shale with thin siltstone and sandstone beds
- Waterford Formation: consists of sandstone, siltstone, mudstone, thin cherty beds and shale

The Tanqua equivalents of the Laingsburg subbasin are as follows:

- Tierberg Formation (Vischkuil): composed mainly of mudstones and shale
- Skoorsteenberg Formation (Laingsburg): sandstone, shale and sand-rich turbidites interbedded with mudstones
- Kookfontein Formation (Fort Brown): shale, siltstone, pro-delta and delta-front mudstones and sandstones

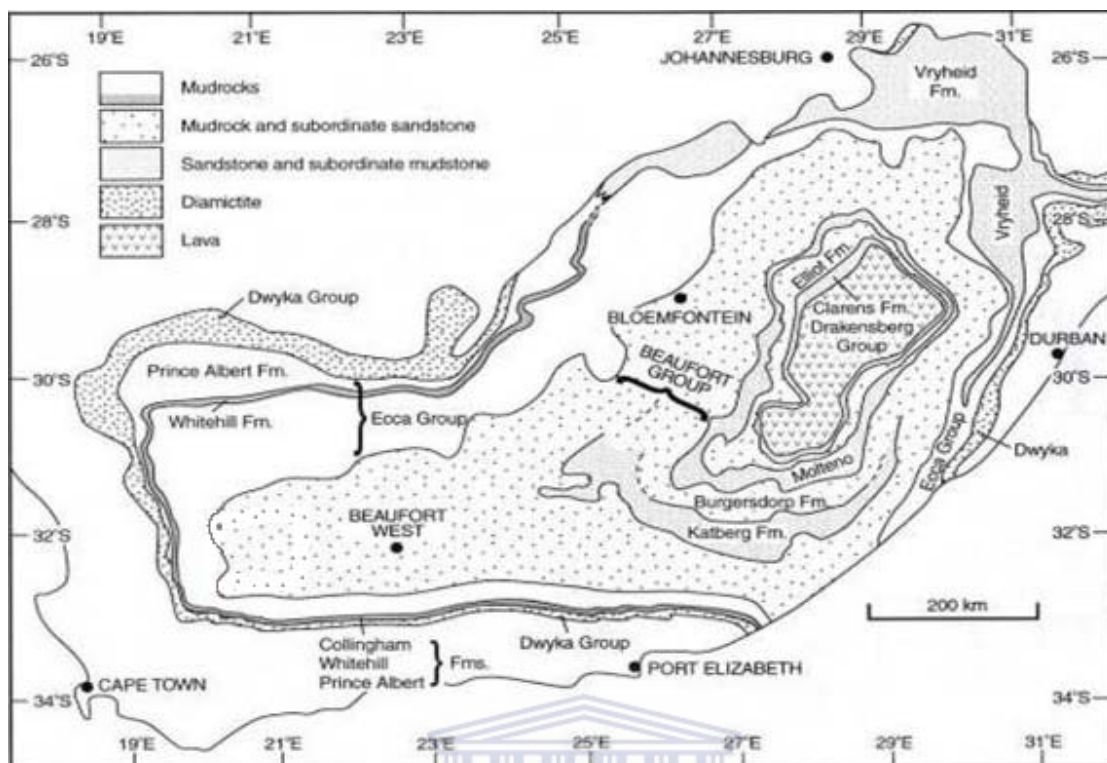
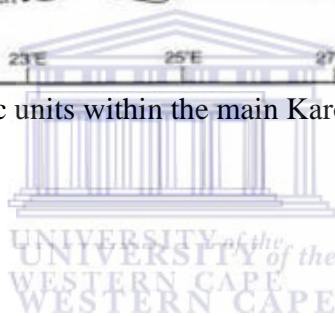


Figure 1.5.2: Lithostratigraphic units within the main Karoo Basin (adapted from Johnson et al., 1996a)



1.6 Tectonic Setting

The Karoo is a retro-arc foreland basin (Catuneanu & Bowker, 2001), situated behind a magmatic arc, and developed in front of the Cape Fold Belt (thrust belt), which was created by the northern subduction of the oceanic lithosphere situated in the south of the arc (Johnson et al., 1996b). This event occurred during the Late-Palaeozoic to early Mesozoic, in which the palaeo-Pacific plate was subducted underneath the Gondwana plate (Catuneanu & Bowker, 2001).

The Cape Fold Belt was a component of the Pan Gondwana Belt developed through impact and terrain accretion along the southern margin of Gondwana (Catuneanu & Bowker, 2001). The related foreland basin, disjointed due to the Gondwana break-up and, (Catuneanu & Bowker, 2001) is contained at present day within the South America (Parana Basin), South Africa (Karoo Basin), Antarctica (Beacon Basin) and Australian (Bowen Basin) continents. The Cape mountain building event was produced beside the

Late Proterozoic structural trends, resulting in the weak and collapsed areas of the continental lithosphere (Catuneanu & Bowker, 2001).

The Karoo basin formed as a result of supralithospheric loading, produced in response to crustal shortening and thickening in the Cape Fold Belt (Catuneanu et al., 2002). The Karoo foreland is classified into (Catuneanu & Bowker, 2001) three flexural provinces, (Catuneanu et al., 2002) although eight tectonic paroxysms have been recognised in the Cape Fold Belt. The three flexural provinces are: foredeep, forebulge and back-bulge (displayed in Figure 1.6.2 adapted from Catuneanu et al., 2002). Before the break-up of Gondwana this foreland structure was as long as 6000km along the strike and more than 1000km along the dip (Catuneanu & Bowker, 2001). Majority of the Ecca and Beaufort Group in the southern foredeep of the basin originated from the arc (Johnson et al., 1996a). The Cape Fold Belt contributed to the basin fill throughout the Triassic and was the main foundation for the Molteno and Elliot formations (Johnson et al., 1996a). The southern Karoo appears to display intracratonic thermal sag basins, although there is evidence in the southwestern part of the Kalahari basin for marine sway in the untimely part of its advancement (Johnson et al., 1996a).

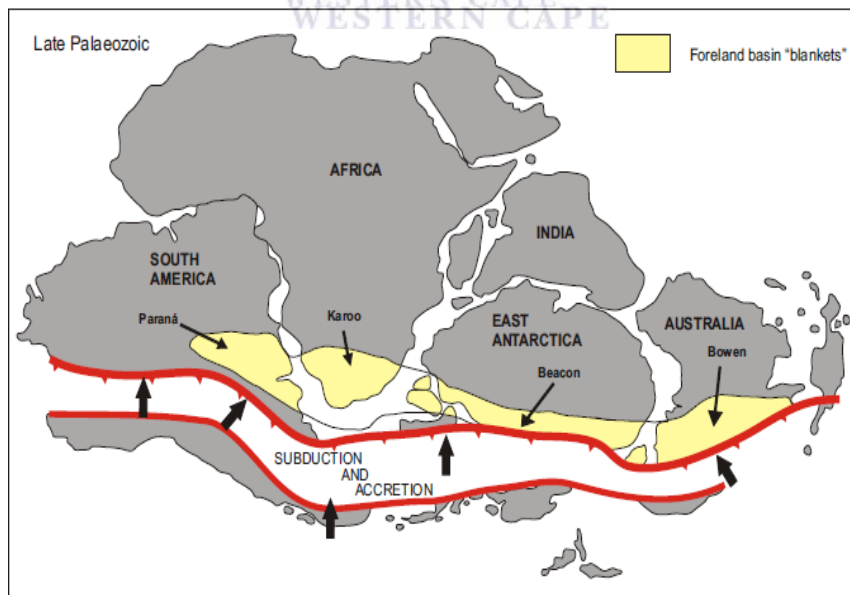


Figure 1.6.1: The Karoo basin shown in perspective to the Pan Gondwanian foreland arrangement (modified from Catuneanu & Bowker, 2001).

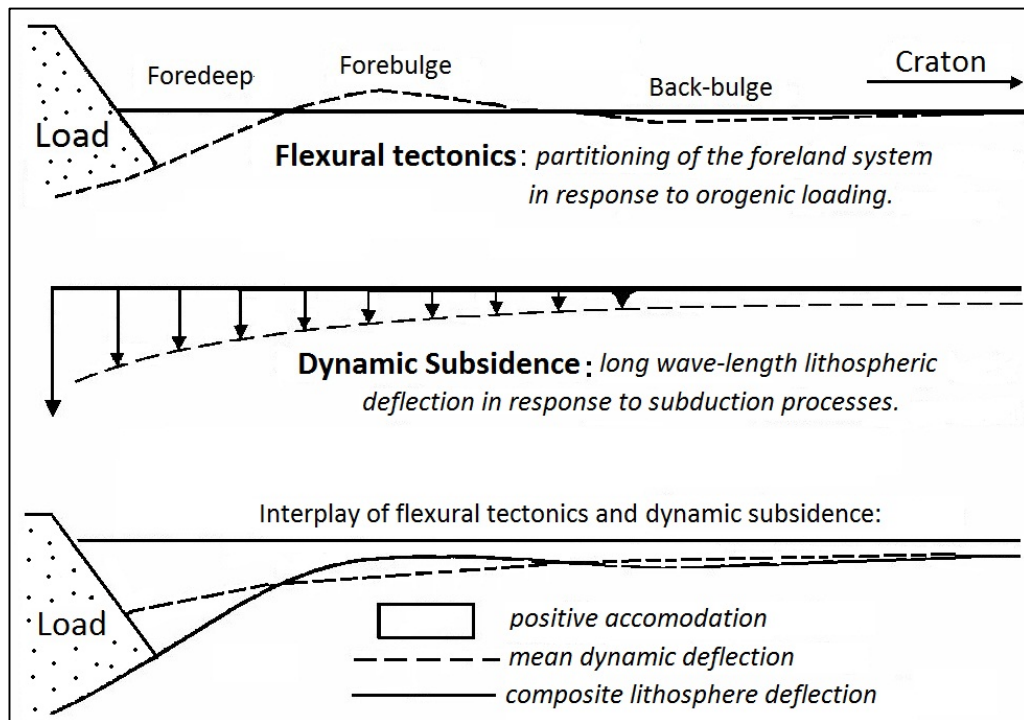


Figure 1.6.2: The three flexural provinces present within the Karoo, which are: foredeep, forebulge and back-bulge (modified from Catuneanu et al., 2002).

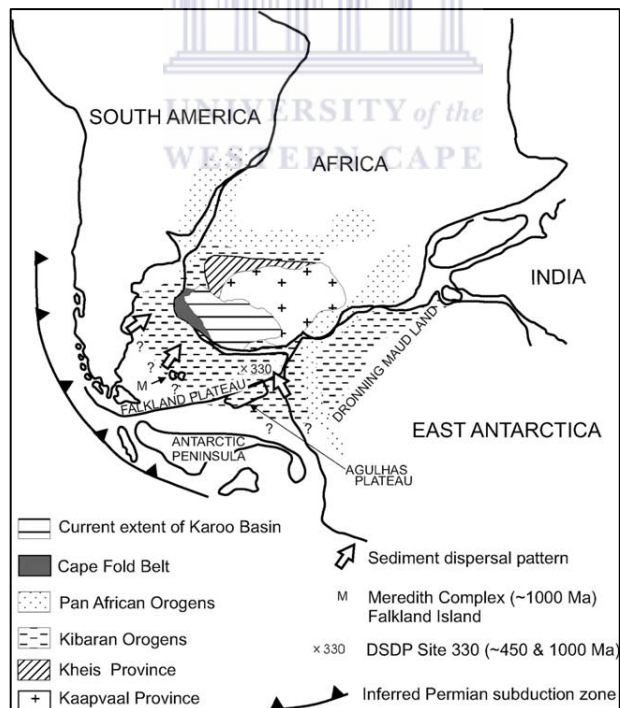


Figure 1.6.3: Locality of the Karoo Basin and crustal terranes of South Africa, Antarctica and the Falkland Plateau. The diagram depicts the terranes before the break-up of Gondwana (adapted by Andersson et al., 2004).

1.7 Lithostratigraphy

The Karoo Basin produced the thickest and largest amount of stratigraphically absolute sequence of numerous depositories from Permo-Carboniferous to Jurassic age in southwestern Gondwana (Catuneanu & Bowker, 2001). The Karoo reaches a thickness that exceeds 6km, adjacent to the Cape Fold Belt (Catuneanu & Bowker, 2001). The sedimentary succession within the Karoo displays shifting environments from glacial to deep marine, deltaic, fluvial and aeolian (Catuneanu & Bowker, 2001). The orogenesis of the Cape Fold Belt is thought to have been linked to the basin fill of the Karoo (Catuneanu & Bowker, 2001).

The Karoo Supergroup (Catuneanu & Bowker, 2001) is subdivided into five focal groups, which are: the Dwyka, Ecca, Beaufort, Stormberg and Drakensberg. The lithostratigraphic sub divisions can be seen in Figure 1.7.1. The deeper marine facies of the Dwyka and early Ecca groups, accumulated for the duration of the underfilled stage of the foreland structure (Catuneanu & Bowker, 2001). The shallow marine facies of the late Ecca Group is related to the filled stage of the basin, which was proceeded by an overfilled stage overpowered (Catuneanu & Bowker, 2001) by fluvial sedimentation beginning with the Beaufort Group.

The Dwyka Group and its equivalents include glacially influenced deposits that accumulated between the 300–290 Ma interval (Catuneanu et al., 2002). The glaciation during the Late Carboniferous–earliest Permian can be linked to the main Karoo Basin in South Africa, Gabon, western Sudan and Somalia (Catuneanu et al., 2002). The accumulation of the Dwyka glacially- predisposed deposits occurred in variable tectonic periods along south-central Africa, encompassing the retro arc foreland system of the main Karoo Basin, to extensional basins (Catuneanu et al., 2002).

Rubidge (1858) claimed the word ‘‘Ecca’’ for argillaceous sedimentary strata bared in the Ecca Pass, near Grahamstown in the Eastern Cape Province, South Africa (Catuneanu et al., 2002). The rocks of the Ecca Group (Catuneanu et al., 2002) are comprised of a

clastic sequence of mudstone, siltstone, sandstone; minor conglomerate and coal (in some parts) outcrop at length in the main Karoo Basin in South Africa (Catuneanu et al., 2002). In the Karoo Basin of South Africa, the Ecca Group formed during the Late Carboniferous Dwyka Group until the Late Permian-Middle Triassic Beaufort Group (Catuneanu et al., 2002). The Ecca Group is comprised of a maximum thickness of 3000 m in the southern division of the main Karoo Basin (Catuneanu et al., 2002). In different places within southern Africa it is significantly thinner (Catuneanu et al., 2002).

The Laingsburg depocentre, elongated from Matjiesfontein in the west to east of Klaarstroom, borders the Swartberg Mountains along the southern margin of the Karoo Basin. The Collingham, Vischkuil, Laingsburg and Fort Brown Formations represent the sequence under study in this depocentre. Sediments in the Laingsburg depocentre were deposited in a tectonically active elongated setting where confinement and basin floor topography have played a chief function in the distribution of the fan systems (Wickens and Bouma, 2000).

The open-marine shales of the Prince Albert Formation are at the bottom of the Ecca Group sharply and conformably overlie the Dwyka diamictites, recording a rapid glacial retreat (Visser, 1991). This dark greenish-grey shale, with some graded silty layers, is of Artinskian to Middle Kungurian age (Visser, 1992) and reaches a thickness of 165 m in the Laingsburg region, but thins out northwards and eastwards (Visser, 1991). Four phases of deposition have been recorded, with the lower branch of the Prince Albert Formation dominated by mudstone containing dropstones and other ice-rafted detritus, the middle and upper part dominated by mudstone and isolated mud-rich turbidite deposits, and the uppermost unit dominated by shale, containing phosphatic nodules (Visser and Loock, 1978; Visser, 1991). Marine fossils and plant remnants have been recognised at the foot of the formation (Johnson et al., 1997). The upper contact with the Whitehill Formation commonly overlies a thin upward-coarsening succession grading from carbonaceous mudrock into silty shale (Johnson et al., 1997).

The Whitehill Formation (early to late Permian) covers much of southern Gondwana and comprises of carbonaceous shale, weathering white, with chert bands and lenses, deposited in a deep water, pelagic, non-marine and reducing environment (Visser, 1992; Catuneanu et al., 1998). The lower contact of the formation is always sharp and well defined. Ferruginous carbonate concretions of a dolomitic nature are dispersed all the way through the formation, whereas the biostratigraphy suggests synchronous deposition in the Karoo Basin (Johnson et al., 1997). The succeeding deposits of the overlying formations were deposited in deeper, fully marine environments.

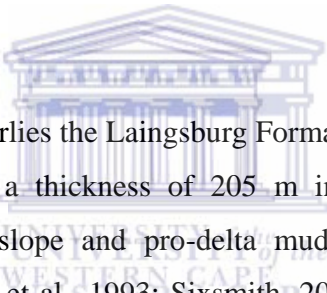
The Collingham Formation (thickness of 30 – 70 m) overlies the Whitehill Formation with a sharp conformable contact and consists of alternating beds of dark grey mudstone and cherty mudstone, yellowish tuff beds, siltstone and very fine- to fine-grained sandstone (Viljoen, 1992b). It is interpreted as a distal submarine fan facies of late Permian age, related to pelagic sedimentation and windward interbedded volcanic ash (Martini, 1974; Cole, 1992; Viljoen, 1995). The volcanic ash indicates a dramatic change in the tectonomagmatic activity along the Panthalassan continental margin of Gondwana, which were most probably the consequent of volcanoes situated in northern Patagonia, in which Permian silicic-andesitic volcanic and plutonic rocks crop out (Wickens and Bouma, 2000). The tuff layers, deposited from suspension, range in thickness from 1 – 20 cm (commonly < 5 cm thick) and are sharp-based and infrequently reworked in their upper portions (Viljoen, 1992b). The Matjiesfontein Chert Bed, a regionally extensive marker bed, developed in the lower part of the formation. Tractional structures and occasional sole structures exhibited by the fine siltstone and sandstone beds, and their association with typical deep-water shale, confirm a turbiditic origin (Viljoen, 1992b; Wickens, 1994).

The contact of the Vischkuil Formation with the Collingham Formation is conformable and clearly defined. The Vischkuil Formation attains a thickness of 200 to 400 m and contains predominantly mudstone, siltstone and fine-grained sandstone (Viljoen and Wickens, 1992; Wickens, 1994). The lower part of the Vischkuil Formation is dominated by mudstone, with occasional thin siltstone beds and several slump horizons, whereas the

upper 40 m consists of meter-scale fining-upward beds separated by mudstone (Viljoen and Wickens, 1992; Wickens, 1994). The thickest beds of this facies (max. 15 m) occur in the lower half of the formation where they contain calcareous and phosphatic lenses and ferruginous layers (Johnson et al., 1997). Tuff layers (1 to 20 cm in thickness) occur sporadically throughout the formation and are laterally persistent, lack any traction structures and sometimes show normal grading with slight mottling near the base (Johnson et al., 1997). Theron (1967) interpreted the Vischkuil Formation as the distal end of a turbidite system, which becomes gradually more proximal in the upper parts. The slump zones in the upper Vischkuil Formation were interpreted by Wickens (1994) as an indication of slope conditions, and the entire formation itself as “background” hemipelagic deposits, interrupted by mud-rich and very fine-grained, low-density turbidites in the distal deep part of the basin.

The boundary between the Vischkuil and Laingsburg Formation is gradational and defined as a horizon above which sandstone predominates over mudrock (Viljoen, 1992b). The Laingsburg Formation, consisting predominantly of very fine- to medium-grained sandstone and comprises a thickness of 750 m, is made up of six turbidite fan systems, informally called Fans A to F, each separated by a significant thickness (10 – 90 m) of hemipelagic and turbiditic mudstone (Sixsmith, 2000). Fan A is interpreted as being deposited in a basin floor setting, constituting ~40% of the Laingsburg Formation with a thickness of 350 m southeast of Laingsburg. Fan B, deposited in a base of slope setting, attains a thickness of 80 – 150 m, and Fans C to F (slope depositional setting) have thicknesses ranging between 10 – 100 m (Grecula, 2000; Sixsmith, 2000). Sixsmith (2000) developed a high-resolution stratigraphic framework for Fan A in the Laingsburg area. He subdivided Fan A into seven time-stratigraphic depositional units (Units 1 to 7), bounded by regionally correlatable key surfaces, interpreted as flooding surfaces and sequence boundaries. Fan A is predominantly composed of alternating sheet-like, medium- to thick-bedded sandstone, rhythmic thin-bedded sandstone/siltstone units and shale units of varying thickness (Wickens, 1994). Fans B to F display a more amalgamated interior nature and stacked channel intervals (Grecula et al., 2003). Fan B is separated from Fan A by a shale unit, which is persistent over the entire outcrop region.

In places along the base of the Fan B succession, are stacked, thick-bedded, mostly amalgamated, sandstone beds that are overlain by progressively thinner beds towards the top; elsewhere thin overbank deposits occur at the base (Grecula, 2000). Fan C is separated from Fan B by a shale unit that attains a thickness of approximately, 150 m. The fan itself is predominantly comprised of thick-bedded, massive and mostly amalgamated sandstone beds at the base, succeeded by thinner-bedded turbidites towards the top (Wickens, 1994; Grecula, 2000). Fan D is comprised of two closely spaced sandstone-rich units and is separated from Fan C by 180 m of basin shale (Wickens, 1994; Grecula, 2000). A thick unit of mudstone separates Fan E from Fan D and is dominated by muddy sandstone and thin beds of massive sandstone (Grecula, 2000). Fan F is separated from Fan E by a thick unit of mudstone as well, and consists predominantly of muddy sandstone and thin beds of massive and parallel laminated sandstone (Grecula, 2000).



The Fort Brown Formation overlies the Laingsburg Formation with a gradational contact at the top of Fan F, attains a thickness of 205 m in the Laingsburg area, and is predominantly comprised of slope and pro-delta mudstones with thick intervals of siltstone and sandstone (Smith et al., 1993; Sixsmith, 2000). The lower part of the Fort Brown Formation is dominantly mud-rich, whereas the upper part becomes silt-dominated and exhibits traction structures, with high-frequency thickening upward cycles of 2 – 10 m thick (Wickens, 1994; Sixsmith, 2000). Soft-sediment deformation, including large-scale slumping, indicates the presence of unstable slope conditions from time to time. Slow mud deposition characterised the initial stage of sedimentation of the Fort Brown Formation (Kingsley, 1981). Subsequent fast regression occurred during which time a typical coarsening-upward sequence was formed. This is characteristic of progradation of a delta front into a relatively shallow water body with a depth above wave base. Cole (1992:91) interpreted the Fort Brown Formation to have been deposited in an “overall regressive shallow marine environment during the late Permian”.

The Tanqua depocentre is positioned in the southwestern portion of the Karoo foreland basin and is bounded by the western and southern branches of the CFB (Wickens, 1994).

The Skoorsteenberg Formation represents gravity flow deposits; whereas the Tierberg Formation, which is overlain by the Skoorsteenberg Formation, consists of grey shale and subordinate thin siltstone layers and represents deposition mainly from suspension (Wickens, 1994). Water depths are not greater than 500 m and the dominant sedimentary process was the deposition of mud from suspension (Visser and Loock, 1978). The Skoorsteenberg, Kookfontein and Waterford Formations represent the sequence under study in the Tanqua depocentre.

The Tierberg formation is predominantly argillaceous succession, which reaches a maximum thickness of approximately 700m along the southern margin of the basin, thinning to 35cm towards the northeast (Johnson et al., 1996a). It has a sharp contact with the Collingham or Whitehill formation and grades upwards into the Waterford formation. The Tierberg is composed of well laminated dark shale. Yellowish tuff beds, up to 10cm thick, arise in the lower division of the succession. Calcareous concretions are common at the topmost part of the formation (Johnson et al., 1996a). The planar lamination of the shale suggests suspension settling in a low energy environment.

The Skoorsteenberg Formation comprises five deep-water turbidite fan systems, roughly exposed over 650 km². The formation thins out in a northerly and easterly direction. A progradational trend can be seen in the approximately 450 m thick succession, from distal basin-floor (Fan 1) through basin-floor sub-environments (Fans 2, 3 and 4) to a slope setting for Fan 5 (Goldhammer et al., 2000; Wach et al., 2000; Wickens and Bouma, 2000; Johnson et al., 2001). Deposition was unrestricted in the broad, open style N-S trending Tanqua depocentre and the sandstones are very fine- to fine-grained. Each fan system has a high sandstone-to-shale ratio, whereas the interfan units comprise finely laminated shale and silty shales of hemipelagic and tubiditic origin (Wickens and Bouma, 2000). The thickness of the sand-rich turbidite systems vary from 20 – 60 m, and are separated by basin shales, with varying thickness of 20 – 75 m (Wickens and Bouma, 2000). The sandstones are virtually without any porosity or permeability, resulting from high-grade diagenetic to low-grade metamorphic changes during burial to depths of about 7 km (Rowell and De Swardt, 1976; Wickens and Bouma, 2000). Five major lithofacies

have been recognised, namely massively bedded sandstone, horizontally and ripple cross-laminated sandstone, parallel-laminated siltstone, parallel laminated shale and a micaceous, silty plant-fragment facies (Wickens and Bouma, 2000). Tuff, limestone beds, calcareous concretions, and cherty layers are present as subordinate facies.

The Kookfontein Formation occurs above the turbidite fan complex and is an upwards coarsening succession, reflecting progressive shallowing conditions associated with deltaic progradation (Wickens, 1994). The upper part of the formation shows very subtle, upward thickening cycles (2 – 10 m thick) that generally commence with dark grey shale and siltstone derived from suspension, followed upwards by a rhythmic alternation of shale, siltstone and sandstone (Wickens, 1994). Traction and wave-produced ripple-lamination become more pronounced upwards in the succession. The thin lower beds mostly resulted from suspension settling, whereas the thicker beds (up to 20 cm) towards the top resulted from sediment-laden traction currents (Wickens, 1994). Thick-bedded mouth bar sandstones, in places modified by wave and tide produced structures, arise in countless areas and are often related to soft sediment deformational features (Flint et al., 2004).

The Waterford Formation consists of delta front, lower delta plain and upper delta plain deposits, dominated by fine- to medium-grained sandstone and a thickness of ca. 200 m (Wickens, 1994). The proximal delta front succession is arenaceous and contrasts sharply with the distal delta front and pro-delta deposits. Characteristic to the delta front succession is the vertically stacked, upward coarsening cycles (10 – 20 m in thickness) and a variety of syn- and post depositional deformational structures (Wickens, 1994). The lower delta plain deposits accumulated as distributory channel-fills, crevasse channel-fills, crevasse splays and interdistributory bay-fill deposits, whereas deposition in the upper delta plain environment took place landward of the prograding delta lobes, mainly in the form of aggrading overbank mud deposits and thin-bedded sandy overbank splays (Wickens, 1994). The boundary between the upper and lower delta plain deposits separates subaqueous from subaerial deposition, i.e. the position taken as the Ecca-Beaufort boundary.

The marine deposits of the Ecca group was proceeded by the nonmarine Beaufort and Stormberg group deposits, which are capped by the volcanic Drakensberg Group that is linked to the break-up of Gondwana (Catuneanu et al., 2002). The Stormberg Group (Svensen et al., 2008:4930) contains, “the Molteno Formation (coarse sandstone, shale, and coal), the Elliot Formation (sandstone, shale), and the Clarens Formation (sandstone with intermittent siltstone horizons)”.

The word Beaufort “Beds” was expressed by Jones (1867) *for sedimentary rocks of the lower division of the Karoo Supergroup series at Beaufort West in South Africa but has later been expanded to include a wider range of fluviially deposited Permo-Triassic rocks in the main Karoo Basin* (Catuneanu et al., 2002).

The Stormberg Series forms part of the Molteno, Elliot and Clarens Formations, and the Drakensberg Group of the main Karoo (Catuneanu et al., 2002). An angular unconformity is established at the bottom of the Molteno formation; it is fully produced in many basins and presents a major tectonic occurrence that brought about Stormberg sedimentation (Catuneanu et al., 2002). Of the three sedimentary Stormberg formations, the Clarens and equivalents have the largest part of consistent distinctiveness (Catuneanu et al., 2002).

The deposition of submarine fans in the Karoo foredeep occurred within three discrete depozones, divided by structural highs (Van der Werff & Johnson, 2003). The three subbasins are: the Tanqua, Laingsburg and southern subbasin. The western (Tanqua) and central (Laingsburg) subbasins are separated by the Baviaanshoek and Hex River-Bontberg anticlines (Van der Werff & Johnson, 2003).

Time-scale	Age	Key	Formations	Key	Group	Supergroup	
~135 Ma ~225 Ma	Cretaceous - Recent			PS	Post-Stromberg		
	Trias-Jurassic			S	Stromberg		
~280 Ma	Permian	Pte	Teekloof	B	Beaufort	Karoo	
		Pa	Abrahamskraal				
		Pwa	Waterford	E	Ecca		
		Pk	Kookfontein				Fortbrown
		Ps	Skoorsteenberg				Laingsburg
		Pt	Tierberg				Vischkuil
		Pl					
		Pv					
		Pc	Collingham				
		Pw	Whitehill				
Pp	Prince Albert						
C-Pd		Dwyka					
~345 Ma	Carboniferous	Cw	Waaipoort	W	Witteberg	Cape	
		Cf	Floriskraal				
		Ck	Kweekvlei				
		Dwi	Witpoort				
		Ds	Swartruggens				
		Dbi	Blinkberg				
		Dwa	Wagen Drift				
		Dka	Karooport				
		Do	Osberg				
		Dkl	Klipbokkop				
~395 Ma	Devonian	Dwu	Wuppertal	B	Bokkeveld		
		Dw	Waboomborg				
		Db	Boplaas				
		Dt	Tra-Tra				
		Dh	Hexriver				
		Dv	Voorstehoek				
		Dga	Gamka				
		Dg	Gydo				
		Dr	Reitvlei				
		Ss	Skurweberg				
~435 Ma	Silurian	Sg	Goudini	TM	Table Mountain		
		O-Sc	Cederberge				
~500 Ma ~600 Ma	Ordovician	Opa	Pakhuis				
		Ope	Peninsula				
		Og	Graafwater				
~500 Ma ~600 Ma	Cambrian Namibian	Op	Piekenierskloof	PT	Pre-Table Mountain		

Figure 1.7.1: Lithostratigraphic column for the Cape Fold Belt and SW Karoo Basin (after Besaans, 1973; Dingle & Siesser, 1977; Steyn, 1983; Theron, 1986; Cole, 1992; Wickens, 1994; Thomas, 1997; De Beer, 1999; Flint et al., 2004).

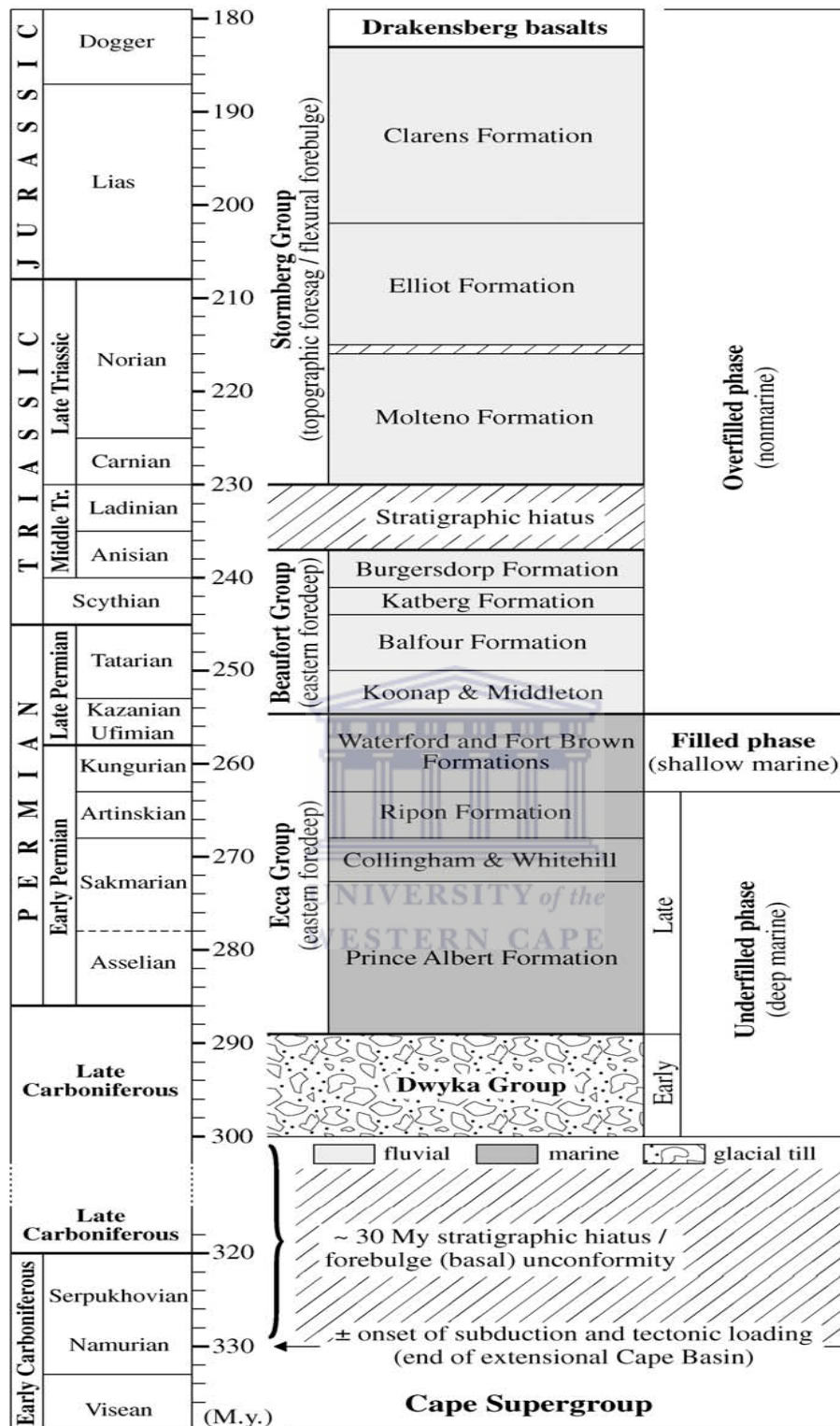
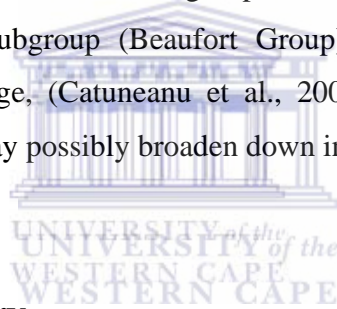


Figure 1.7.2: Stratigraphic diagram of the main lithostratigraphic subdivisions of the Karoo Supergroup in the main Karoo Basin of South Africa (modified from Catuneanu et al., 2005).

1.8 Chronostratigraphy

The sedimentary and volcanic documentation of the Karoo Supergroup ranged from the Late Carboniferous to the Early Jurassic (Catuneanu et al., 2002). In the *main Karoo basin the Dwyka Group ranges from the Late Carboniferous to the Early Permian, the Eccca Group is dated from the Early-Late Permian margin and the Adelaide Subgroup (Beaufort Group) makes up the remainder of the Late Permian* (Catuneanu et al., 2002). The age of the Whitehill Formation (Catuneanu et al., 2002), has been dated using different methods as Late Sakmarian (Early Permian), late Kungurian to early Ufimian (Early-Late Permian) or late Kazanian (Late Permian) (Catuneanu et al., 2002). The Permo-Triassic coincides with the foot of the Lystrosaurus group which is situated underneath the pinnacle of the Adelaide Subgroup of the Beaufort Group (Catuneanu et al., 2002). The Tarkastad Subgroup (Beaufort Group) and the Molteno and Elliot Formations are of Triassic age, (Catuneanu et al., 2002), whilst the overlying Early Jurassic Clarens Formation may possibly broaden down into the Late Triassic (Catuneanu et al., 2002).



1.9 Depositional History

Decreases in temperature during the mid-Carboniferous caused a global regression, accompanied by the buildup of an extensive ice cover over the southern mountain chain fringing the paleo- Pacific margin and the cratonic highlands to the north and east of the main Karoo basin (Johnson et al., 1996a). According to Catuneanu et al., (2002) the Karoo depositional cycle commenced with an assortment of glaciogene rock types. These represented ground moraine, which are remainders of receding glaciers and the melt-out products of floating ice sheets, with fluvioglacial outwash material and seasonal varvites resulting from suspension settling under quiet water conditions forming a subsidiary constituent (Catuneanu, 2002). Deposition of the Dwyka took place from grounded ice sheet, but the onset of warmer climates resulted in rain out debris accumulating from floating ice shelf (Johnson et al., 1996a). Further warming led to the dissolution of the ice

sheet during the Early Permian, with glacial deposition confined mostly to valleys bordering the cratonic high lands (Johnson et al., 1996a).

In the southern part of the main Karoo basin the glacial event was preceded by the deposition of a thick mudrock sequence (Prince Albert, Whitehill, Tierberg Formations), indicative to suspension settling in moderately deep water (Catuneanu, 2002). *Beside the southern rim of the main Karoo basin the sandstones of the Ripon, Laingsburg and Skoorsteenberg Formations characterise turbidites deposited as submarine fan complexes at the base of developing delta slopes* (Catuneanu, 2002). *The mudrocks and rhythmites of the Fort Brown Formation and the upper parts of the Kookfontein and Tierberg Formations comprise distal deltaic deposits which grade upwards during coarsening-upward cycles into the sandstone-rich delta front Waterford Formation* (Catuneanu, 2002). In the northeastern division of the basin the coal-bearing Vryheid Formation is composed of equally coarsening-upward deltaic cycles and fining-upward fluvial cycles, with the latter taking place in the center division of the formation (Catuneanu, 2002). The regressive Vryheid Formation is established within the mudrocks of the Pietermaritzburg and Volksrust Formations representing transgressive shelf sediments (Catuneanu, 2002). The Beaufort Group and overlying Molteno and Elliot Formations are mostly comprised of fining upward fluvial sediments (Catuneanu, 2002). The rivers were chief high sinuosity types, with widespread floodplain muds predominating over lenticular channel sands (Catuneanu, 2002). On the other hand, the sandstone-rich Molteno Formation seems to have been deposited by braided low-sinuosity rivers (Catuneanu, 2002). Arid, aeolian settings occurred during the deposition of the Clarens Formation with enormous, loess-type deposits (Catuneanu, 2002). Fluvial and playa lake settings display wetter climatic episodes. A progressive change from glacial, to warm, to arid settings has occurred in most places (Catuneanu, 2002).

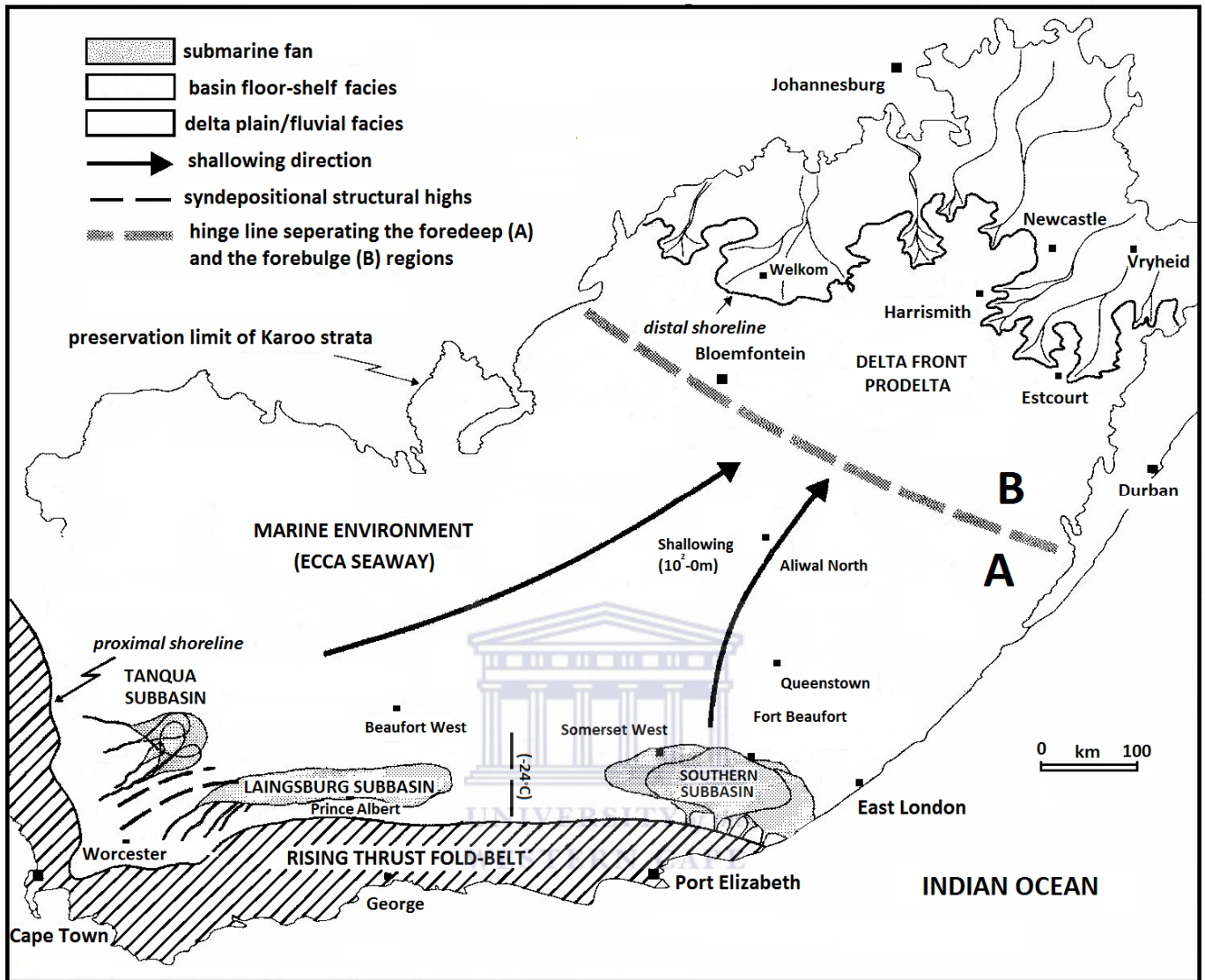


Figure 1.9.1: Palaeogeographic re-enactment of the environments recognised in relation to the Ecca interior seaway of the Karoo basin during the Artinskian (modified from Catuneanu et al., 2002).

Chapter Two

Concepts

There are seven geochemical methods that can be utilised to determine source rock quality and maturity. The seven methods are vitrinite reflectance, Thermal Alteration Index (TAI), Time-Temperature Index (TTI), elemental analyses/composition, extent of kerogen reaction, rock eval pyrolysis and Gas Chromatography (GC). In this study rock eval pyrolysis and TOC was used, which is explained in more detail below.

2.1 Geochemical Methods

Source rock studies require some form of geochemical analyses. Researchers utilise all or some of the methods available depending upon their work. The method is displayed in Figure 2.1.1. Rock or core (preferably core) samples of around 50g is required for most of the analyses. The rocks are dried in an oven at 60°C and then grinded and milled to a powder form. The powdered sample is sent for Total organic carbon (TOC) content analyses (to screen samples, to see which are suitable for rock eval). After, TOC samples are sent for rock eval analyses to determine the kerogen type and content. Other geochemical methods requires that the soxhlet extraction for 48hrs, using chloroform, which is then concentrated by rotary evaporation and weighed to determine the extractable organic matter. Asphaltenes are removed from n-pentane by precipitation or septic tank treatment and then weighed. Column chromatography requires 12g of silica to produce aromatics, polars and saturates. Aromatics are used for GCMS methyl phenanthrenes, monoaromatic and triaromatic steroids, whereas saturates are used for GCMS of biomarkers and GC n-alkane profiles.

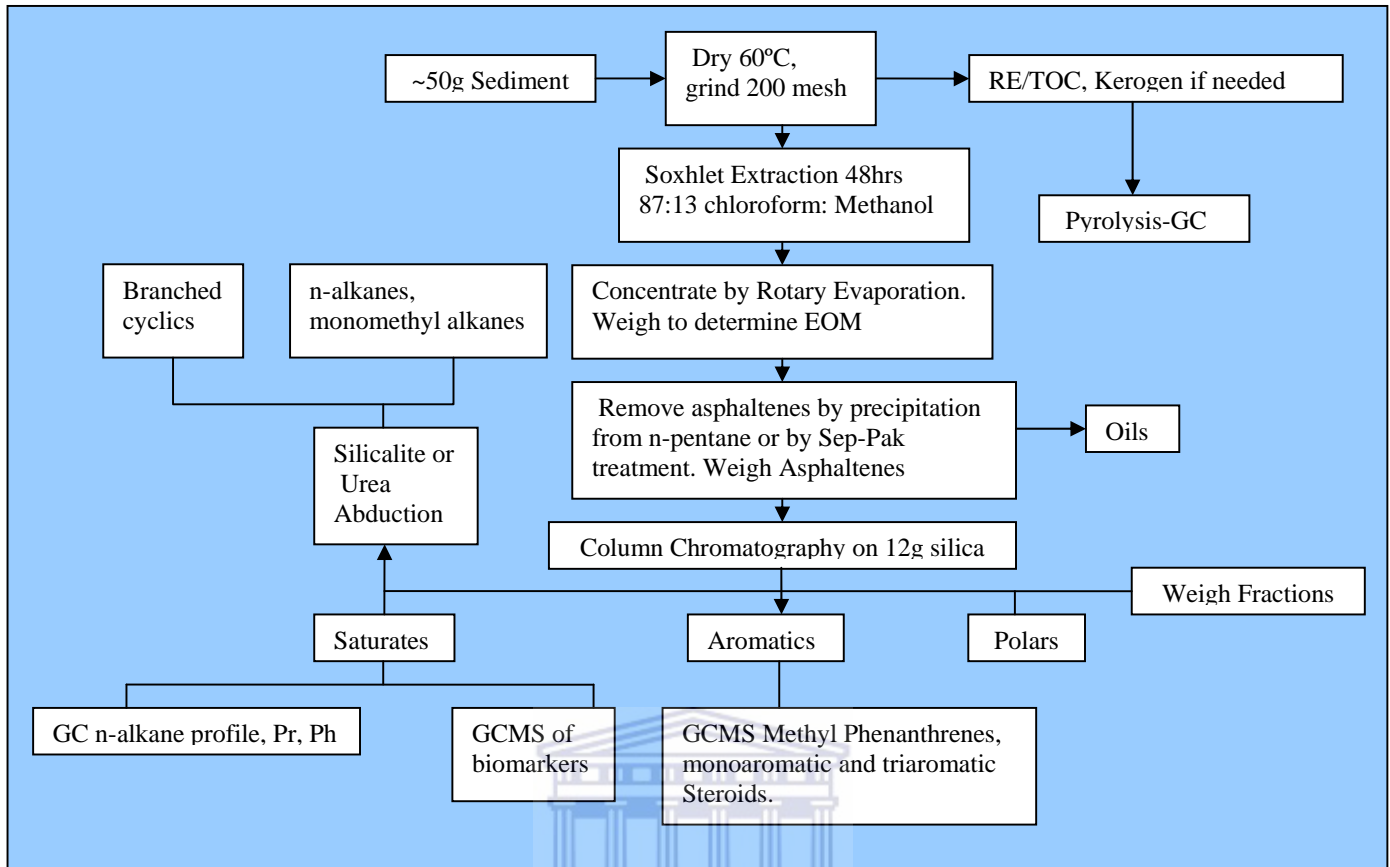


Figure 2.1.1: A characteristic geochemical analyses diagram for a potential source rock sample¹.

2.2 Time Temperature Index (TTI)

The time temperature index is a measure of the maturity and oil generation. The burial history (depth vs. time) needs to be determined to estimate the geothermal history².

1) Hydrocarbon Prospects and Exploration Plays: www.ccop.or.th/ppm/document/CAEXV2/CAEXV2DOC02.pdf (Visited on 16 October 2009).

2) Basin Modelling: www.landforms.eu/Orkney/Geology/Oil/OIL%20orkney%20devonian%20source%20rock%20quality.htm (Visited on 13 February 2010).

2.3 Vitrinite Reflectance (R_o)

Vitrinite reflectance is the extent of the maturity of organic matter (in relation to whether it has formed hydrocarbons or could be an efficient source rock)³. The vitrinite reflectance of a minimum of thirty (depending on sample collection) singular grains of vitrinite from a rock sample is calculated using a microscope. The measurement is given in units of reflectance, % R_o , with typical values ranging from 0% R_o to 3% R_o ³.

2.4 Thermal Alteration Index (TAI)

Thermal Alteration Index (TAI) is a method used to describe the colour change in palynomorphs¹. The colour of the kerogen is indicative of the degree of catagenesis. The scale ranges from 1 to 4¹.



2.5 Elemental Analyses

An elemental analysis is a process whereby kerogen is separated from the rock and the solvent is extracted¹. The solvent is burned in a furnace and the produced CO_2 , H_2O , N_2 and ash are measured¹. Carbon, hydrogen, and nitrogen are subsequently determined based on their original weight of the kerogen. The sum of oxygen is calculated by separate analyses¹.

2.6 Extent of Kerogen Reaction

An estimate of the total kerogen that has been converted to oil/gas, will be an indication of the source rock maturity (Opuwari, 2011). The formula $dC/C = dt.Ae^{-E_a/Rt}$ whereby:
 dC/C = Extent of reaction, R = Gas constant $kJ/mol^\circ K$, E_a = Activation energy of reaction

3) Schlumberger: www.glossary.oilfield.slb.com/Display.cfm?Term=vitrinite%20reflectance (Visited on 20 August 2009).

T = time over which reaction occurs and A = frequency factor S^{-1} . When $dC/C = 1$, total reaction of kerogen produces petroleum products, but when $dC/C < 1$, then the kerogen is overmature (no oil or gas generation).

2.7 Gas Chromatography (GC)

Gas chromatography removes different components of saturates (paraffin's and naphthenes) and aromatics based principally on their boiling point and create a graphic representation (chromatogram) of the severance¹.

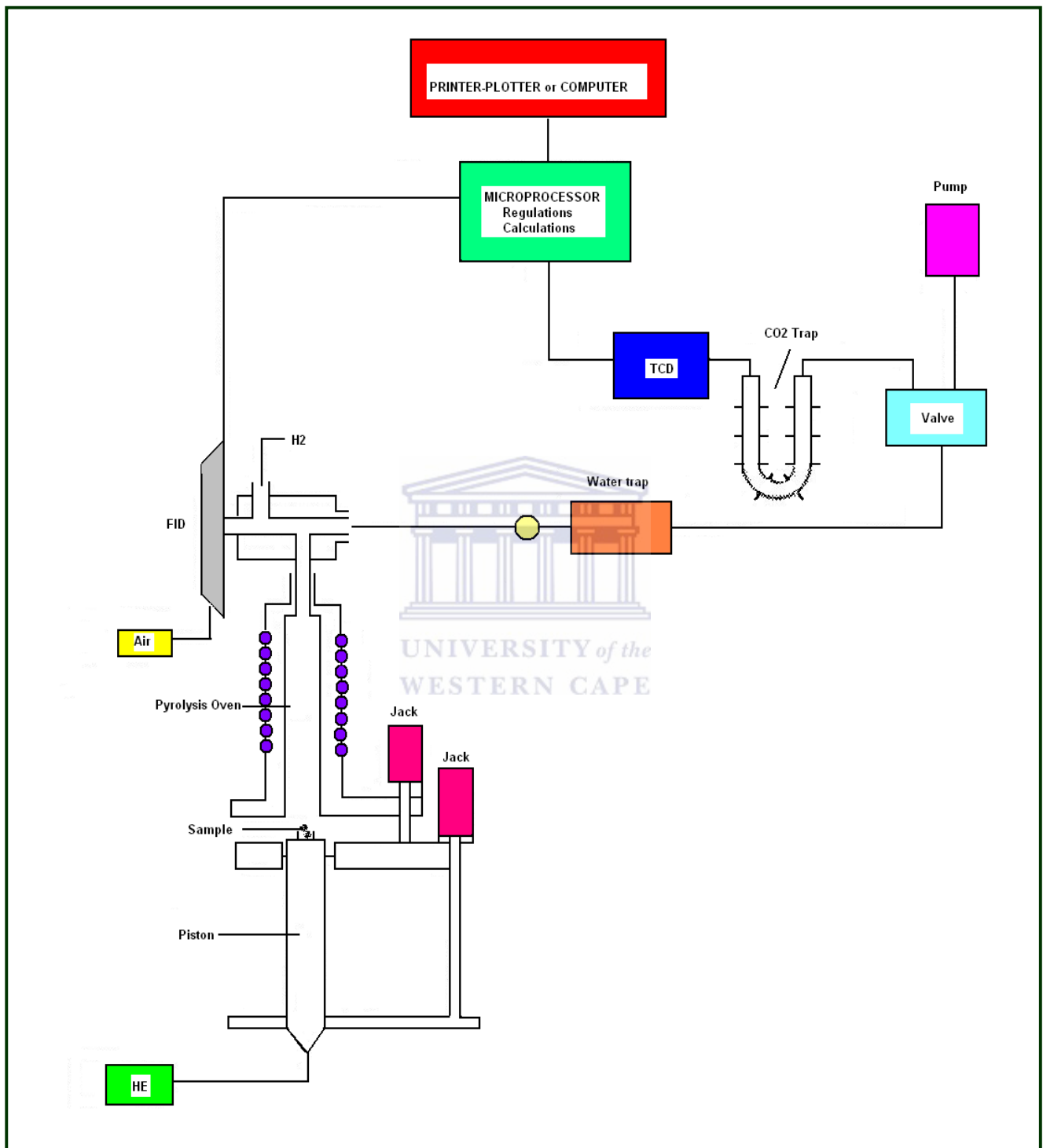
2.8 Rock Eval Pyrolysis

Rock Eval Pyrolysis is a routine method that is used to determine the hydrocarbon potential of a source rock (which is done by looking at the type and maturity of kerogen). The technique involves programmed temperature heating of a small amount of sample in a pyrolysis oven. Data from rock eval is used to quantitatively determine the⁴:

- the sum of free hydrocarbons (S1)
- the sum of hydrocarbons formed during thermal cracking of nonvolatile organic matter (S2)
- the sum of CO₂ formed for the duration of pyrolysis of kerogen (S3)
- the temperature at which the highest discharge of hydrocarbons from cracking of kerogen occurs throughout pyrolysis. T_{max} is the temperature at the period of maturation of the organic matter.

4) Kerogen: <http://www.eaps.mit.edu/geobiology/biomarkers/kerogen.html> (Visited on 10 February 2010).

Figure 2.8.1 below represents the pyrolysis method of source rock analysis¹.



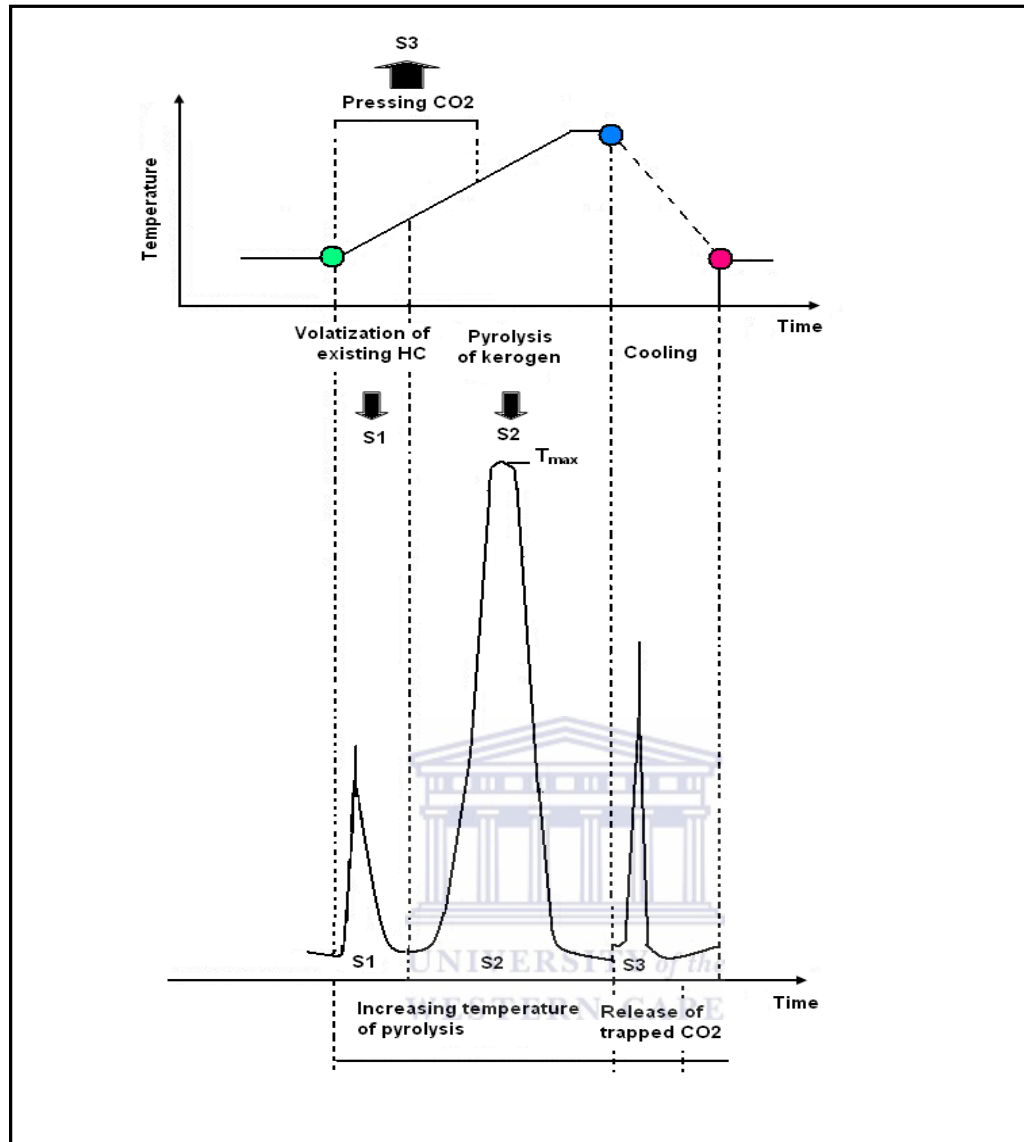


Figure 2.8.2: S1 peak represents products evolved at temperatures of 300°C. The area below the peak corresponds to the thermal distillation of free or absorbed organic matter. The S2 peak represents products that have evolved at temperatures from 300-500°C¹. The region below this peak represents the quantity of hydrocarbon like products cracked from the kerogen and indicates the major percentage of the convertible carbon. S3 relates to the carbon dioxide released in the procedure¹.

The nature and maturity of organic matter in source rocks can be identified from rock eval pyrolysis data by means of the subsequent conditions⁴:

- H/C ratio. This is used to characterise the source of organic matter. Marine organisms and algae are comprised of lipid- and protein-rich organic matter, where the ratio of H to C is greater than in the carbohydrate-rich components of land plants.
- O/C ratio. This ratio is high for polysaccharide-rich remains of ground plants and inert organic substances.

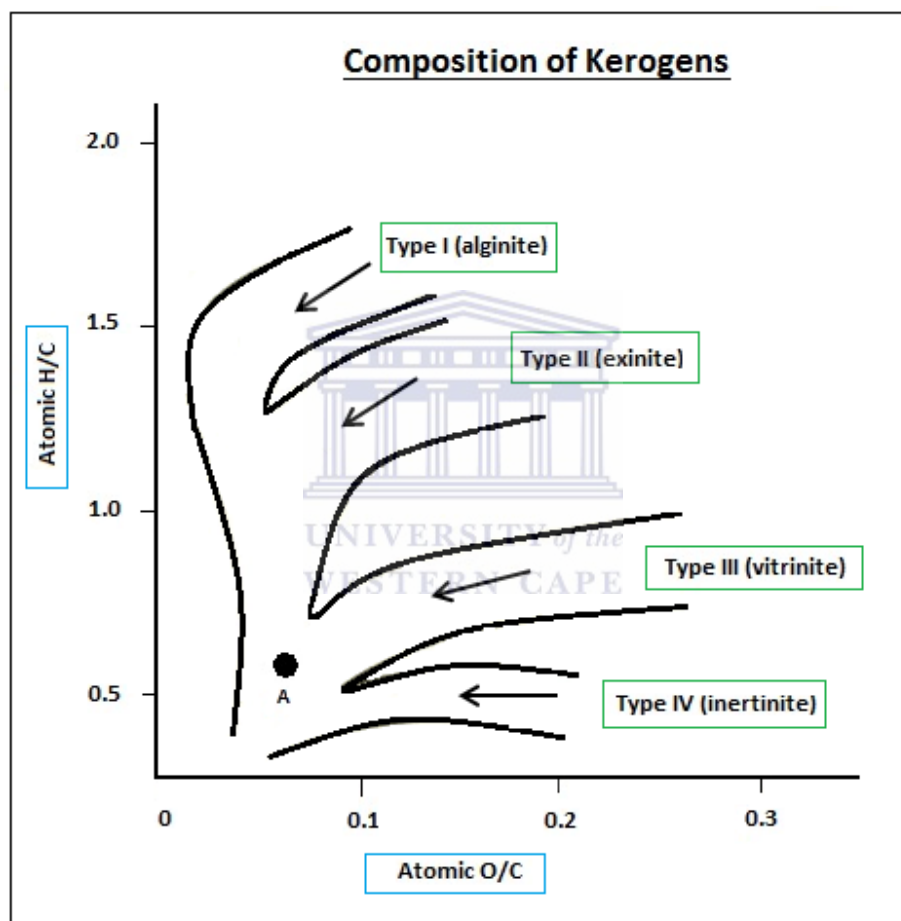


Figure 2.8.3: The van Krevelen diagram is a plot of the bulk element ratios, H/C vs. O/C. The four varying kerogen types, in the chart above, mature along four dissimilar evolutionary paths. When a sedimentary rock evolves to a more mature state during burial, the kerogen becomes further exhausted in hydrogen and oxygen in relation to carbon⁴.

2.9 Total Organic Carbon (TOC)

TOC is the measure of the carbon present in a rock in the form of both bitumen and kerogen (Allen & Allen, 1990). Total Organic Carbon (TOC) - weight percent total organic carbon in a sample. It is comprised of¹:

- *extractable organic matter (EOM): carbon that is the oil in the sample*
- *convertible carbon :which can be used in petroleum generation*
- *residual carbon: which is non-reactive carbon, thus it cannot yield hydrocarbons*

Organic matter in soils and sediments is extensively circulated over the earth's surface taking place in nearly all terrestrial and aquatic environments (Schnitzer, 1978). There are three carbon forms, inorganic, organic and elemental. Elemental carbon types consist of charcoal, soot, graphite, and coal (Schnitzer, 1978). The principal sources for elemental carbon in soils and sediments are partial combustion products of organic matter, from geologic sources, or the distribution of these carbon forms throughout mining, processing, or combustion of these materials (Schumacher, 2002). Inorganic carbon forms are resultant from geologic or soil parent substances. Inorganic carbon forms are at hand in soils and sediments usually as carbonates (Schumacher, 2002). Naturally-occurring organic carbon forms are derivative from the decomposition of plants and animals (Schumacher, 2002). In soils and sediments, an ample assortment of organic carbon forms are present and vary from plant constituents to highly decomposed matter such as humus(Schumacher, 2002).

TOC classification Table	
Poor/Inadequate	< 0.5
Fair/Marginal	0.5-1.0
Good/Adequate	1.0-2.0
Very Good/Adequate	2.0-5.0
Excellent/Adequate	> 5.0

Table 2.9.1: TOC classification table with relative percentages¹.

Both destructive and non-destructive methods are utilised to determine the TOC and total carbon in soils and sediments (Tiessen and Moir, 1993). The three fundamental characteristics of the destructive techniques are (Tiessen and Moir, 1993): (1) Wet oxidation proceeded by titration with ferrous ammonium sulfate or photometric determination of Cr^{3+} (2) Wet oxidation proceeded by the compilation and measurement of altered CO_2 , and (3) dry combustion at elevated temperatures in a furnace with the assortment and detection of altered CO_2 (Tiessen and Moir, 1993).

Sample preparation for sediment samples, requires the elimination of huge particles (usually the particles are not greater than 2-mm in diameter) and sample homogenisation (Schumacher, 2002).

The standard wet chemistry method (Walkley Black method) for the sample removal requires the fast dichromate oxidation of organic matter. In this process, potassium dichromate ($\text{K}_2\text{Cr}_2\text{O}_7$) and concentrated H_2SO_4 are supplemented to between 0.5 g and 1.0 g (however the assortment may be up to 10g depending on organic carbon content) of soil or sediment (Schumacher, 2002). The solution is swirled and permitted to cool before adding water to stop the reaction. The addition of H_3PO_4 to the digestive mix after the sample has cooled has been used to eradicate interferences from the ferric (Fe^{3+}) iron that may be present in the sample (Tiessen and Moir, 1993).

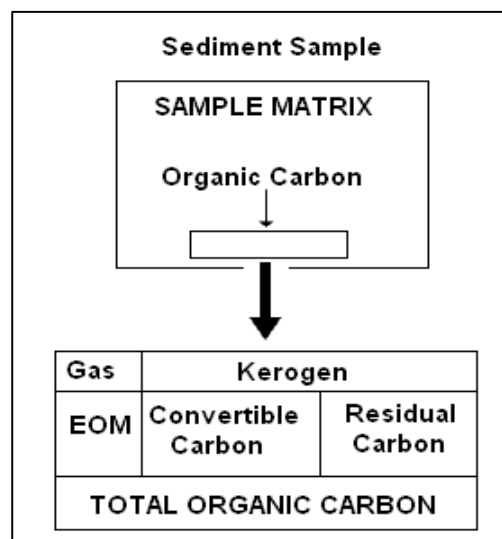


Figure 2.9.1: Components and classification of TOC¹

The rock eval pyrolysis machinery can be used to measure the TOC of a sample by oxidizing (in an oxidation oven maintained at 600°C) the organic matter remaining in the sample after pyrolysis (residual organic carbon)⁵. The TOC is then calculated by totaling the residual organic carbon recognised to the pyrolyzed organic carbon, which in turn is calculated from the hydrocarbon compounds given from pyrolysis⁵. TOC that contains carbon content less than 0.5% is inadequate, TOC between 0.5-1.0 is marginal and TOC from 1.0 to greater than 5.0 is adequate for oil or gas accumulation (Peters, 1986).

2.10. X-Ray Diffraction (XRD)

Before one can determine the precise mineralogy, X-ray diffraction (XRD) analyses, is completed⁶. X-ray diffraction (XRD) is a flexible, non-destructive method that displays thorough data about the chemical composition and crystallographic arrangement of natural and artificial materials⁶.

There are two types of XRD methods; one is qualitative whereas the other is quantitative. Qualitative analysis typically requires the recognition of a phase or phases in a sample by comparing the sample with customary patterns (i.e., data gathered or measured by someone else), and relative estimation of proportions of various phases in multiphase data by comparing peak intensities ascribed to the recognised phases⁷.

Quantitative analysis of diffraction data refers to the determination of sum of varying phases in multi-phase samples. In quantitative analysis, the structural types and phase proportions are dealt with, with great precision⁷. Excellent quantitative analysis relies on modelling diffraction patterns calculated in such a way that it exhibits the same properties as the experimental pattern⁷. All quantitative analysis needs exact and precise deductions of the diffraction pattern for a sample both by means of peak localities and intensities.

5) Publication Services: www.odp.tamu.edu/publications/tnotes/tn30/tn30_12.htm (Visited on 10 February 2010).

6) X-Ray Diffraction: www.panalytical.com/index.cfm?pid=135 (Visited on 5 February 2011).

7) Introduction Quantitative X-Ray Diffraction Method: www.unm.edu/xrd/xrdclass/09-Quant-intro.pdf (Visited on 20 June 2010).

Whilst a number of analyses depend upon the favored orientation, the majority involves a uniformly sized, erratically oriented fine (ideally 1-2 μm) powder specimens to create intensities which precisely display the structure and composition of the phase or phases analysed⁷.

XRD is a process in which X-rays of a recognised wavelength strike crystal lattice planes separated by a distance d . $\text{Wavelength} = 2d \sin(\theta)$ When the values of θ and 2θ are identified the resultant values of d can be calculated. Using the calculated values of d it is probable to deduce information pertaining to the sample such as⁸.

- Qualitative & quantitative mineral content
- Crystallographic structure determination
- Identification of unknown substances

In this study qualitative analyses mineral content was undertaken⁸

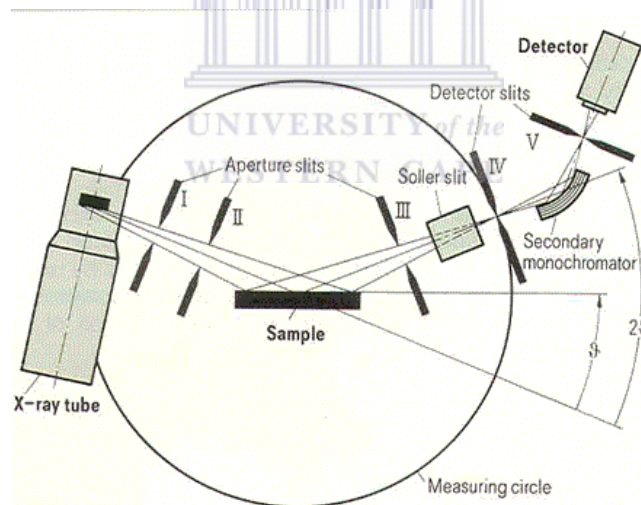


Figure 2.10.1: The diagram shows a common configuration for an XRD unit⁸.

8) Operational Theory: <http://ks-analytical.com/service-and-support> (Visited on 10 February 2010).

Methodology and Data

2.11 Research Design

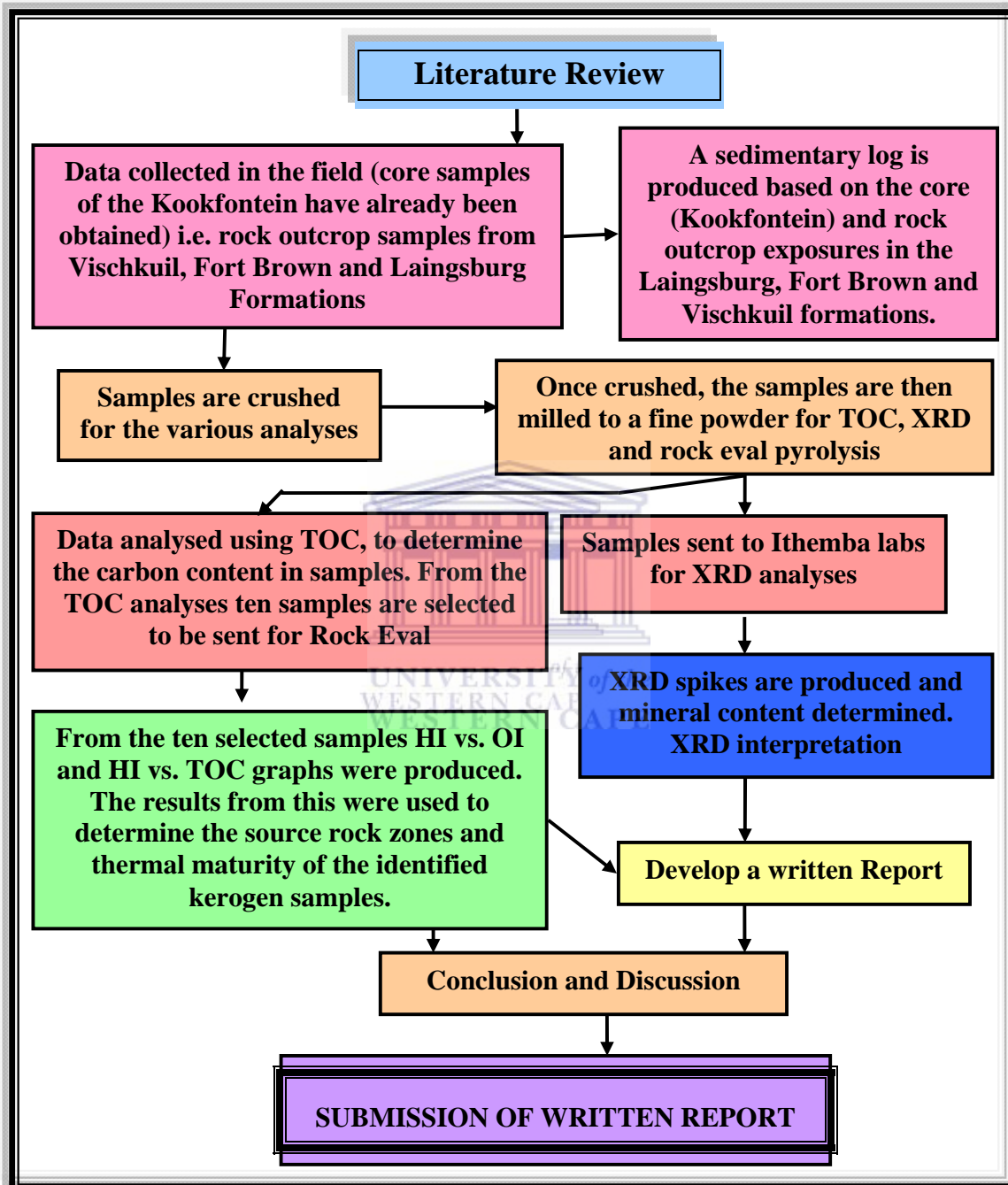


Figure 2.11.1: Flow chart of the methodology

2.12 Analytical Techniques

Rock outcrop and core samples were collected, grinded, milled and then weighed for TOC, XRD and rock eval analyses. TOC was done first to screen the samples before it was sent for rock eval analyses. Samples above 0.5% were selected for rock eval, which was used to determine the thermal maturity and kerogen type. XRD was done to determine the mineralogical content.

A total of forty samples were collected from the Laingsburg, Fort Brown, Vischkuil and Kookfontein Formations. Thirty rock outcrop samples were collected from various localities within the Laingsburg subbasin, whereas ten core samples were collected from the Tanqua basin. Samples were selected on core availability and places of interest within the study areas.

After sample selection the rock and core samples were grinded using a rock grinder at UWC (University of the Western Cape), the machine was switched on to remove the excess shards that were left over from the previous run. The tray that the samples were in was then washed and dosed in some ethanol to remove contamination of the previous samples. The samples was then placed in the sterilised draw and crushed using the rock grinder, this process was repeated for every sample. Once all the samples were grinded it was then sent to be milled.

The samples were placed within the milling container in which it was then milled to a fine powder (in some cases the samples had to be milled twice or thrice owing to the large quantity of sample collected), once milled the container would be washed and dosed in ethanol as well (to remove impurities) and the next sample would then be placed in the milling machine (at the UWC). Milling took approximately 5min-10min in the machine depending upon the quantity of each sample.

After the samples had been prepared (in the form of a fine powder) it was then weighed in the laboratory. Forty samples of 5grams each was then sent for TOC at Bemlab. The

Walkley Black/ Dichromate Oxidation method was utilised to perform the analysis. The method involves boiling the samples at 150°C for 30 minutes, allowing the samples to cool and then adding water to halt the reaction. The TOC data from Bemlab was analysed and ten samples were selected from the TOC to be sent away for rock eval analysis.



Formation	Sample	TOC %	Result
Fort Brown	1	0.3	inadequate
Fort Brown	2	0.35	inadequate
Fort Brown	3	0.11	inadequate
Fort Brown	4	0.32	inadequate
Fort Brown	5	0.25	inadequate
Fort Brown	6	0.29	inadequate
Fort Brown	7	0.1	inadequate
Fort Brown	8	0.22	inadequate
Fort Brown	9	0.19	inadequate
Fort Brown	10	0.35	inadequate
Vischkuil	1	0.43	inadequate
Vischkuil	2	0.56	marginal
Vischkuil	3	0.11	inadequate
Vischkuil	4	0.21	inadequate
Vischkuil	5	0.48	inadequate
Vischkuil	6	0.36	inadequate
Vischkuil	7	0.43	inadequate
Vischkuil	8	0.12	inadequate
Vischkuil	9	0.31	inadequate
Vischkuil	10	0.62	marginal
Kookfontein	12	0.8	marginal
Kookfontein	16	0.35	inadequate
Kookfontein	20	0.22	inadequate
Kookfontein	28	0.46	inadequate
Kookfontein	47	0.22	inadequate
Kookfontein	53	1.04	adequate
Kookfontein	57	0.35	inadequate
Kookfontein	65	0.37	inadequate
Kookfontein	72	0.3	inadequate
Kookfontein	75	0.24	inadequate
Laingsburg	1	0.51	marginal
Laingsburg	2	0.64	marginal
Laingsburg	3	0.27	inadequate
Laingsburg	4	0.4	inadequate
Laingsburg	5	0.54	marginal
Laingsburg	6	0.53	marginal
Laingsburg	7	0.33	inadequate
Laingsburg	8	0.21	inadequate
Laingsburg	9	0.25	inadequate
Laingsburg	10	0.22	inadequate

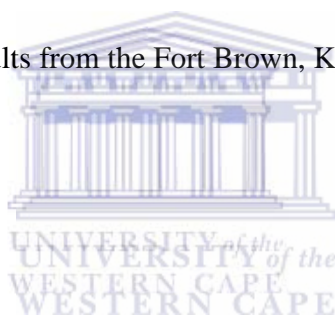
Table 2.12.1: TOC results from the Laingsburg, Kookfontein, Vischkuil and Fort Brown.

Rock eval six was used for its varying functionalities and accuracy. Some of the new capabilities of rock eval 6 are the change in the temperature ovens, relocation of the thermocouple and the introduction of infrared detectors (Lafarge et al., n.d.). Rock eval six ovens start from 100°C to 850°C, as opposed to rock eval two that started at 180°C and went up to 600°C (Lafarge et al., n.d.). Higher temperatures are essential for absolute thermal degradation of type III organic matter. The temperature increase in rock eval six yields a more accurate HI (S2/TOC) index. The legitimacy of Tmax is extended to higher temperatures with rock eval six. The reduced starting temperature from 180°C to 100°C allows for a more detailed study of the hydrocarbons found within rocks (Lafarge et al., n.d.). The new location of the thermocouple at the crucible below the sample (instead of the wall in the case of rock eval II), accounts for a more real measurement of the sample temperatures (Lafarge et al., n.d.). Infrared detectors into the Rock-Eval 6 are capable of constant on-line footage of the quantity of both CO and CO₂ released during pyrolysis and oxidation of samples (Lafarge et al., n.d.).

Rock Eval 6 was utilised to determine the kerogen type, thermal maturity, S1 (mg HC/g rock), S2 (mg HC/g rock), S3 (mg CO₂/g rock), Tmax (°C). Details of the analytical procedure and discussion can be found in chapter 3.

Sample No	RE			Tmax (°C)	HI	OI	S2/S3	S1/TOC * 100	PI
	S1	S2	S3						
Fort Brown 2	0.03	0.04	0.13	310	11	37	0.3	8.57	0.43
Fort Brown 10	0.03	0.04	0.2	325	11	37	0.2	8.57	0.43
Kookfontein 12	0.28	0.54	0.2	514	68	25	2.7	35	0.34
Kookfontein 53	0.06	0.31	0.17	532	30	16	1.8	5.77	0.16
Laingsburg 1	0.04	0.05	0.16	357	10	31	0.3	7.84	0.44
Laingsburg 2	0.04	0.07	0.15	337	11	23	0.5	6.25	0.36
Laingsburg 5	0.04	0.08	0.19	336	15	35	0.4	7.41	0.33
Laingsburg 6	0.07	0.13	0.12	378	25	23	1.1	13.21	0.35
Vischkuil 2	0.04	0.07	0.34	325	13	61	0.2	7.14	0.36
Vischkuil 10	0.03	0.03	0.37	349	5	60	0.1	4.84	0.5

Table 2.12.2: Rock Eval 6 results from the Fort Brown, Kookfontein, Laingsburg and Vischkuil formations.



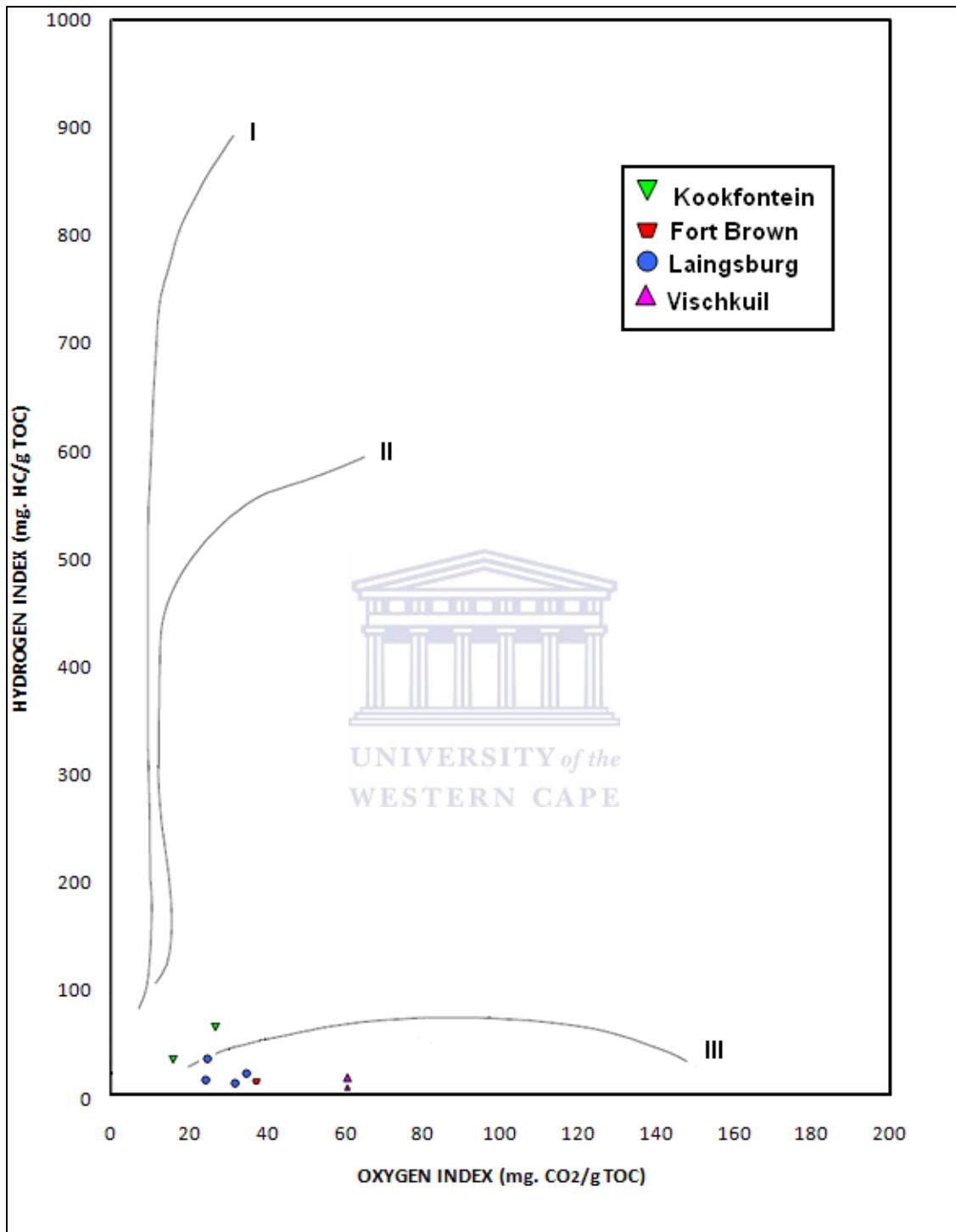


Figure 2.12.1: HI vs. OI diagram, displaying the kerogen type present within the plotted formations

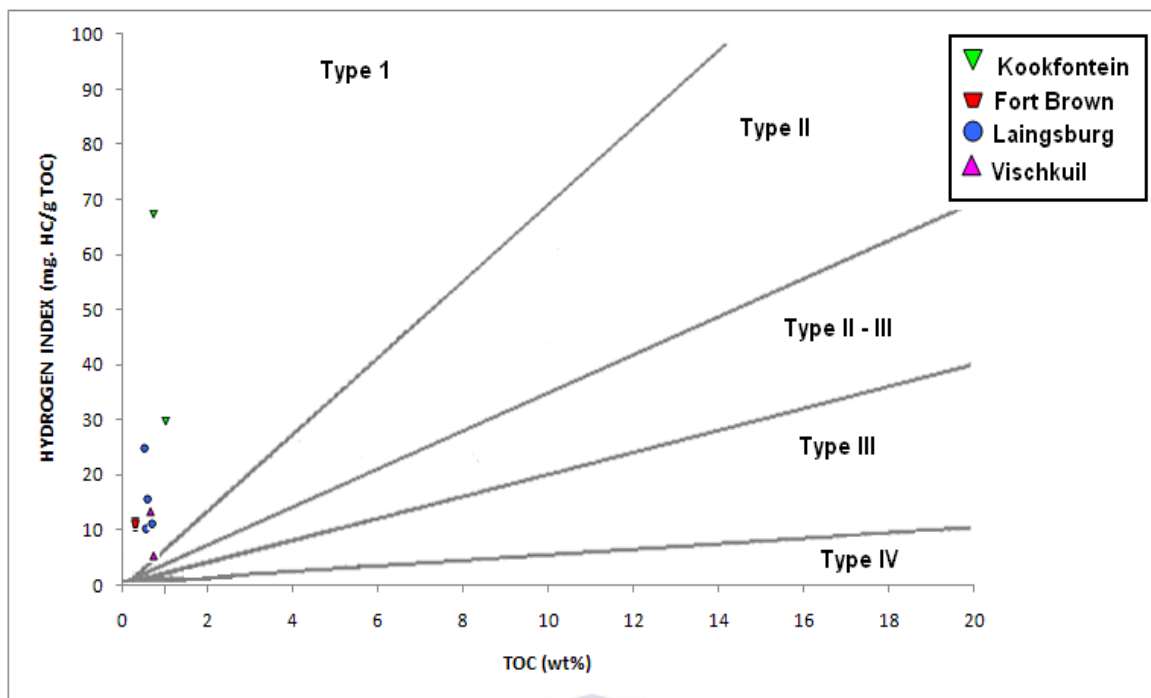


Figure 2.12.2: HI vs. TOC diagram displaying the kerogen type plots.

A qualitative XRD analysis was done at iThemba labs. Forty samples of 5 grams each was needed for the analysis. Minerals were identified based on existing literature of the rocks present in the Karoo region. It took 3 weeks for the samples to be prepared before the XRD graphs could be constructed. A day was spent at Ithemba to produce the graphs based upon the formations in this study.

Quartz, syn

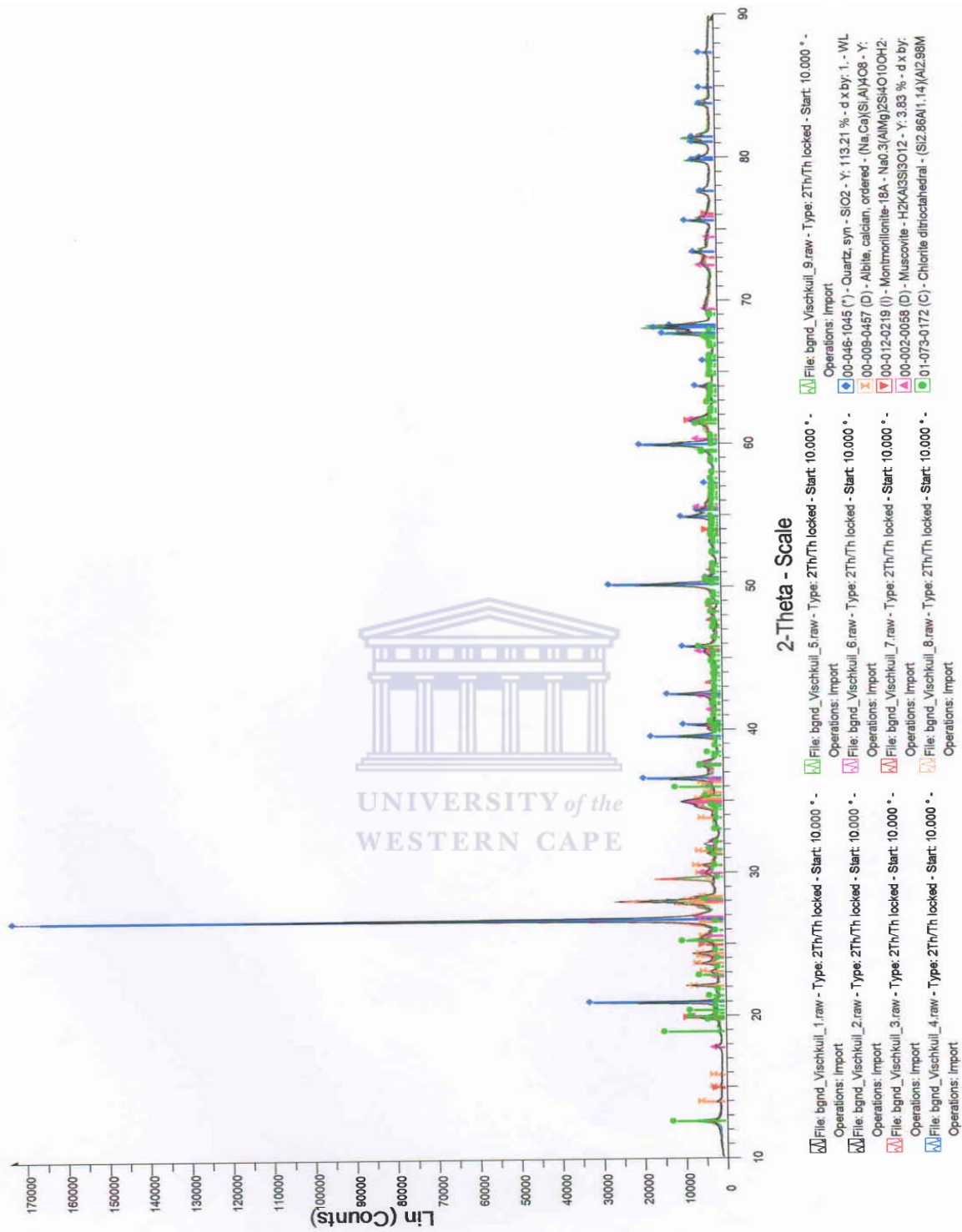


Figure 2.12.3: The Vischkuil formation minerals displayed by the XRD spikes. The minerals are represented in different colours which are: blue – quartz; orange – albite, red –montmorillonite; pink – muscovite; green – chlorite.

Quartz, syn

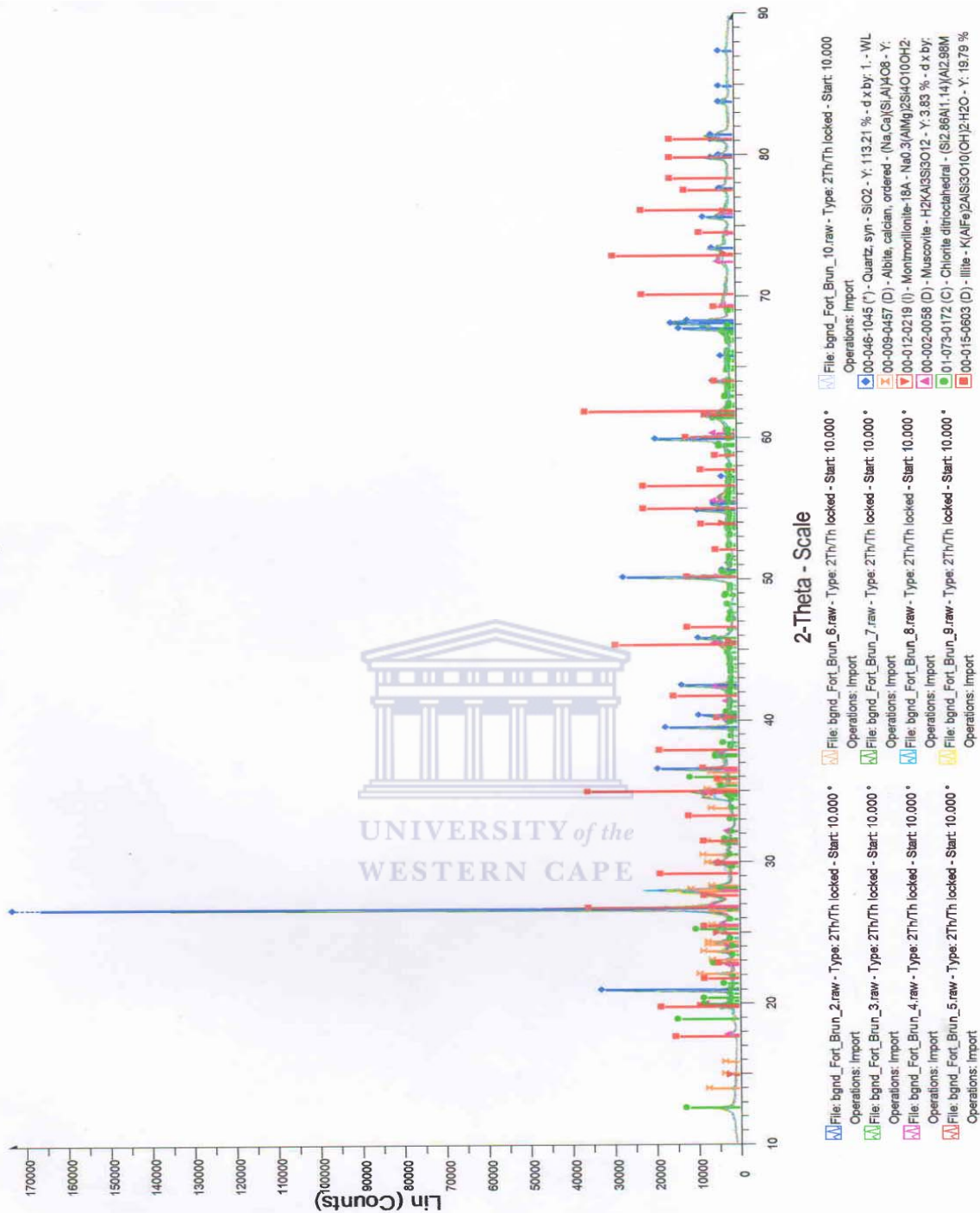


Figure 2.12.4: The Fort Brown formation minerals displayed by the XRD spikes. The minerals are represented in different colours which are: blue – quartz; orange – albite, red –montmorillonite; pink – muscovite; green – chlorite; dark red – illite.

Quartz, syn

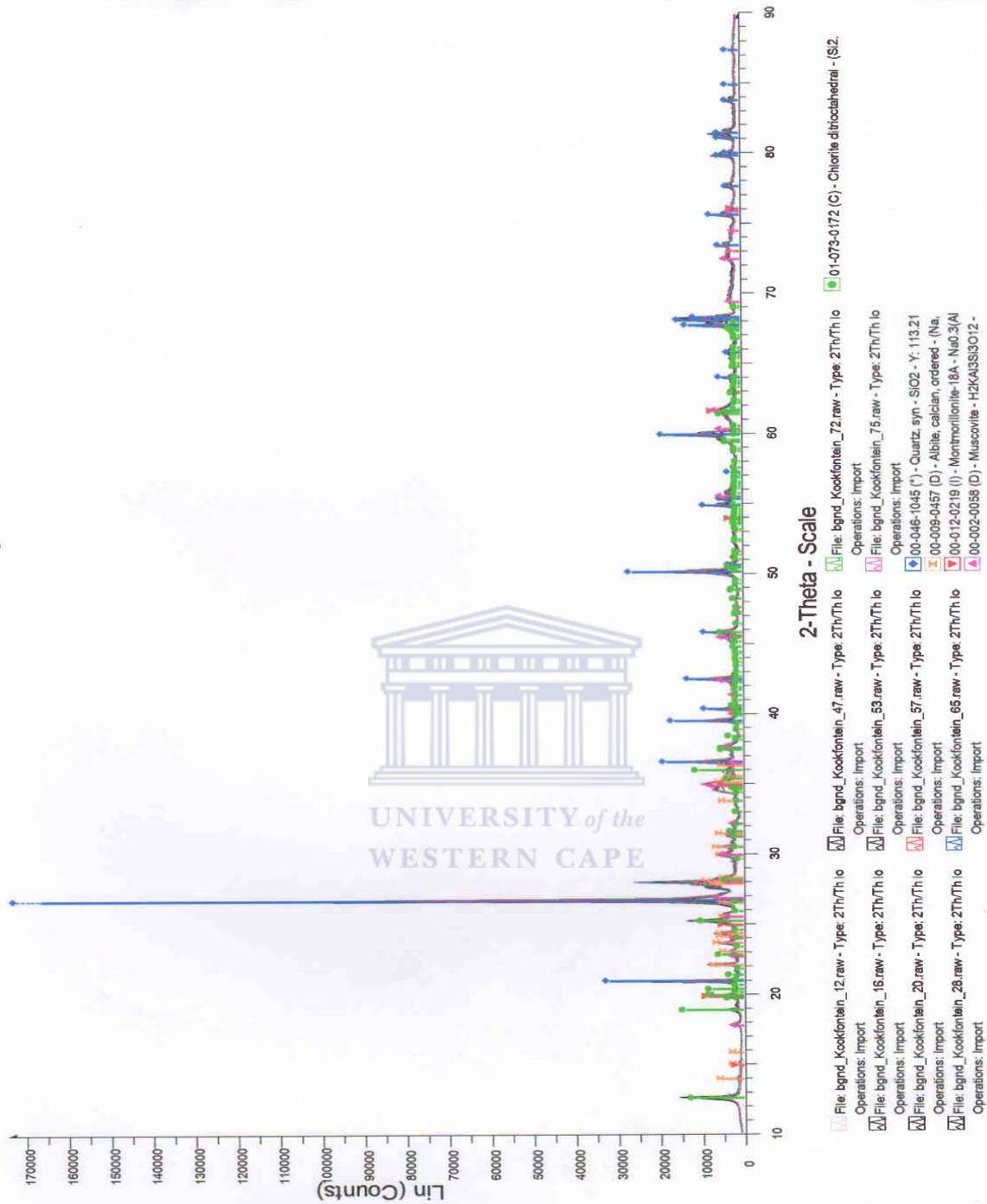


Figure 2.12.5: The Kookfontein formation minerals displayed by the XRD spikes. The minerals are represented in different colours which are: blue – quartz; orange – albite, red –montmorillonite; pink – muscovite; green – chlorite.

Quartz, syn

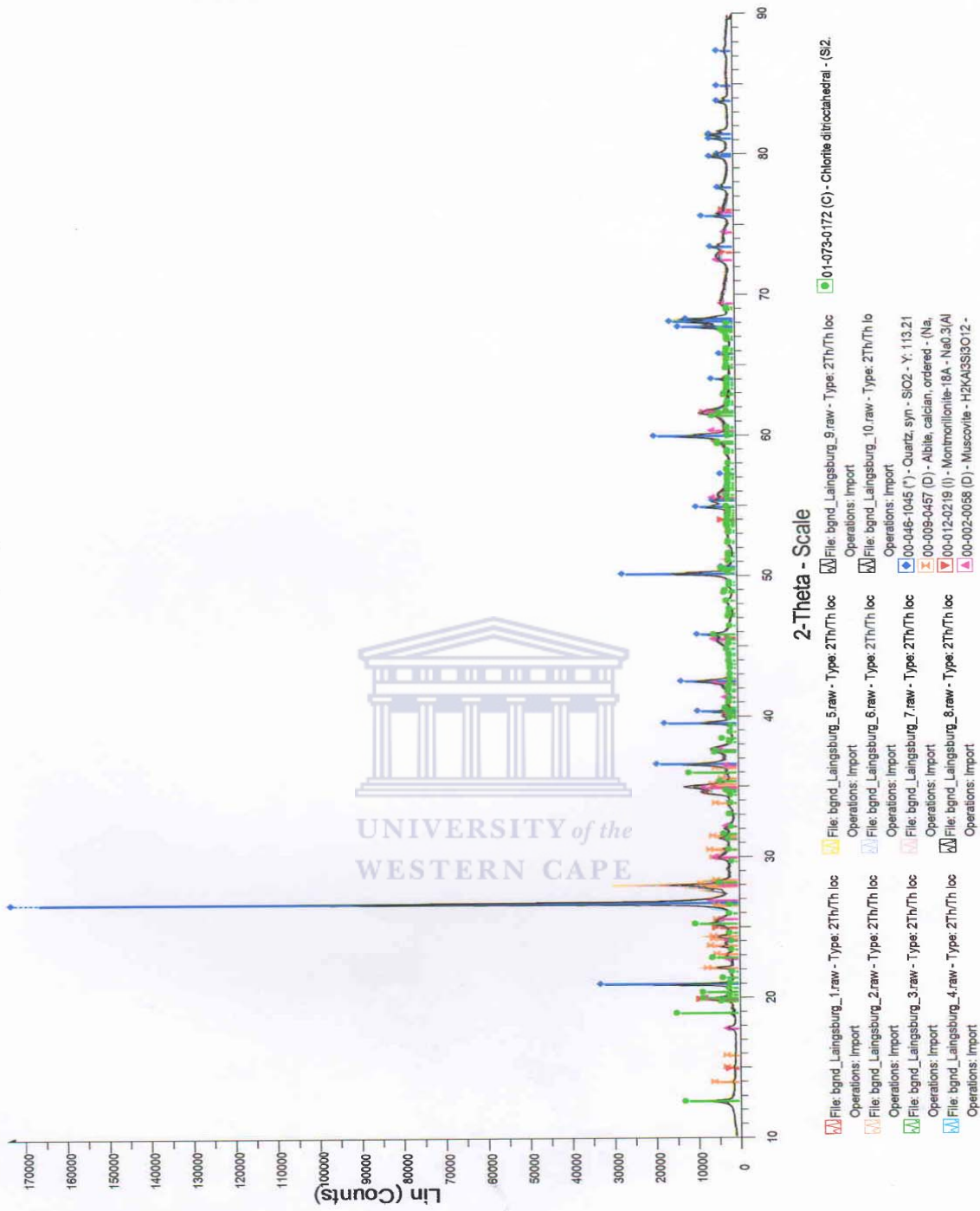
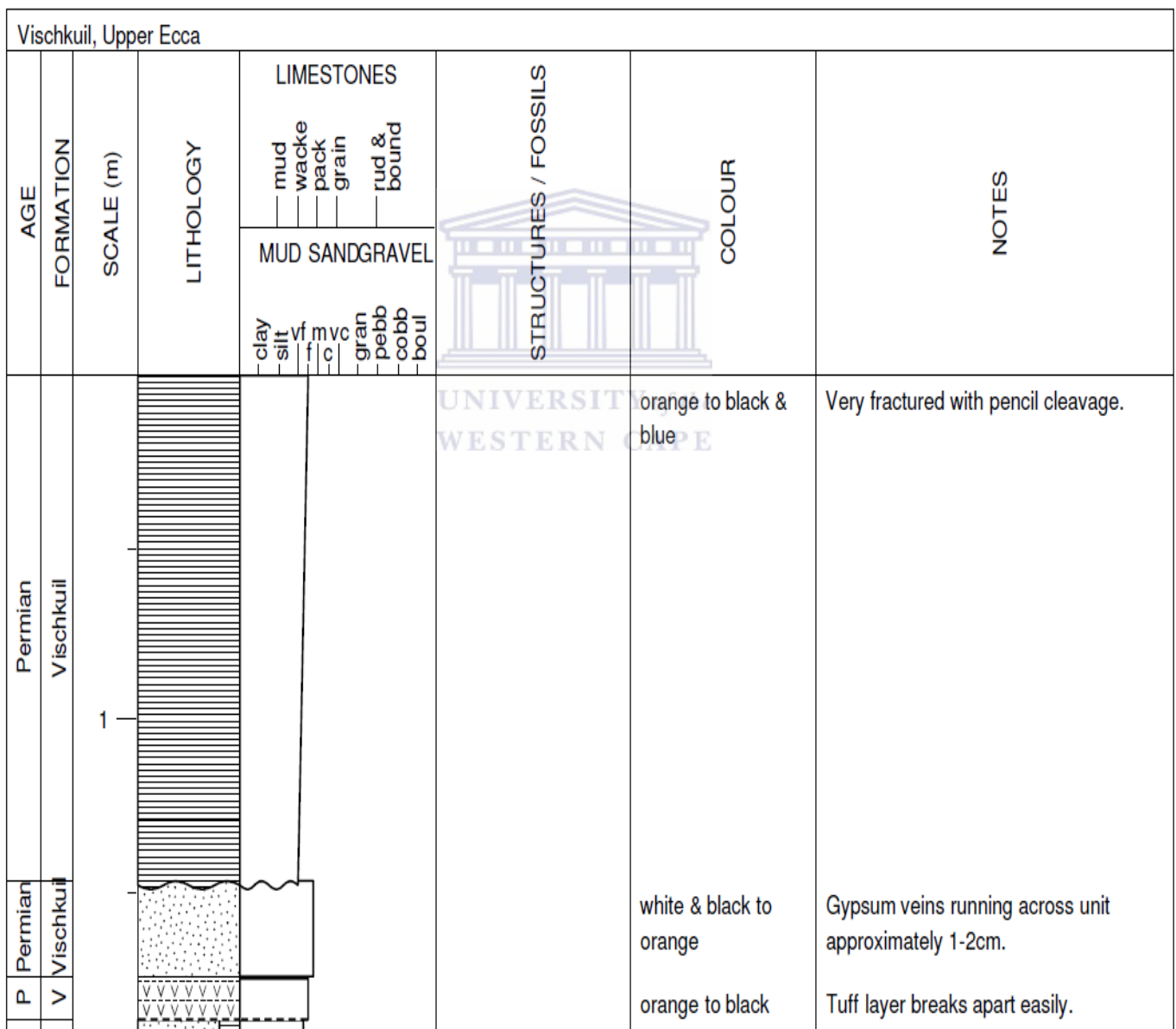


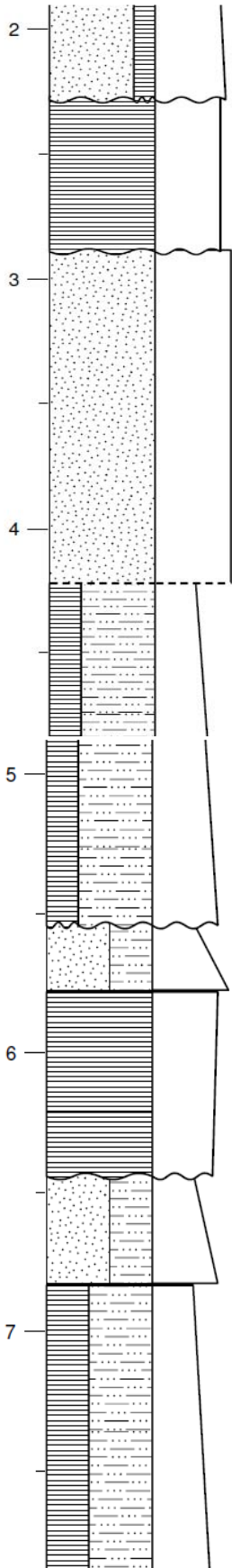
Figure 2.12.6: The Laingsburg formation minerals displayed by the XRD spikes. The minerals are represented in different colours which are: blue – quartz; orange – albite, red –montmorillonite; pink – muscovite; green – chlorite.

Sedimentary logs were produced for each formation. Logs were chosen based upon the best well exposed outcrop and areas of interest in the region. The Kookfontein log was created from the core samples. Four logs were produced and three can be found in the appendix section. Logs were used with the facies interpretation to determine the depositional environments found within the four formations

Figure 2.12.7: Sedimentary log of the Vischkuil Formation taken at: S33°14'16.8", E20°51'56.9".



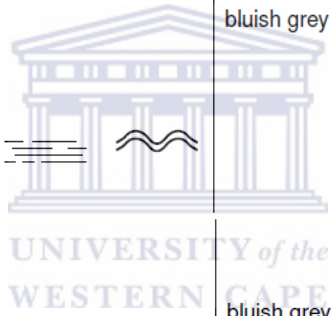
Permian	Permian	Permian	Permian	Permian	Permian
Vischkuil	Vischkuil	Vischkuil	Vischkuil	Vischkuil	Vischkuil



black to beige	Alternation of sandstone and siltstone, sandstone forming the bulk majority of the unit.
blue grey	Fractured with pencil cleavage.
orange to red & yellow	Massive sandstone unit and Lisa Gan weathering
blue grey	Pebbles found along the shale unit. Shale alternating with siltstone beds.
orange to black & yellow	Pebbles with very thin laminae of 1cm thick of the alternating lithologies.
blue grey	Fractured with pencil cleavage.
orangey blue & yellow	Intense Lisa Gan weathering. Concretions found along sandstone unit.
bluish grey black	Black specks, weathered white in some parts.

Permian Vischkuil	Permian Vischkuil	Permian Vischkuil	Permian Vischkuil	Permian Vischkuil	Permian Vischkuil	Permian Vischkuil	Permian Vischkuil
8							
9							
10							
11							
12							
13							
an uil							

bluish orange, yellow & red	Lisa Gan weathering with concretions along the sandstone unit.
bluish grey	Fractured, with very thin laminae 0.02cm of alternating shale, with the presence of wavy lamination along the lower part of the unit.
bluish grey and beige in some parts	Fractured with pencil cleavage.
bluish grey to white	Fractures found along shale unit.
bluish grey and white	Fractures, thin laminae of the alternating lithologies & wavy lamination. Concretions are found along the sandstone unit. Wavy lamination occurs on the top most part of the unit.
orange to red, black & yellow	Lisa Gan weathering with nodules and concretions along the sandstone unit.
orange to red &	Lisa Gan weathering with concretions.



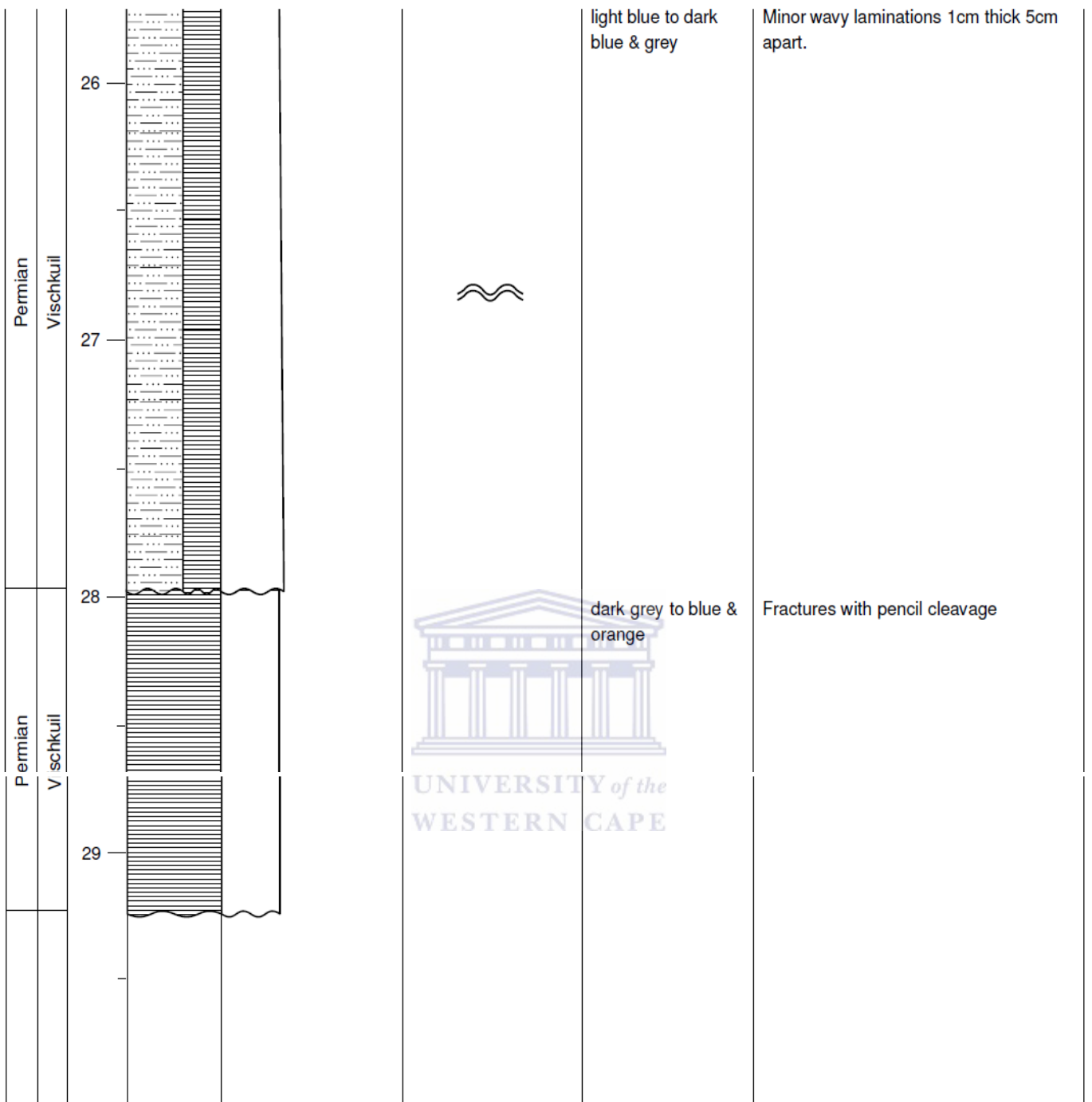
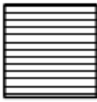
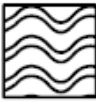

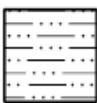

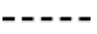
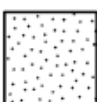






Figure 2.12.8: Vischkuil Formation Legend

Lithologies	Symbols	Base Boundaries
 Shale	 Wave ripple cross-lamination	 Erosion
 Siltstone	 Nodules and concretions	 Gradational
 Sandstone	 Planar cross bedding	 Sharp
 Fine ash	 Horizontal planar lamination	



Chapter Three

Interpretation

Geochemistry

3.1 TOC Interpretation

The amount of organic matter was determined using TOC. Forty samples were sent for TOC analyses at Bemlab. Rock samples were taken at various localities in the Fort Brown, Vischkuil and Laingsburg Formations, within the Laingsburg subbasin, whereas, Kookfontein core samples were obtained from the Tanqua subbasin. The Walkley-Black method was utilised at Bemlab. TOC was done first to screen the samples before it was sent for rock eval pyrolysis.

Samples below 0.5wt% is not reflected to be source rocks, but those at and above 0.5wt% are considered to be source rocks (Tissot & Welte, 1978). The results of the TOC data from most of the aforementioned Formations of interest was classified as inadequate. Two samples from the Vischkuil Formation passed through the marginal mark, which are samples 2 and 10. The Kookfontein samples also fell under the inadequate trend, but two samples showed signs of good and fair data, which are samples 12 and 53. The Laingsburg Formation showed signs of fair data, but poor data was the prominent result. The fair data of the Laingsburg Formation was obtained from samples 1, 2, 5 and 6. The marginal and adequate data from the Formations of interest was selected to be sent for Rock Eval analysis. Fort Brown had relatively low TOC values, so the two highest results were selected to be sent for Rock Eval. Overall, ten samples were selected from the 40 samples that had undergone TOC analysis.

3.2 Rock Eval Interpretation

Many different variables were interpreted using the Rock Eval 6 data. The data gave information pertaining to the hydrocarbon potential, the kerogen type, T_{max}, thermal maturity and the hydrocarbon index.

The Van Krevelen diagram displays three different types of kerogen, which ranges from type 1 to type 3. Type 1 alginite (composed of algal bodies) is from an aquatic environment and has high hydrocarbon content. Type 2 exinite (composed of pollen, spores, and cuticles of leaves of plants) is derived from a terrestrial environment. Type 2 is a high hydrocarbon content and is seen as a precursor for oil or gas. Type 3 vitrinite is also of a terrestrial nature (composed of fibrous, woody plant fragments and structureless colloidal humic matter). Vitrinite has a low hydrocarbon yield, but could be a possible precursor for gas. Type IV kerogen is associated with dead carbon (i.e. no hydrocarbon potential), low H/C and low O/C indices. Inertinite macerals are prominently found within type IV and are derived from reworked or oxidised kerogens.

The Hydrocarbon Index (HI) and Oxygen Index (OI) were used with the production index to obtain the kerogen type and maturity levels within the samples. Espitalié et al. (1977) proposed that the ratio of kerogen-derived hydrocarbons to organic carbon [hydrogen index (HI): S₂/TOC] and the ratio of kerogen-derived CO₂ (S₃) relative to organic carbon [oxygen index (OI): S₃/TOC] are comparable to the atomic H /C and O/C ratios, respectively. The bulk of the organic matter appears to be either type I, II or III, such values reveal the importance of recycled and/or strongly oxidised material as contributors of organic carbon. The elevated levels of oxidation may have been obtained through low-temperature subaerial weathering, biological oxidation (Tissot and Welte, 1978), or forest fires (Pocock, 1982). These data also aids in explaining the poorly defined S₂ peak and consequently the inability to establish a T_{max} value on many samples.

The T_{max} values are inapplicable owing to the fact that the S₂ values are too low, except for sample 12 of the Kookfontein Formation. Values of S₂ was unreliable due to the

TOC value of two of the samples chosen being below 0.5 wt.%, this was as a result of absorption of pyrolytic compounds onto the mineral matrix, which is also common in type 3 kerogen. Kookfontein 12 displayed a T_{max} value of 514°C, which has gas potential. The high T_{max} value of Kookfontein 12 has very little to no evidence of oil. The high T_{max} value was attributed to the partial absorption of clay in the rock sample that resulted in delays in the pyrolyzate. Since the T_{max} values of the rest of the samples could not be utilised the production index was looked at.

The production index gave information pertaining to the maturity levels within the rock and core samples. The Fort Brown samples were over mature. The Kookfontein samples displayed opposing levels of maturity, whereas sample 12 had reached peak maturity, sample 53 showed signs of immaturity. Samples 2, 5 and 6 of the Laingsburg Formation showed signs of peak maturity; whereas sample 1 from the same formation was over mature. Vischkuil sample 2 has reached peak maturity and sample 6 of the same formation was found to be over mature. The kerogen type formula of S2/S3 gave erroneous results, owing to the low peak produced by S2.

The hydrocarbon source potential of all the samples was very poor. The kerogen types predominant in the samples are type I, II and III, which is relevant owing to the fact that the depositional environments predominant in the Vischkuil and Laingsburg Formations are deep marine (Theron, 1967), the Kookfontein is deltaic (Wickens, 1994) and the Fort Brown is shallow marine (Cole, 1992). The Fort Brown, Laingsburg, Kookfontein and Vischkuil Formations exhibited type I-III kerogen. Type 1 and 2 are associated with oil potential, whereas type 3 is associated with gas potential. These samples contain alginite, exinite and vitrinite.

Overall the results of the rock eval were not good enough to be exploitable. This was due to the fact that majority of the samples were rock outcrop samples and were highly weathered and eroded thus displaying signs of oxidation and a low S2 peak. This resulted in errors in the T_{max} and kerogen type values. The only formation that showed greater results was the Kookfontein Formation, but only a limited amount of samples was looked

at within this formation. The hydrocarbon source potential of all the samples was very poor. The kerogen type in the samples ranges from type 1 to type 3.

3.3 XRD Interpretation

Qualitative XRD analyses were used to determine and evaluate the elemental concentrations⁸. Qualitative XRD was performed on the shale samples of the Vischkuil, Kookfontein, Laingsburg and the Fort Brown formations. The identification of clay minerals was determined by the peak positions and intensities. The qualitative identification looks at minerals that have the greatest peaks, then confirming the selection by searching for weaker peaks of the same mineral. Once the set of peaks was confirmed as belonging to a specific mineral, these peaks were eliminated from consideration. From the residual peaks, a mineral was used to determine the greatest remaining peak was looked at and then confirmed by identifying peaks of lesser intensity. This procedure was repeated until all peaks were identified.

The Vischkuil formation is comprised of quartz, chlorite, albite, montmorillonite and muscovite. Quartz is the most abundant mineral identified from the diffraction peaks. Chlorite is the second most abundant mineral displayed from the diffraction patterns, with minor traces of albite, montmorillonite and muscovite.

The Fort Brown formation contains minerals such as: quartz, chlorite, illite, albite and muscovite from the XRD data. Quartz, illite and chlorite are the major components displayed by the diffraction peaks, whereas albite and muscovite make up the remainder of the mineral assemblage.

The Kookfontein formation is comprised of chlorite, quartz, albite, muscovite and montmorillonite. Albite and quartz are the major minerals seen from the diffraction patterns, whereas montmorillonite, albite and muscovite constitute trace elements.

The Laingsburg formation contains minerals such as: quartz, chlorite, muscovite, albite and montmorillonite. Chlorite and quartz are the major minerals displayed by the diffraction peaks whereas; muscovite, albite and montmorillonite are in minor quantities.

3.3.1 Clay minerals

Clay minerals are formed beneath a fairly restricted range of geological conditions. Environments can range from soil horizons, continental, marine sediments, geothermal fields, volcanic deposits and weathering rock formation (Hillier, 1995).

Clay minerals are part of a essential group of the phyllosilicate group of minerals, which are recognised by layered structures composed of polymeric sheets of SiO_4 tetrahedra correlated to sheets of $(\text{Al, Mg, Fe})(\text{O,OH})_6$ octahedra⁹. Clay minerals are of great significance geochemically because of the abundance of clay in soils and sediments⁹.

There are four main groups of clay minerals, which are: kaolinite, illite, smectite and vermiculite⁹.

The kaolinite group of clay minerals includes kaolinite, dickite, nacrite and halloysite; produced by the decomposition of orthoclase feldspar⁹.

Illite clays also known as hydromicas are triple layered aluminosilicates with up to 8% K_2O (Hillier, 1995). The illite group of clay minerals contains hydrous micas, phengite, brammalite, celadonite, and glauconite; produced by the decomposition of several micas and feldspars; mainly in marine clays and shales⁹. The presence of potassium could be the result of partial degradation of potassium feldspars to kaolin, or the diagenesis of kaolin within a marine environment. Illite is the largest quantity of clays found within clay minerals, but is not as readily identified as kaolin because of the lack of crystals recognised under an microscope (Selley, 1982).

9) Introduction to Clay Minerals: [www.mineralatlas.com/General%20introduction/introduction to claymineralogy.htm](http://www.mineralatlas.com/General%20introduction/introduction%20to%20claymineralogy.htm)(Visited on 8 July 2010).

The smectite group of clay minerals contains montmorillonite, bentonite, nontronite, hectorite, saponite and saucanite; created by the variation of mafic igneous rocks rich in calcium and magnesium; weak connectivity by cations leads to high swelling or shrinking potential⁹.

Smectites are phyllosilicates containing a layered lattice configuration in which two-dimensional oxoanions are detached by layers of hydrated cations⁹. The oxygen atoms characterise the higher and lower sheets enveloping the tetrahedral zones, and the innermost sheet has brucite or gibbsite structure enclosing octahedral zones (Velde, 1995). Smectites that contain two tetrahedral sheets around the innermost octahedral sheet are referred to as phyllosilicates⁹. “A smectite is dioctahedral if two-thirds of the octahedral sites are occupied by trivalent cations and trioctahedral if all octahedral sites are filled with bivalent cations” (Velde, 1995:5).

Vermiculite is a highly charged phyllosilicate clay mineral. It is formed as the result of weathering of micas⁹. Vermiculite is hydrated and is capable of expanding, however at a much lower rate than smectite because of its comparatively high charge⁹.

3.3.2 Clay minerals in the studied samples

Illite, montmorillonite and chlorite are the most abundant clay minerals found within the studied shale samples. The clay samples were identified based on their peak position, intensity, shape and width.

3.3.2.1 Montmorillonite

Smectites are derived from various diagenetic sequence of events (Brosse, 1982), such as the modification of volcanic rocks (Fisher, 1977), or in soils beneath hydrolyzing surroundings (Chamley, 1989). The chemical composition of smectites changes depending upon the inherent environment⁵.

Montmorillonite consists of a three layered lattice which has unusual properties of expanding and constricting to adsorb water (Selley, 1982). Montmorillonite can absorb around 20% of water in addition to calcium and magnesium (Selley, 1982). Mudrocks comprised of a large quantity of smectite clays are referred to as bentonites (Hillier, 1995). Montmorillonite is a group of resilient 2:1 phyllosilicate clays containing a stable layered charge because of isomorphous substitution in the octahedral sheet (Hillier, 1995).

The dominant type of smectite is montmorillonite, with a chemical formula of: “ $(\frac{1}{2}\text{Ca}, \text{Na}) (\text{Al}, \text{Mg}, \text{Fe})_4 (\text{Si}, \text{Al})_8 \text{O}_{20} (\text{OH})_4 \cdot n\text{H}_2\text{O}$ ” (Hillier, 1995:12). Montmorillonite is the chief component of bentonite, originating from the weathering of volcanic ash (Selley, 1982). Montmorillonite can expand by several times its original volume when it comes in contact with water (Selley, 1982).

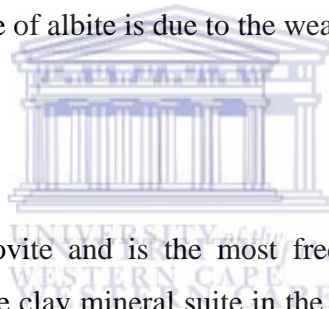
Montmorillonite (which is a form of smectite) was established within the Fort Brown, Laingsburg, Vischkuil and Kookfontein formation. A large content of detrital aluminum (beidelite) is produced as the result of chemical weathering, thus the alteration in the montmorillonite content in the samples can be associated with climate change (Chamley, 1989). Montmorillonite is associated with marine conditions. Increasing marine conditions can be monitored by the transformation of montmorillonite to chlorite (Velde, 1995). The montmorillonite samples is composed of $\text{Na}_{0.3} (\text{AlMg})_2 \text{Si}_4 \text{O}_{10} \text{OH}_2 \cdot 6\text{H}_2\text{O}$. The occurrence of albite in the shales samples is the result of weathering of feldspar.

3.3.2.2 Chlorite

Chlorites are comparable to clay minerals and share several affinities to the mica mineral group (Selley, 1982). Chlorites are assorted layered lattice clays of around 9% iron oxide and 30% magnesium oxide (Selley, 1982). Chlorites are produced as a varied result of primary micas and are a general accessory detrital mineral in immature sands and mudrock (Selley, 1982). On the other hand chlorite replaces illite and other clay minerals in which diagenesis combines with metamorphism (Selley, 1982).

The chlorite group minerals have a large variety of chemical compositions with Mg^{2+} , Fe^{2+} , Fe^{3+} and Al^{3+} contending for octahedral positions (Wenk and Bulakh, 2006). The two major members of the chlorite group are clinocllore ($Mg_3(OH)6Mg_2Al(HO)2Si_3AlO_{10}$) and chamosite ($Fe^{2+}_3(HO)6Fe_{2+2.5}Al_{0.5}(HO)2Si_{3.5}Al_{0.5}O_{10}$).

Chlorite group of minerals occurs in the Kookfontein, Vischkuil, and Fort Brown and Laingsburg formations. Chlorite is easily weathered and seldom found within the dominant mica of source rocks. Chlorite may have formed in marine environment, but it is postulated that the basic lattice is detrital in origin and that the only interlayer material is authigenic (Powers, 1957). The chlorite samples have a chemical composition of $Si_{2.86}Al_{1.14}.Al_{2.98}Mg$, which is related to the vermiculite group of clays, it is synonymous with biotite (which is present in the form of muscovite in the studied shale samples), whereas the presence of albite is due to the weathering of feldspars.



3.3.2.3 Illite

Illite is comparable to muscovite and is the most frequent clay mineral, comprising greater than fifty percent of the clay mineral suite in the deep marine (Velde, 1995). Illite forms due to the weathering of material in varying climates and reaches the ocean through river and wind action (Velde, 1995). Illite clays comprise a configuration related to that of muscovite, but are usually lacking in alkalies, with minor aluminium replacement of silicon. Consequently, the universal formula for the illites is: $K_yAl_4(Si_{8-y}, Aly)O_{20}(OH)_4$, typically with $1 < y < 1.5$, however y is constantly less than 2 (Velde, 1995). The charge imbalance between calcium and magnesium can result in the substitution of potassium (Velde, 1995). The potassium, calcium or magnesium interlayer cations avert water from entering the arrangement (Velde, 1995). In consequence of the aforementioned cations forces illite are non-swelling clays (Velde, 1995).

The illite group of minerals only occurs in the Fort Brown formation. Illite varieties of clays are produced from weathering of potassium and aluminium rich rocks during elevated pH conditions (Hillier, 1995). Hence, they develop by the modification of

minerals such as muscovite and feldspar. (Hillier, 1995) Illite clays are the foremost component of shales (Hillier, 1995). The illite samples have a chemical composition of $K (AlFe)_2 AlSi_3 O_{10} (OH)_2 \cdot 2H_2O$. In this case it is likely that illite is the result of the alteration products of muscovite and potassium feldspar.



Chapter Four

4.1 Conclusion and Discussion

This study includes the interpretation of the mineralogy, source rock types, kerogen type and source rock potential.

Three minerals were prominent in all four formations (based upon XRD analyses) which are: illite, montmorillonite and chlorite. Montmorillonite was established within the Fort Brown, Laingsburg, Vischkuil and Kookfontein formation. Montmorillonite is associated with marine conditions. Chlorite group of minerals occurred in the Kookfontein, Vischkuil, and Fort Brown and Laingsburg formations. Chlorite may have formed in a marine environment, but it is postulated that the basic lattice is detrital in origin and that the only interlayer material is authigenic. The illite group of minerals only occurred in the Fort Brown formation. In this study it is likely that illite is the result of the alteration products of muscovite and potassium feldspar.

Shale and claystone were the predominant source rocks identified. Forty samples were screened from TOC analyses for rock eval pyrolysis. The TOC revealed only ten samples viable for rock eval analyses.

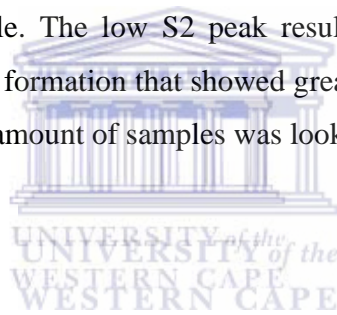
The Van Krevelen diagram displayed three different types of kerogen, which ranged from type 1 to type 3. Type 1 alginite is derived from an aquatic environment and has high hydrocarbon content. Type 2 exinite is derived from a terrestrial environment. Type 2 has high hydrocarbon content and is seen as a precursor for oil or gas. Type 3 vitrinite is also of a terrestrial nature. Vitrinite has a low hydrocarbon yield, but could be a possible precursor for gas.

The bulk of the organic matter appeared to be either type I, II or III, such values revealed the importance of recycled and/or strongly oxidised material as contributors of organic carbon. The elevated levels of oxidation may have been obtained through low-temperature subaerial weathering, biological oxidation, or forest fires. This data aids in

explaining the poorly defined S2 peak and consequently the inability to establish a Tmax value on many samples.

The production index gave information pertaining to the maturity levels within the rock and core samples. The Fort Brown samples were over mature. The Kookfontein samples displayed opposing levels of maturity. The Laingsburg formation and Vischkuil formations fell under the same trends as the Kookfontein formation samples

The hydrocarbon source potential of all the samples was very poor. Some discrepancies were found in the rock eval data between the HI vs. OI and HI vs. TOC diagrams. The errors arose from the fact that the S2 peak was very low and that the rock outcrop samples were highly weathered and oxidised. Overall the results of the rock eval were not good enough to be exploitable. The low S2 peak resulted in errors in the Tmax and kerogen type values. The only formation that showed greater results was the Kookfontein Formation, but only a limited amount of samples was looked at within this formation.



4.2 Recommendation

A series of analyses needs to be done based upon the rock eval findings, to further look at the lithological characteristics and ascertain the extent of the source potential within the upper Ecca. The inability to obtain a core samples from the all the formations brought about limitations to the extent at which analyses can be carried out. Additional studies in this area need to be undertaken to produce more concrete findings. Some petrographic analyses can still be carried out e.g. XRF and SEM to explain the diagenetic history of the area.



References

- **Allen, P.A. & Allen, J.R.** (1990). *Basin Analysis, Principles and Applications*. United Kingdom: Blackwell Publishing, p.335-338.
- **Almond, J.E.** (2010). Falcon Oil & Gas Ltd Exploration Right – southern Main Karoo Basin, Western, Northern and Eastern Cape Provinces, RSA.
- **Andersson, P.O.D., Worden, R.H.** (2004). Mudstones of the Tanqua Basin, South Africa: an analysis of lateral and stratigraphic turbidite fans. *Sedimentology*, 51(10): 479-502. Available from Science Direct database: <http://www.sciencedirect.com> (Accessed 26 July 2009).
- **Andersson, P.O.D., Worden R.H., Hodgson D.M. & Flint, S.** (2004). Provenance evolution and chemostratigraphy of a Palaeozoic submarine fan complex: Tanqua Karoo basin, South Africa. *Marine and Petroleum Geology*, 21:555-557. Available from Elsevier database: <http://www.elsevier.com> (Accessed 26 July 2009).
- **Anketell, J.M. Cegla, J. & Dzulynski S.** (1970). On the deformational structures in systems with reversed density gradients. *Annual Geologic Society of Poland*, 40: 3–30.
- **Basin Modelling** wwwoil (n.d.). Available from: [http://www.landforms.eu/Orkney/Geology/Oil/OIL%20orkney%20devonian%20source%20rock%20quality.htm#THE ABUNDANCE](http://www.landforms.eu/Orkney/Geology/Oil/OIL%20orkney%20devonian%20source%20rock%20quality.htm#THE%20ABUNDANCE) (Accessed 13 February 2010).
- **Bates, C.C.** (1953). Rational Theory of Delta Formation: *American Association of Petroleum Geologists, Bulletin*. 37: 2119.

- **Besaans, A. J.** (1970-98). Geological Map of South Africa. *Ladismith, southwestern sheet*, 3320, 1:250 000, Pretoria: Geological Survey of the Republic of South Africa.
- **Boggs, S., Jr.** (2001). *Principles of Sedimentology and Stratigraphy*, 3rd Edition. Upper Saddle River, New Jersey: Prentice-Hall, p.162-168.
- **Bouma, A.H.** (1962). *Sedimentology of some Flysch Deposits: a graphic approach to facies interpretation*. Amsterdam: Elsevier, p.168.
- **Bouma, A.H. & Hollister, C.D.** (1973). Deep ocean basin sedimentation. In *Turbidites and Deepwater Sedimentation*. Society of Economic Paleontology and Mineralogy. California: Pacific, p.79-118. [Short course notes].
- **Brosse, R.** (1982). *Sedimentary processes in the river Loire*. Doctoral dissertation. France: University of Angers.
- **Cairncross, B.** (2001). An overview of the Permian (Karoo) coal deposits of southern Africa. *Journal of African Earth Sciences*, 33:529-562. Available from Scencedirect database: <http://www.sciencedirect.com> (Accessed 21 July 2009).
- **Catuneanu, O. & Bowker, D.** (2001). Sequence stratigraphy of the Koonap and Middleton fluvial formations in the Karoo foredeep South Africa. *Journal of African Earth Sciences*, 33:579-595. Available from Scencedirect database: <http://www.sciencedirect.com> (Accessed 6 July 2009).
- **Catuneanu, O., Hancox, P. J. & Rubidge, B. S.** (1998). Reciprocal flexural behaviour and contrasting stratigraphies: a new basin development model for the Karoo retroarc foreland system, South Africa. *Basin Research*, 10: 417 – 439. Available from Scencedirect database: <http://www.sciencedirect.com> (Accessed 6 July 2009).

- **Catuneanu, O., Hancox, P.J., Cairncross, B. & Rubidge, B.S.** (2002). Foredeep submarine fans and the forebulge delta; orogenic off-loading in the underfilled Karoo basin. *Journal of African Earth Sciences*, 35:489-502. Available from Elsevier database: <http://www.elsevier.com> (Accessed 6 July 2009).
- **Catuneanu, O., Wopfner, H., Eriksson, P.G., Cairncross, B., Rubidge, B.S., Smith, R.M.H. & Hancox, P.J.** (2005). The Karoo basins of south-central Africa. *Journal of African Earth Sciences*, 43: 211-253. Available from Sciencedirect database: <http://www.sciencedirect.com> (Accessed 6 July 2009).
- **Chamley, H.** (1989). *Clay Sedimentology*. New York: Springer – Verlag, p. 623.
- **Clay minerals** www mineralogy (n.d.). Available from: http://earth.usc.edu/~dfarris/Mineralogy/17_ClayMinerals.pdf (Accessed 25 August 2010).
- **Cole, D.I.** (1992). Evolution and development of the Karoo Basin. In *Inversion Tectonics of the Cape Fold Belt, Karoo and Cretaceous Basins of Southern Africa*. Edited by de Wit, M.J. & Ransome, I.G.D. Rotterdam: Balkema, p. 87–100.
- **Coleman, J.M. & Wright, L.D.** (1971). Analysis of major river systems and their deltas, procedures and rationale, with two examples. *Louisiana State University., Coastal Studies Institute of Technology*, Report. 95, p.125.
- **Connolly, J.R.** (2010). *Introduction Quantitative X-Ray Diffraction Methods*. Available from: <http://epswww.unm.edu/xrd/xrdclass/09-Quant-intro.pdf> (Accessed 20 June 2010).

- **Cramez, C.** (2001). *Turbidite Systems in Hydrocarbon Exploration*, University of Fernando Pessoa, Portugal. Available from: <http://homepage.ufp.pt/biblioteca/WEBTurDiDepSystems/Pages/Page4.htm> (Accessed 15 August 2010).
- **Curray, J.R.** (1960) Sediments and history of Holocene transgression, continental shelf, northwest Gulf of Mexico. In *Recent Sediments, Northwestern Gulf of Mexico*. Edited by Shepard, F.P., Phleger, F.B. & Van Andel, T.H. American Association of Petroleum Geologists, p. 221-236.
- **De Beer, C. H.** (1999). Structure of the Cape Fold belt in the Ceres Arc. *Geological Survey of South Africa, Bulletin.123*, p.93.
- **Dingle, R. V. & Siesser, W.G.** (1977). *Geology of the continental margin between Walvis Bay and Ponta Do Ouro: Volume two of Marine Geosciences Series*. Geological Survey (South Africa), Pretoria: The Government Printer.
- **Dumas, D. & Arnott, R.W.C.** (2006). Origin of hummocky and swaley cross-stratification – The controlling influence of unidirectional current strength and aggradation rate (Abstract) *Geology*, 34 (12) 1073-1076. Available from: Geoscience World <http://geology.geoscienceworld.org/cgi/content/abstract/34/12/> (Accessed 20 August 2010).
- **Espitalie, J. M., Madec, M., Tissot, B., Mennig, J. J. & Leplat, P.** (1977). *Source rock characterization method for petroleum exploration*. 9th Annual Offshore Technology Conference held in Houston, Texas. Conducted by Preprints, p.439-448.
- **Falcon-Lange, H.J.** (2003). Small cordaitalean trees in a marine-influenced coastal habitat in the Pennsylvanian Joggins Formation, Nova Scotia. *Journal of Geological Society*, 162(3): 485-500.

- **Faure, K. and Cole, D.** (1999). Geochemical evidence for lacustrine microbial blooms in the vast Permian main Karoo, Parana, Falkland Islands and Huab basins of southwestern Gondwana. *Palaeogeography, Palaeoclimatology and Palaeoecology*, 152 (3-4): 189–213.
- **Fisher, G.W.** (1977). Non-equilibrium thermodynamics in metamorphism. In *Thermodynamics in Geology*. Edited by Fraser, D.G. Boston: Reidel Publishing. p. 381-403.
- **Fisk, H.N.** (1944). Geological Investigations of the Alluvial Valley of the Lower Mississippi River. *U.S. Department of the Army, Mississippi River Commission*, p.78.
- **Fisk, H.N.** (1947). Fine-Grained Alluvial Deposits and Their Effects on Mississippi River Activity. *U.S. Cooperation of Engineers, Mississippi River Commission Vicksburg, Mississippi*.
- **Flint, S. S., Hodgson, D. M., King, R. C., Potts, G. J., Van Lente, B. & Wild, R. J.** (2004). *The Karoo Basin Slope Project – Final Report: Phase 1. Industry consortium report* (unpublished). The Universities of Liverpool and Stellenbosch. (CD-ROM).
- **Folk, R.L.** (1959). Practical petrographic classification of limestones. *American Association of Petroleum Geologists. Bulletin*.43, p. 1-38.
- **Folk, R.L.** (1962). Spectral subdivision of limestone types. In *Classification of Carbonate Rocks-A Symposium*. Edited by Ham, W.E. American Association of Petroleum Geologists, Memoir 1, p. 62-84.
- **Galloway, W.E.** (1975). Process framework for describing the Morphologic and Stratigraphic Evolution of Deltaic Depositional Systems. In *Deltas, models for*

exploration. Edited by Broussard, M.L. Texas: Houston Geological Society. p.555.

- **Gier, S. & Johns, W.D.** (2005). Clay mineral diagenesis in interbedded sandstones and shales (Aderklaa-78, Vienna Basin): Comparisons and correlations (Abstract). 7:5448. Available from: <http://meetings.copernicus.org/www.cosis.net/abstracts/EGU05/05448/EGU05-J-05448.pdf> (Accessed 13 June 2010).
- **Glaister, R.P. & Hopkins, J.** (1983). Turbidity-current and Debris-flow Deposits *Canadian Society of Petroleum Geologists*. p. 23-25.
- **Goldhammer, R. K., Wickens, H. DeV., Bouma, A. H. and Wach, G.** (2000). Sequence stratigraphic architecture of the Late Permian Tanqua submarine fan complex, Karoo Basin, South Africa. In *Fine-grained turbidite systems*. Edited by Bouma, A.H. & Stone, C.G. AAPG Memoir 72: SEPM Special Publication 68, p. 165 - 172.
- **Google Earth** (2005-2011). (Free Computer Software). Available from: <http://www.google.com/earth/download/ge/agree.html>.
- **Grecula, M.** (2000). *Stratigraphy and architecture of tectonically controlled turbidite systems: Laingsburg Formation, Karoo Basin, South Africa*. Doctoral dissertation. United Kingdom: University of Liverpool, p. 291.
- **Grecula, M., Flint, S. S. Wickens, H. DeV. & Johnson, S. D.** (2003). Upward-thickening patterns and lateral continuity of Permian sand-rich turbidite channel fills, Laingsburg Karoo, South Africa. *The Journal of the International Association of Sedimentologists*, 50 (5): 831 – 853.
- **Haszeldine, R.S., Cavanagh, A.J. & England, G.L.** (2003). Effects of oil charge on illite dates and stopping quartz cement: calibration of basin models (Abstract).

Journal of Geochemical Exploration, 78-79: 373-376. Available from Sciencedirect database: <http://www.sciencedirect.com> (Accessed 8 August 2010).

- **Herbert, C.T & Compton, J.S.** (2007). Depositional environments of the lower Permian Dwyka diamictite and Prince Albert shale inferred from the geochemistry of early diagenetic concretions, southwest Karoo Basin, South Africa. *Sedimentary Geology*, 194: 263-277. Available from Sciencedirect database: <http://www.sciencedirect.com> (Accessed 6 July 2010).
- **Herbert, S.Z. & Shaffer, P.R.** (1971). *Rocks and Minerals*. England; Paul Hamlyn.
- **Hillier, S.** (1995). *Erosion and Sedimentation and Sedimentary Origin of clays*. New York: Springer-Verlag, p.162-219.
- **Hydrocarbon Prospects and Exploration Plays** (n.d.). Available from: <http://www.ccop.or.th/ppm/document/CAEXV2/CAEXV2DOC02.pdf> (Accessed 16 October 2009).
- **Introduction to Clay Mineralogy** www introduction to clay mineralogy (2008). Available from: [http://www.mineralatlas.com/General%20introduction/introduction to clay mineralogy.htm](http://www.mineralatlas.com/General%20introduction/introduction%20to%20clay%20mineralogy.htm)(Accessed 8 July 2010).
- **Johnson, A.H.** (1970). *Physical processes in geology*. San Francisco, California: Freeman, Cooper and Co., p. 577.
- **Johnson, M. R.** (1991). Sandstone petrography, provenance and plate tectonic setting in Gondwana context of the southeastern Cape-Karoo Basin. *South African Journal of Geology*, 94(2-3): 137-154. Available from Sciencedirect database: <http://www.sciencedirect.com> (Accessed 6 July 2010).

- **Johnson, S.D., Flint, S.S., Hinds, D. & Wickens, H. de V.** (2001). Anatomy, geometry and sequence stratigraphy of basin floor to toe of slope basin turbidite systems, Tanqua Karoo, South Africa. *Sedimentology*, 48: 987-1024.
- **Johnson, M.R., Van Vuuren, C.J., Hegenberger, W.F., Key, R. & Shoko, U.** (1996a). Stratigraphy of the Karoo Supergroup in southern Africa: an overview. *Journal of African Science*, 23(1): 3-15. Available from Sciencedirect database: <http://www.sciencedirect.com> (Accessed 6 July 2010).
- **Johnson, M. R., Van Vuuren, C. J., Visser, J. N. J., Cole, D. I., Wickens, H. DeV., Christie, A. D. M., Roberts, D. L. & Brandl, G.** (1996b). Sedimentary rocks of the Karoo Supergroup In *The Geology of South Africa*. Edited by Johnson, M.R., Anhaeusser, C.R. & Thomas, R.J. Council for Geoscience, p. 461 – 490.
- **Johnson, M. R., Van Vuuren, C. J., Visser, J. N. J., Cole, D. I., Wickens, H. DeV., Christie, A. D. M. & Roberts, D. L.** (1997). The Foreland Karoo Basin, South Africa. In *Sedimentary basins of the world*. Edited Hsü, K.J. & Selley, R.C. Elsevier, p. 269 – 317.
- **Johnston, W.A.** (1921) Sedimentation of the Fraser River Delta. *Geological Survey of Canada*, Memoir 125, p.46.
- **Karmakar, R., Manna, S.S. & Dutta, T.** (2003). A geometrical model of diagenesis using percolation theory, *Physica A*, 318: 113.
- **Kearey, P.** (1996). *Dictionary of Geology*. England: Penguin Books.
- **Kerogen** www kerogen (n.d.). Available from: <http://www.eaps.mit.edu/geobiology/biomarkers/kerogen.html> (Accessed 10 February 2010).

- **Kingsley, C. S.** (1981). A composite submarine fan-delta-fluvial model for the Ecca and lower Beaufort Groups of Permian age in the Eastern Cape Province, South Africa. *Transactions of the Geological Society South Africa*, 84: 27 – 40.
- **Kuntcheva, B., Kruhl, J.H. & Kunze, K.** (2006). Crystallographic orientations of high-angle grain boundaries in dynamically recrystallised quartz: First results. *Tectonophysics*, 421: 331-346.
- **MacDonald, J. G., Burton, C. J., Winstanley, I. & Lapidus, D. F.** (2003). *Collins Dictionary of Geology*. Glasgow: Harper Collins
- **Lafargue, E., Espitalié, J., Marquis, F. & Pillot, D.** (n.d.). Rock-Eval 6 applications in hydrocarbon exploration, production and in soil contamination studies. In *Revue de l'Institut Français du Pétrole*. France: Vinci Technologies, 53(4): 421-437.
- **Lee, Y.I., Sur, K.H. & Hisada, K.** (2005). Assymmetric diagenetic changes in a half-graben basin: the Kanmon Group (Lower Cretaceous), SW Japan. *Cretaceous Research*, 26: 73-84.
- **Long, D.** (1993). *The Burgsvik Beds, an Upper Silurian storm generated sand ridge complex in southern Gotland, Sweden*. GFF 115: 299–226.
- **Loon, Van M.** (1 March 2007). *South Africa's license round is on the road*. Available from First Break: <http://fb.eage.org/content.php?id=27371> (Accessed 2 August 2009).
- **Martini, J. E. J.** (1974). On the presence of ash beds and volcanic fragments in the greywackes of the Karoo System in the southern Cape Province (South Africa). *Transactions of the Geological Society South Africa*, 77: 113 – 116.

- **Matthews, G.P. & Ridgway, C.J.** (1996). Modelling of simulated clay precipitation within reservoir sandstones. *Marine and Petroleum Geology*, 13(5): 581-589.
- **McGraw-Hill.** (2003). *McGraw-Hill dictionary of earth science*, 2nd Edition. United States: McGraw-Hill, p.326.
- **McHardy, W.J., Wilson, M.J. & Tait, J.M.** (1982). Electron microscope and X-ray diffraction studies of filamentous illitic clay from sandstones of the Magnus Field. *Clay Minerals*, 17: 23-39.
- **Middleton, G.V.** (1967). Experiments on density and turbidity currents: III Deposition of sediment. *Canadian Journal of Earth Sciences*, 4: 475-505.
- **Moore, G.T. & Asquith, D.O.** (1971). Delta-Term and Concept. *Geological Society of America*, Bulletin.82: 2563-2568.
- **Morgan, J.P.** (1970). Depositional processes and products in the deltaic environment. In *Deltaic Sedimentation, Modern and Ancient*. Edited by Morgan, J.P. Special Publication, Economic Society of Paleontology and Mineralogy, 15: 31-47.
- **Nichols, G.** (2009). *Sedimentary and Stratigraphy*, 2nd Edition. United Kingdom: Wiley- Blackwell.
- **Operational Theory www service and support** (n.d.). Available from: <http://ks-analytical.com/service-and-support> (Accessed 10 February 2010).
- **Opuwari, M.** (2011). *Field Development Geology 1*, p.46. [Lecture Notes].

- **Pasquini, C., Lualdi, A. & Vercesi, P.** (2004). Depositional dynamics of glaucony-rich deposits in the Lower Cretaceous of the Nice arc, southeast France. *Cretaceous Research*, 25: 179-189.
- **Peters, K. E.** (1986). Guidelines for evaluating petroleum source rock using programmed pyrolysis. *American Association of Petroleum Geologists, Bulletin*. 70(3): 318 – 329.
- **Pocock, S.A.J.** (1982). Identification and recording of particulate sedimentary organic matter. In *How to Assess Maturation and Palaeotemperatures*. Edited by Staplin, F. L. Tulsa (Economic Society of Paleontology and Mineralogy), p. 13-131.
- **Powers, M.C.** (1957). Adjustment of clays to chemical change and the concept of the equivalence level. *Clays Clay Minerals, Proceedings of the Geology National Conference*, 6: 309-326.
- **Press, F., Siever, R. Grotzinger, J. & Jordan, T.H.** (2004). *Understanding Earth*, 4th Edition, England: W.H. Freeman and Co., p.165-169.
- **Publication Services** www tn30 (n.d.). Available from: http://www.odp.tamu.edu/publications/tnotes/tn30/tn30_12.htm (Accessed 10 February 2010).
- **Raseroka, L. & McLachlan, I.R.** (5 June 2009). *The Petroleum Potential of South Africa's Onshore Karoo Basins* Available from Search and Discovery: <http://www.searchanddiscovery.com/documents/2009/10196raseroka/index.htm> (Accessed 2 August 2009).
- **Rasmussen, B.** (2005). Radiometric dating of sedimentary rocks: the application of diagenetic xenotime geochronology. *Earth Science Reviews* 68 (3-4): 197-243.

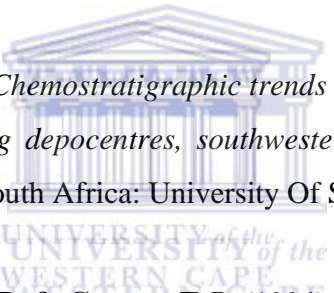
- **Reading, H.G.** (1986). Facies. In *Sedimentary Environments and Facies*, 2nd Edition. Edited by Reading, H.G. Department of Earth Sciences, University of Oxford: Blackwell Science.
- **Reineck, H.** (1967). Layered Sediments of Tidal Flats, Beaches, and Shelf Bottoms of the North Sea. In *Estuaries*. Edited by Lauff, G.H. American Association of Advanced Science Publisher, 83: 191-206.
- **Reineck, H.E. & Singh, I.B.** (1980). *Depositional Sedimentary Environments with reference to Terrigenous Clastics*. New York: Springer-Verlag, p.5-7.
- **Renard, F., Ortoleva, P. & Gratier, J.P.** (1997). Pressure solution in sandstones: influence of clays and dependence on temperature and stress. *Tectonophysics*, 280(3-4): 257-266. Available from Sciencedirect database: <http://www.sciencedirect.com> (Accessed 6 July 2010).
- **Rowell, D. M. & De Swardt, A. M. J.** (1976). Diagenesis in Cape and Karoo sediments, South Africa, and its bearing on their hydrocarbon potential. *Geological Society of South Africa.*, 79 (1): 81-145.
- **Rubidge, B.S.** (1995). Biostratigraphy of the Beaufort Group (Karoo Supergroup). Edited by Rubidge, B.S. *South African Committee for Stratigraphy*. Biostratigraphic Series 1:46.
- **Russell, R.J.** (1936). Physiography of Lower Mississippi River Delta. In *Lower Mississippi River Delta*. Conservation Geology, Bulletin. 8, p. 1–199.
- **Russell, R.J. & Russell, R.D.** (1939). Mississippi river delta sedimentation. In *Recent marine sediments*. Edited by Trask, P.D. p.153-177.

- **Schlumberger.** (2009). *Vitrinite reflectance*. Available from: <http://www.glossary.oilfield.slb.com/Display.cfm?Term=vitrinite%20reflectance> (Accessed 20 August 2009).
- **Schnitzer, M.** (1978). Humic substances: Chemistry and reactions. In *Soil Organic Matter*. Edited by Schnitzer and, M. & Khan, S.U. New York: Elsevier Scientific Publishing Co., p. 1-64.
- **Schumacher, A.B.** (2002). *Methods for the Determination of Total Organic Carbon (TOC) in Soils and Sediments*. Doctoral dissertation. U.S. Environmental Protection Agency. Las Vegas: Office of research and Development, p.1-25. Available from U.S. Environmental Protection Agency: <http://www.epa.gov/esd/cmb/research/papers/bs116.pdf> (Accessed 12 May 2011).
- **Selley, R.C.** (1982). *Introduction to sedimentology*, 2nd edition. London: Academic Press, 417p.
- **Shanmugam, G.** (2000). 50 years of the turbidite paradigm (1950s – 1990s): deep-water processes and facies models – a critical perspective. *Marine and Petroleum Geology*, 17(2): 285 – 342. Available from Sciencedirect database: <http://www.sciencedirect.com> (Accessed 6 July 2010).
- **Shawa, M.S., Lee, P.J. & Young F.G.** (1983). Recognition of deltas: A general review. *Canadian Society of Petroleum Geologists*, p.3-7.
- **Shepard, F.P & Dill, R.F.** (1966). *Submarine Canyons and other Sea Valleys*. Chicago: Rand McNally and Co., p.381.
- **Sixsmith, P. J.** (2000). *Stratigraphic development of a Permian turbidite system on a deforming basin floor: turbidite systems: Laingsburg Formation, Karoo*

Basin, South Africa. Doctoral dissertation. United Kingdom: University of Liverpool.

- **Smith, R.M.H.** (1990). A review of stratigraphy and sedimentary environments of the Karoo Basin South Africa. *Journal of African Earth Sciences*, 10:117-137.
- **Smith, R. M. H., Erickson, P. A. & Botha W. J.** (1993). A review of the stratigraphy and sedimentary environments of the Karoo-aged basins of southern Africa. *Journal of African Earth Sciences*, 16(1-2): 143 – 169. Available from Sciencedirect database: <http://www.sciencedirect.com> (Accessed 1 April 2010).
- **Storvoll, V., Bjørlykke, K. Karlsen, D. & Saigal, G.** (2002). Porosity preservation in reservoir sandstones due to grain-coating illite: a study of the Jurassic Garn Formation from the Kristin and Lavrans fields, offshore Mid-Norway. *Marine and Petroleum Geology*, 6(19): 767-781. Available from Sciencedirect database: <http://www.sciencedirect.com> (Accessed 25 September 2009).
- **Stow, A.V.D.** (2009) *Sedimentary Rocks in the Field: A Color Guide*. New York: Academic Press.
- **Svensen, H., Bebout, G., Kronz, A., Li L., Planke, S., Chevallier, L. & Bjørn, J.** (2008). Nitrogen geochemistry as a tracer of fluid flow in a hydrothermal vent complex in the Karoo Basin, South Africa. *Geochimica et Cosmochimica Acta*, 72: 4929–4947. Available from Sciencedirect database: <http://www.sciencedirect.com> (Accessed 15 June 2009).
- **Steyn, J. H.** (1983). Geological Map of South Africa. *Sutherland*, 3320, 1:250 000, Pretoria: Geological Survey of the Republic of South Africa.

- **Tasa Clips Images for the Geoscience** www illustrations (n.d.): Available from : <http://tasaclips.com/illustrations.html> (Accessed 25 September 2009).
- **Taylor, K.G., Gawthorpe, R.L. & Fannon-Howell, S.** (2004). Basin-scale diagenetic alteration of shoreface sandstones in the Upper Cretaceous Spring Canyon and Aberdeen Members, Blackhawk Formation, Book Cliffs, Utah. *Sedimentary Geology*, 172: 99-115. Available from Sciencedirect database: <http://www.sciencedirect.com> (Accessed 25 September 2009).
- **Terwindt, J. H. J. & Breusers, H. H. C.** (1971). Experiments on the Origin of Flaser, Lenticular and Sand-Clay Alternating Bedding. *Sedimentology*, 19: 85-98. Available from Sciencedirect database: <http://www.sciencedirect.com> (Accessed 16 October 2009).
- **Theron, A. C.** (1967). *The sedimentology of the Koup Subgroup near Laingsburg*. Masters dissertation. South Africa: University of Stellenbosch.
- **Theron, J. N.** (1986). Geological Map of South Africa. *Ladismith*, 3320, 1:250 000, Pretoria: Geological Survey of the Republic of South Africa.
- **Thomas, C.** (1997). Geological Map of South Africa. *Worcester*, 3319, 1:250 000, Pretoria: Geological Survey of the Republic of South Africa.
- **Tiessen, H. & Moir, J.O.** (1993). Total and organic carbon. In *Soil Sampling and Methods of Analysis*. Edited by Carter, M.E. Florida: Lewis Publ., p. 187-211.
- **Tissot, B.P. & Welte, D.H.** (1978). *Petroleum Formation and Occurrence*. New York: Springer-Verlag, p.699.
- **Trowbridge, A.C.** (1930). Building of Mississippi Delta. *American Association of Petroleum Geologists, Bulletin*. 14, p. 867-901.

- **Turner, B.R.** (1975). *The stratigraphy and sedimentary history of the Molteno Formation in the main Karoo basin of South Africa and Lesotho*. Unpublished doctoral dissertation. Johannesburg: University of the Witwatersrand.
- Vance, D.J.** (1992). Activity patterns of juvenile penaeid prawns. In response to artificial tidal and day-night cycles; a comparison of three species. *March Ecological Program Series*, 87: 215-226
- **Van der Werff, W. & Johnson, S.** (2003). High resolution stratigraphic analysis of a turbidite system, Tanqua Karoo Basin, South Africa. *Marine and Petroleum Geology*, 20: 45–69. Available from Sciencedirect database: <http://www.sciencedirect.com> (Accessed 16 October 2009).
- 

UNIVERSITY of the
WESTERN CAPE
- **Van Lente, B.** (2004). *Chemostratigraphic trends and provenance of the Permian Tanqua and Laingsburg depocentres, southwestern Karoo Basin, South Africa*. Masters Dissertation, South Africa: University Of Stellenbosch.
 - **Veevers, J.J., Cole, D.I. & Cowan, E.J.** (1994). Southern Africa: Karoo Basin and Cape Fold Belt. In *Permian-Triassic Pangean basins and fold belts along the Panthalassan Margin of Gondwana*. Edited by Veevers, J.J. & Powell, C. McA. Geological Society of America, Memoir, p.184, 223–279.
 - **Velde, B.** (1995). Composition and mineralogy of clay minerals. In *Origin and mineralogy of clays*. Edited by Velde, B. New York: Springer-Verlag, p.8-42.
 - **Viljoen, J. H. A.** (1992a). Lithostratigraphy of the Laingsburg Formation (Ecca Group). *South African Committee for Stratigraphy*, Lithostratigraphic Series 20, p. 7.
 - **Viljoen, J. H. A.** (1992b). Lithostratigraphy of the Collingham Formation (Ecca Group), including the Zoute Kloof, Buffels River and Wilgehout River members

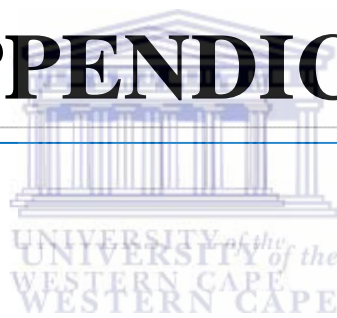
and the Matjiesfontein Chert Bed. *South African Committee for Stratigraphy*, Lithostratigraphic Series 22, p.10.

- **Viljoen, J. H. A.** (1995). *Piroklastiese afsettings van Perm-ouderdom in die hoof-Karookom met spesiale verwysing na die Collingham Formasie, Ecca Groep* [Pyroclastic deposits of Permian age in the main Karoo with special reference to the Collingham Formation, Ecca Group]. Doctoral dissertation. South Africa: University of Stellenbosch, p.274.
- **Viljoen, J. H. A. & Wickens, H. DeV.** (1992). Lithostratigraphy of the Vischkuil Formation (Ecca Group). *South African Committee for Stratigraphy*, Lithostratigraphic Series 19, p.7.
- **Visser, J.N.J.** (1986). Lateral lithofacies relationships in the glaciogene Dwyka Formation in the western and central parts of the Karoo Basin. *Transactions of the Geological Society of South Africa*, p. 89, 373–383.
- **Visser, J. N. J.** (1991). Self-destructive collapse of the Permo-Carboniferous marine ice sheet in the Karoo Basin: evidence from the southern Karoo. *South African Journal of Geology* 94: 255 – 262. Available from Scencedirect database: <http://www.sciencedirect.com> (Accessed 25 September 2009).
- **Visser, J. N. J.** (1992). Basin tectonics in southwestern Gondwana during the Carboniferous and Permian. In: *Inversion Tectonics of the Cape Fold Belt, Karoo and Cretaceous Basins of Southern Africa*. Edited by M. J. De Wit M.J. & I. G. D. Ransome I.G.D. p. 109 – 115.
- **Visser, J. N. J. & Loock, J. C.** (1978). Water depth in the main Karoo Basin in South Africa during Permian sedimentation. *Transactions of the Geological Society of South Africa*, 81:185 – 191. Available from Scencedirect database: <http://www.sciencedirect.com> (Accessed 5 October 2009).

- **Wach, G. D., Lukas, T. C., Goldhammer, R. K., Wickens, H. DeV., Bouma, A. H. & Wach, G. (2000).** Submarine fan through slope to deltaic transition basin-fill succession, Tanqua Karoo, South Africa. In *Fine-grained turbidite systems*. Edited by Bouma A.H. & C. G. Stone C.G. AAPG Memoir 72: SEPM Special Publication 68, p. 173-180.
- **Walker, R.G. (1967).** Turbidite Sedimentary Structures and their Relationship to Proximal and Distal Depositional Environments. *Journal of Sedimentary Petrology*, 37: 25-443. Available from Sciencedirect database: <http://www.sciencedirect.com> (Accessed 16 July 2010).
- **Walther, J. (1894).** Lithogenesis der Gegenwart. Beobachtungen über die Bildung der Gesteine von der heutigen Erdoberfläche. Dritter Teil einer Einleitung in die Geologie als historische Wissenschaft, *Jena: Verlag Gustaf Fischer* [Lithogenesis the present. Observations on the rocks of the today Building earth's surface. Third part of an introduction to the geology as a historical science, *Jena: Gustav Fischer Verlag*] p. 535-1055.
- **Weaver, C. E. & Beck, K. C. (1977).** Miocene of the S.E. United States: A Model for Chemical Sedimentation in a Peri-marine Environment. *Developments in Sedimentology*, Amsterdam: Elsevier, 22: 201-225.
- **Weaver, C.E. & Pollard, L.D. (1975).** Chemistry of Clay Minerals, *Developments in Sedimentology*, Amsterdam: Elsevier.
- **Wenk, H.R. & Bulakh, A. (2006).** *Minerals: their constitution and origin*. New York: Cambridge University Press.
- **Wickens, H. DeV. (1994).** *Basin floor fan building turbidites of the southwestern Karoo Basin, Permian Ecca Group, South Africa*. Doctoral dissertation, South Africa: University of Port Elizabeth, p.233.

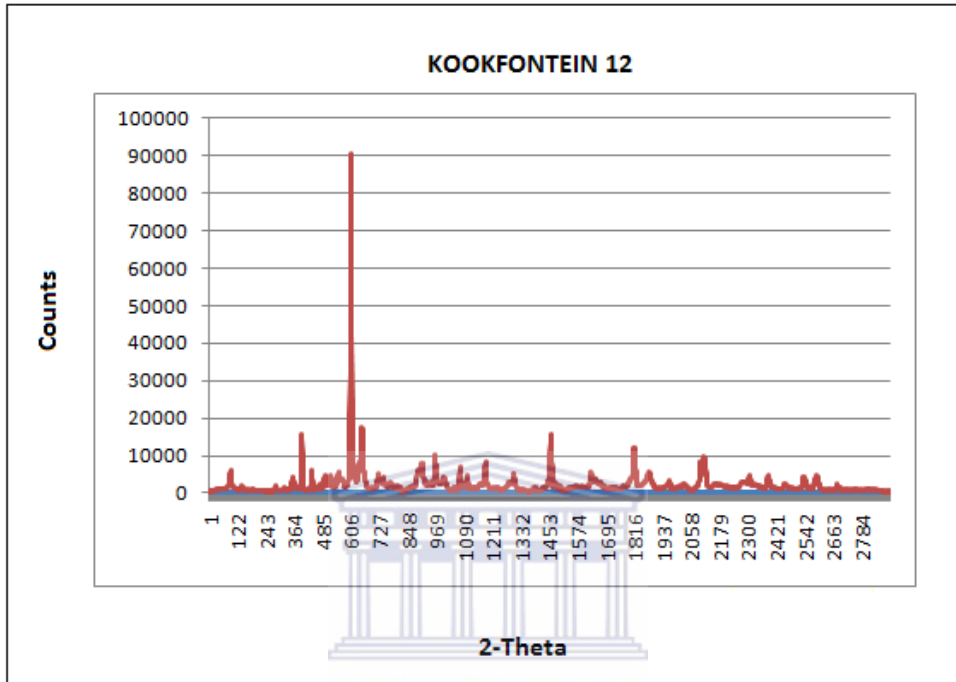
- **Wickens, H. DeV. & Bouma, A. H.** (2000). The Tanqua Fan Complex, Karoo Basin, South Africa – Outcrop analog for fine-grained, deepwater deposits. In *Fine-grained turbidite systems*. Edited by Bouma, A. H. & Stone C. G., AAPG Memoir 72: SEPM Special Publication 68, p. 153 – 164.
- AAPG Field Seminar (1992). *The Tanqua turbidite and deltaic complexes: Depositional models, reservoir realities and the application of sequence stratigraphy* (Guidebook), 180 p. **Wickens, H. DeV., Brink, G. J., Van Rooyen, W., Bouma, A. H. and Brown, L. F., Jr.:** Authors
- **Wild, R., Flint, S.S. & Hodgson, D.M.** (2009). Stratigraphic evolution of the upper slope and shelf edge in the Karoo Basin, South Africa. *Basin Research*, Department of Earth and Ocean Sciences, United Kingdom: University of Liverpool, p.1-26.
- **Wilkinson, M., Milliken, K.L. & Haszeldine, R.S.** (2001). Systematic Destruction of K-feldspar in deeply buried rift and passive margin sandstones. *Journal of the Geological Society*, 158: 675-683.
- **X-Ray Diffraction** www index (2011). Available from: <http://www.panalytical.com/index.cfm?pid=135> (Accessed 5 February 2011).

APPENDICES

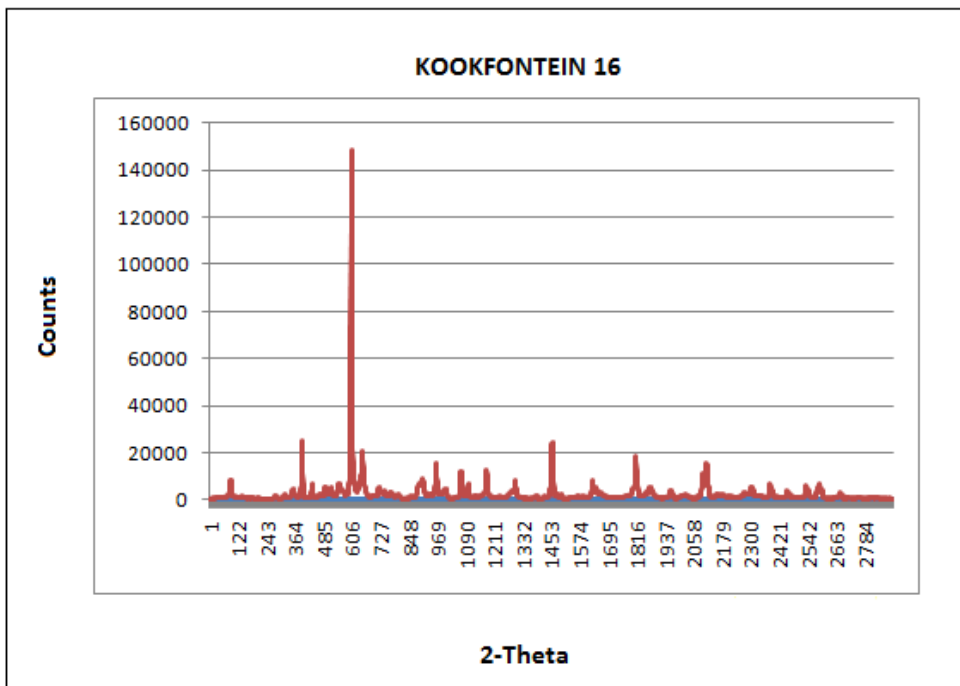


APPENDIX A

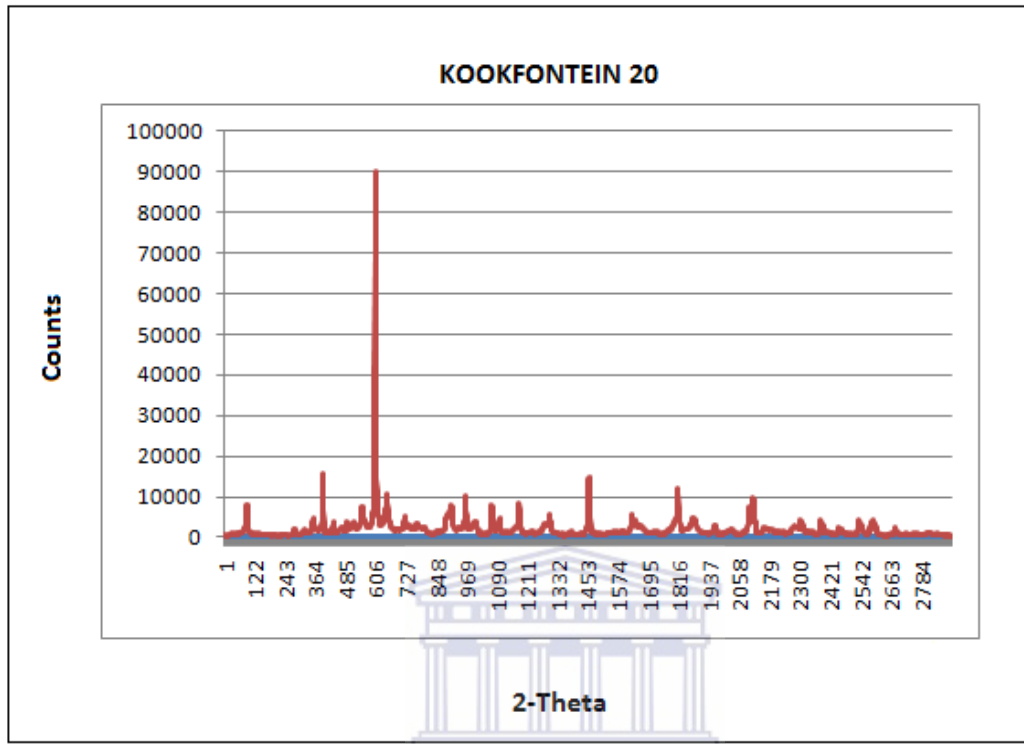
Appendix A-1: X-ray diffraction patterns profile, as an indication of the Kookfontein Formation shale samples obtained during this study.



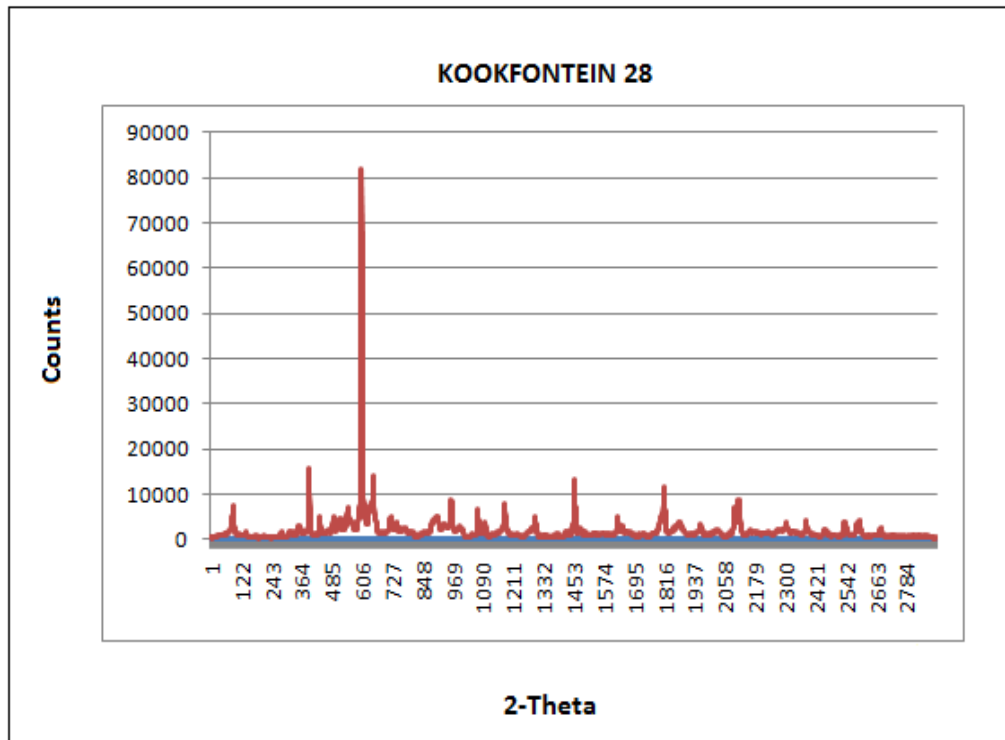
Appendix A-2: X-ray diffraction patterns profile, as an indication of the Kookfontein Formation shale samples obtained during this study.



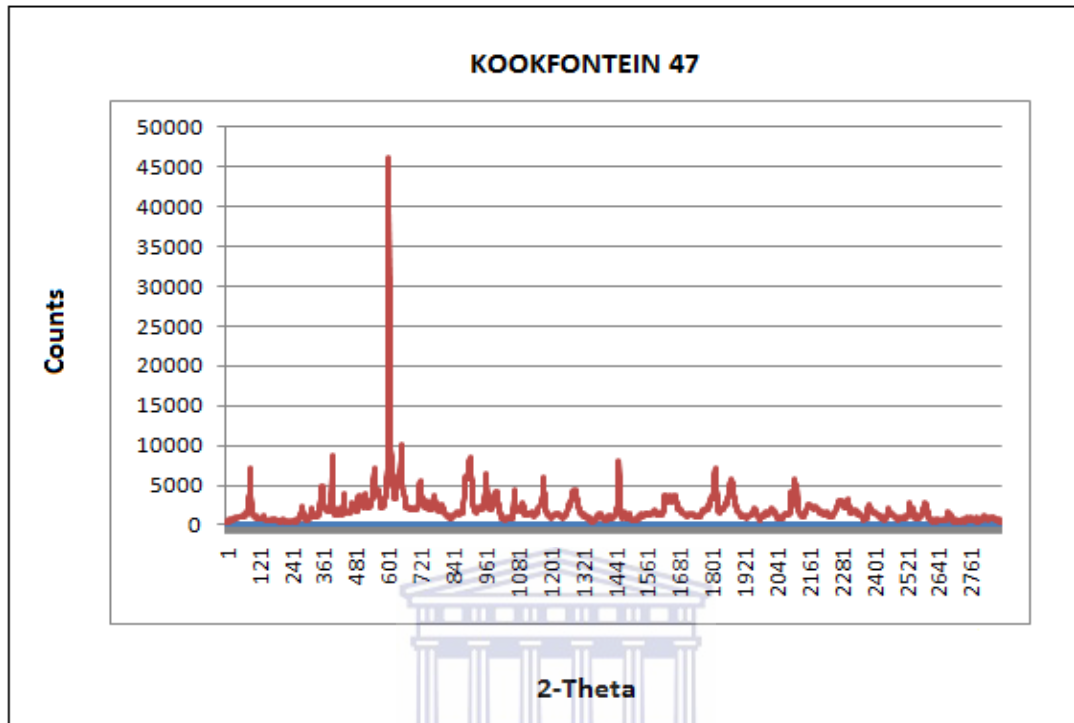
Appendix A-3: X-ray diffraction patterns profile, as an indication of the Kookfontein Formation shale samples obtained during this study.



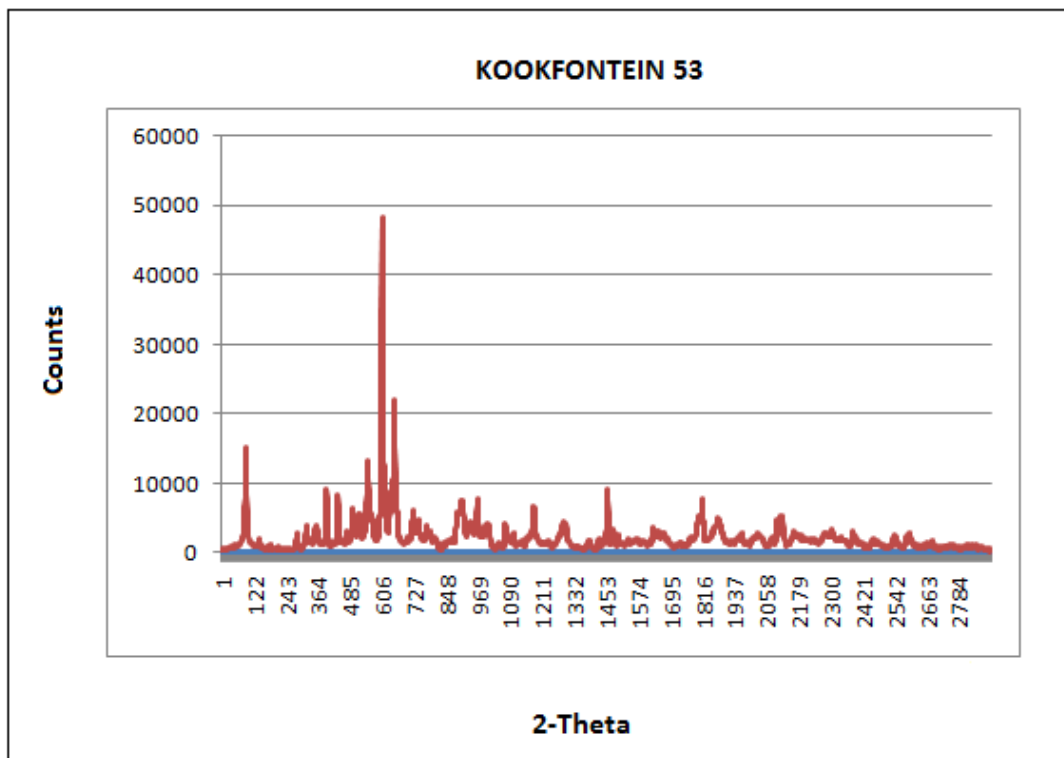
Appendix A-4: X-ray diffraction patterns profile, as an indication of the Kookfontein Formation shale samples obtained during this study.



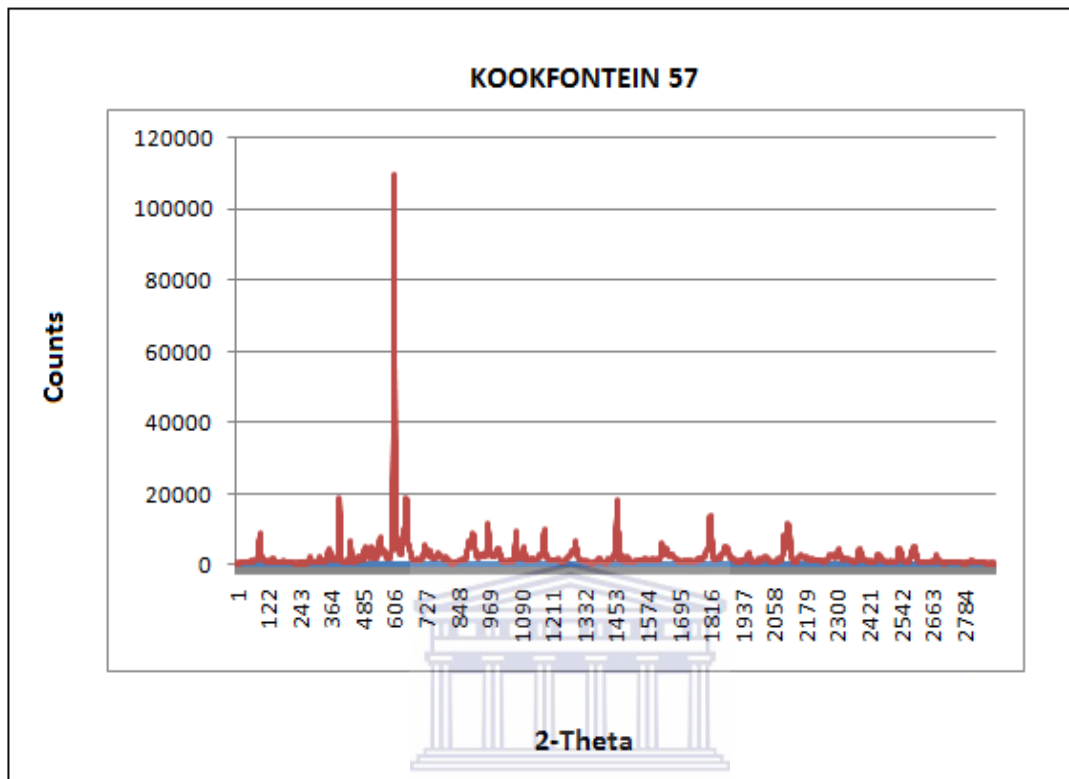
Appendix A-5: X-ray diffraction patterns profile, as an indication of the Kookfontein Formation shale samples obtained during this study.



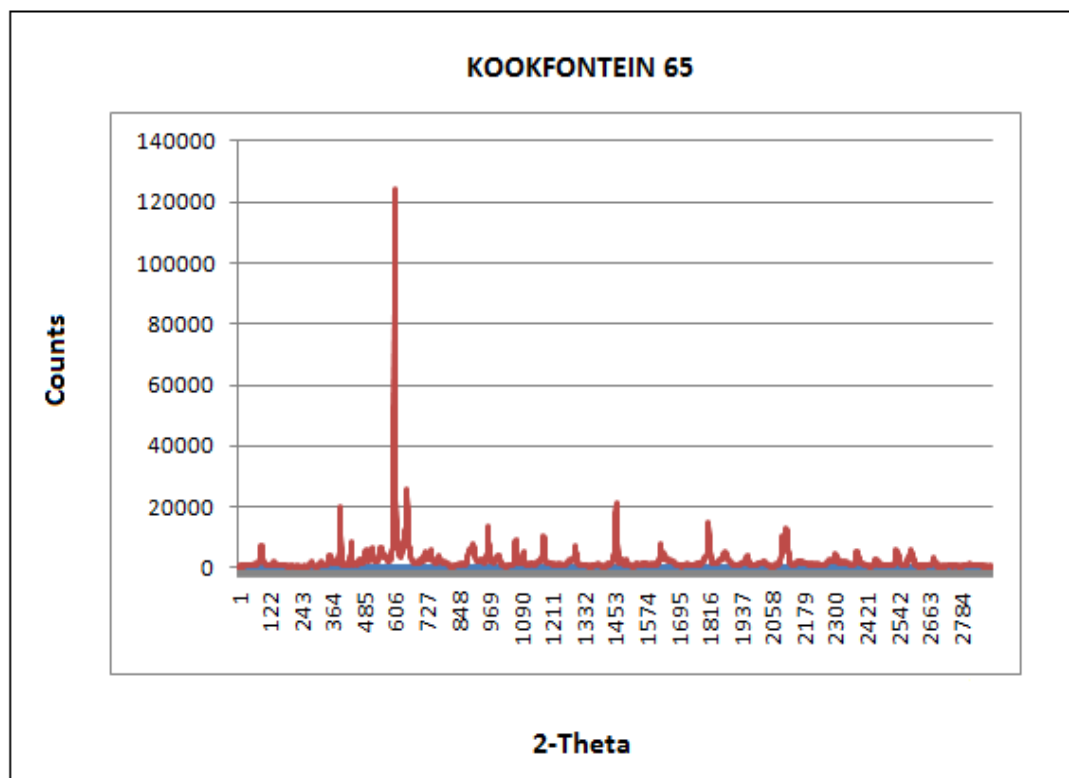
Appendix A-6: X-ray diffraction patterns profile, as an indication of the Kookfontein Formation shale samples obtained during this study.



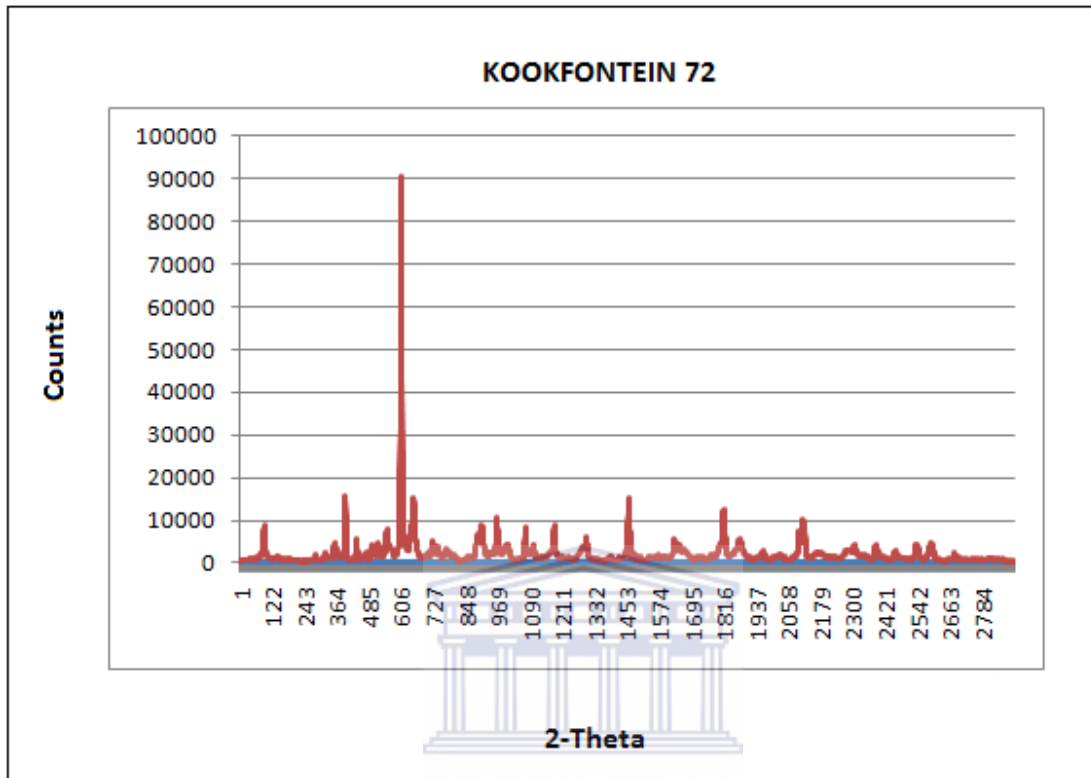
Appendix A-7: X-ray diffraction patterns profile, as an indication of the Kookfontein Formation shale samples obtained during this study.



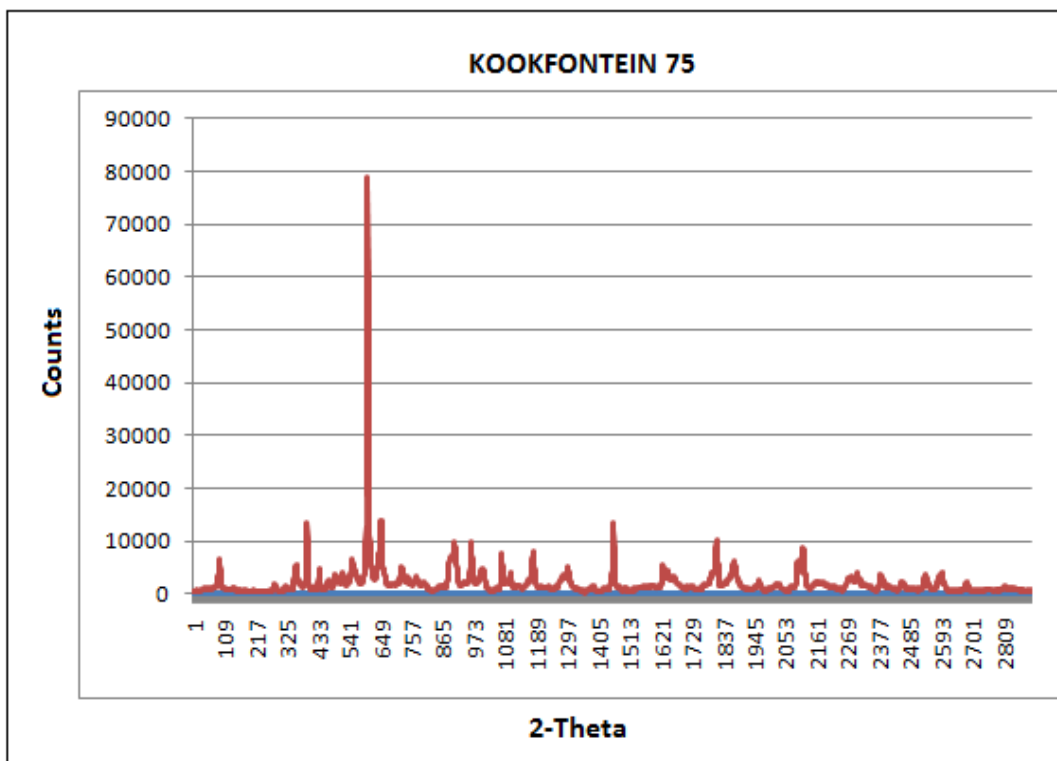
Appendix A-8: X-ray diffraction patterns profile, as an indication of the Kookfontein Formation shale samples obtained during this study.



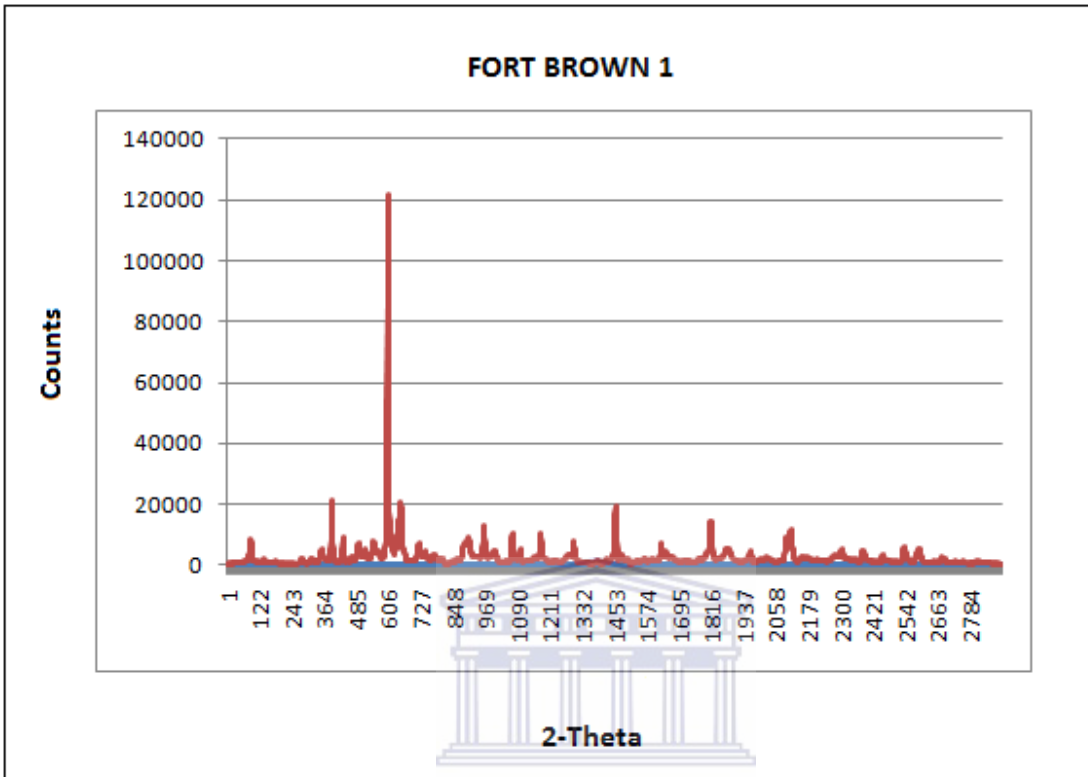
Appendix A-9: X-ray diffraction patterns profile, as an indication of the Kookfontein Formation shale samples obtained during this study.



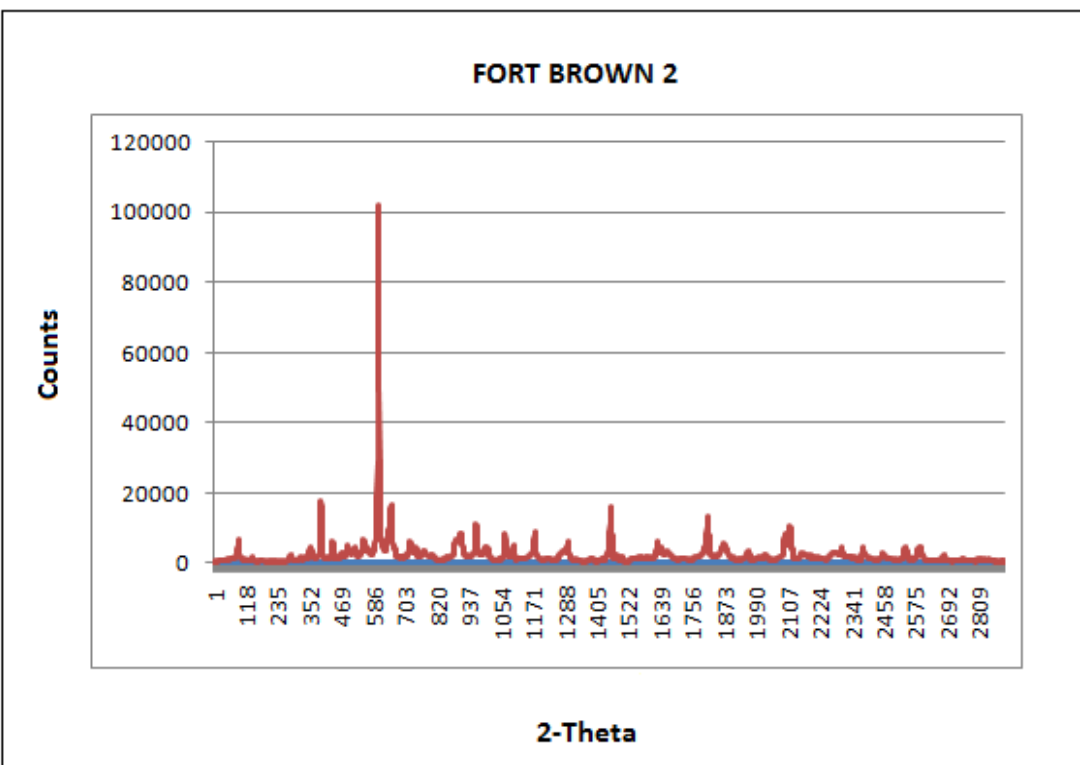
Appendix A-10: X-ray diffraction patterns profile, as an indication of the Kookfontein Formation shale samples obtained during this study.



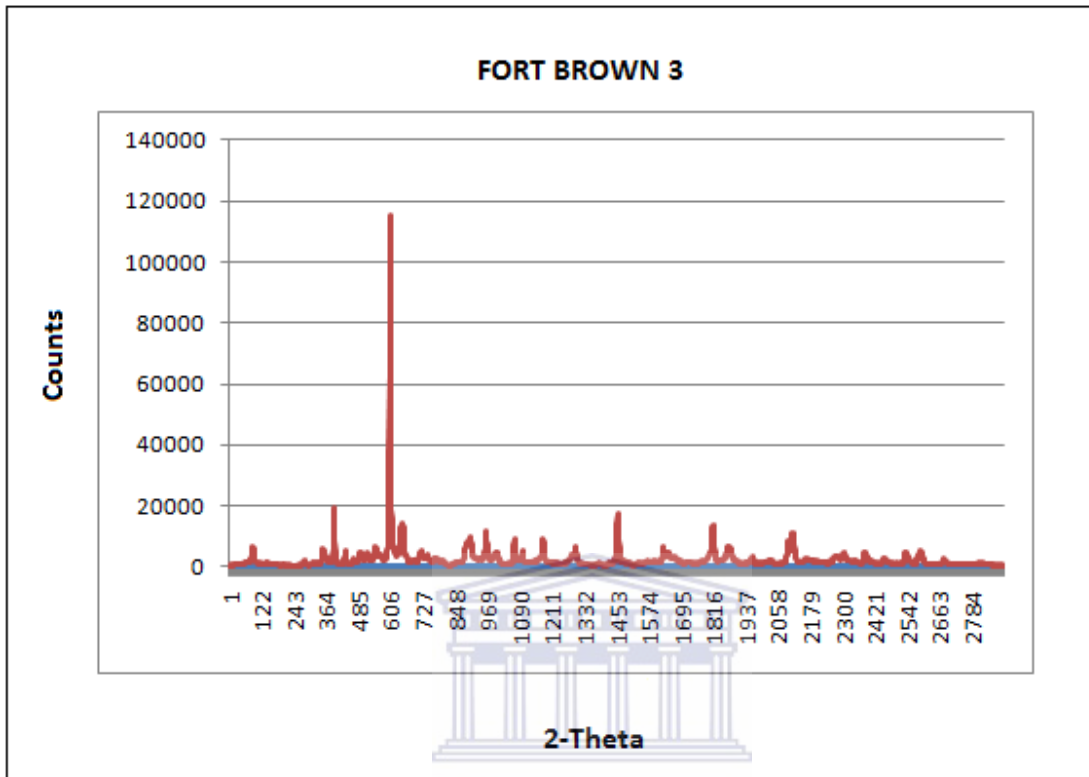
Appendix A-11: X-ray diffraction patterns profile, as an indication of the Fort Brown Formation shale samples obtained during this study.



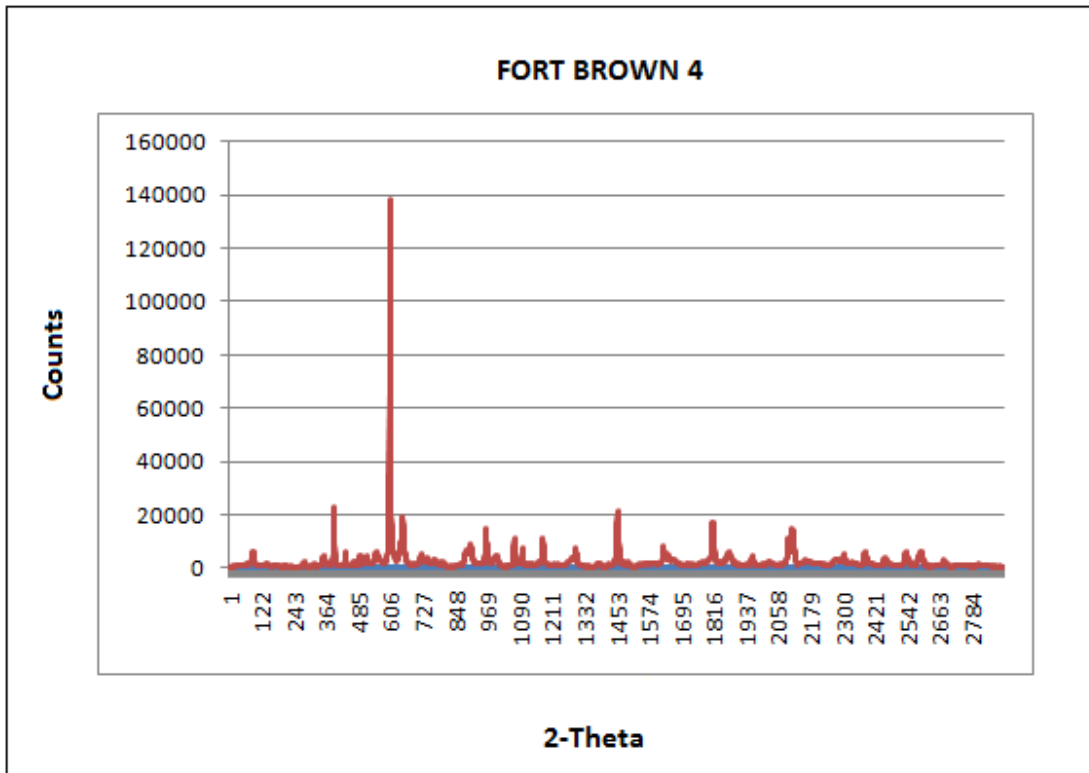
Appendix A-12: X-ray diffraction patterns profile, as an indication of the Fort Brown Formation shale samples obtained during this study.



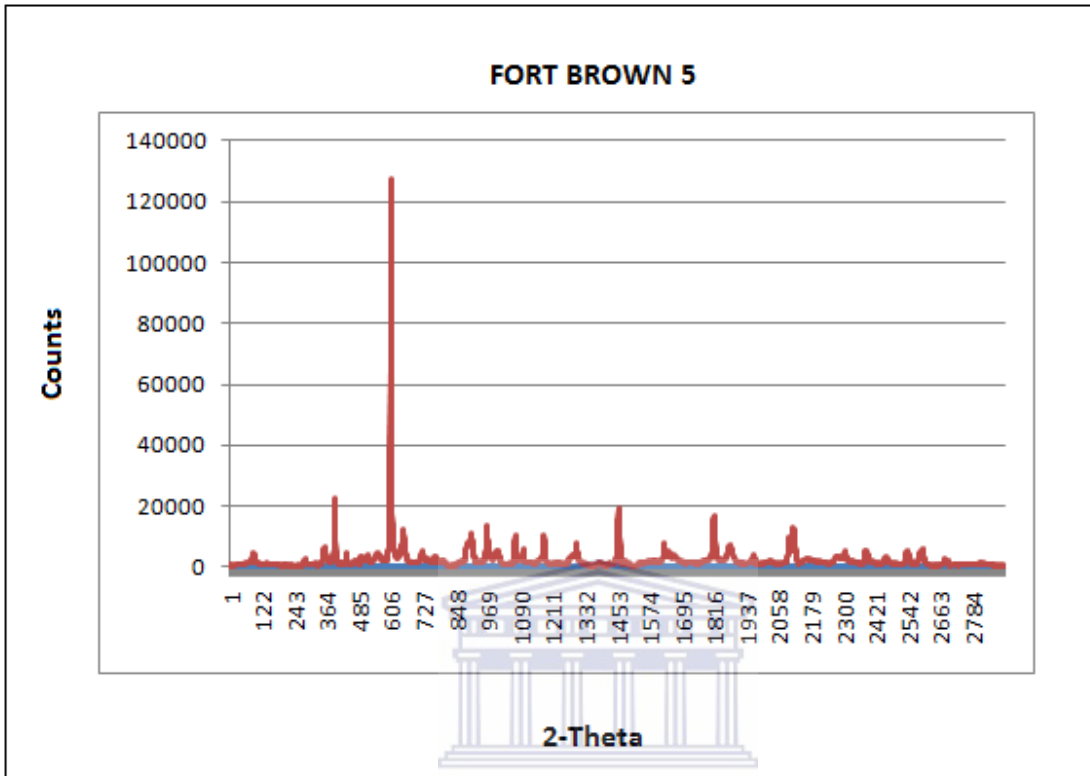
Appendix A-13: X-ray diffraction patterns profile, as an indication of the Fort Brown Formation shale samples obtained during this study.



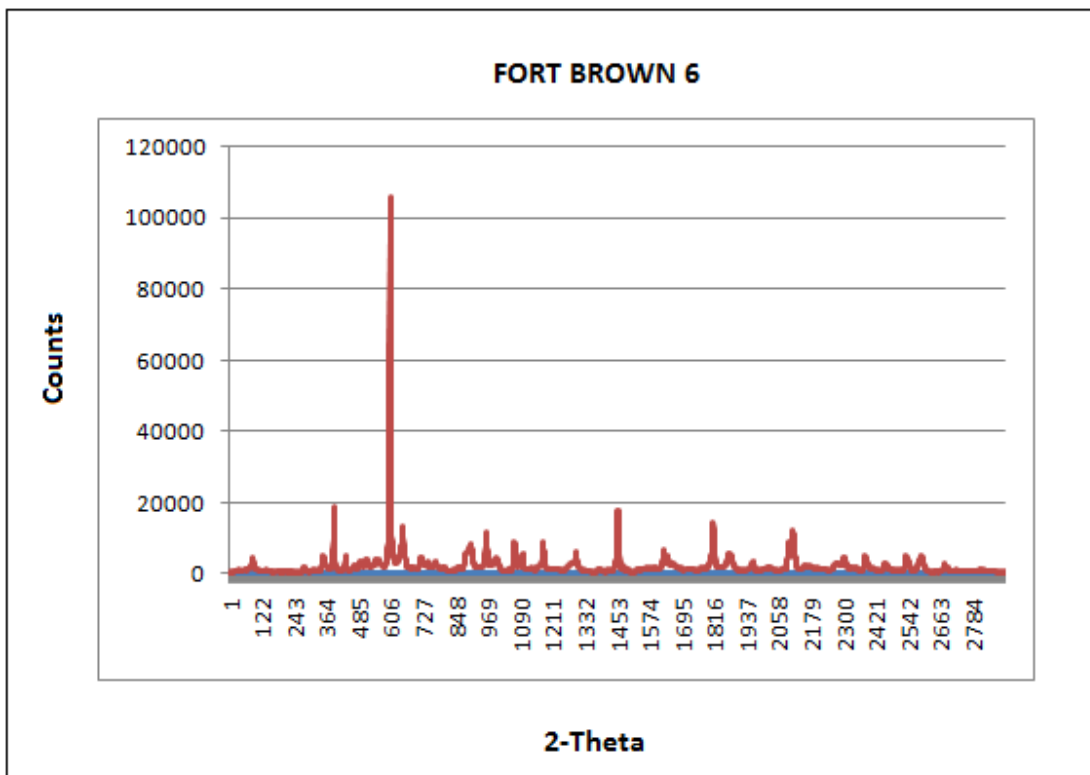
Appendix A-14: X-ray diffraction patterns profile, as an indication of the Fort Brown Formation shale samples obtained during this study.



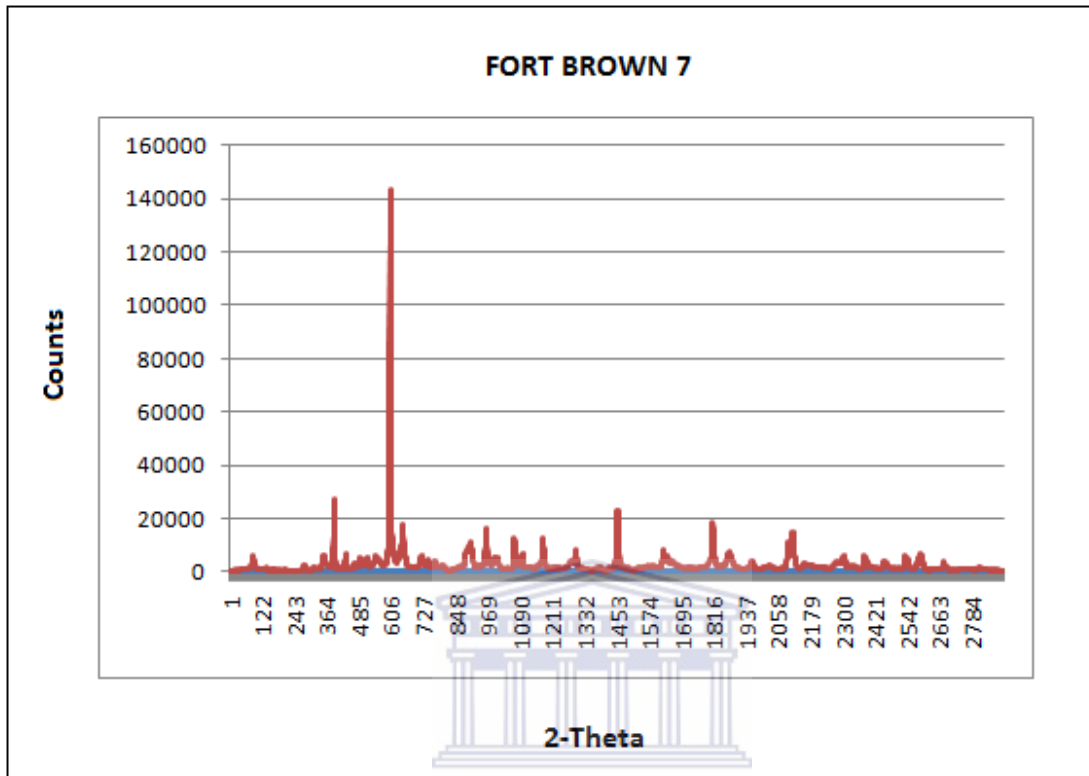
Appendix A-15: X-ray diffraction patterns profile, as an indication of the Fort Brown Formation shale samples obtained during this study.



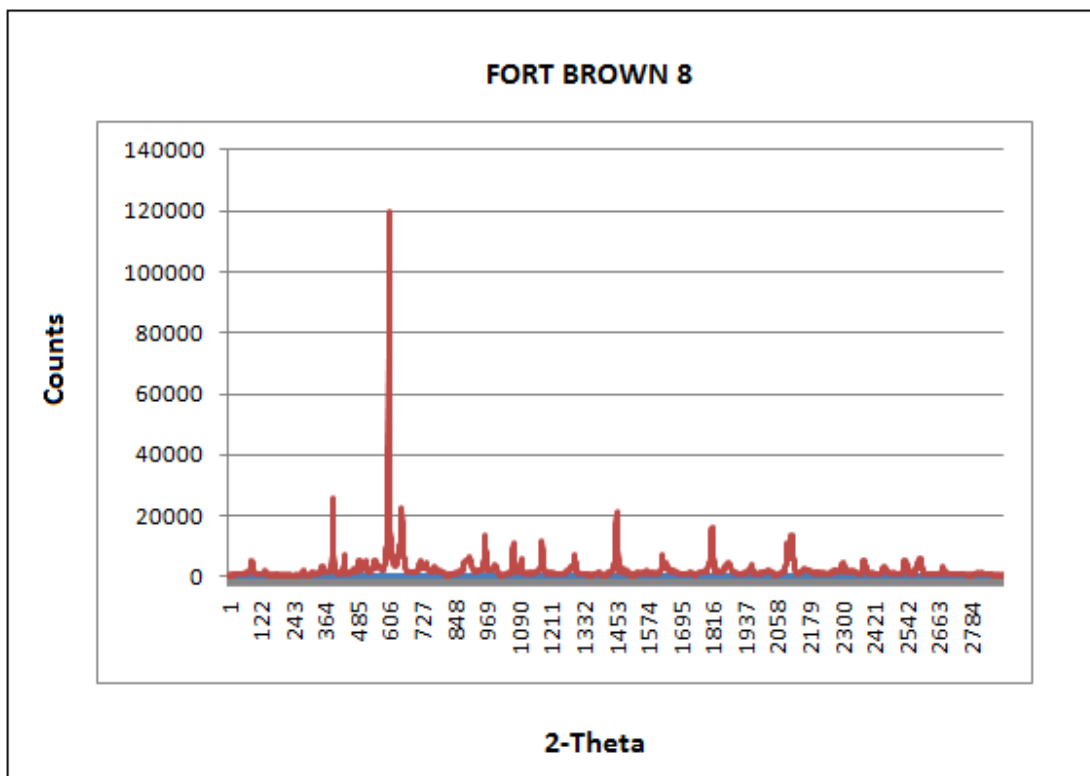
Appendix A-16: X-ray diffraction patterns profile, as an indication of the Fort Brown Formation shale samples obtained during this study.



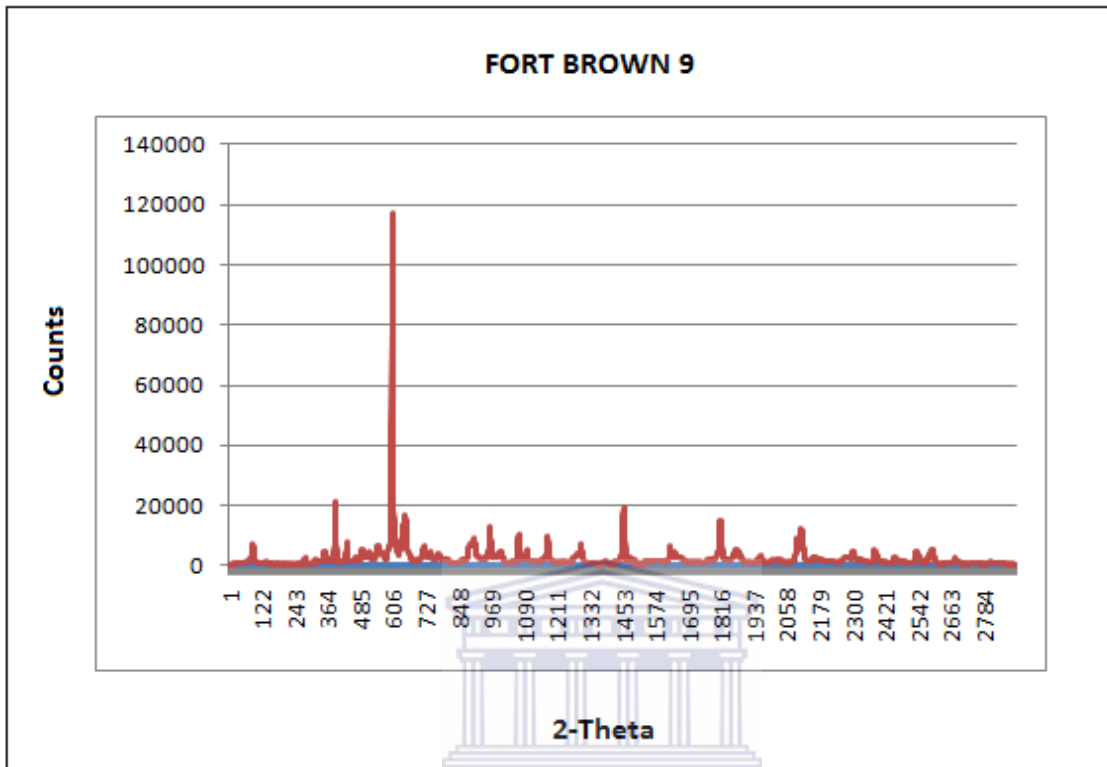
Appendix A-17: X-ray diffraction patterns profile, as an indication of the Fort Brown Formation shale samples obtained during this study.



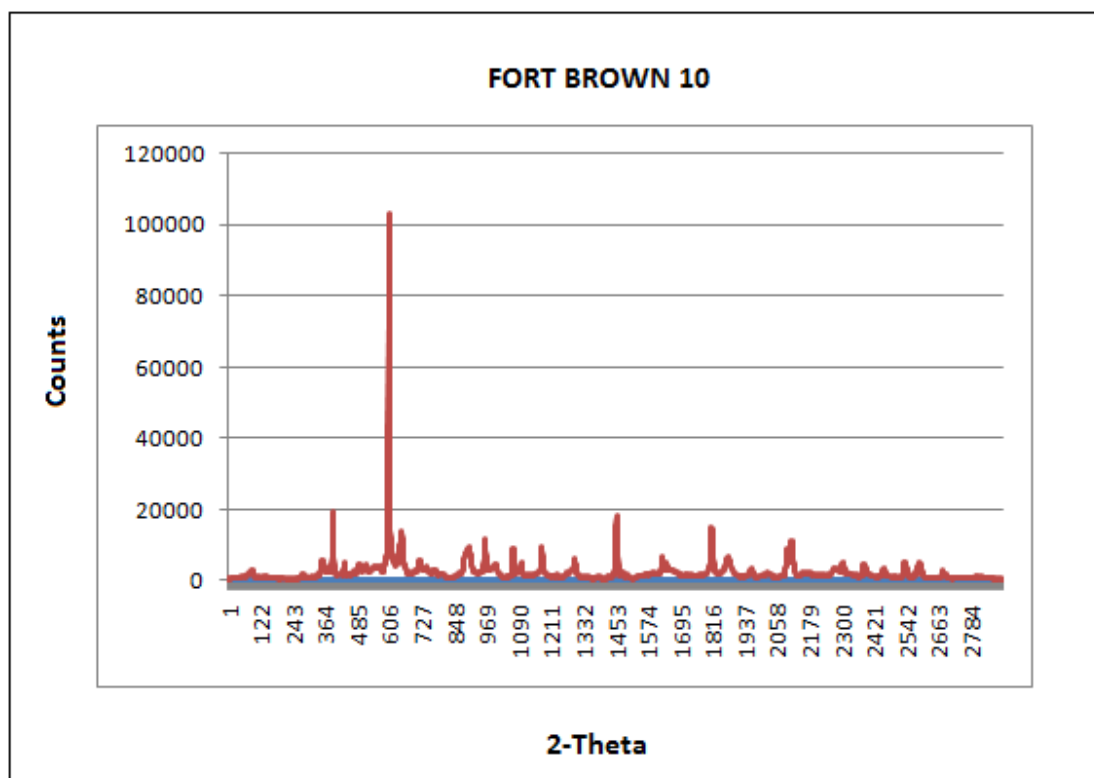
Appendix A-18: X-ray diffraction patterns profile, as an indication of the Fort Brown Formation shale samples obtained during this study.



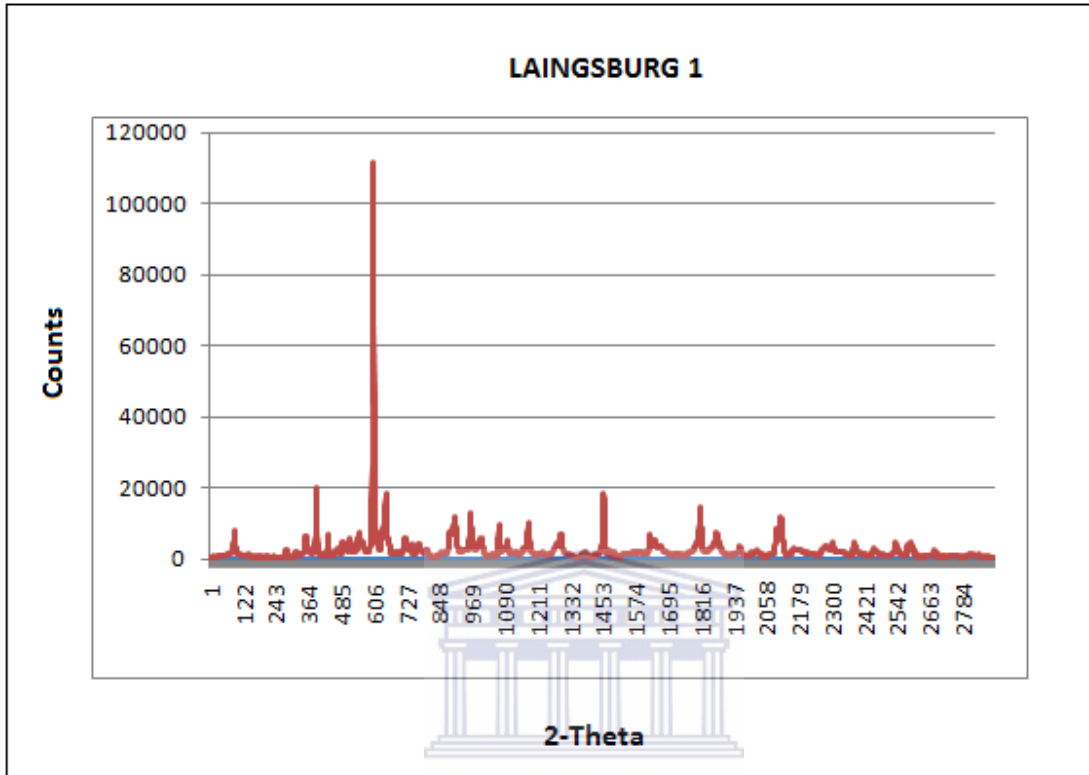
Appendix A-19: X-ray diffraction patterns profile, as an indication of the Fort Brown Formation shale samples obtained during this study.



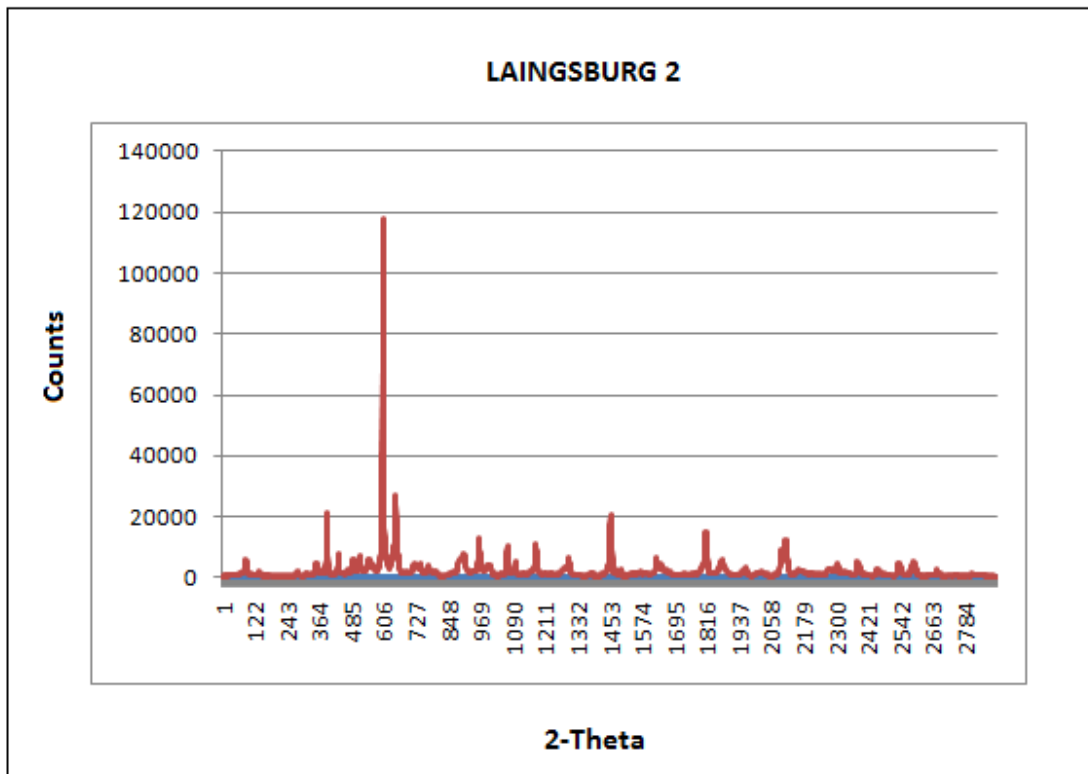
Appendix A-20: X-ray diffraction patterns profile, as an indication of the Fort Brown Formation shale samples obtained during this study.



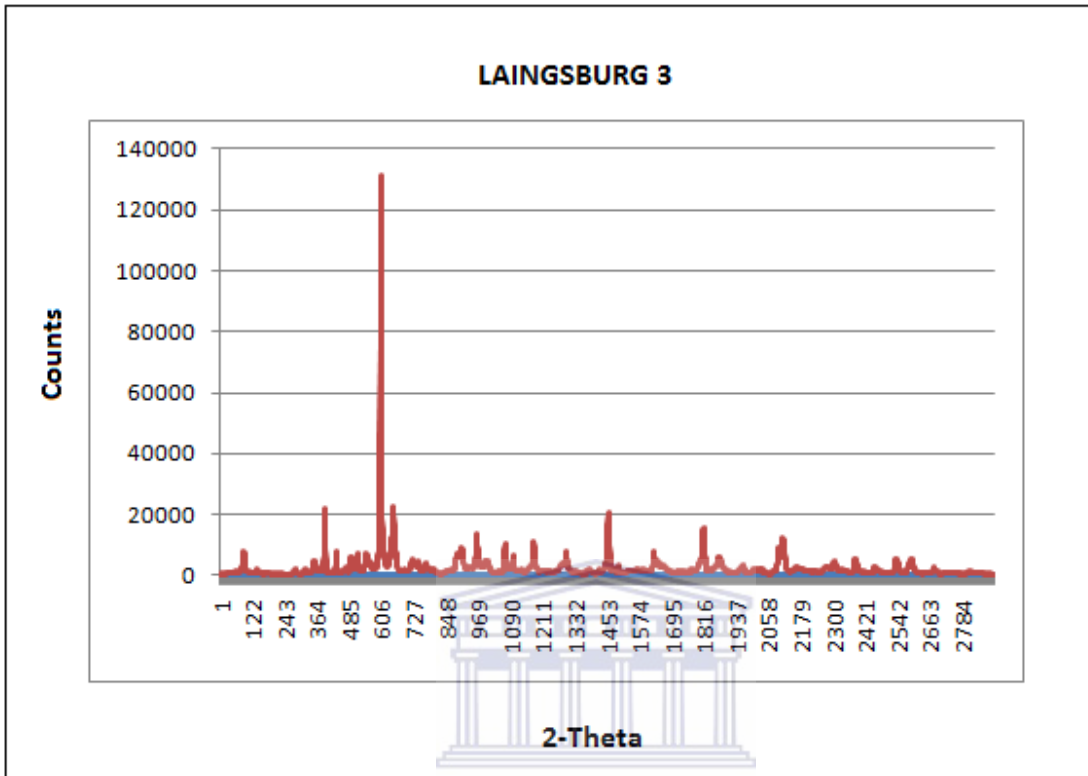
Appendix A-21: X-ray diffraction patterns profile, as an indication of the Laingsburg Formation shale samples obtained during this study.



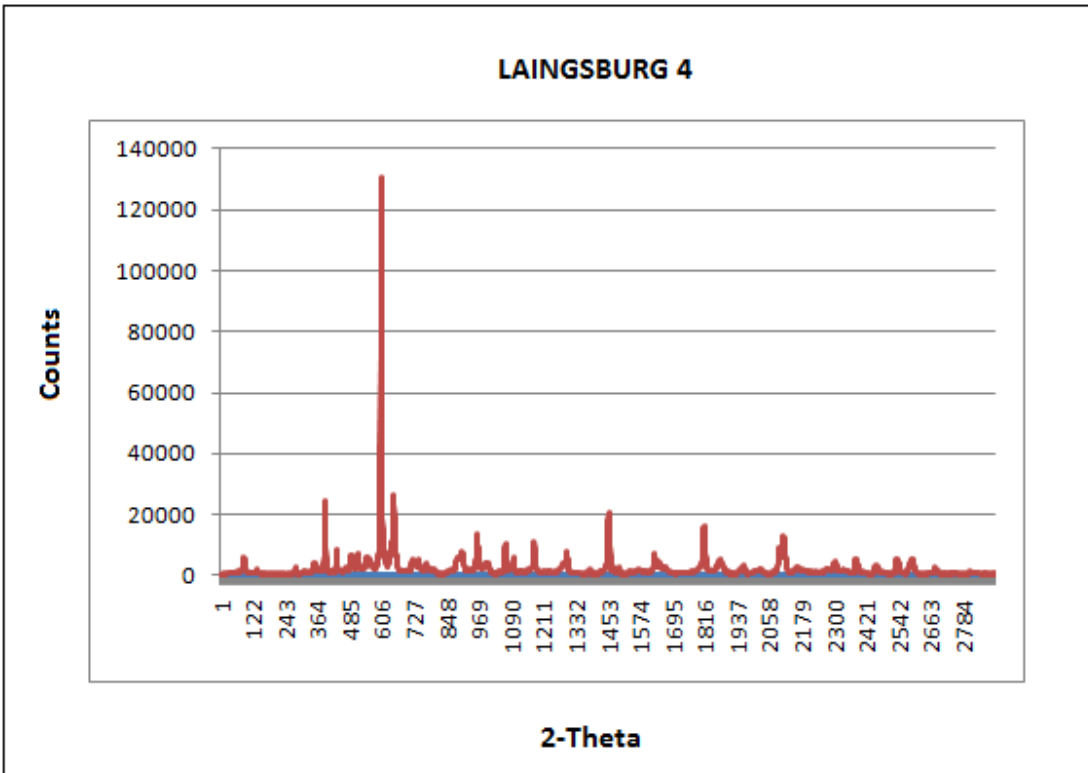
Appendix A-22: X-ray diffraction patterns profile, as an indication of the Laingsburg Formation shale samples obtained during this study.



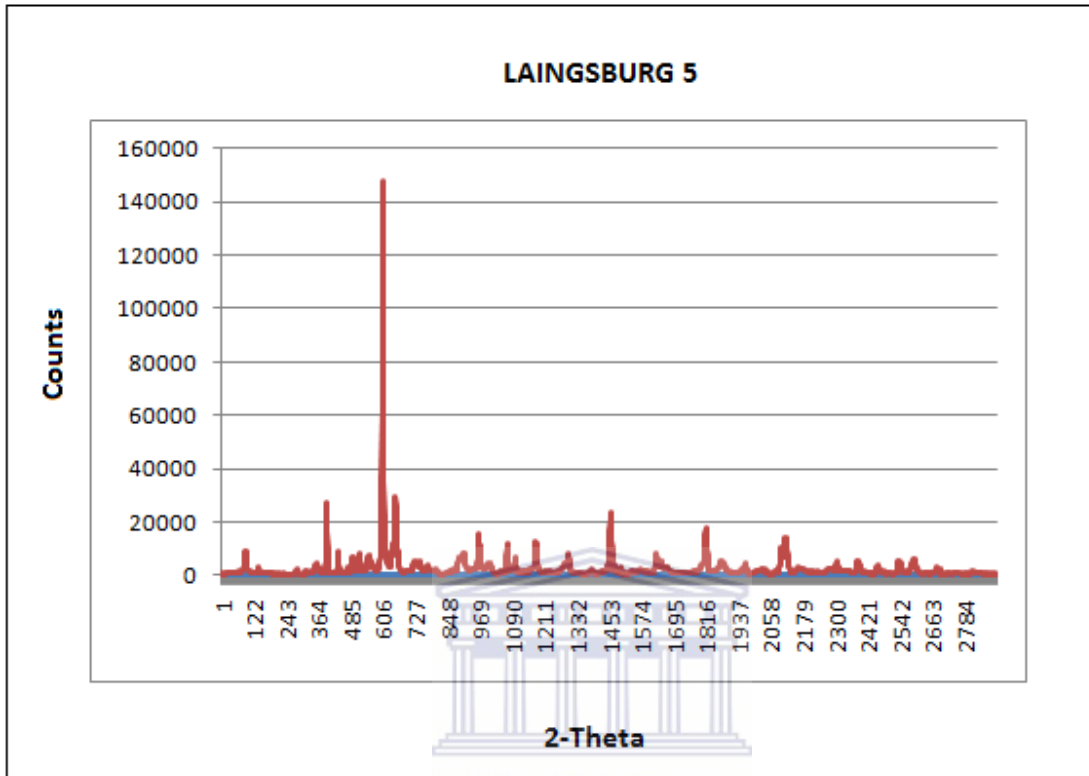
Appendix A-23: X-ray diffraction patterns profile, as an indication of the Laingsburg Formation shale samples obtained during this study.



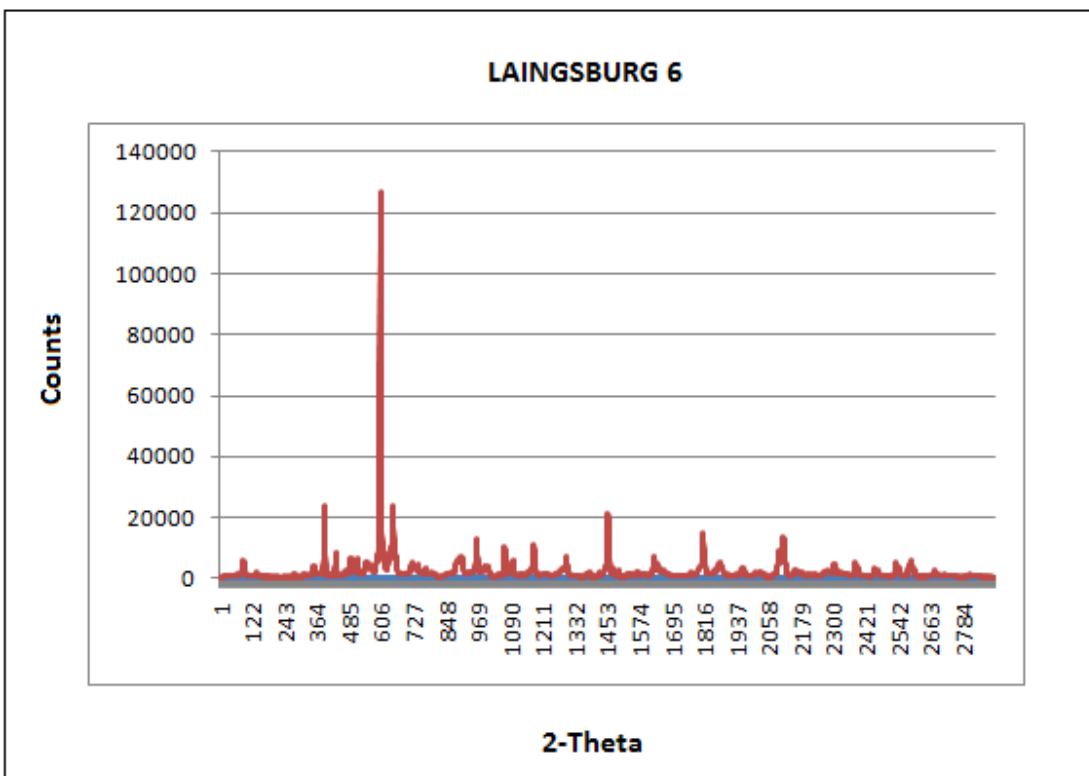
Appendix A-24: X-ray diffraction patterns profile, as an indication of the Laingsburg Formation shale samples obtained during this study.



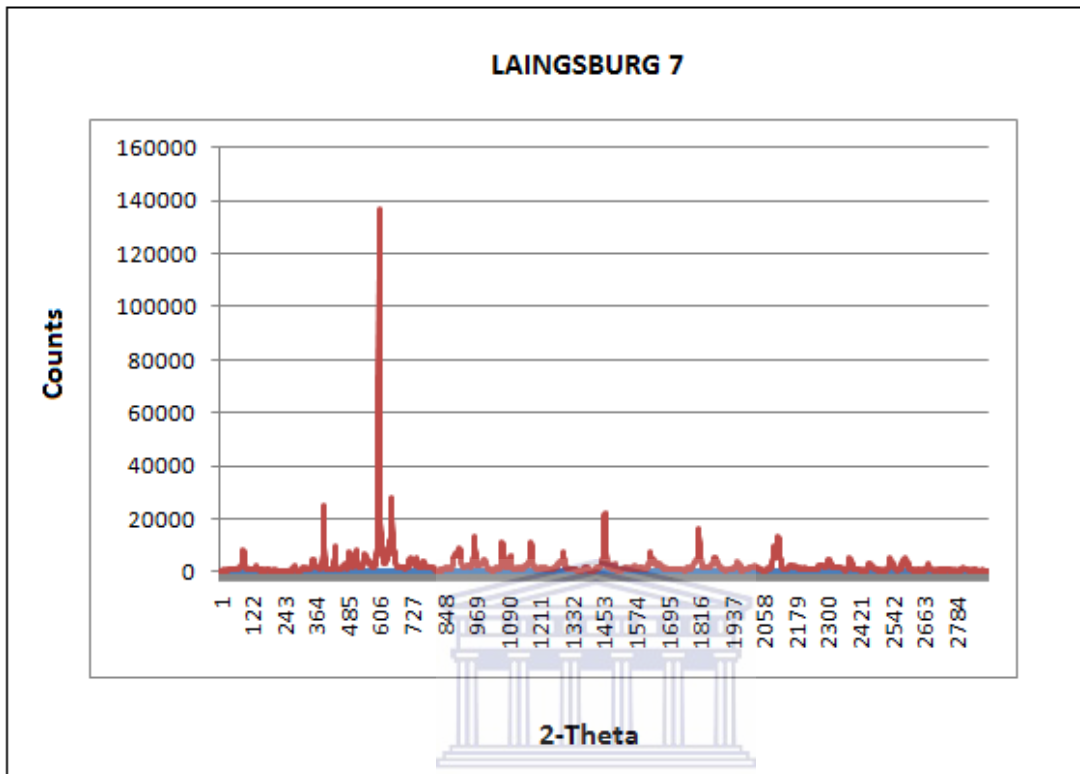
Appendix A-25: X-ray diffraction patterns profile, as an indication of the Laingsburg Formation shale samples obtained during this study.



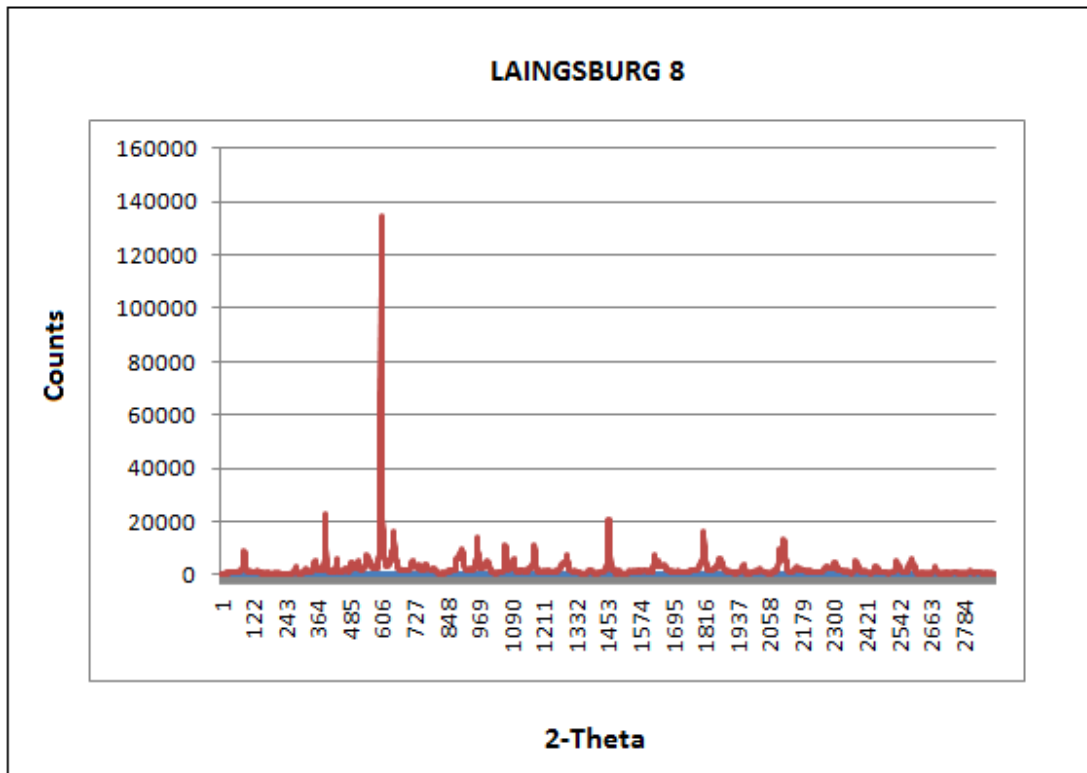
Appendix A-26: X-ray diffraction patterns profile, as an indication of the Laingsburg Formation shale samples obtained during this study.



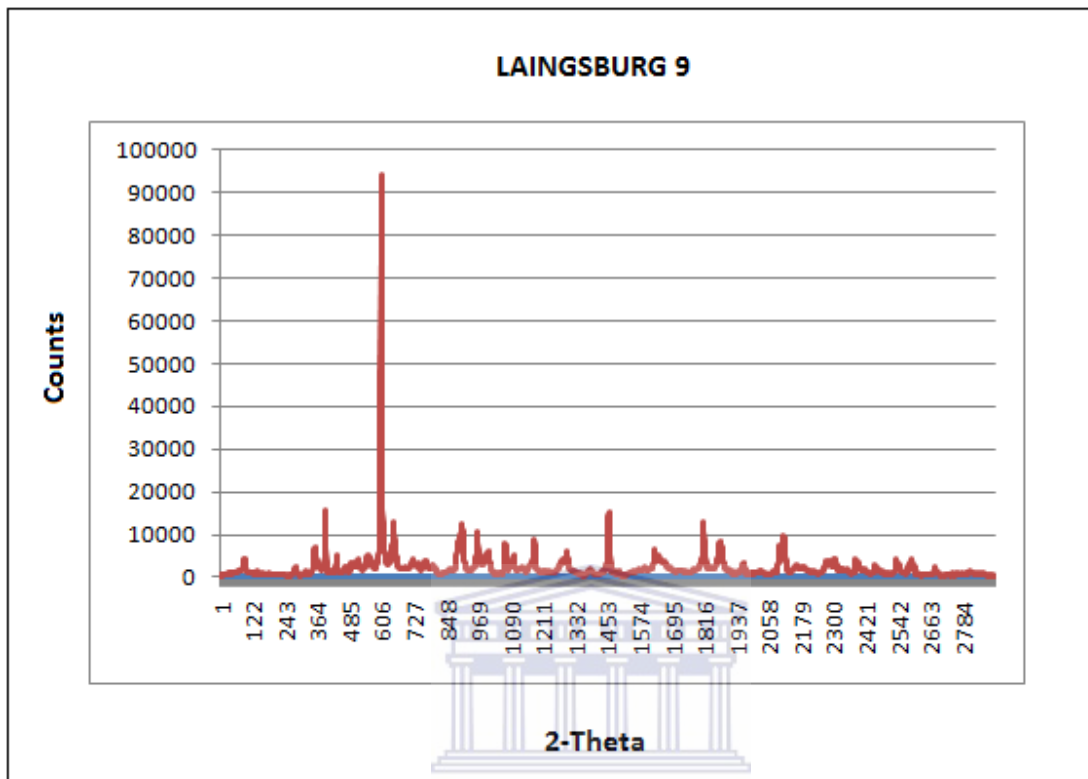
Appendix A-27: X-ray diffraction patterns profile, as an indication of the Laingsburg Formation shale samples obtained during this study.



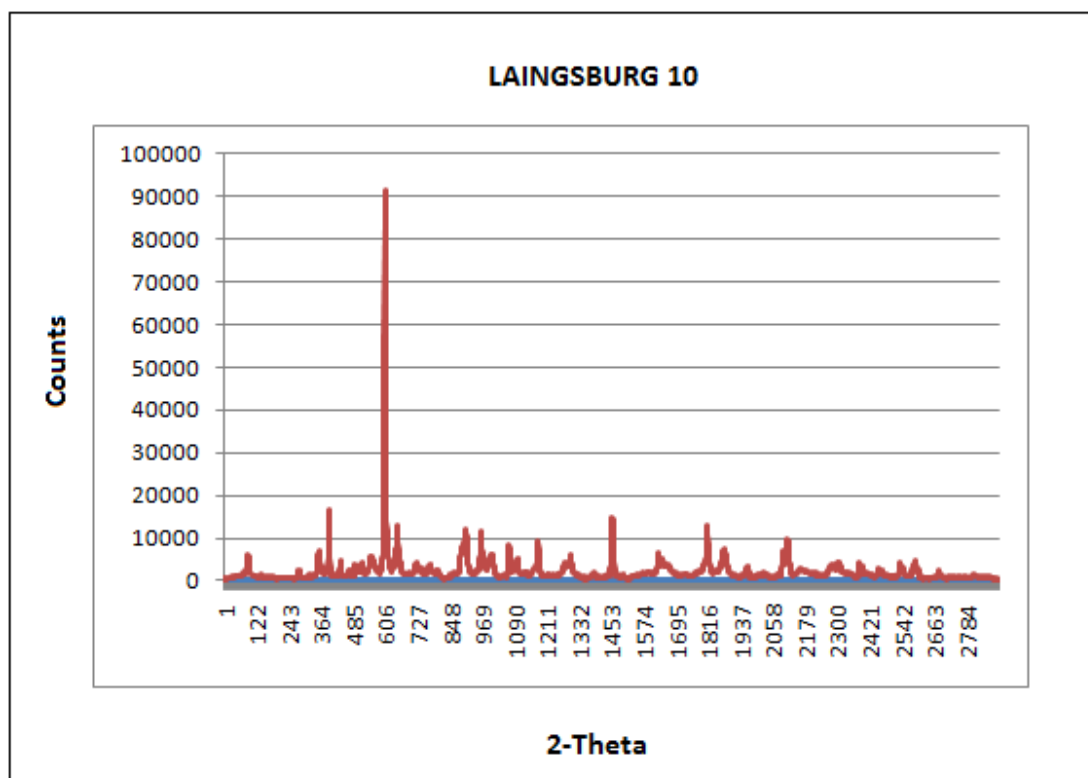
Appendix A-28: X-ray diffraction patterns profile, as an indication of the Laingsburg Formation shale samples obtained during this study.



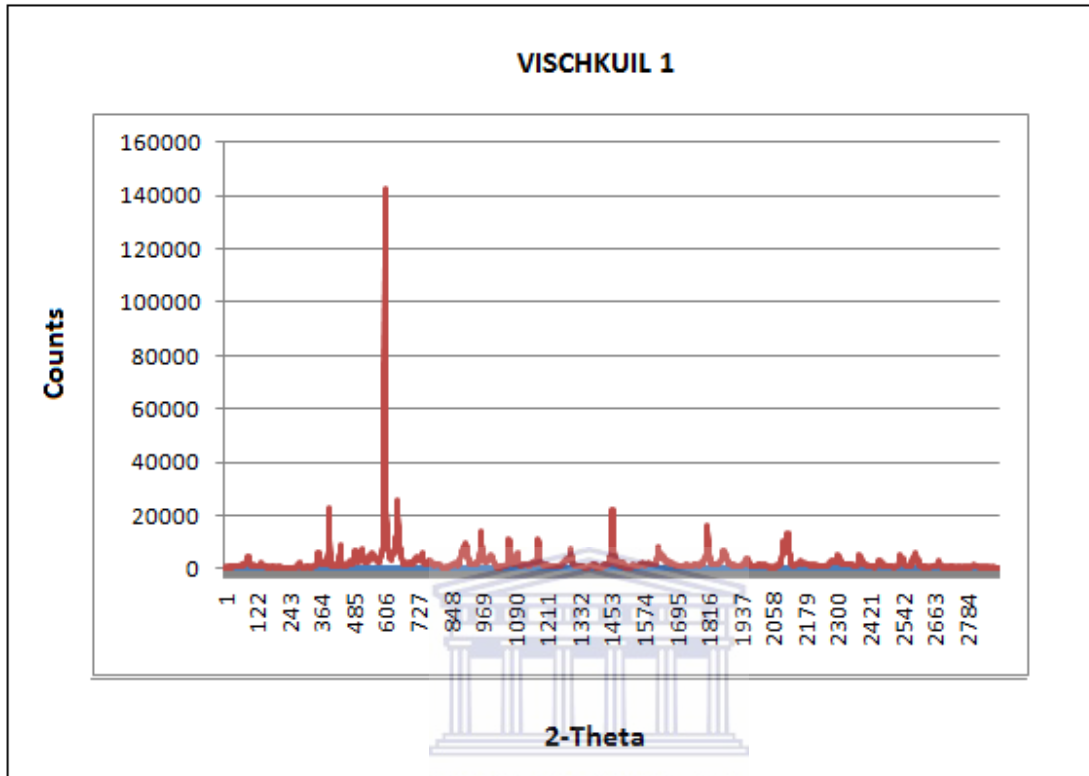
Appendix A-29: X-ray diffraction patterns profile, as an indication of the Laingsburg Formation shale samples obtained during this study.



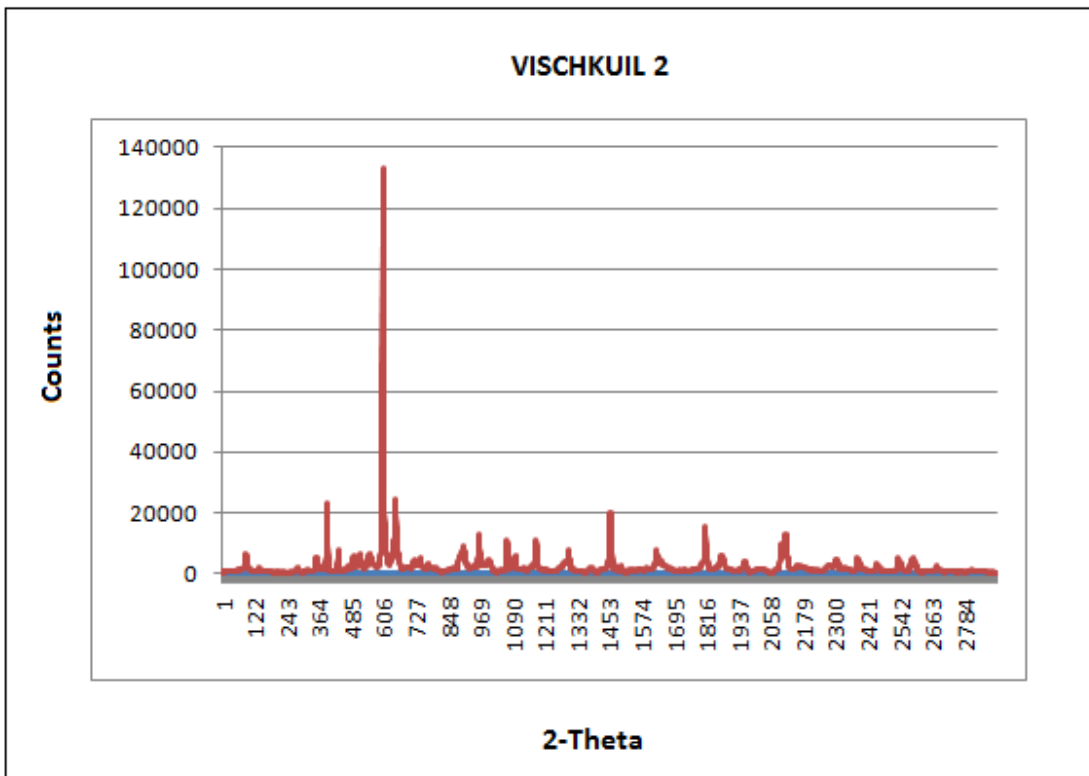
Appendix A-30: X-ray diffraction patterns profile, as an indication of the Laingsburg Formation shale samples obtained during this study.



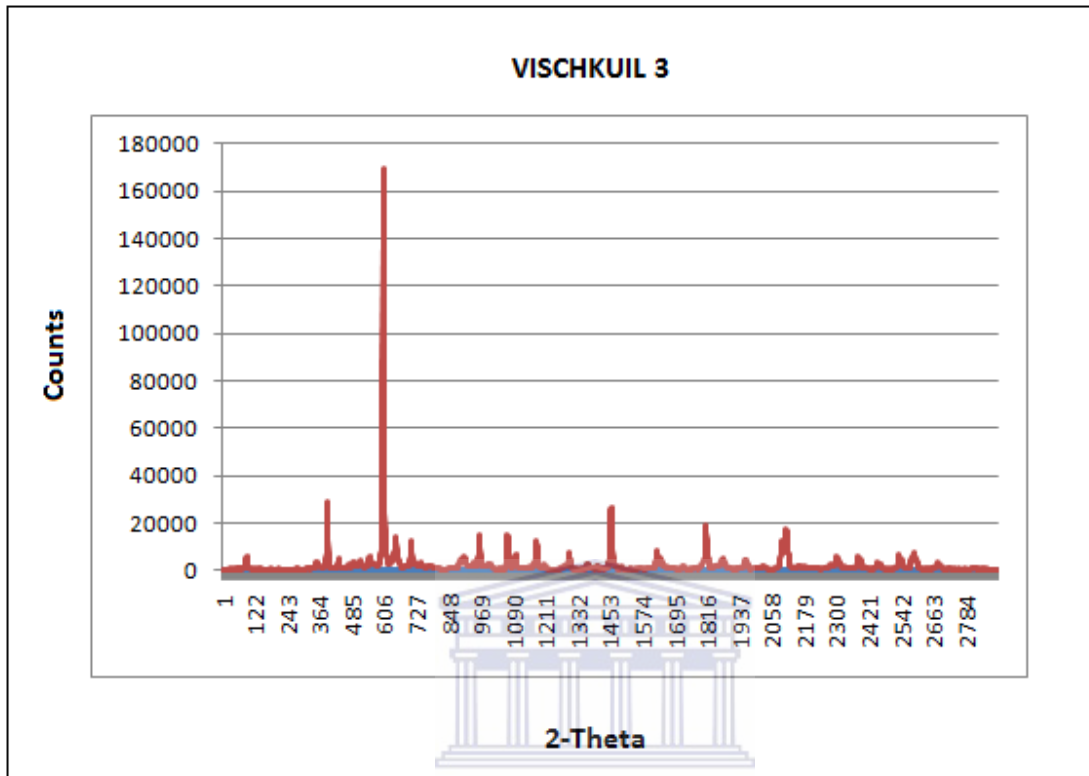
Appendix A-31: X-ray diffraction patterns profile, as an indication of the Vischkuil Formation shale samples obtained during this study.



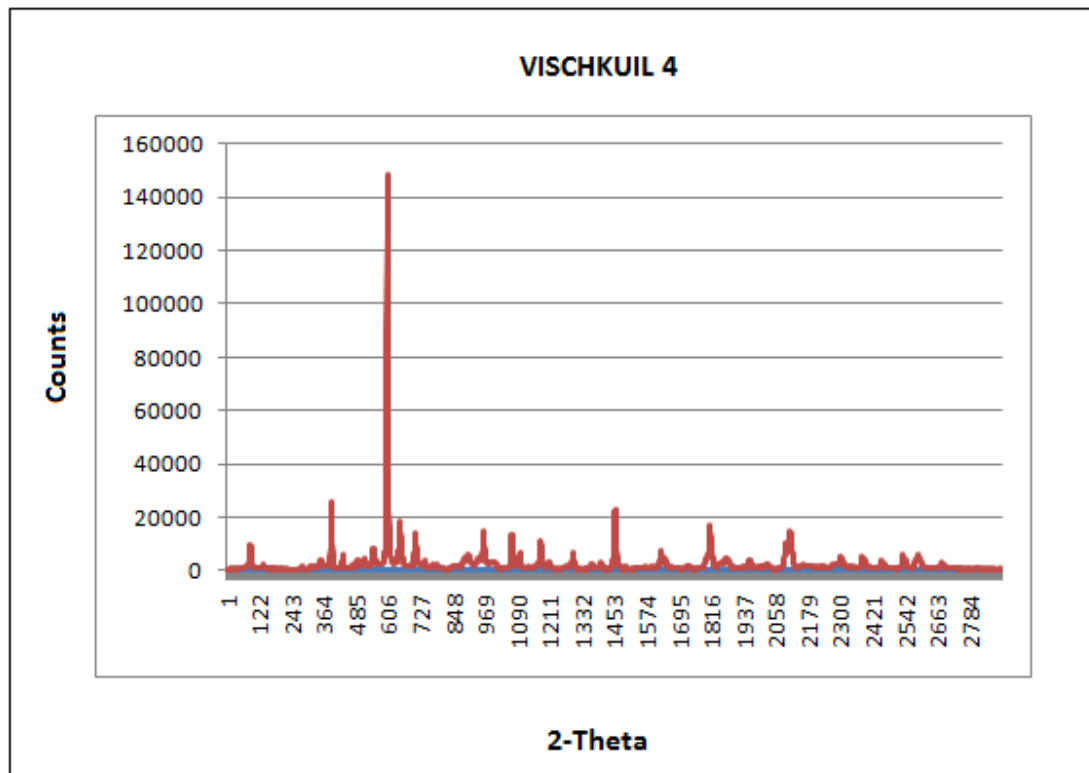
Appendix A-32: X-ray diffraction patterns profile, as an indication of the Vischkuil Formation shale samples obtained during this study.



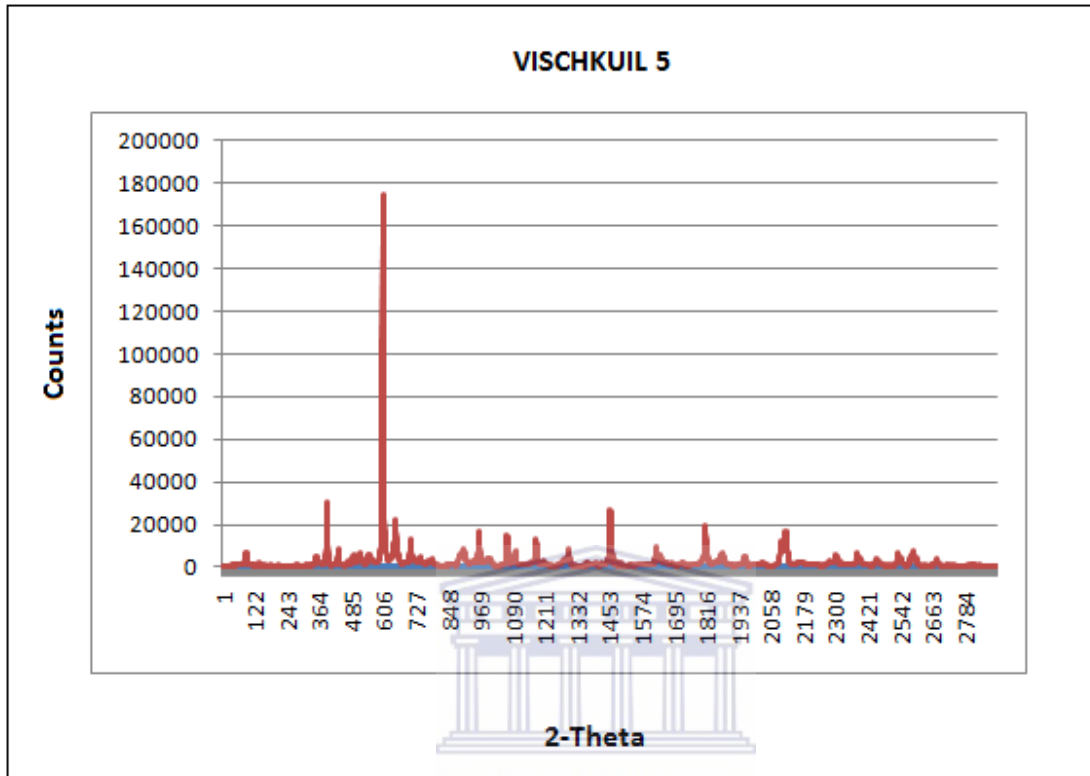
Appendix A-33: X-ray diffraction patterns profile, as an indication of the Vischkuil Formation shale samples obtained during this study.



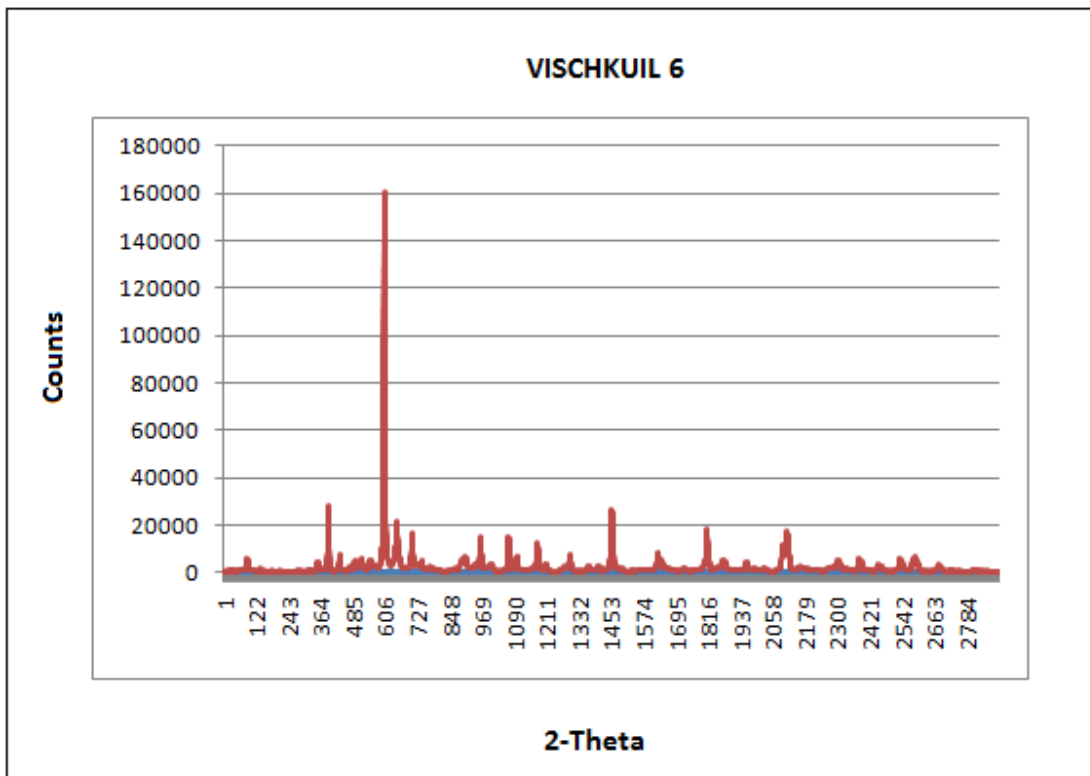
Appendix A-34: X-ray diffraction patterns profile, as an indication of the Vischkuil Formation shale samples obtained during this study.



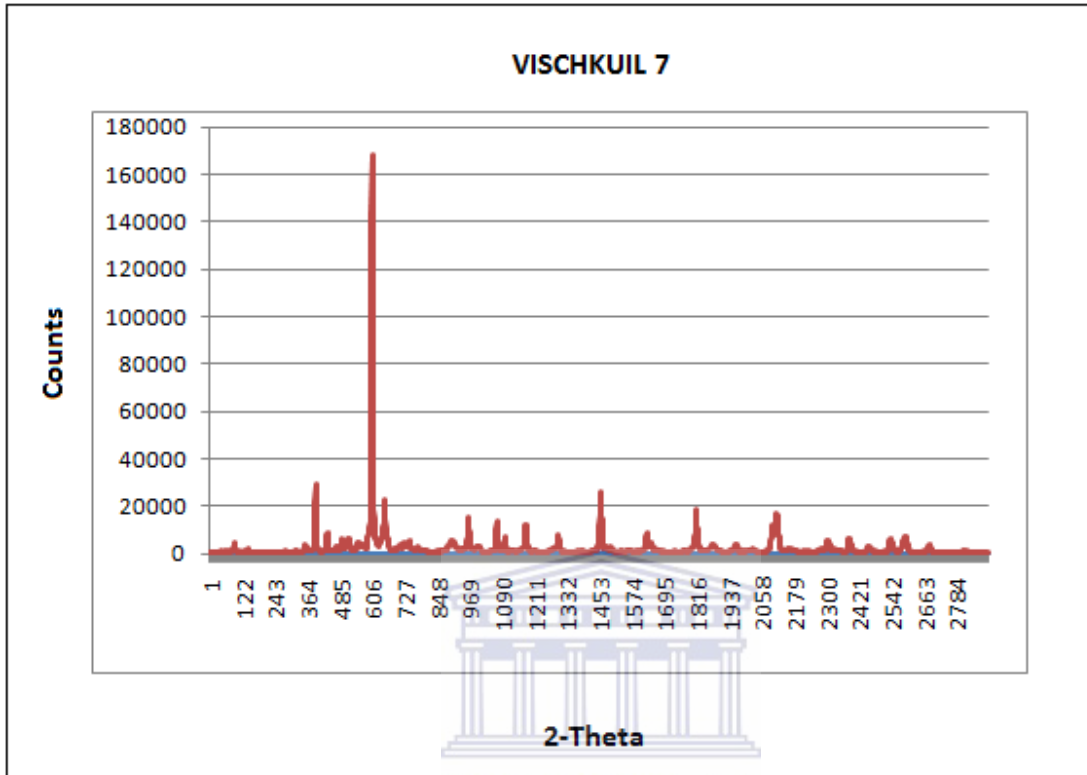
Appendix A-35: X-ray diffraction patterns profile, as an indication of the Vischkuil Formation shale samples obtained during this study.



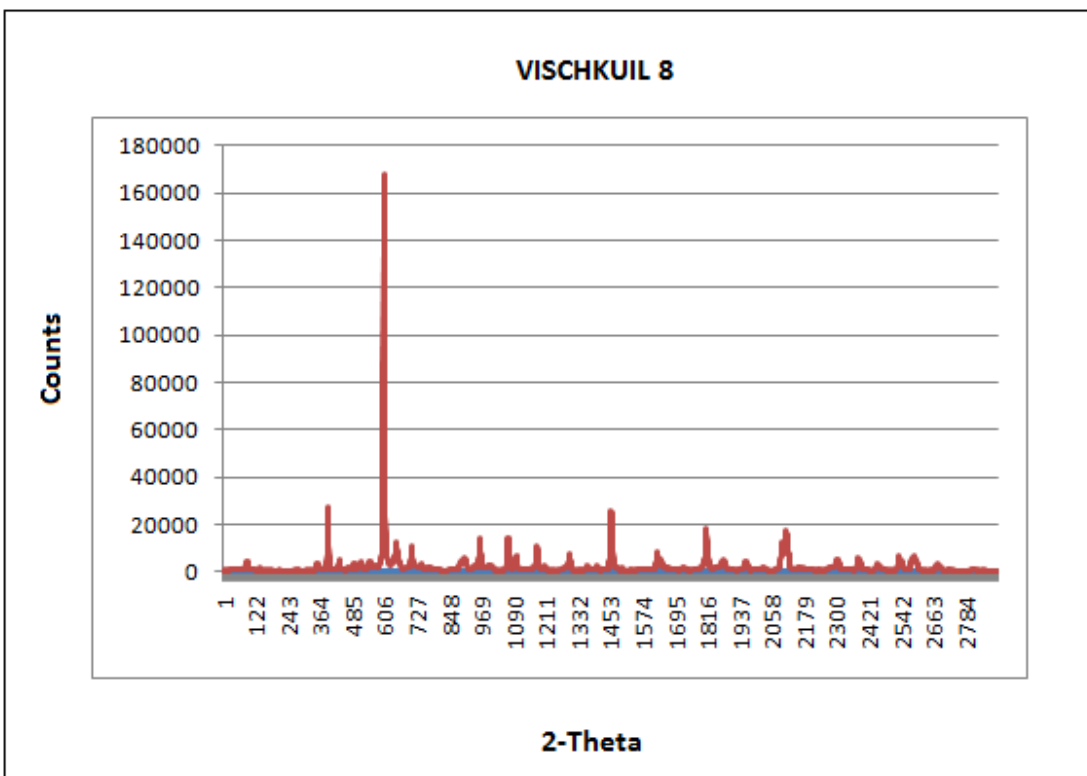
Appendix A-36: X-ray diffraction patterns profile, as an indication of the Vischkuil Formation shale samples obtained during this study.



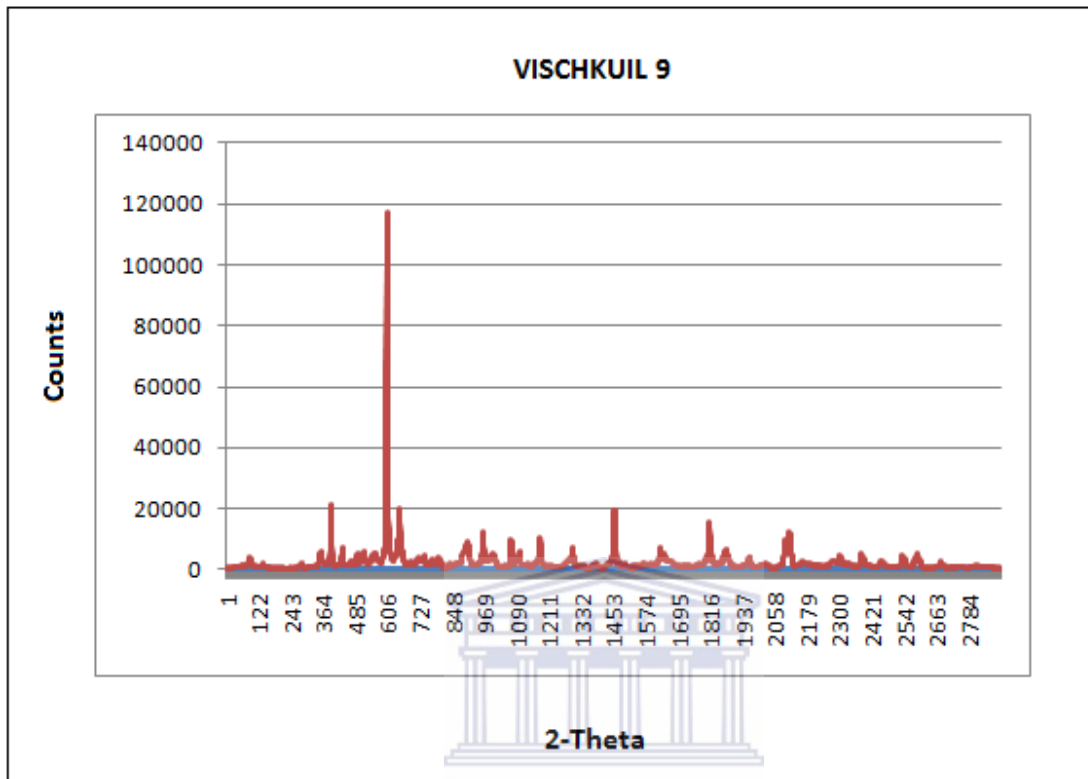
Appendix A-37: X-ray diffraction patterns profile, as an indication of the Vischkuil Formation shale samples obtained during this study.



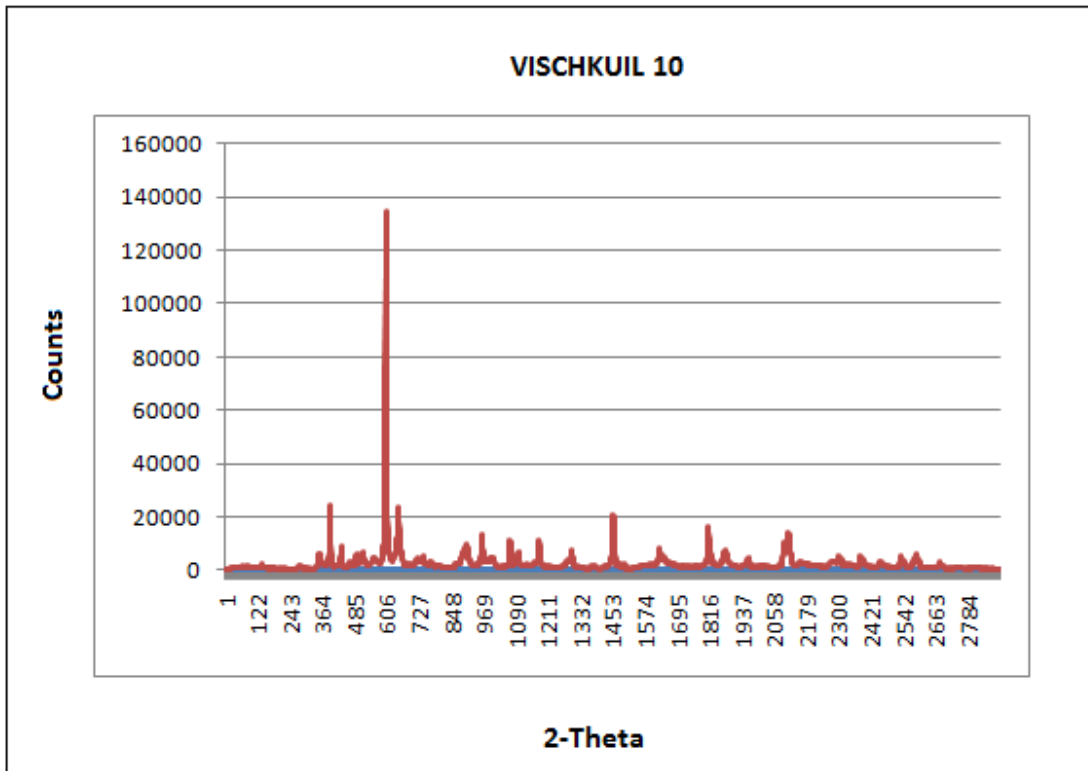
Appendix A-38: X-ray diffraction patterns profile, as an indication of the Vischkuil Formation shale samples obtained during this study.



Appendix A-39: X-ray diffraction patterns profile, as an indication of the Vischkuil Formation shale samples obtained during this study.



Appendix A-40: X-ray diffraction patterns profile, as an indication of the Vischkuil Formation shale samples obtained during this study.



APPENDIX B

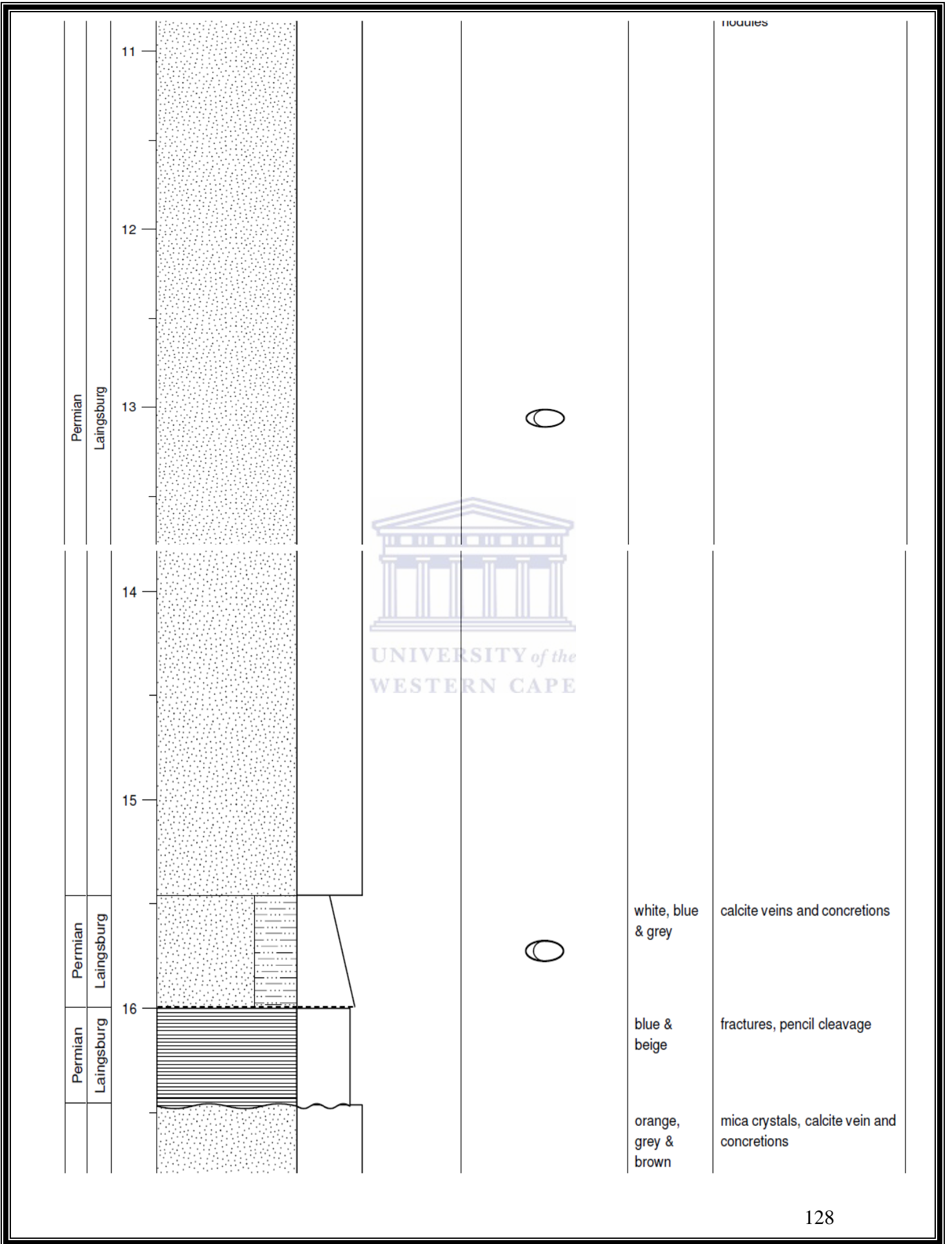
Appendix B-1: Sedimentary log of the Laingsburg Formation taken at: S33°11' 09.1",
E20°51'58.9".

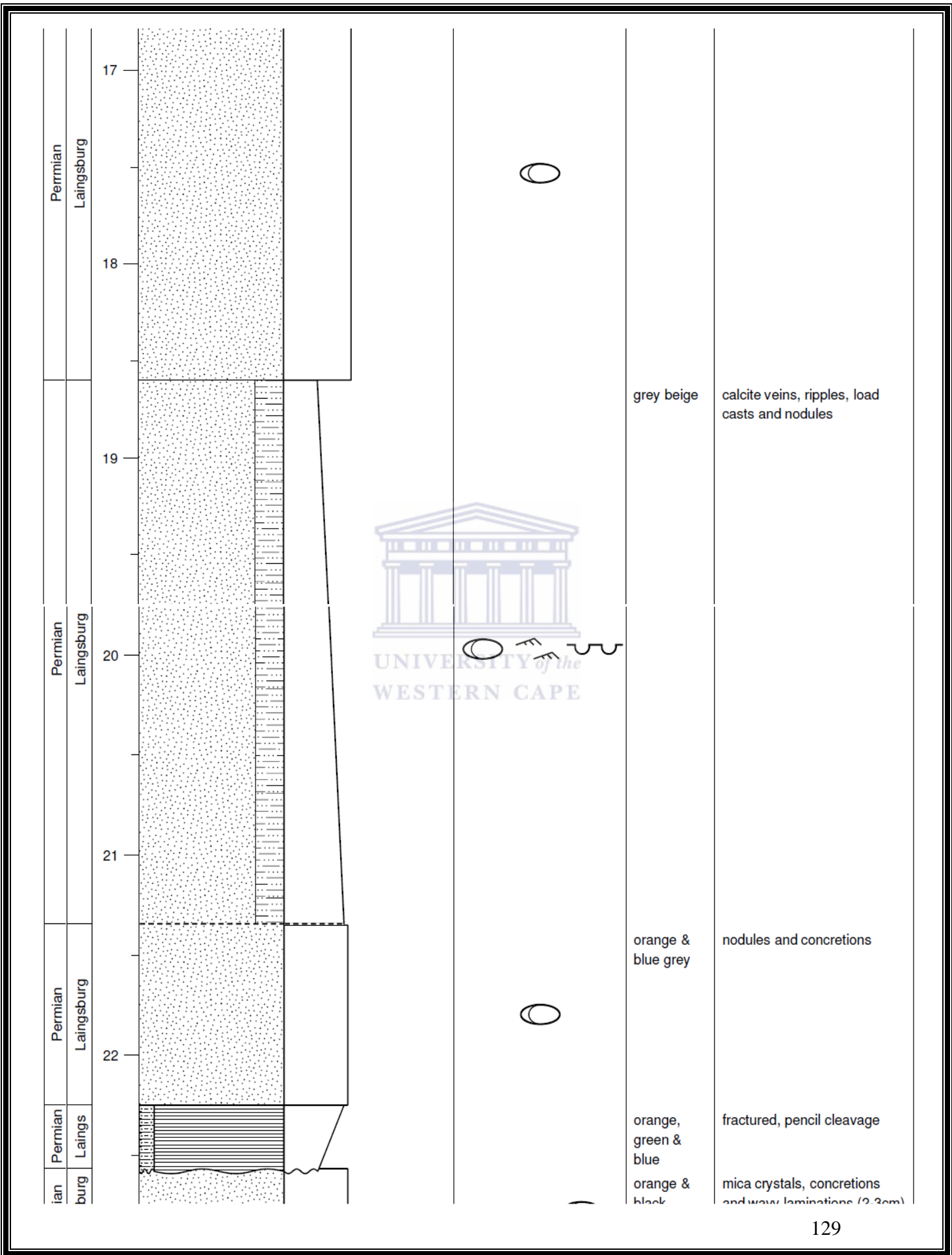
Laingsburg, Upper Eccla		SCALE (m)	LITHOLOGY	LIMESTONES						STRUCTURES / FOSSILS	COLOUR	NOTES
AGE	FORMATION			MUD		SAND		GRAVEL				
				mud	wacke	pack	grain	rud &	bound			
				clay	silt	vf	m	vc	gran			
Permian	Laingsburg	1	[Lithology: horizontal lines]							light blue grey	concretion found within the unit	
Permian	Laingsburg	2	[Lithology: dotted]							grey to beige	mudcracks mica crystals	
Permian	Laingsburg	3	[Lithology: horizontal lines]							grey	wavy laminations 3cm thick and nodules	
Permian	Laingsburg	4	[Lithology: dotted]							grey and brown	wavy laminations approximately 2cm thick	
Permian	Laingsburg	5	[Lithology: horizontal lines]							grey, beige	calcite veins and wavy laminations (5-6cm) thick	
Permian	Laingsburg	6	[Lithology: dotted]							grey, brown & white	mica crystals, calcite veins, concretions	
Permian	Laingsburg	7	[Lithology: horizontal lines]							orange, yellow, beige and grey	fractured, pencil cleavage and wavy laminations (1-2cm) thick	
Permian	Laingsburg	8	[Lithology: dotted]							blue grey	calcite veins, mica crystals, parallel laminae, ripples and nodules	
Permian	Laingsburg	9	[Lithology: horizontal lines]							brown, orangy grey	concretions found within the unit	

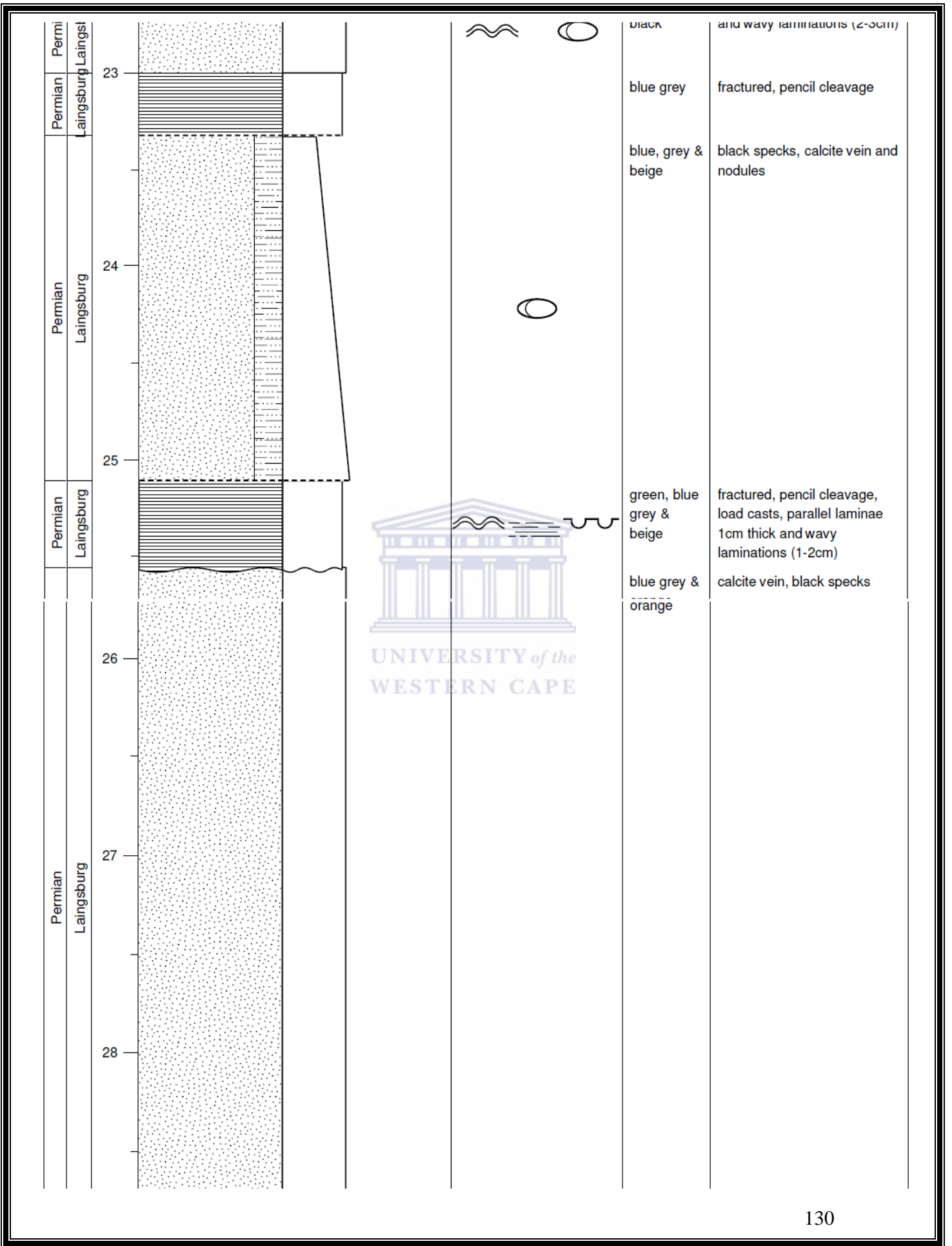
Permian Laingsburg	Permian Laingsburg	Permian Laingsburg	Permian Laingsburg	Permian Laingsburg	Permian Laingsburg	Permian Laingsburg	Permian Laingsburg
5							
6							
7							
8							
9							
10							

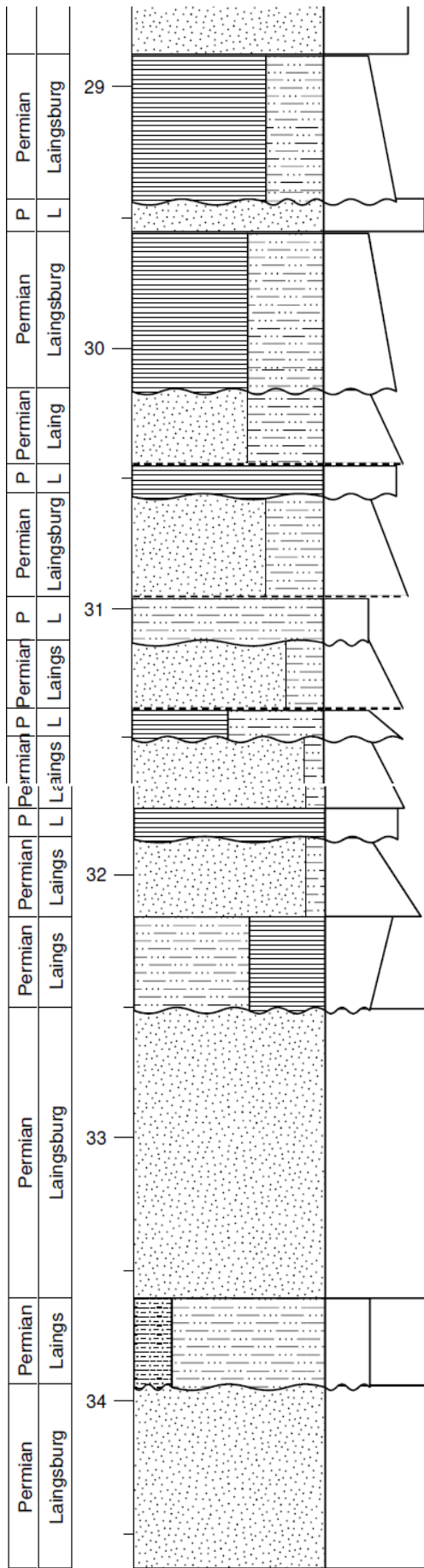
	beige & grey blue grey	calcite veins and wavy laminations (1-2cm) thick calcite veins and concretions
	bluish brown	fractures, pencil cleavage and wavy laminations(1-2cm) thick
	orange, blue grey	nodules, plumos structures and cross beds are visible on the unit
	blue grey	fractures, pencil cleavage, mica crystals, calcite veins and nodules
	beige	
	blue grey	fractured, pencil cleavage, nodules, load casts and wavy laminations (3-4cm) thick
	dark grey and beige	calcite veins, concretions and load casts
	blue grey	calcite veins, concretions and nodules



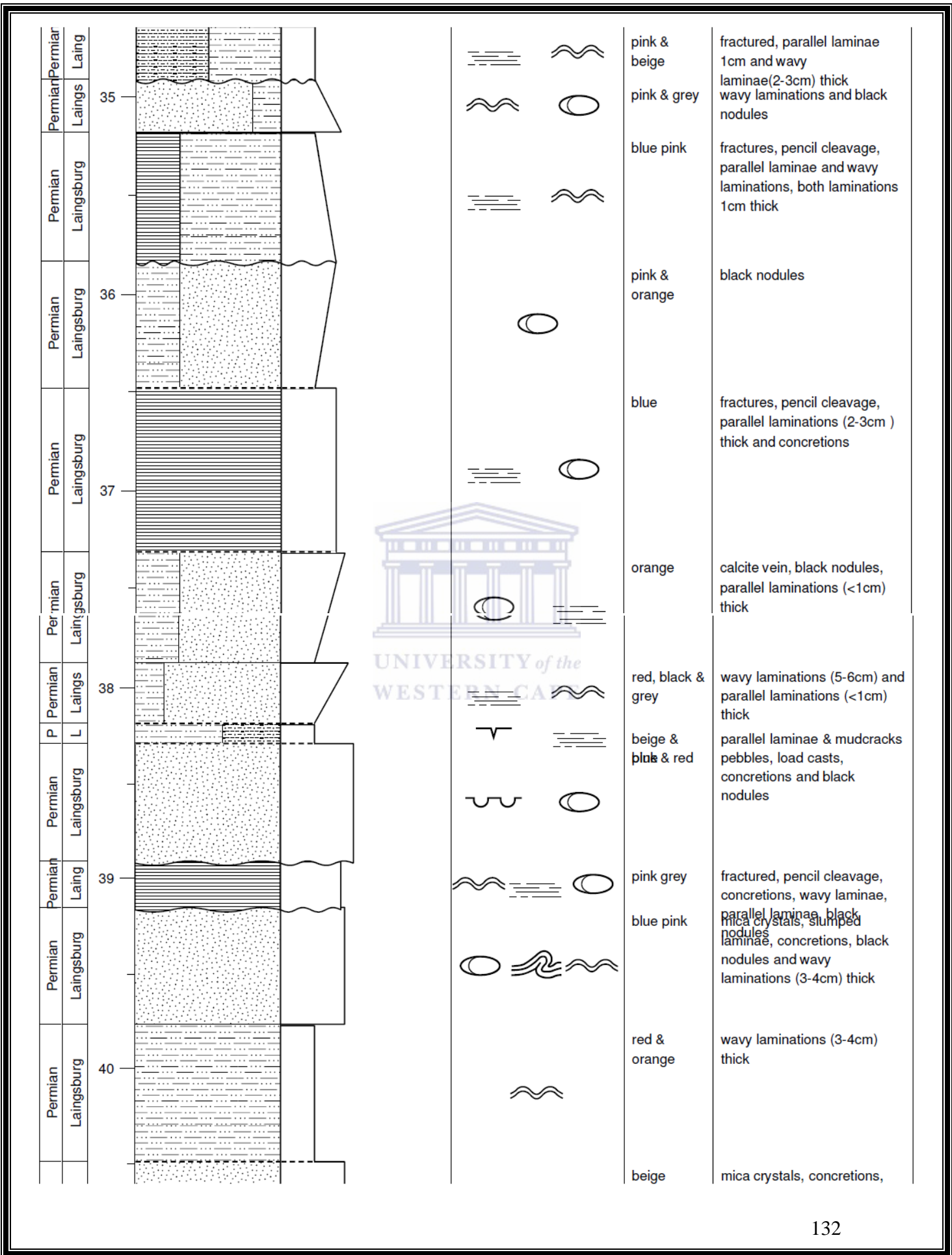


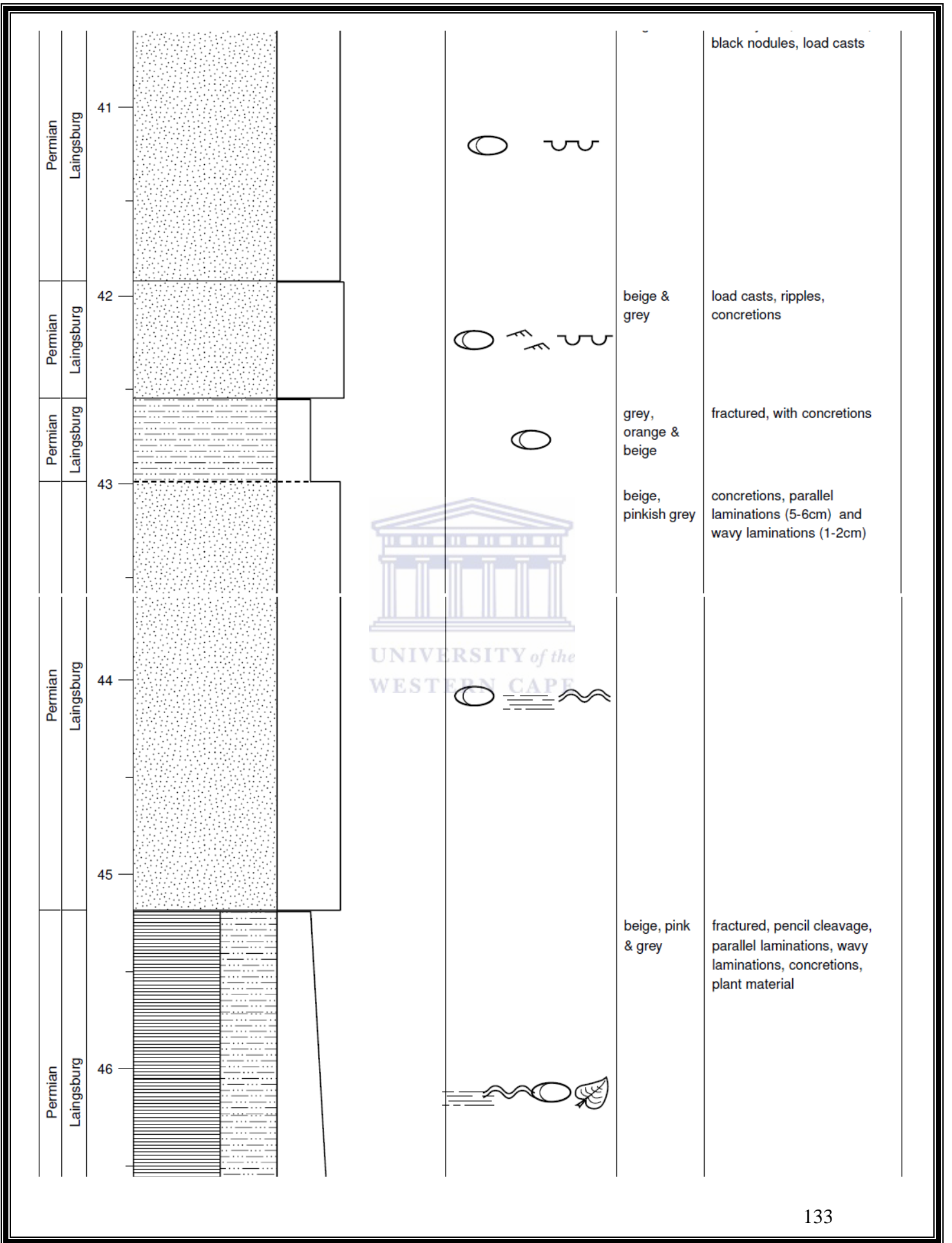


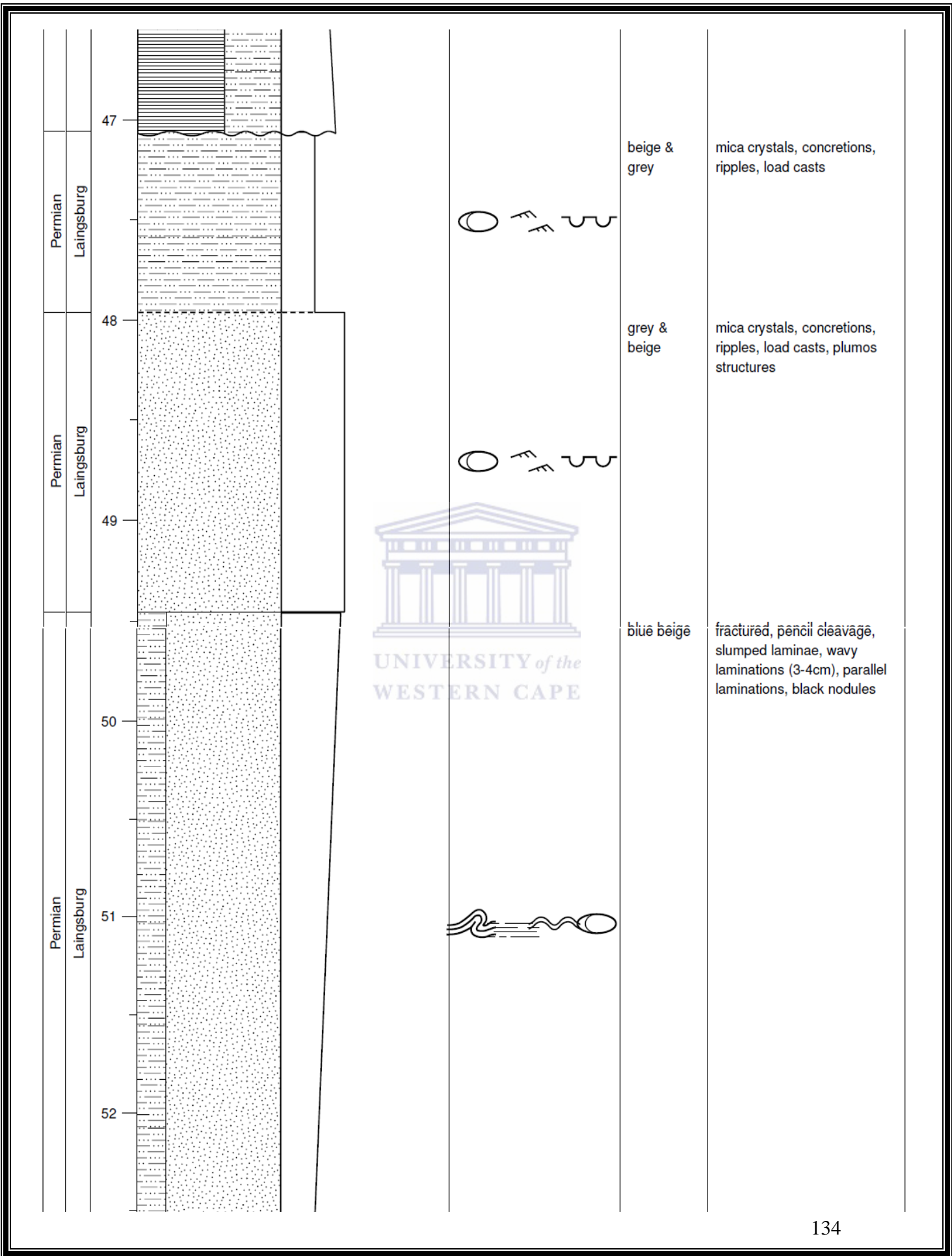


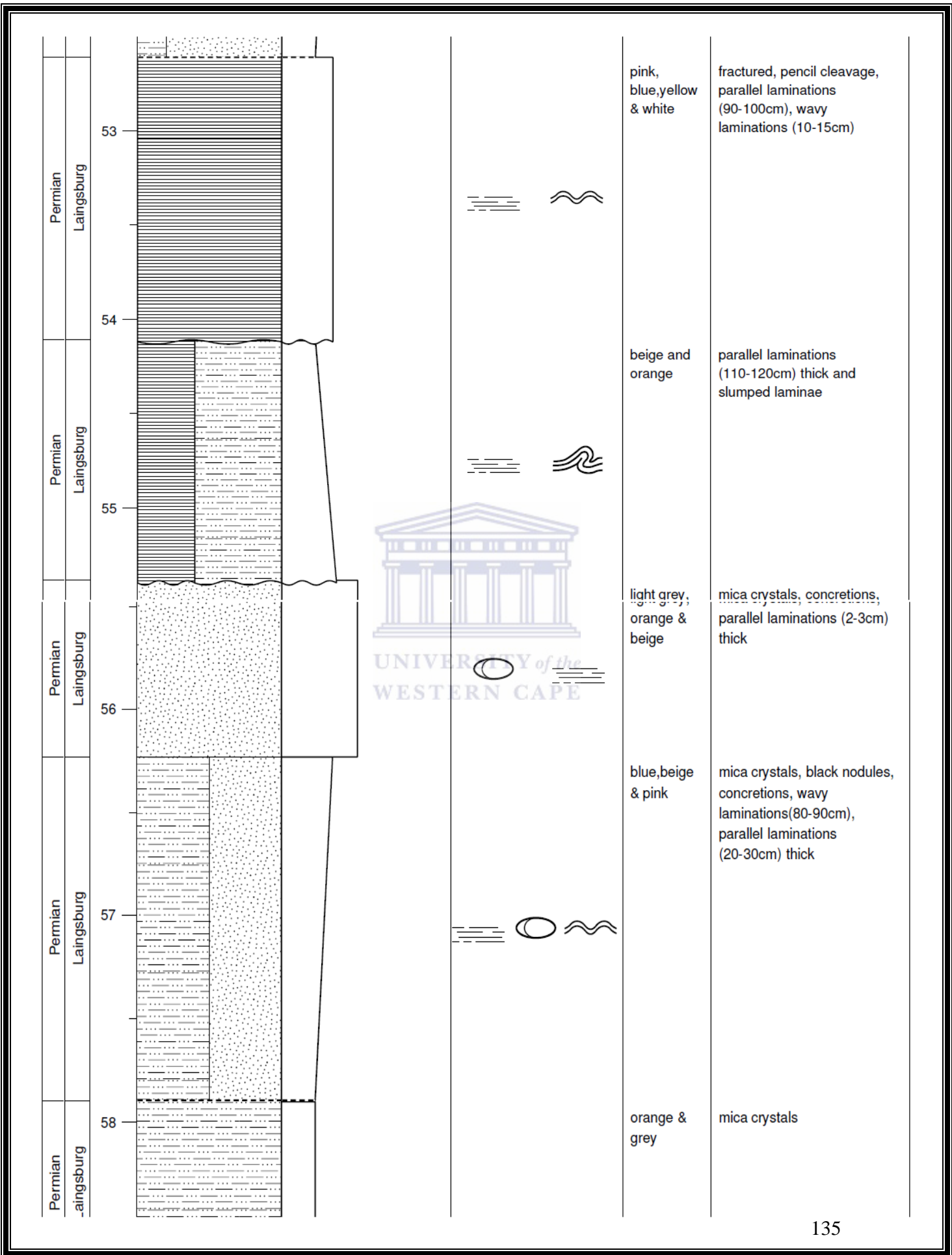


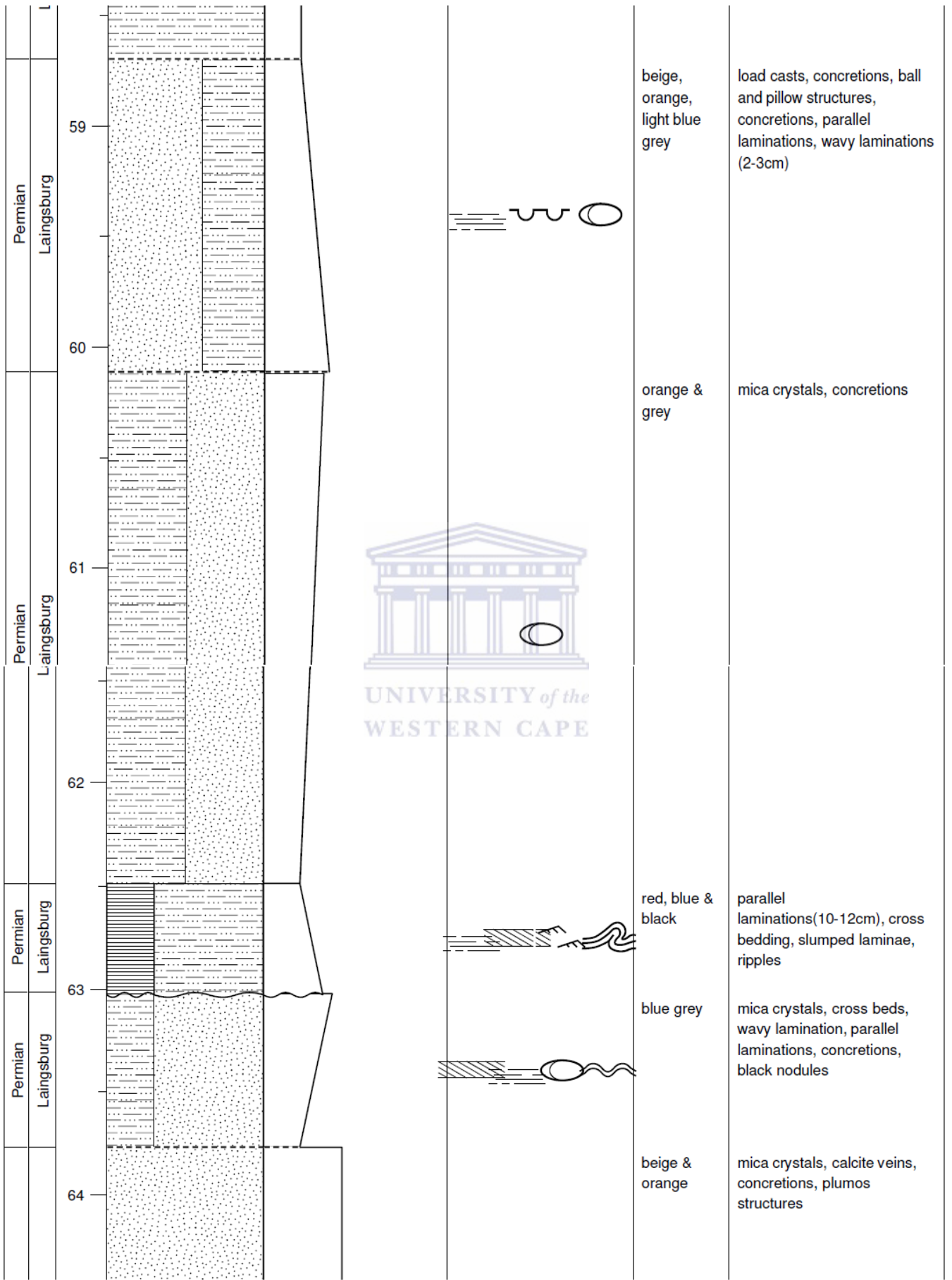
blue grey	fractures, pencil cleavage, concretions, parallel laminae 3cm and wavy laminations 1cm thick respectively
light grey	black specks, mica crystals
blue grey & beige	ripples and wavy laminations 4cm thick
dark to light grey	black specks
beige & grey & dark grey	fractured, pencil cleavage concretions and black nodules found within the unit
beige & grey dark & light blue & orange dark blue & beige	concretions, slumped laminae and wavy laminations fractured, pencil cleavage mica crystals, weathered black
blue grey greyish pink	cleavage and wavy laminae black nodules
greyish pink	fractured, pencil cleavage and wavy laminations (3-4cm) thick
greyish pink	plumos structures and concretions
grey, pink & beige	fractured and parallel laminations (<1cm) thick
pink & grey	mica crystals, ripples, concretions and wavy laminations (2-3cm) thick

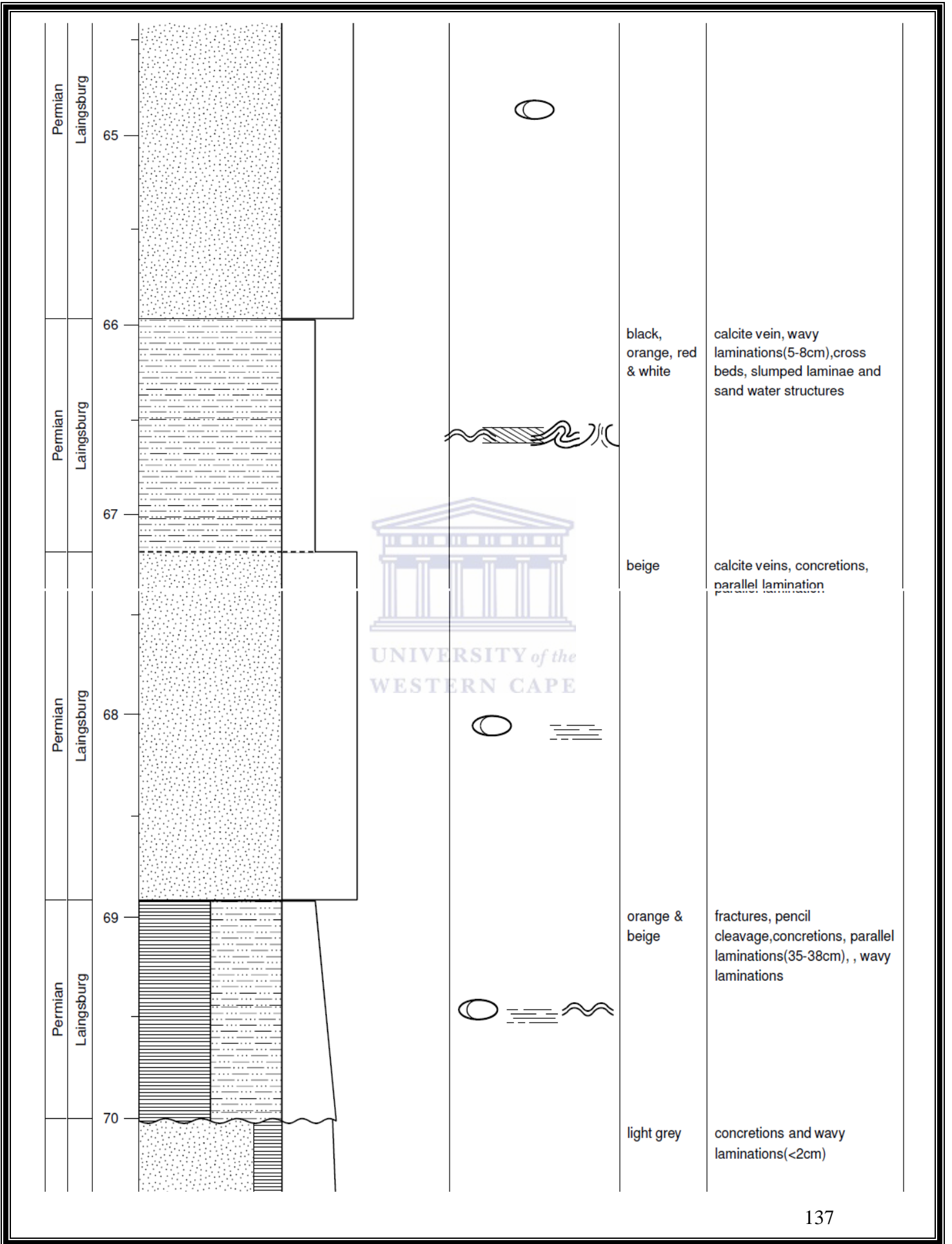


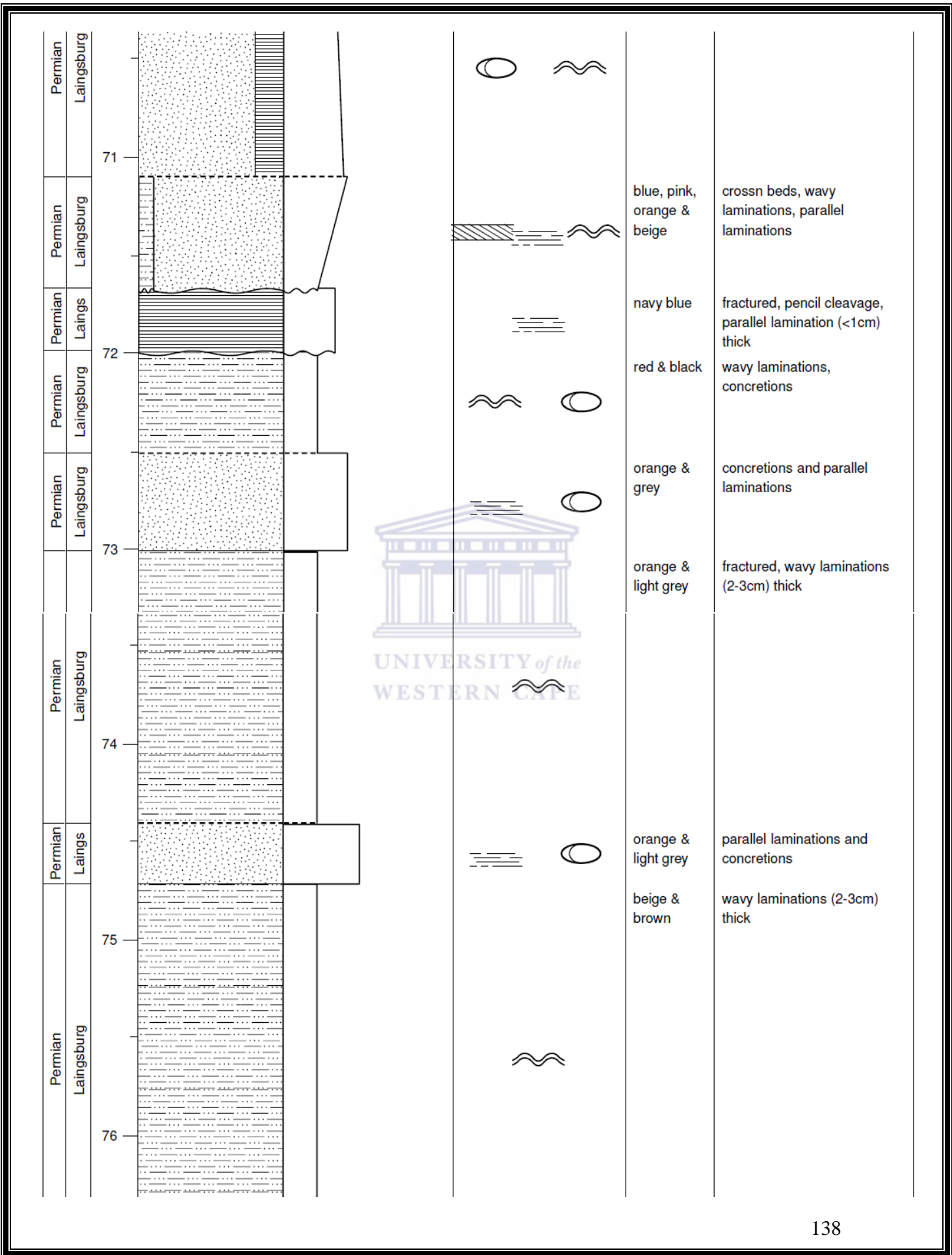


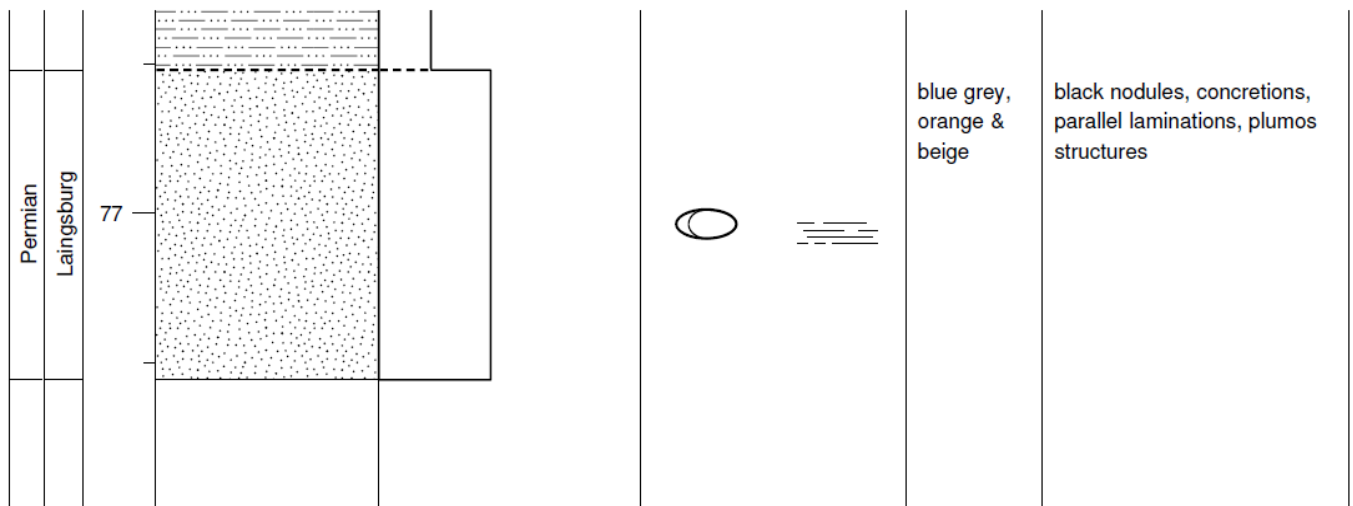












Appendix B-2: Laingsburg Formation Legend

Lithologies	Symbols	Base Boundaries
Sandstone	Nodules and concretions	Sharp
Siltstone	Horizontal planar lamination	Gradational
Shale	Wave ripple cross-lamination	Erosion
Mudstone	Planar cross bedding	
	Convolute lamination	
	Water structures	
	Current ripple cross-lamination	
	Load casts	
	Plant material	
	Mudcracks	

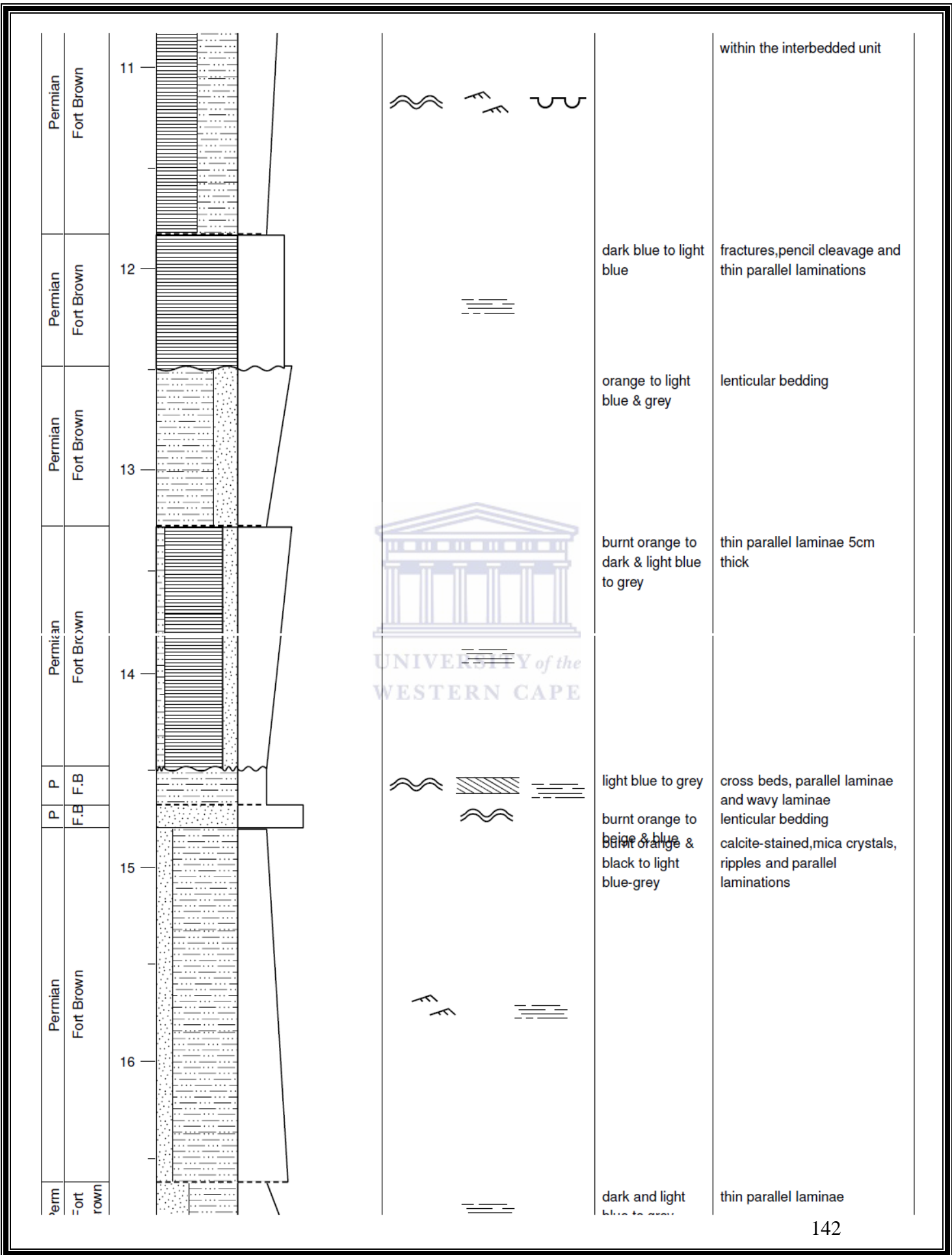
APPENDIX C

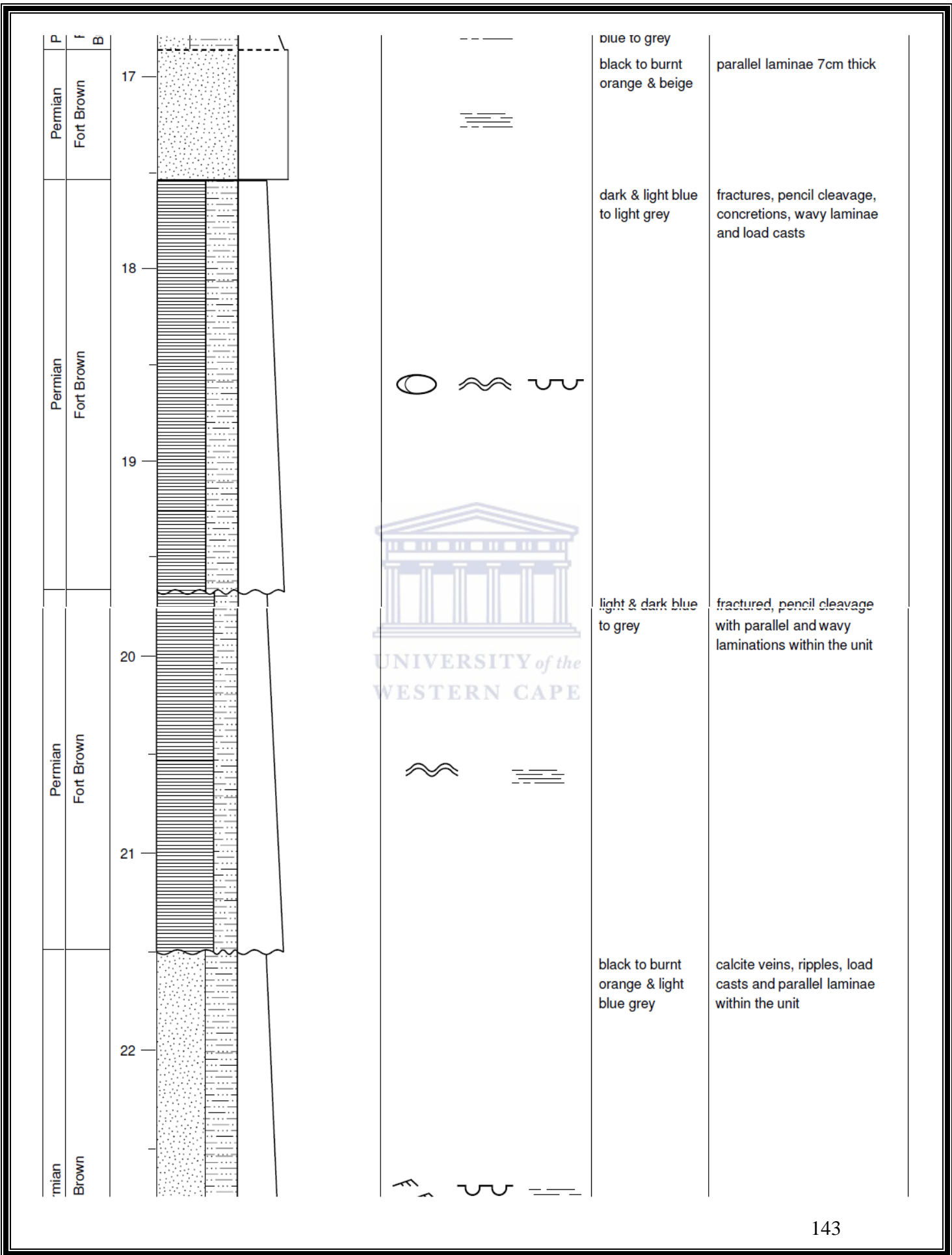
Appendix C-1: Sedimentary log of the Fort Brown Formation taken at: S33°12' 07.0",
E20°51'20.2"

Fort Brown, Upper Eccla			SCALE (m)	LITHOLOGY	LIMESTONES						STRUCTURES / FOSSILS	COLOUR	NOTES		
AGE	FORMATION				MUD SANDGRAVEL										
					mud	wacke	pack	grain	rud & bound	clay				silt	vf
Permian	Fort Brown		1 2 3 4	[Lithology pattern]								[Structures]	orange to beige & black	mica crystals, with parallel laminae, some wavy laminae as well as load casts on the underside of the unit.	
P	F.B.			[Lithology pattern]									[Structures]	bluish grey orange to beige	fractures with wavy laminae small parallel laminae 5cm thick
Permian	Fort Brown			[Lithology pattern]									[Structures]	bluish grey	fractured with wavy laminae
Permian	Fort Brown			[Lithology pattern]									[Structures]	bluish grey, reddish beige & black	wavy laminae, minor parallel laminae and ripples on the underside of the unit
P	F.B.F.	B		[Lithology pattern]									[Structures]	bluish grey greyish blue	wavy laminae around 5cm thick parallel and wavy laminae
Permian	Fort Brown			[Lithology pattern]									[Structures]	light grey to blue	wavy laminae, ripples and nodules are visible
Permian	Fort Brown			[Lithology pattern]									[Structures]	orange & beige to light bluish grey	parallel laminae around 10 cm and wavy laminae 40cm thick
Permian	Fort Brown			[Lithology pattern]									[Structures]	orange & beige to bluish grey	ripples and wavy laminations 10cm thick
Permian	Fort Brown			[Lithology pattern]									[Structures]	orangey beige to black in some parts bluish grey orange beige	parallel laminations 20cm thick wavy laminae parallel laminae
Permian	Fort Brown			[Lithology pattern]									[Structures]	bluish grey burnt orange bluish grey orange to beige burnt orange to bluish grey & black	wavy laminae parallel laminae wavy laminae parallel laminae load casts and parallel laminae bedding, concretions and thin laminae

Pt	Permian	Fort Brown	5		orange to bluish grey	ripples, wavy laminations as well as parallel laminae
	Permian	Fort Brown	6		orange to bluish grey dark orange & black to bluish grey	thin parallel laminae 5cm long mica crystals
	Permian	Fort Brown	7		bluish to light grey	thin parallel laminae, concretions, wavy laminae and ripples found within the unit
	Permian	Fort Brown	8		orange & beige to bluish grey	cross beds, ripple marks and wavy laminae
	Permian	Fort Brown	9		bluish grey	flame structure, with ripple marks, concretions and wavy laminations on the unit
	Permian	Fort Brown	10		burnt orange to beige & bluish grey	calcite veins 2cm thick and wavy laminae
					dark to light blue & grey	fractured, pencil cleavage, wavy laminae, ripple marks and load casts are found



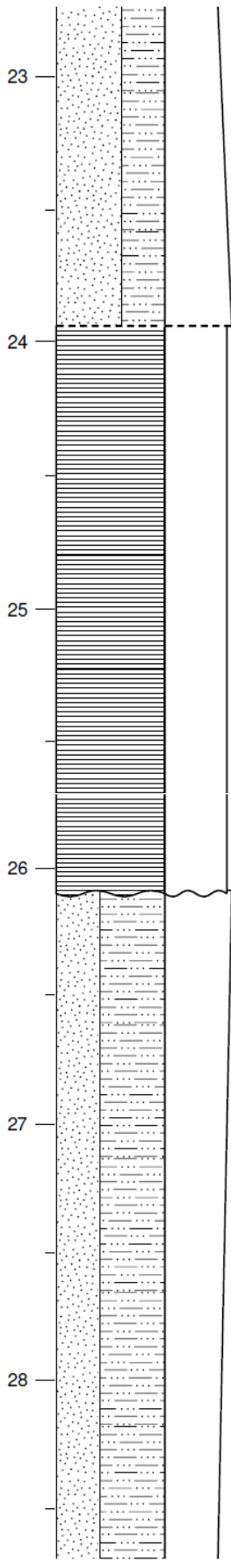




an
own

Permian
Fort Brown

Per
Fort

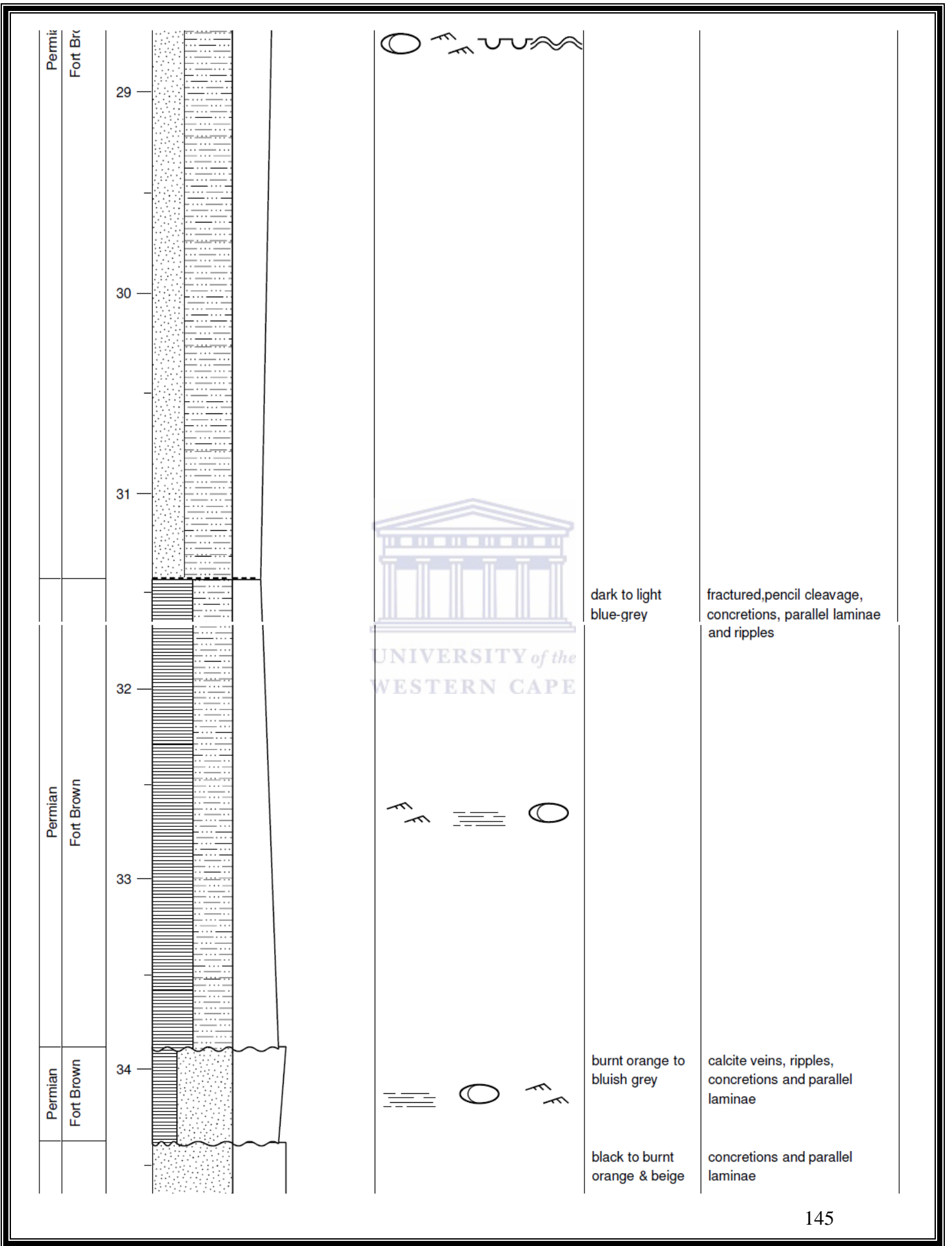


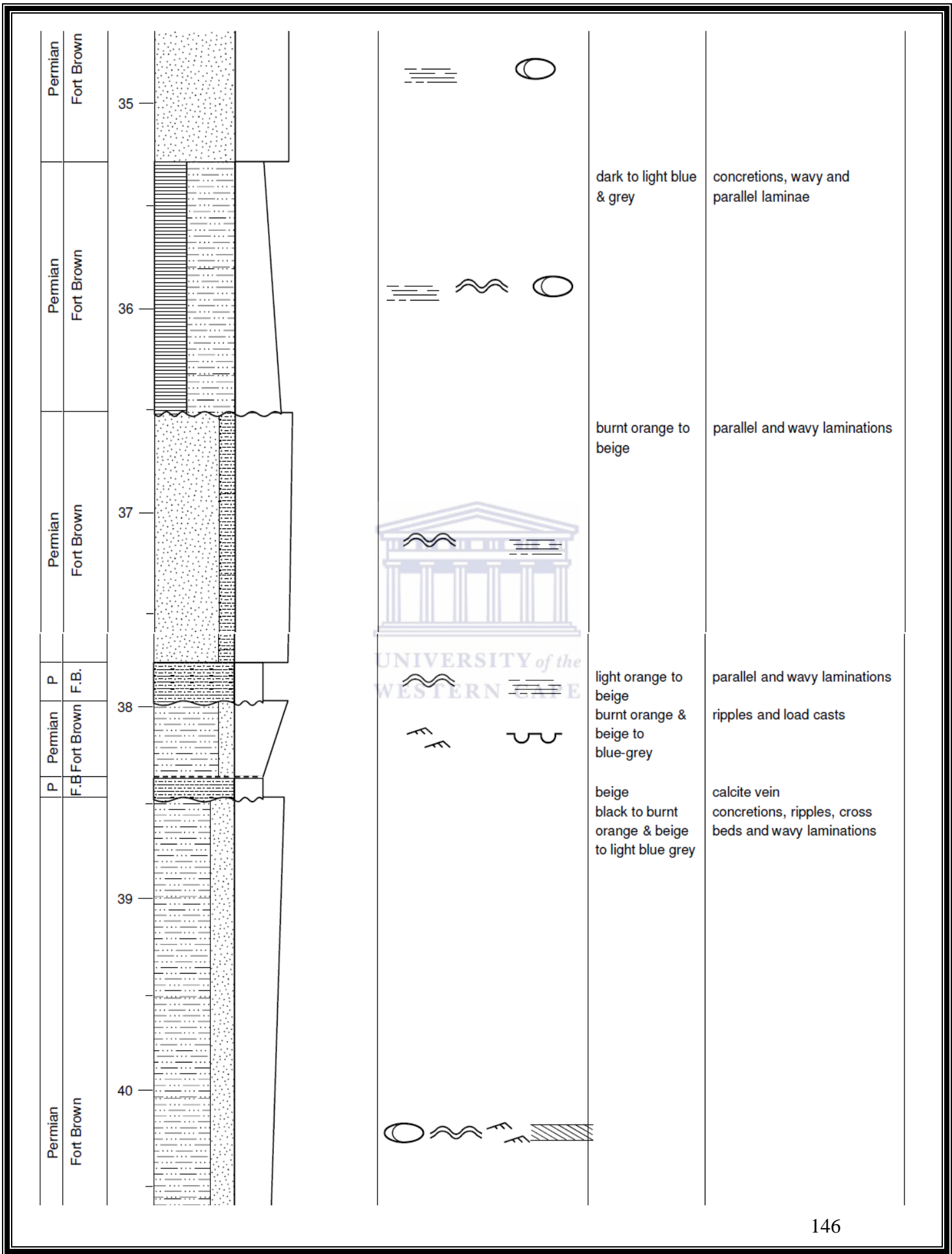
dark to light
blue-grey

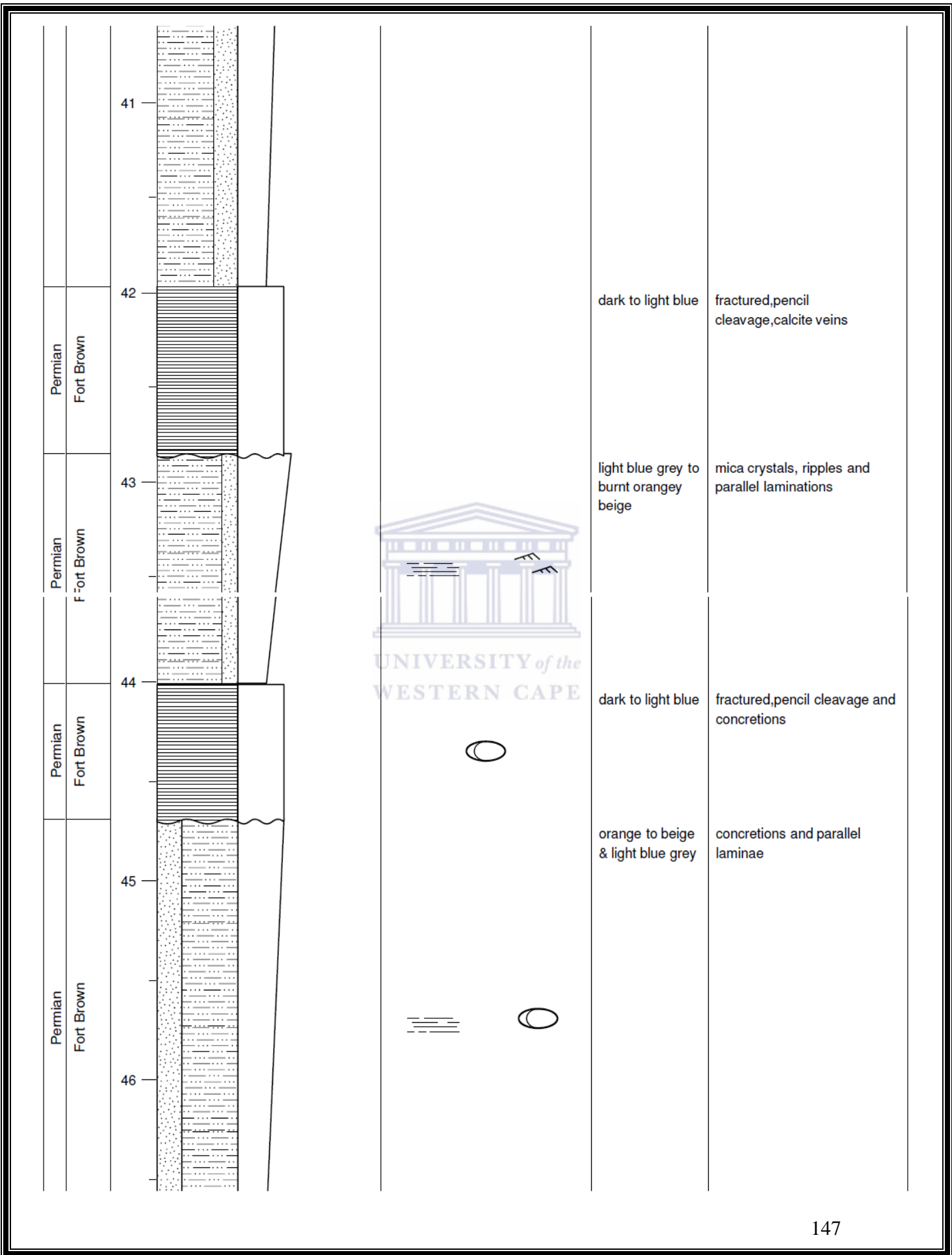
fractured, pencil cleavage and
parallel laminations

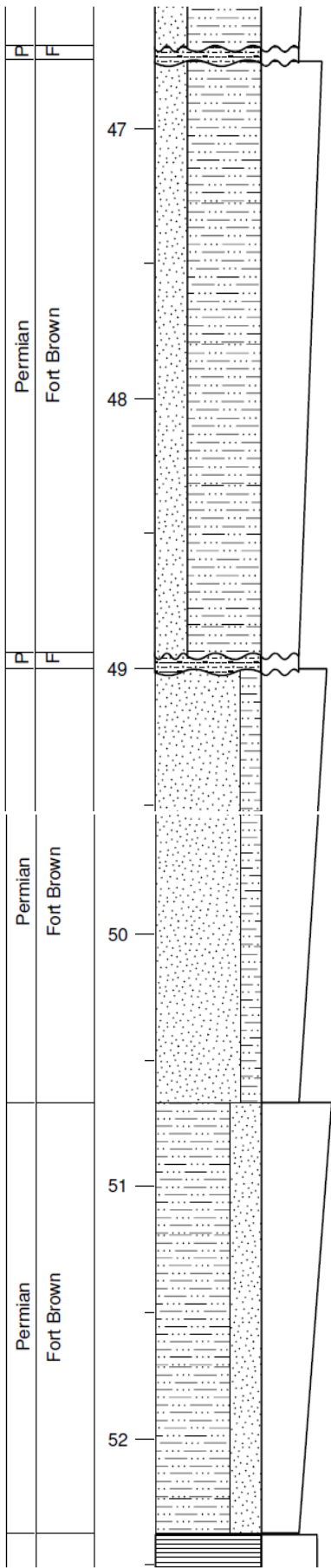
dark orange to
light blue grey

mica crystals, concretions,
load casts, ripples and wavy
laminations are present









beige
burnt orange to
light blue grey &
beige

wavy lamination
concretions and parallel
laminae

beige
burnt orange to
light blue grey

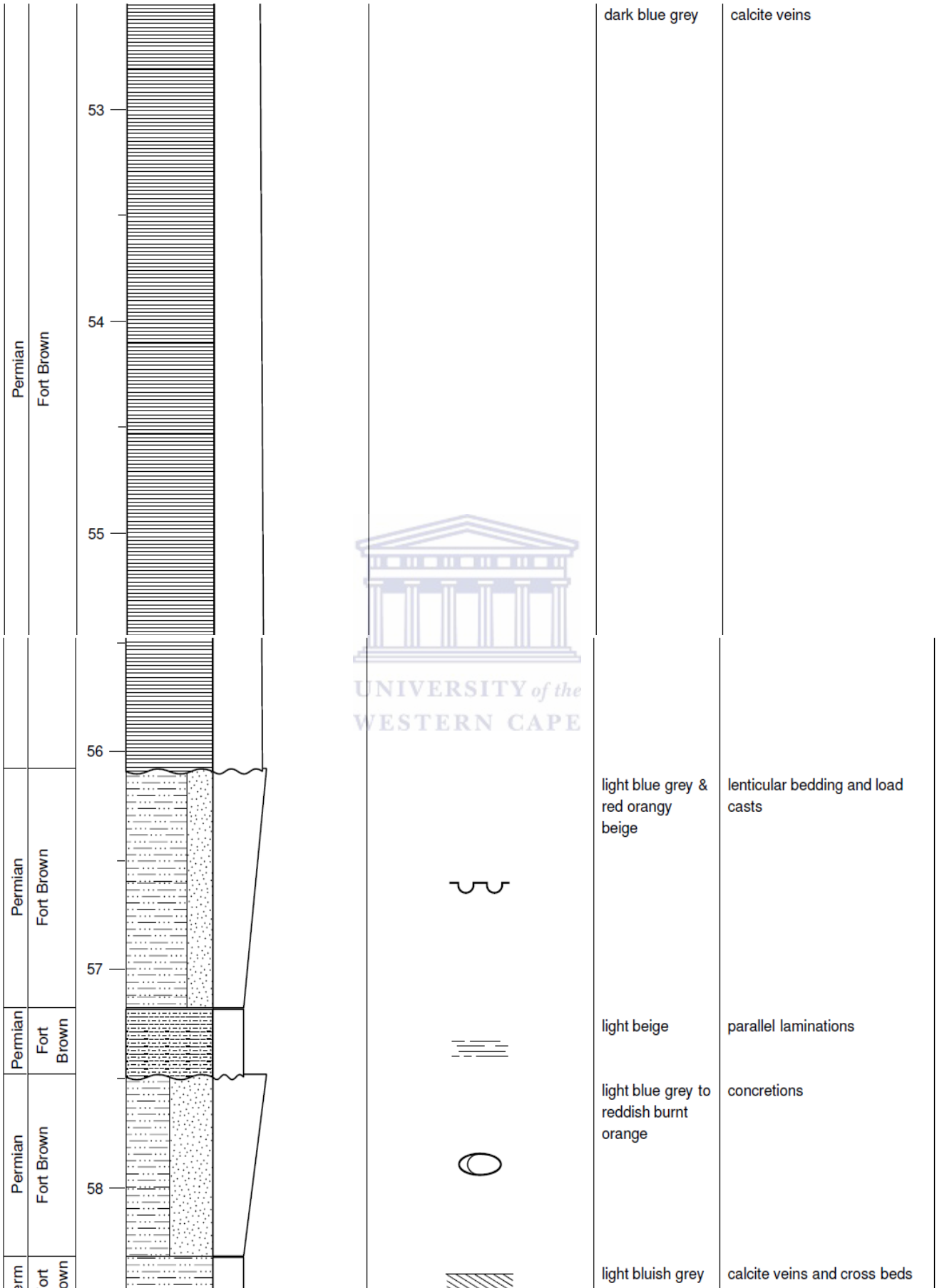
calcite vein and parallel
calcite veins and parallel
lamination

light blue grey to
burnt orangy
beige

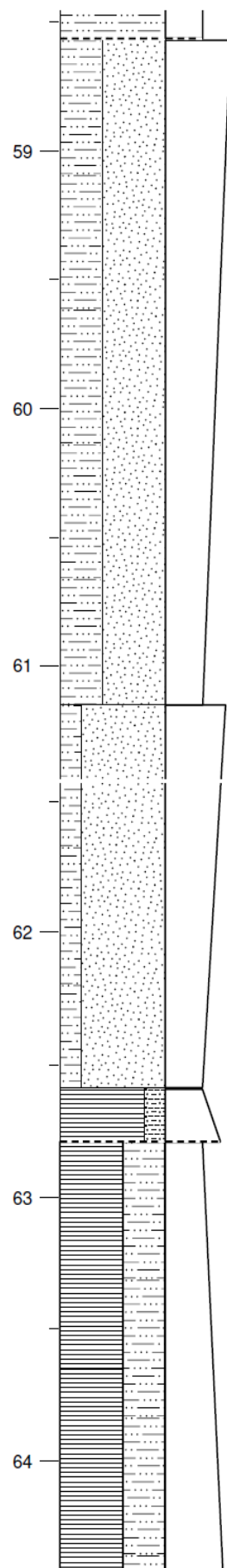
concretions and wavy
laminations

red, orange to

fractured, pencil cleavage,



Permian Fort Brown	Permian Fort Brown	Permian Fort Brown	Permian Fort Brown
64	63	62	61
60	59		



light bluish grey to reddish orangy beige

orange to beige & light grey

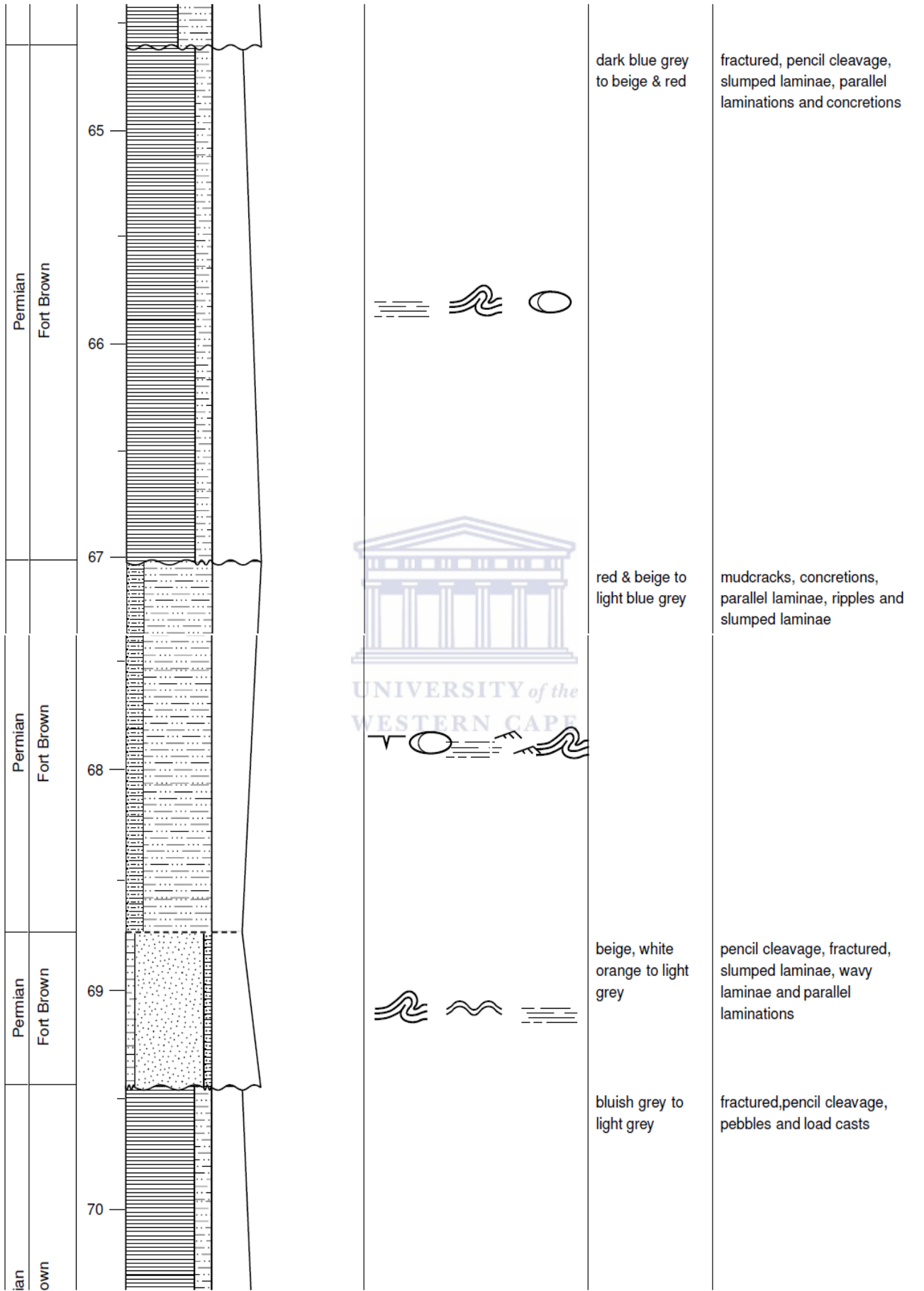
dark blue and grey burnt orange, dark grey & blue

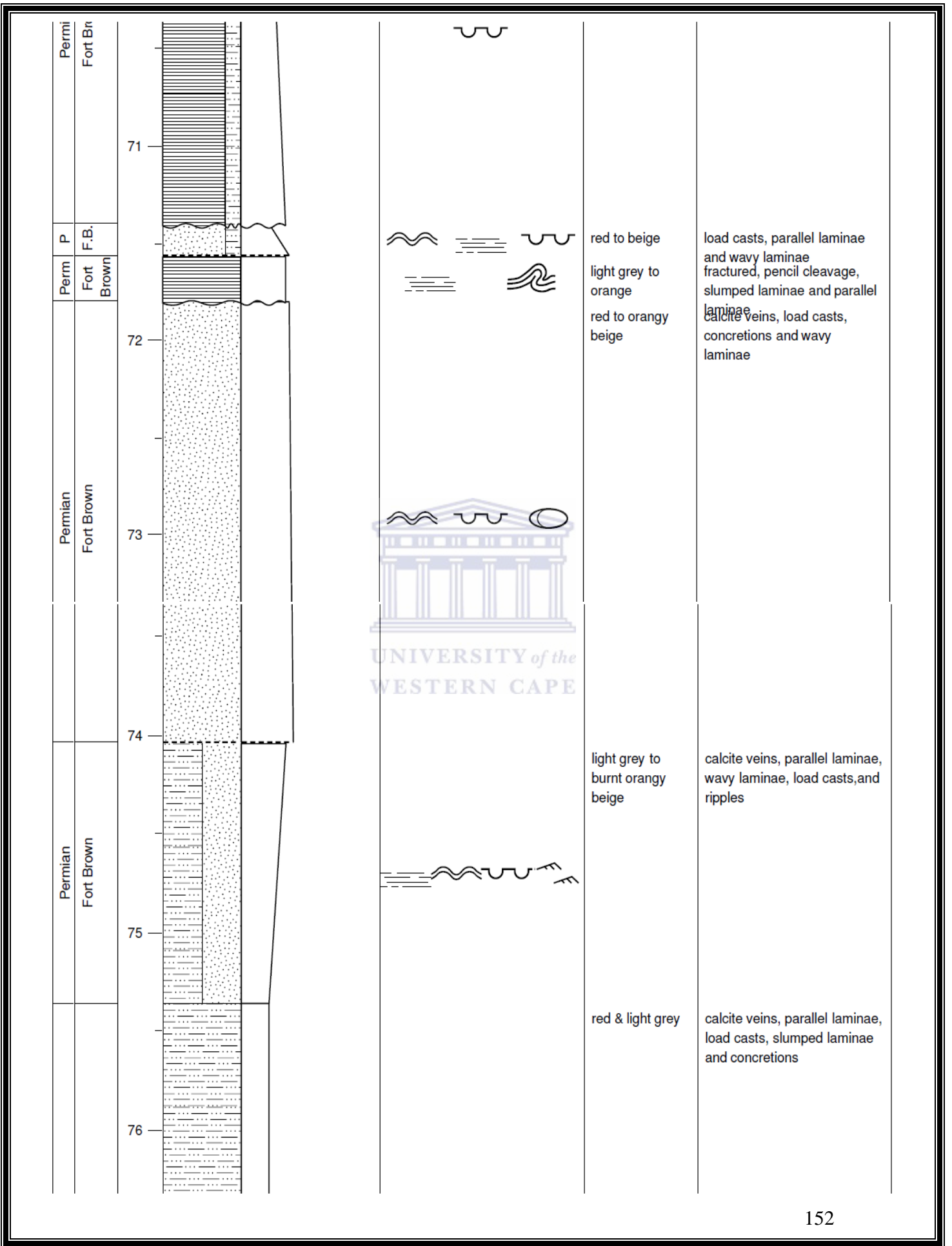
concretions, parallel laminations and wavy laminae

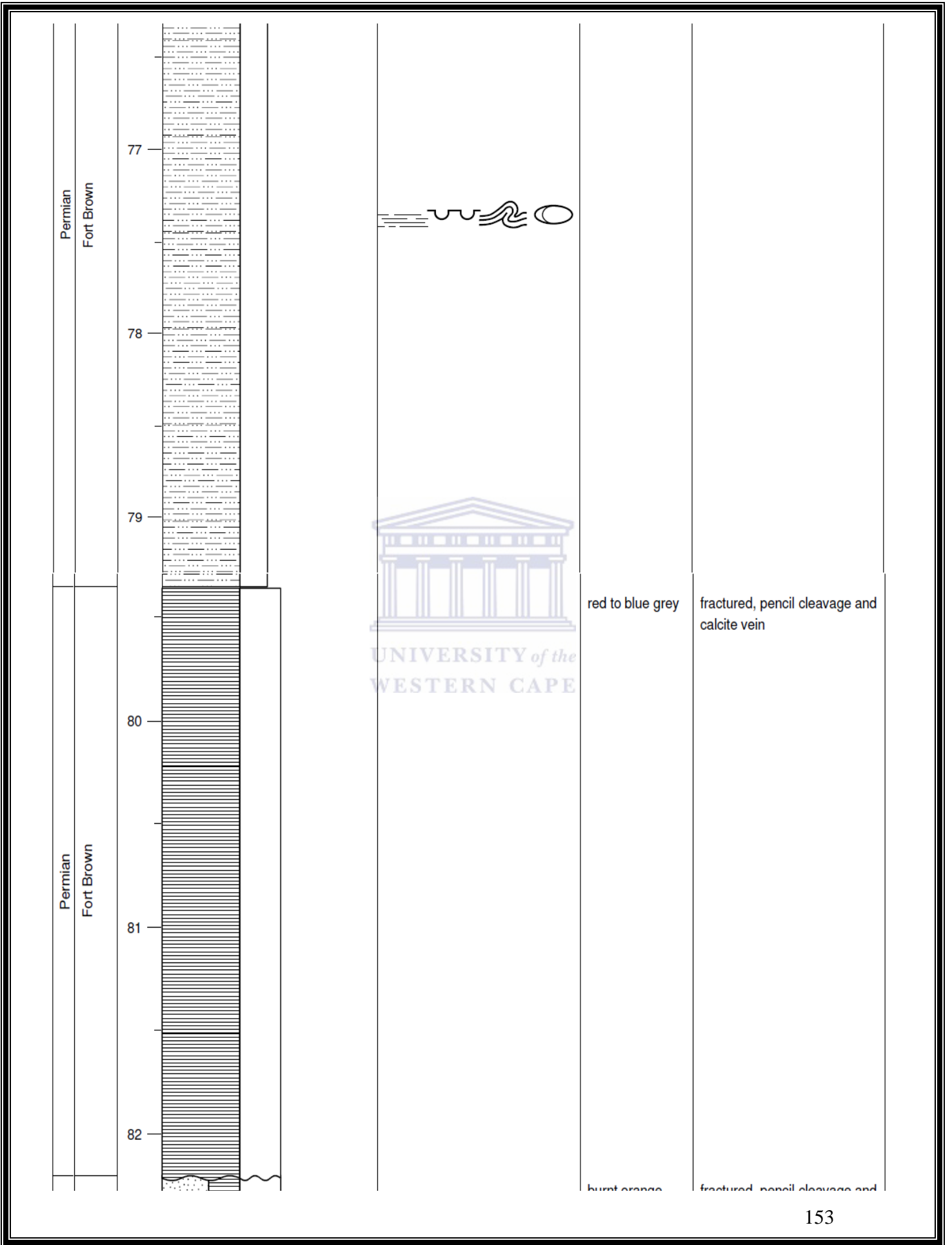
pebbles, concretions, load casts and parallel laminae

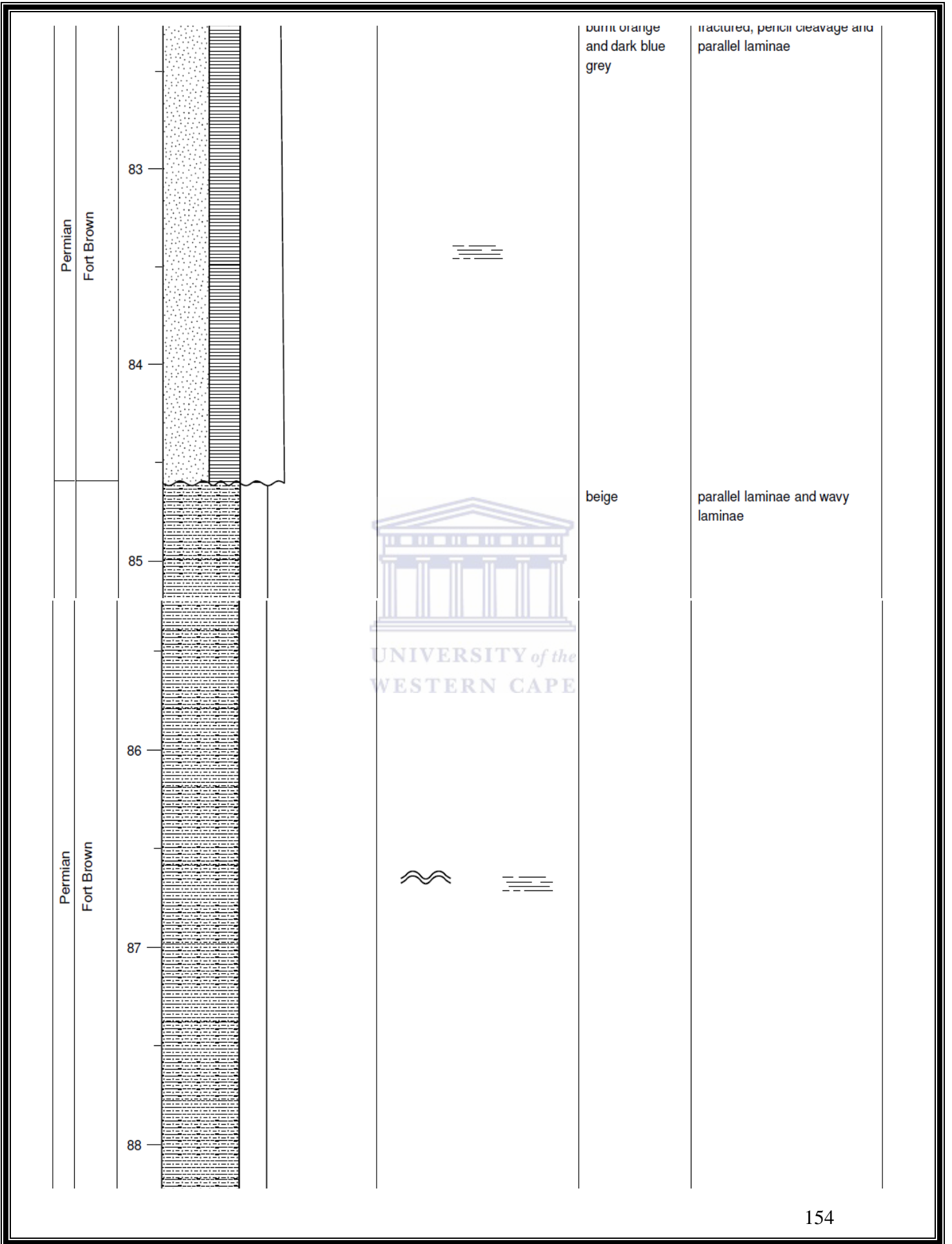
fractured, pencil cleavage and concretions
fractured, slumped laminae, cross beds, concretions, ripples and parallel laminae

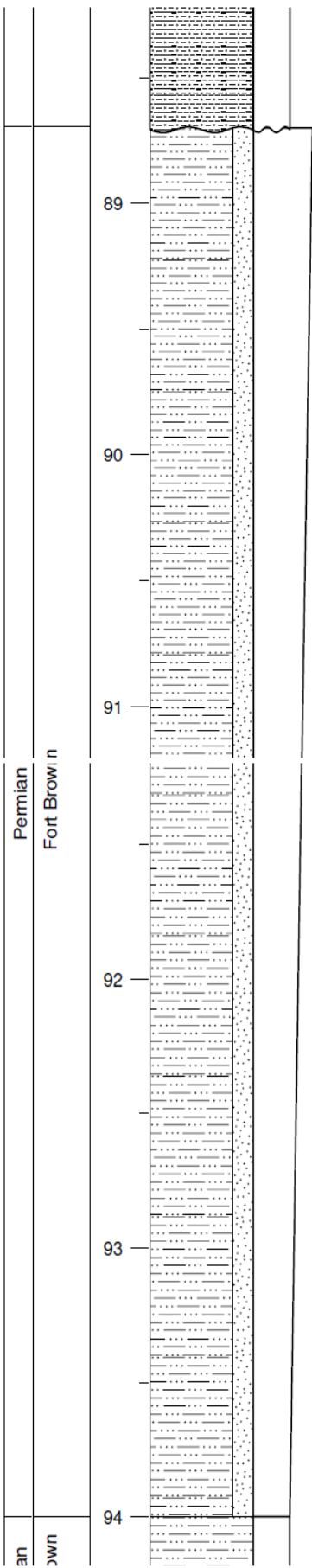












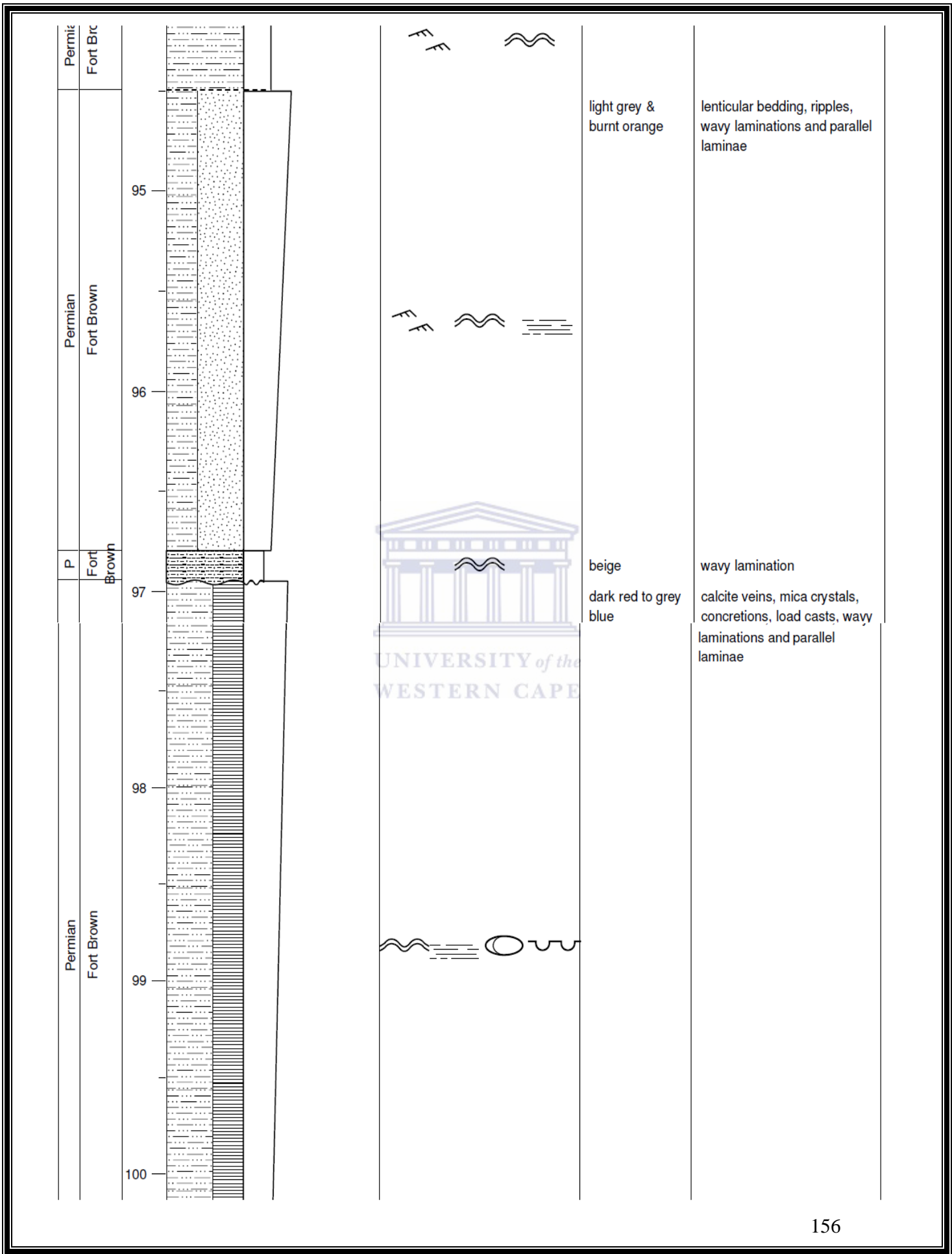
light grey to
burnt orange

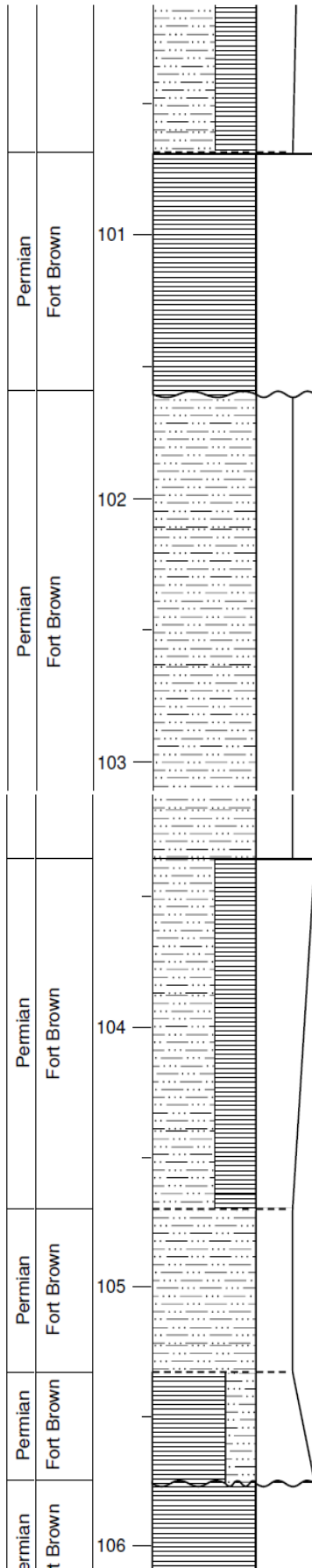
calcite veins, load casts,
ripples and concretions



light blue grey

wavy lamination and ripples





dark blue grey

fractured, pencil cleavage, concretions, wavy laminations and parallel laminae

light brown to light grey

nodules, fractures, concretions, pencil cleavage and wavy laminations

light brown to blue grey

fractured, pencil cleavage, nodules and wavy lamination

light blue grey

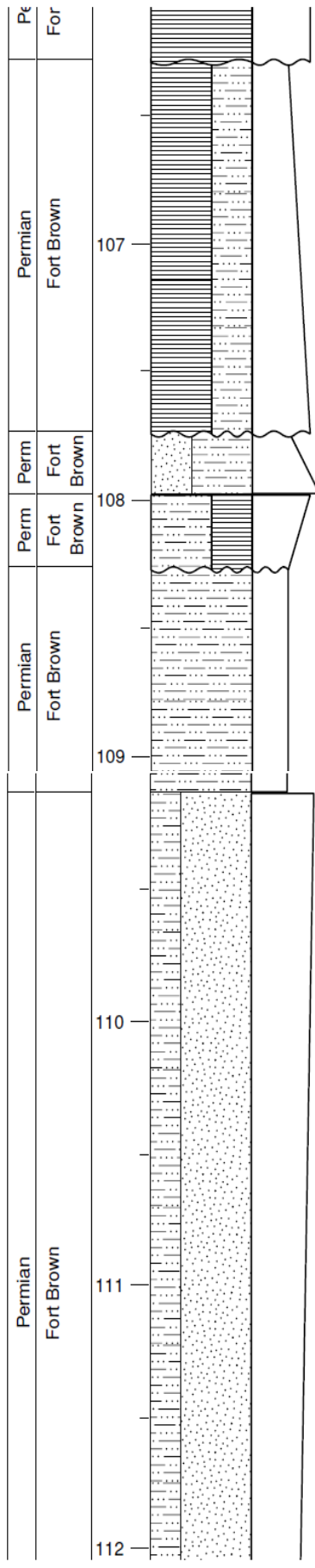
ripples, parallel and wavy lamination

beige to light blue grey

fractured, pencil cleavage and parallel laminations

white & red to dark bluish grey

fractured, pencil cleavage, concretions and wavy laminations



dark to light
bluish grey

fractured, pencil cleavage,
slumped laminae, wavy
laminations and parallel
laminations

orange to light
grey

concretions and ripples

dark to light
bluish grey

fractured, pencil cleavage,
calcite vein

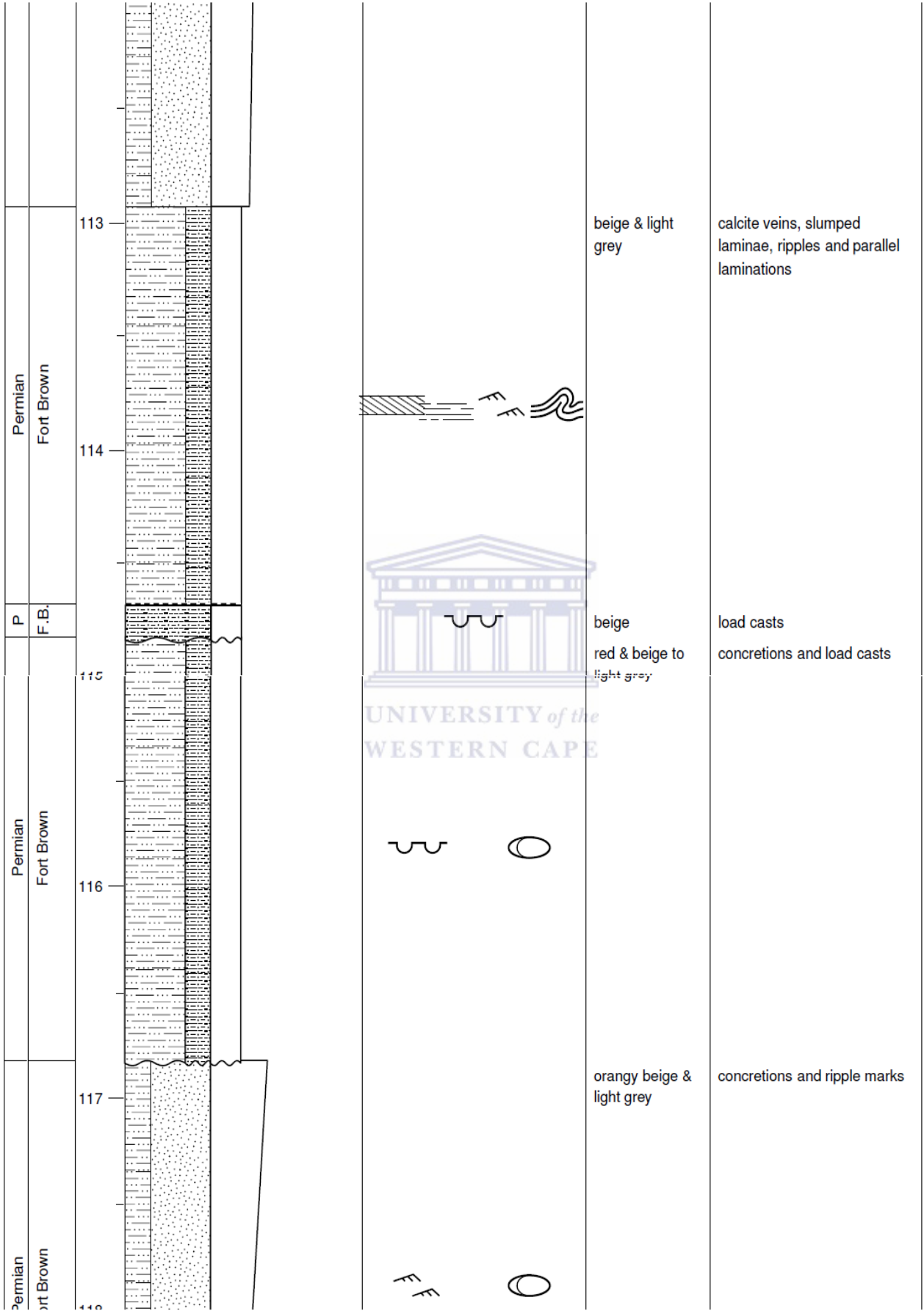
beige to light
blue grey

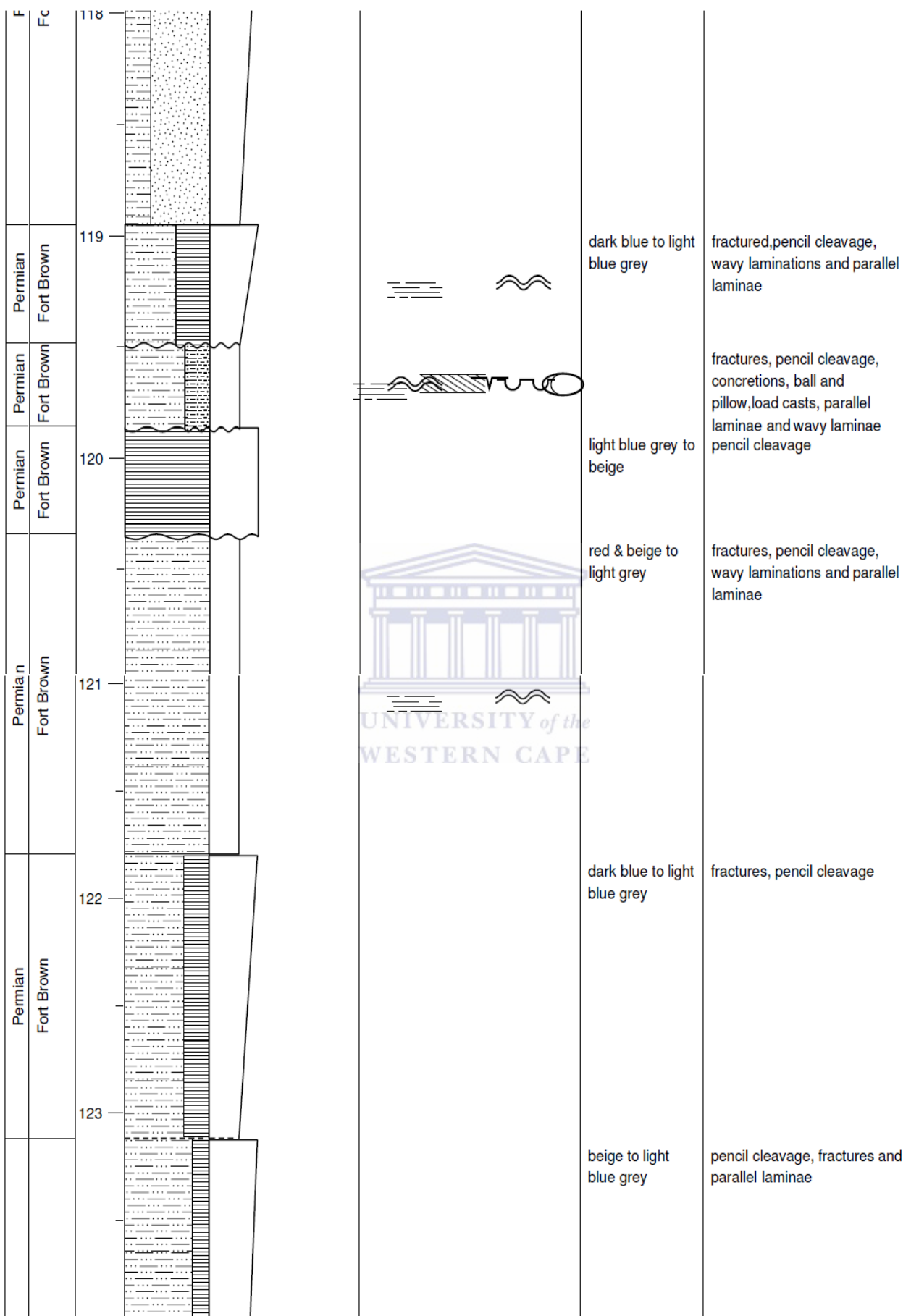
concretions and parallel
laminae

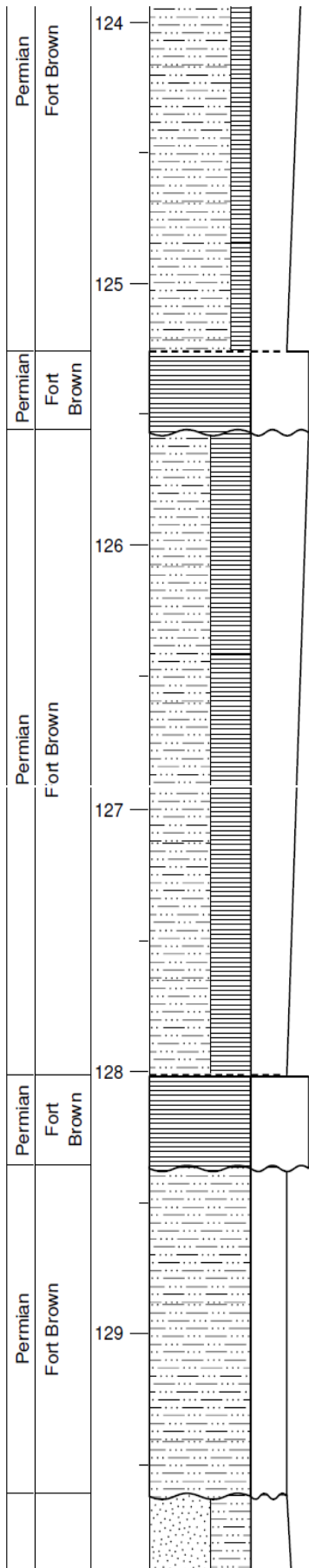
light grey &
orangy red

calcite veins, slumped
laminae, concretions and
parallel laminae









— — — — —

beige to bluish grey

fractures, pencil cleavage

red to light bluish grey

fractures, pencil cleavage, concretions, wavy laminae and parallel laminae

beige to bluish grey

fractures, pencil cleavage

beige to light grey

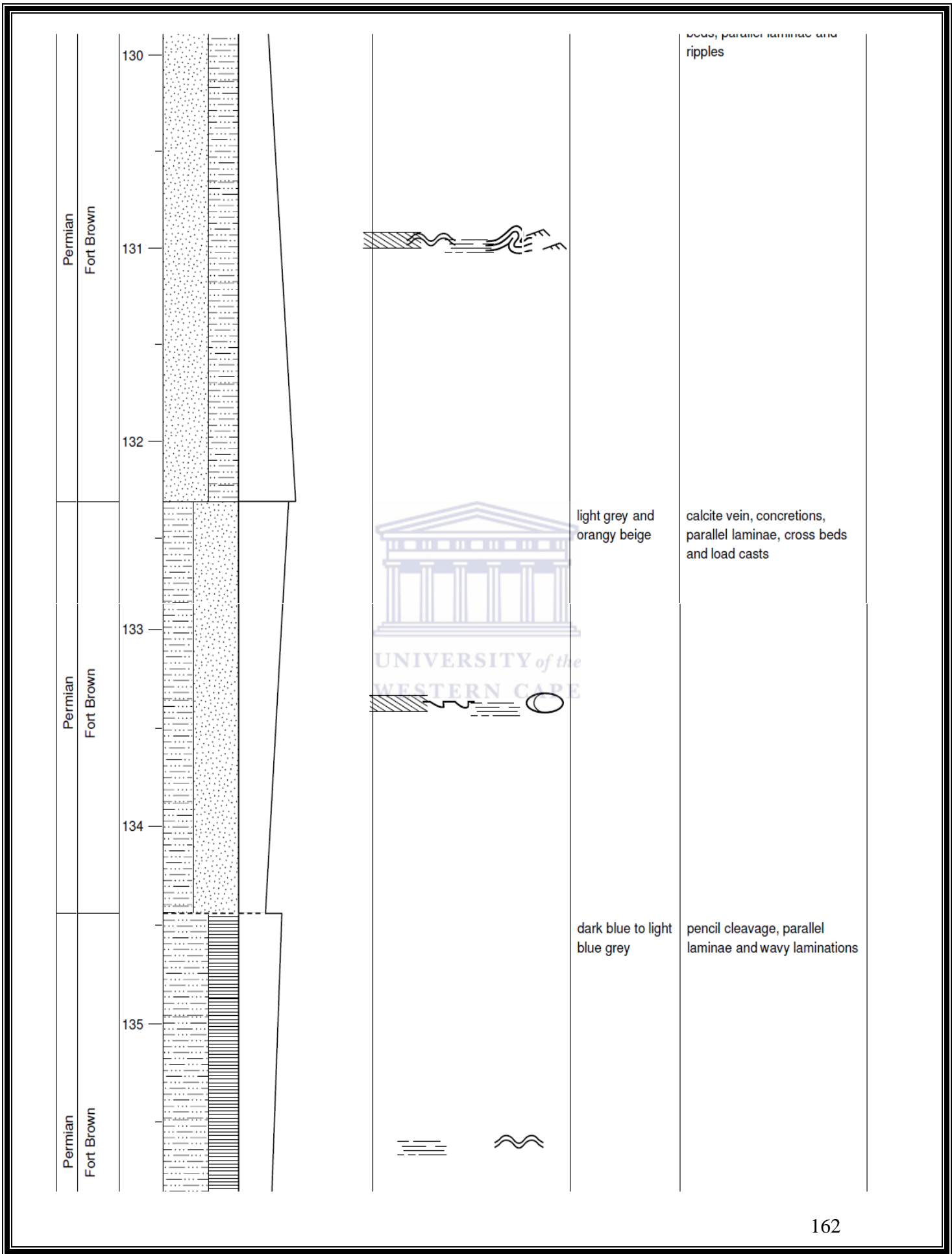
fractured, pencil cleavage, cross beds and wavy laminations

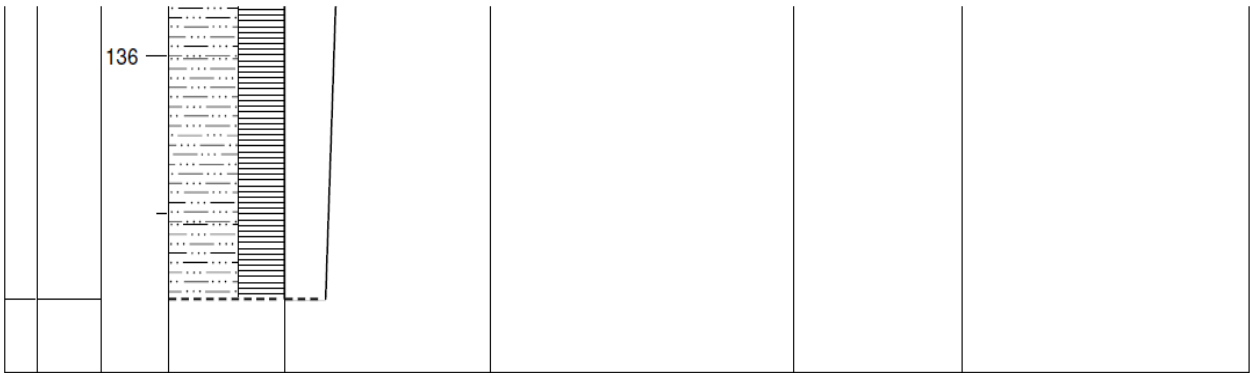
~ ~ ~ ~ ~

▨ ▨ ▨ ▨ ▨

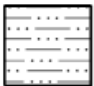


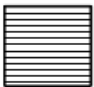
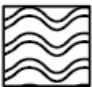

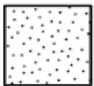


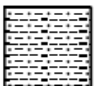
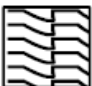



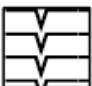


burnt orange and light grey

lenticular bedding, slumped laminae, wavy laminae, cross beds, parallel laminae and





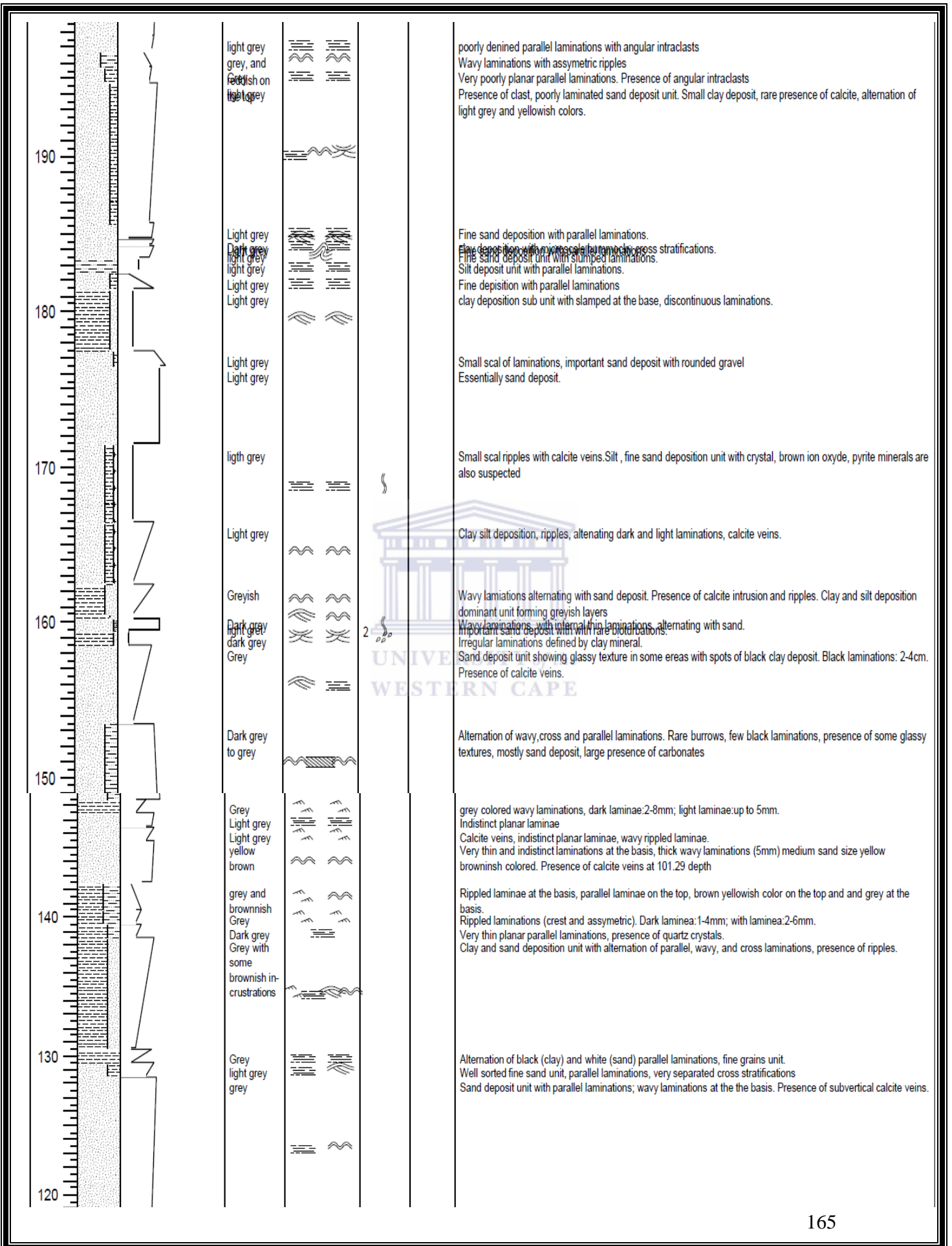
Appendix C-2: Fort Brown Formation Legend

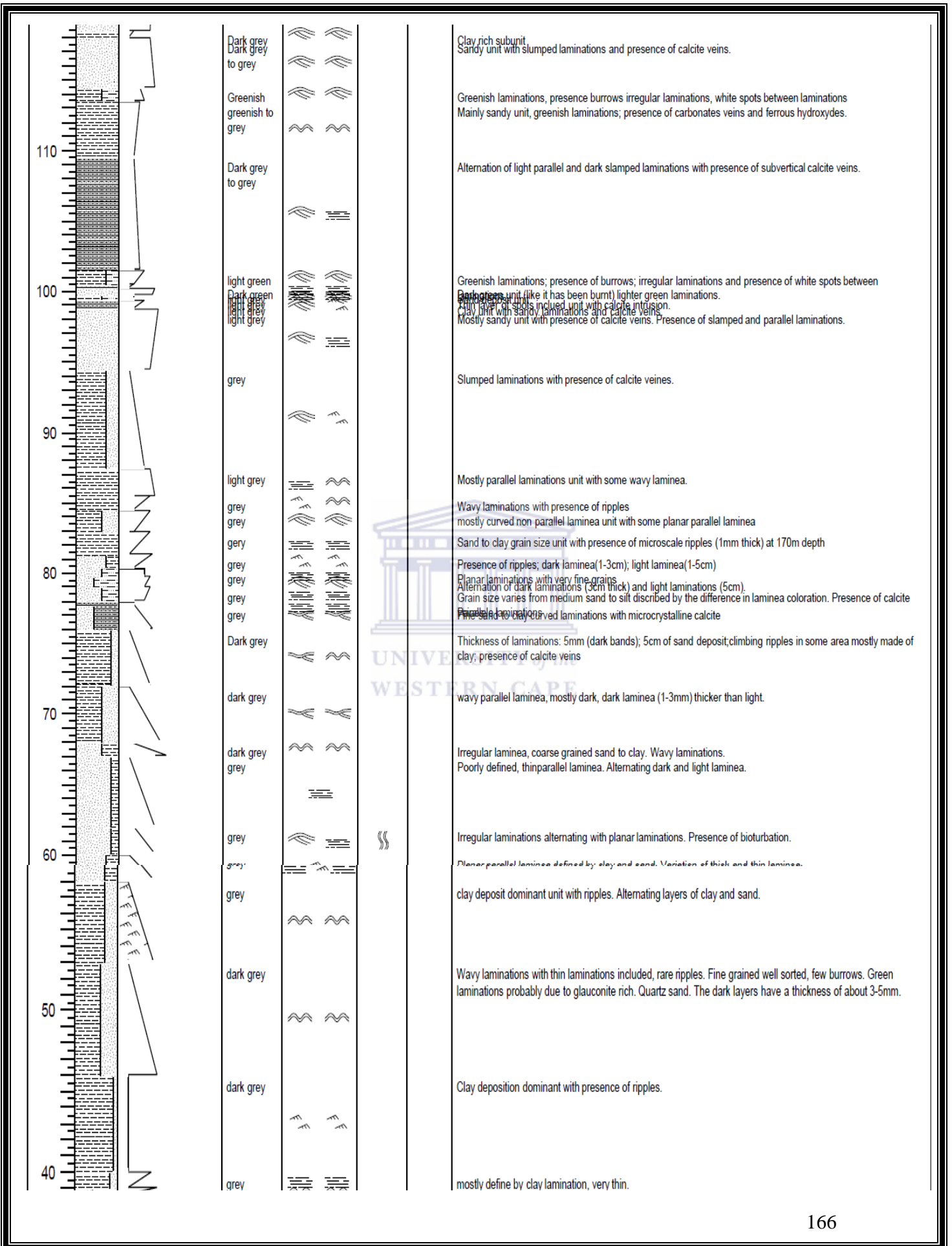
Lithologies	Symbols	Base Boundaries
 Siltstone	 Horizontal planar lamination	 Gradational
 Shale	 Wave ripple cross-lamination	 Sharp
 Sandstone	 Planar cross bedding	 Erosion
 Mudstone	 Scours	
	 Nodules and concretions	
	 Convolute lamination	
	 Current ripple cross-lamination	
	 Mudcracks	
	 Load casts	
	 Water structures	

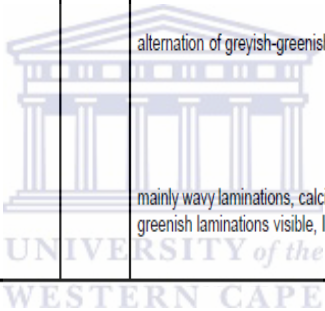
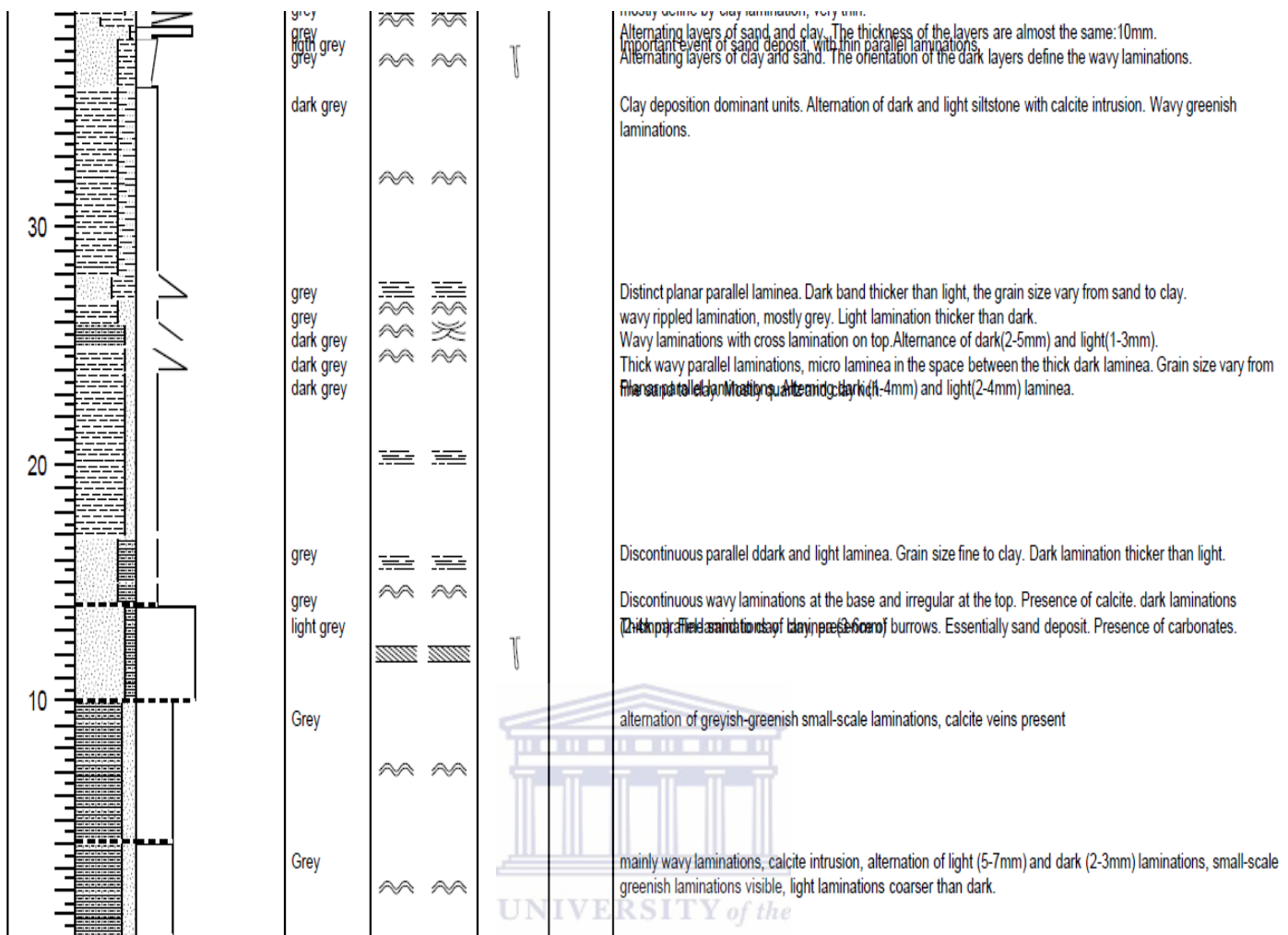
APPENDIX D

Appendix D-1: Sedimentary log of the Kookfontein Formation taken at the Bitterberg area, core SL1: S32°39' 00.12", E 20°07' 59.58" (Courtesy of Dr.Mikesh Stellenbosch University, 2010).

Untitled							
SCALE (m)	LITHOLOGY	MUDSANDGRAVEL	COLOUR	STRUCTURES / FOSSILS	BIOTURBATION	PALAEOCURRENT	NOTES
		clay silt fine medium coarse grain pebb cobb boul					
240	[Lithology symbols]		Yellowish	[Symbol]			Essentially sand deposit subunit with slumped laminations. Sandy unit, with no laminae.
			Yellowish	[Symbol]			Sand deposit unit with parallel laminae of 5-6cm thick
			Yellowish	[Symbol]			Essentially sand deposit unit, small amount of clay deposit, few spots of clay in some areas.
			yellowish	[Symbol]			Essentially sand deposit unit with poorly defined parallel laminations and wavy and slumped laminations on the top (25cm), presence of clasts, clay deposit (0.5-1cm)
			Yellowish	[Symbol]			Erosion of sand deposit then clay deposit (18cm), parallel laminations, presence of calcite veins.
			Yellowish	[Symbol]			Slumped laminations with thin parallel laminations, medium grains
			Yellowish	[Symbol]			sand deposit, parallel laminations, medium grain
			Dark grey	[Symbol]			Parallel and slumped laminations, clay rich, dark grey fine grains, rare green laminations
			Grey	[Symbol]			Very poorly defined parallel laminations unit with sand deposition and subvertical calcite intrusion
230			Dark grey unit	[Symbol]			Silt and clay deposition unit with thin laminae and vertical calcite intrusions. Very poorly defined parallel laminations yellowish sandy unit subvertical calcite.
			Dark grey	[Symbol]			Clay deposition subunit fine laminations with subvertical calcite intrusions.
			yellowish	[Symbol]			Very poorly defined parallel laminations yellowish sandy unit with subvertical calcite veins and calcite.
			Grey	[Symbol]			Alternation of dark and light tick laminae(5cm each)
220			Grey	[Symbol]			Slumped lamination unit with vertical calcite veins
			Grey	[Symbol]			Alternation of very well defined thin laminae (1-2mm) and slumped lamination subunits.
			Yellowish	[Symbol]			Very poorly defined planar parallel laminations with thicker wavy laminae (3mm) and white oblic calcite veins.
210			Grey	[Symbol]			Very well defined wavy planar parallel laminations (1-3mm dark laminae; 2-4mm light laminae)
			Yellowish	[Symbol]			very poorly defined thin planar parallel laminae well sorted medium to fine sand yellowish and reddish colored, and presence of white calcite.
			Grey to yellowish	[Symbol]			Poorly defined parallel laminations yellowish colored unit with well sorted sand grains and presence of calcite veins at 49 and 48m depth.
200				[Symbol]			







Appendix D-2: Kookfontein Formation Legend (Courtesy of Dr. Mikesh Stellenbosch University, 2010).

Lithologies	Symbols	Base Boundaries
Mudstone	Wave ripple cross-lamination	Gradational
Sandstone	Planar cross bedding	
Claystone	Vertical burrows	
Siltstone	Horizontal planar lamination	
Halite	Trough cross bedding	



Current ripple cross-lamination



Hummocky cross stratification



Moderate bioturbation



Swaley cross stratification



Tracks



Minor bioturbation



Convolute lamination

